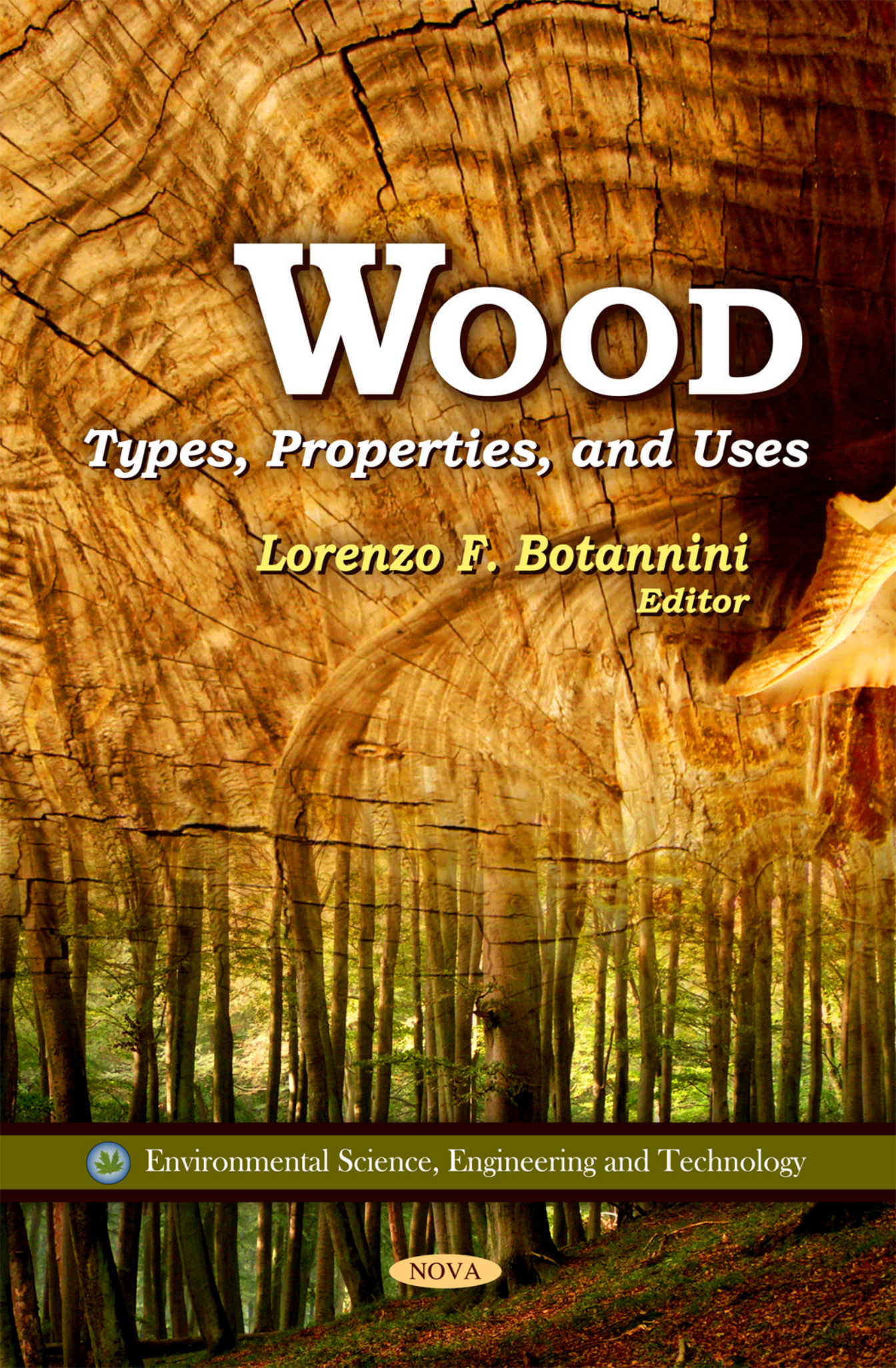
WOOD
Types, Properties, and Uses
Lorenzo F. Botannini
Editor
Environmental Science, Engineering and Technology
NOVA

ENVIRONMENTAL SCIENCE, ENGINEERING AND TECHNOLOGY

WOOD: TYPES, PROPERTIES, AND USES

ENVIRONMENTAL SCIENCE, ENGINEERING AND TECHNOLOGY

Additional books in this series can be found on Nova's website under the Series tab.

Additional E-books in this series can be found on Nova's website under the E-books tab.

ENVIRONMENTAL SCIENCE, ENGINEERING AND TECHNOLOGY

WOOD: TYPES, PROPERTIES, AND USES

LORENZO F. BOTANNINI
EDITOR

Nova Science Publishers, Inc.
New York

LIBRARY OF CONGRESS CATALOGING-IN-PUBLICATION DATA
Wood : types, properties, and uses / editor, Lorenzo F. Botannini.
p. cm.
Includes bibliographical references and index.
ISBN978-1-61728-046-7 (eBook)
1. Wood. I. Botannini, Lorenzo F.
TA419.W838 2009
620.1'2--dc22
2010012263

Published by Nova Science Publishers, Inc. † New York

CONTENTS

PREFACE

Wood is the most accessible and renewable material used by humankind during its history. Today, the consumption of wood exceeds all other known materials. The industry of various products made of wood grows continuously. This new book reviews research on hydrothermal treatment and modification of wood in the drying and impregnation process; the decomposition of coarse woody debris as an important component of the carbon cycle and biodiversity of forest ecosystems; and the potential of agroforestry as a carbon sequestration strategy. Also discussed is the importance of fossil woods, types of preservation, and their significance in reconstructing the palaeo-climatology and paleo-environment of a region as well as the limitation in identifying the fossil woods.

Chapter 1 - Wood is the most accessible and renewable material used by humankind during its history. Today, the consumption of wood exceeds all other known materials. The industry of various products made of wood grows continuously. Green lumber, being usually a raw material for final consumer products, possesses a number of properties that limit its application. For example, wood reduces its geometrical dimensions and can crack during drying, it is a highly hygroscopic material, has an ability to decay, burn, etc. Of the wide variety of lumber treatment technologies, typically two of them are used in producing the majority of wood products. These are a process for removing the fluid (dehydration, drying, extraction) and a process for introducing into wood certain substances in the form of a liquid or vapor.

In most cases, for carrying out these treatments it is necessary to heat the wood in an environment of gases and liquids, which modify its properties. These processes are termed hydrothermal treatment. In this Chapter the processes of drying, heat treatment, combined thermal and mechanical effects, as well as methods for wood modification, including those by impregnating of wood with various liquids, are discussed.

A typical feature of modern dewatering and drying technologies is the significant role played by the hydrodynamic transfer of vapor and liquid in the timber. In the first part of the Chapter, the authors describe some features of this technology. The results (of tests) on thermal-mechanical wood drying by the method of depressurization are presented. This method permits intensifying the movement of moisture in the wood structure and removing free water from the material in the form of drops without evaporation. The authors describe the original results of the study of high-temperature drying of cylinder-shaped articles in a vacuum-compression experimental setup using the depressurization method. This drying rate

increases by 4–5 times as compared with traditional drying kilns. The method allowed the authors to produce good quality products.

The second part is devoted to the modification of wood by impregnation. The urgent technological problem is to create a desired distribution of impregnating liquid throughout the timber volume. The proposed methods allow impregnating the wood at any depth up to full saturation.The research has shown that this problem can be efficiently solved by using a wide class of liquids (solutions of salts, polymers, hydrocarbons, dyes, melts, etc.), including emulsions. The effects of the impregnation method, temperature, cyclic pressure and other factors on the absorption of liquids are described.

Chapter 2 - Productive direct conversion of lignocelluloses into liquid organic products by electron distillation of crude wood or by dry distillation of preliminarily irradiated wood is considered. Electron-beam conversion is several times more effective than ordinary hydrolytic, pyrogenous or enzymatic processing of wood. Distillation of wood by electron-beam energy yields a number of the useful reagents for heavy organic synthesis and fuel productions. In particular, this path results in high yield of furans - perspective raw materials for production of high-quality alternative fuel which is compatible to conventional engine fuel and the up-to-date types of automobile engines. Electron-beam processing of intermixtures of wood with others synthetic and natural organics (plasts, bitumen, oil, etc.) also can be perspective. An experiments have shown that the electron-beam irradiation of binary wood-bitumen or wood-polymer intermixtures is characterized by sinergistic destruction of components. Such effect can be the innovative base in the alternative fuel production, in recovery of complex polymer-cellulose waste, in processing of native bitumens and heavy petroleum residue, in practical regeneration of synthetic monomers and in synthesis of industrial inhibitors of radical polymerization.

Chapter 3 - Biomass in a holistic view produces food, fodder, fuel, fiber and fertilizer. There are a number of simple, efficient and convenient biomass-based systems for different domestic, agro-industrial and agricultural applications. The replacement of conventional fossil fuels with biomass for thermal energy production results both in a net reduction of greenhouse gas emissions and in the replacement of conventional energy sources. Biomass energy accounts for about 11% of the global primary energy supply, and about 2 billion people worldwide depend on biomass for their energy needs. Modern applications of biomass cover not only industrial thermal application and electricity production, but also include domestic applications through improved cookstoves, wood gas stoves and gasifier. Combustible producer gas extracted from gasifier is effectively and economically converted from low value solid biomass fuel to a gaseous mixture. This gaseous mixture can be used to generate processing heat for thermal application. In this chapter, various biomass conversion routes such as thermo chemical, bio-chemical and agro chemical conversion have been covered, which includes improved cookstoves and biomass gasifier. The thermo chemical conversion process starts from a direct combustion process to more efficient gasification process, which includes pyrolysis, gasification and improved cookstoves. A gasification system to generate processing heat for baking bakery items and drying of phosphoric acid through open core down draft type; durable biomass cookstove for domestic, agro industrial and community applications; and a gasification-based wood stove for cooking application are discussed. The natural draft gasifier to generate thermal heat to extract chemical components from medicinal plants, fuel replacement and greenhouse gas mitigation potential through installation of biomass gasifier and cookstoves are also discussed in this chapter.

Chapter 4 - The aboveground biomass and nutrient content are important measures of the characteristics and individual requirements of the plant species. Also, a previous evaluation of the areas to be planted is essential to a successful establishment of forests with native or exotic species. The aim of this review is to explore the current information on the total aboveground biomass, nutrient content and the benefit of symbiosis in some native woody species and exotic *Eucalyptus* plantations in Brazil. The methodology for native and exotic plant species used for agroforestry is illustrated. The *Eucalyptus* species presented an aboveground wood biomass (AWB) of 26.9 to 44.4 Mg ha^{-1}, and the aboveground wood volume varied for 42.8 to 75.9 m^3ha^{-1}. The biomass of the stem wood, leaves, branches, and stem bark accounted for 64–66%, 16–19%, 15–17%, and 0.2–0.6% of the total biomass, respectively. The wood localized in superior parts of the trunk presented a higher concentration of P and bark containing significant amounts of nutrients. On the other hand, the native species evaluated, presented a higher total aboveground biomass when inoculated with arbuscular mycorrhizal fungi and *Rhizobium* bacteria. Leguminous trees showed greater height and diameter growth, as well as, higher dry matter and nutrient concentration when inoculated. The AWB varied for 0.48 to 0.76 Mg ha^{-1} for *Anadenanthera peregrina*. The agroforestry trees exhibited mycorrhizal mycotrophy. The potential of agroforestry as a carbon sequestration strategy (carbon storage potential in its multiple plant species and soil) as well as its applicability in agricultural lands and in reforestation must be more exploited. Research directions that are needed to increase understanding of mycorrhizal associations in tropical cropping systems and to increase mycorrhizal benefit are indicated. The benefits and problems encountered are discussed in this chapter, in order to highlight the need for a continual study of the forestry species.

Chapter 5 - Decomposition of coarse woody debris (CWD) is an important component of the carbon cycle and biodiversity of forest ecosystems. Dynamics of organic chemicals, nutrients and occurrence of fungi during CWD decomposition have been studied intensively in coniferous boreal forests. However, little attention has been paid to the CWD of angiosperms that dominate temperate areas and to the relation between the organic chemical dynamics and fungal succession during CWD decomposition. Thus, the purpose of the present study is to clarify the mechanism of fungal decomposition of CWD of an angiosperm tree, Japanese beech (*Fagus crenata* Blume).

First, the dynamics of the physicochemical properties of beech CWD during decomposition were estimated. A chronosequence method with a five decay class system was used to estimates the decay process of CWD. Second, a mycological survey was conducted for macrofungi fruiting on CWD and microfungi isolated from CWD, and the relationships between fungal succession and physicochemical changes during CWD decomposition were detected. In light of the results, fungal decomposition of beech CWD and the implication for soil humus accumulation were discussed.

Chapter 6 - The stable-carbon-isotope ratio ($\delta^{13}C$) of plants is strongly related to the ratio of CO_2 assimilation rate and stomatal conductance, and water use efficiency (WUE), and thus $\delta^{13}C$ analysis of tree rings gives long-term records on carbon gain and water use associated with wood formation. To identify the effective rainfall seasons for early and late wood formation of Chinese pine (*Pinus tabulaeformis* Carr.) and black locust (*Robinia pseudoacacia* L.) in the Loess Plateau, China, we examined correlations of seasonal precipitation with annual values of $\delta^{13}C$ and tree-ring width for early and late wood. The

correlations with precipitation were examined for each month and for periods of all possible lengths from 2 to 22 months starting from January of the previous year to October of the current year. The period with the highest correlation was adopted as the most effective rainfall season for interannual variations in tree-ring $\delta^{13}C$ and width. In early wood, precipitation during the dry season (October to May) before the growing season was negatively correlated with $\delta^{13}C$ of pine trees and positively correlated with ring width of pine and locust trees. In late wood, rainfall during the growing season in the current year was negatively correlated with $\delta^{13}C$ of pine and locust trees, and positively correlated with ring width of locust trees. Our results demonstrated the different water use strategies between pine and locust trees. The lower $\delta^{13}C$ of pine trees indicated higher WUE and more conservative water use compared to locust trees. Precipitation during the dry season affected the interannual variation in tree-ring $\delta^{13}C$ and width of pine and locust trees, indicating that the rainfall during the dry season before the growing season is important for wood formation in the Loess Plateau.

Chapter 7 - Palaeo-environmental interpretation using the fossil remains has attained a world wide attention and the palaeontological studies coupled with geochronology and stratigraphy could bring many dimensions to certain obstinate facets of biogeography and promote not only the theory of evolution, but the concept of plate tectonics also. Throughout geological time the omnipresence of fossil wood has provided researchers with a potentially rich archive of data for exploring questions concerning extinct and extant arboreal plant systematics. Fossil woods, both petrified and carbonized wood remains, provide information on bio-geographical trends over space and time. Also, the past distribution and diversity of woody taxa are important for reconstructing the timing of diversification and migration patterns. They have also provided vital information on palaeo-climatic fluxes in reconstructing the palaeo-environmental scenario of a region. The present chapter deals with the importance of fossils woods, types of preservation, their significance in reconstructing the palaeo-climatology and palaeo-environment of a region as well as the limitation in identifying the fossil woods.

Chapter 8 - The effects of chemical modification of pine wood fiber on the moldability of this material were examined. Pine wood fiber was chemically modified with benzyl chloride under alkaline conditions at various mole ratios of benzyl chloride to wood hydroxyl groups (ratio = 1 to 4) and at different reaction times (2 to 8 h). The extent of benzylation was assessed by weight gain and FTIR and NMR spectroscopies. FTIR spectroscopy revealed the reduction of wood hydroxyl group bands, an increase in aromatic bands, a reduction in cellulose crystallinity, and an increase in acryl and alkyl ether bands, which were consistent with etherification. The thermal and mechanical properties of the benzylated wood fiber were assessed by a combination of differential scanning calorimetry (DSC), dynamic rheometry and dynamic mechanical analysis (DMA). The results from DSC were consistent with data from rheometry. The data have shown that the benzylated wood thermal transition temperature and mechanical properties can be tailored by the extent of benzylation.

Chapter 9 - This chapter highlights the deforming behavior of PF resin-impregnated wood under transverse compression aiming at obtaining high strength wood at low pressing pressure. The impregnation of PF resin caused significant softening of cell walls resulting in cell wall collapse at low pressing pressure. Pressure holding causing creep deformation of resin impregnated wood was also effective in initiating collapse at lower pressure. Thus, by

controlling the processing parameters (resin content, pre-curing temperature, pressing temperature and pressing speed) high strength wood having MOR of 240 MPa and MOE of 22 GPa can be obtained at a pressing pressure of 2 MPa. Removal of matrix substances by $NaClO_2$ treatment prior to resin impregnation is also effective for further enhancing the mechanical properties of resin impregnated wood at lower pressing pressure. This treatment is attractive; nevertheless it is complicated in processing and somewhat difficult to remove the harmful chemical $NaClO_2$ completely from the treated wood, posing a major drawback in the commercial application. Hence, the potentials of steam pretreatment as a substitute of chemical treatment for making highly compressed PF resin-impregnated wood at low pressing pressure was highlighted. Such treated wood elements present a promising surface material in the manufacture of sandwich panels, giving high strength and dimensional stabilization with a moderate specific gravity as a whole product using single shot application.

Chapter 10 - Wood polymer composites (WPC's) are a new generation of reinforcing materials, using polymeric thermoplastic matrices such as polyolefins, and renewable materials such as woodflour. As a contrast to other mineral fillers, WPC materials have experienced growing interest over recent years due to the combination of a variety of factors, such as high performance, high versatility, processing advances, reasonable costs and biodegradability. However, there are some limitations. The most important disadvantage is their reduced resistance and low efficiency during stress transfer due to the incompatibility between hydrophilic polar fibres and hydrophobic apolar isotactic polypropylene, iPP. This creates repulsion forces that lead to poor adhesion, if at all, during blending. The use of compatibilizers increments the adhesion between components by reducing the interfacial tension and improving the stress transfer between phases. Since iPP is a semicrystalline polymer the understanding of the crystallization and melting behaviour of this matrix in the iPP/WF system, and the study of the influence of the compatibilizer on the crystalline parameters, and both the kinetics and thermodynamics of crystallization of iPP, are essential to the understanding of the solid-state properties in these materials. In this chapter we review the crystallization and melting processes of iPP/wood composites, under both dynamic and isothermal conditions, as a function of the thermal history, the content of the filler and the presence of interfacial agents as compatibilizers. The kinetic parameters and the evolution of the energies associated with crystalline nucleation of polypropylene in this type of composites and their relationship with the possible existence of a compatibilization processes between the polypropylene matrix and the wood reinforcement are discussed.

In: Wood: Types, Properties and Uses
Editor: Lorenzo F. Botannini
ISBN 978-1-61668-837-0

Chapter 1

HYDROTHERMAL TREATMENT AND MODIFICATION OF WOOD: DRYING, IMPREGNATION

V. P. Kozhin[1] and N. M. Gorbachev
A.V.Luikov Heat and Mass Transfer Institute National Academy of Sciences of Belarus

ABSTRACT

Wood is the most accessible and renewable material used by humankind during its history. Today, the consumption of wood exceeds all other known materials. The industry of various products made of wood grows continuously. Green lumber, being usually a raw material for final consumer products, possesses a number of properties that limit its application. For example, wood reduces its geometrical dimensions and can crack during drying, it is a highly hygroscopic material, has an ability to decay, burn, etc. Of the wide variety of lumber treatment technologies, typically two of them are used in producing the majority of wood products. These are a process for removing the fluid (dehydration, drying, extraction) and a process for introducing into wood certain substances in the form of a liquid or vapor.

In most cases, for carrying out these treatments it is necessary to heat the wood in an environment of gases and liquids, which modify its properties. These processes are termed hydrothermal treatment. In this Chapter the processes of drying, heat treatment, combined thermal and mechanical effects, as well as methods for wood modification, including those by impregnating of wood with various liquids, are discussed.

A typical feature of modern dewatering and drying technologies is the significant role played by the hydrodynamic transfer of vapor and liquid in the timber. In the first part of the Chapter, we describe some features of this technology. Our results (of tests) on thermal-mechanical wood drying by the method of depressurization are presented. This method permits intensifying the movement of moisture in the wood structure and removing free water from the material in the form of drops without evaporation. We describe the original results of the study of high-temperature drying of cylinder-shaped articles in a vacuum-compression experimental setup using the depressurization method. This drying rate increases by 4–5 times as compared with traditional drying kilns. The method allowed us to produce good quality products.

[1] e-mail: vpkozhin@yahoo.com.

The second part is devoted to the modification of wood by impregnation. The urgent technological problem is to create a desired distribution of impregnating liquid throughout the timber volume. The proposed methods allow impregnating the wood at any depth up to full saturation. Our research has shown that this problem can be efficiently solved by using a wide class of liquids (solutions of salts, polymers, hydrocarbons, dyes, melts, etc.), including emulsions. The effects of the impregnation method, temperature, cyclic pressure and other factors on the absorption of liquids are described.

INTRODUCTION

People have used wood in the course of the millennia mainly as fuel and building material. Today the volume of wood consumption exceeds all other known materials and it is more widely used.

It is known that every tree, on average, consumes six kilograms of carbon dioxide from the atmosphere a day; every cubic meter of wood is the result of assimilation of 250 pounds of CO_2 from the atmosphere. Wood products play a significant role in moderating the impacts that affect global climate change. The natural properties of wood in themselves provide a simple way to reduce the emission of CO_2, which is probably the main cause of global climate change. Processing wood into finished products requires less energy than a full cycle of production, say, of steel or concrete, and, thus, contributes to reducing CO_2 emissions. Production of one ton of aluminum means the release of 22 tons of CO_2, compared with 15 kilograms emitted in the production of one ton of lumber [[20]].

Wood properties such as carbon content, and the fact that the wood is a renewable resource make the use of wood important not only from the viewpoint of economics, but also of politics [[79]]. Politics is in the context of the fight against global warming and other environmental problems.

The use of wood begins with timber-harvesting operations. After cutting the wood lumber, 40–50% of the wood mass (branches, knots, and roots) are left in the forest [[82], [102]]. Some part of the waste is to remain in the forest to avoid the depletion of soil nutrients. Another part can be used as fuel (firewood, wood chips, pellets), for the production of chipboard, as well as fertilizers, as mulch, for getting charcoal, wood chemical production, etc. In many countries, wood fuel is widely used in the energy sector. In Sweden and Finland, for example, the proportion of wood in the fuel balance is about 60%.

When sawing, the waste can be 40–60% of timber brought from the forest. After treatment, the wood is used for making various products, starting with furniture and building construction and finishing with dishes and souvenirs. Thus, only about 25% of the grown tree is in use to make a final product. So, the reasonable use of wood materials and products is an important task.

Wood has several properties that limit its use: Such products reduce their geometric dimensions and can undergo cracking at shrinkage. The wood is able to decay, burn, etc. Wood should be subjected to hydrothermal treatment in order to give required parameters. This extends the possibilities of its application and widens its consumer properties. By the hydrothermal treatment is meant the process when the properties of material undergo a change (at heating, pressing, saturation, etc.) in gas and liquid media [[83]].

This chapter describes a number of methods of hydrothermal treatment of wood, starting with the traditional methods of timber drying in kilns and modifying impregnation with preservatives in autoclaves and ending with insufficiently explored technology. We describe the drying technology using thermal, mechanical and thermal-mechanical removal of water, the intensification of the process using carbon dioxide, the combined drying methods. The second part of the chapter is concerned with the analysis of the impregnation methods, the model of saturation of timber with liquid, and with some of the results on impregnation with solutions of salts, polymers, oils, emulsions, dyes, melts, etc. This chapter also contains brief descriptions of the traditional and lesser-known drying technology and modifying impregnation with references to the information for a better understanding of the processes.

1. Drying and Heat Treatment of Wood: The Traditional and Non-Traditional Methods

Usually green wood has a moisture content MC = 70-120%. This value depends on the wood specie, the location of growing a tree, and the harvesting time. Moisture in the wood is divided into free and bound (hygroscopic). Free moisture fills the cavity cells (macro-capillaries) and here it is fixed mechanically. Bound water is located in the micro-capillaries of cell walls. The maximum moisture content of wood is about 30% when free water is absent and the cell wall is completely saturated with moisture (fiber saturation point FSP).

Wood is a capillary-porous body with the high porosity to 40-77% depending on tree species. Fully saturated with water timber may have a high moisture content, for example, for pine MC is 185%, for spruce – 212%, for oak – 116% [[101]]. Since wood is an anisotropic material, the permeability of gases and liquids depends on grain direction. For example, the pine permeability in the radial direction is a thousand times less than that in the axial direction [[65]]. Geometric dimensions of wood depend on its moisture content.

When wood is drying out, its size decreases (shrinkage), thus increasing its strength and hardness, thermal conductivity decreases. Electrical conductivity of material decreases million times and dried wood becomes an electrical insulator. The principle of measuring electrical conductivity is based on the most prevailing method of MC controlling.

At MC $\leq$ 20% the wood becomes resistant to bio-deterioration, as it provides uncomfortable conditions for developing microorganisms.

The wood should be dried out to a moisture content, at which a final product will be used. For example, outdoor garden furniture will not be broken because of the shrinkage in Las Vegas, NV, where the equilibrium moisture content (EMC) can reach 4% [[82]], if the furniture material has been dried out to 4%. In more humid air such as in Madison, WI, in Russia or Belarus, it is enough to dry out a material up to MC = 10-12%.

1.1. Drying Methods

The most ancient method of wood drying is the *air drying*, including seasoning under a shed. Air drying is the drying of timber by exposing it to the air. This method usually does not require energy, but the drying process is long and needs several months [[21]].

Almost all commercial sorts of timber are being dried in industrial kilns. The process of kiln drying consists basically of applying heat to the material. As known, there exist three main methods of energy supply to the material: conduction, where heating is carried out by contact of wood with a hot surface; convection, where a material gets heat from the stream of hot gas or liquid, and radiation, where a heat source is infra-red, or high-frequency radiation.

The simplest method of heating timber is its blowing by hot air. To do this, *conventional kilns* are the most widespread [[21], [34], [82], [83], [85], [110]]. Figure 1.1 shows the photo of this-type kilns, including the picture inside the dryer while timber loading.

Typically, material stacks in the dryer are being blown by hot air with specific humidity. Circulated air has a temperature of 60-80^{o}C and a speed of 2-6 m/s. In such kilns we can download up to 1000 m^3 of material, the drying time takes from several days (spruce, pine and other softwood) to several tens of days (hardwood). A long time process is necessary to arrange soft conditions for providing good-quality products.

Figure 1.1. Block of four conventional kilns with a load volume of 50 m^3 of timber each (a). Formation of stacks inside the chamber (b). Klichev Forestry, Belarus.

In this process the drying agent (hot air) provides energy to the material surface, and moisture is transferred from the deep layers of wood to the material surface mainly due to capillary movement and diffusion. The drying process is based on the tendency of wood to hydrothermal equilibrium (EMC) with surrounding media (drying agent). If the water vapor pressure in the timber is higher than the vapor pressure in the environment, then drying occurs, if it is lower – sorption of moisture. Since reducing the moisture content below the fiber saturation point (FSP) causes the timber size to decrease, it is necessary to create the same moisture content at each part (section) of products to obtain a good drying quality. In addition, equal conditions of heat and mass transfer for each unit of dried products must be created.

To heat the drying agent in kilns steam or water heaters are used. Often hot gases (e.g., furnace gases) [[83]] are employed. In some regions solar kilns using free solar energy are built for wood drying [[21], [106]]. Sometimes aerodynamic drying kilns having no heaters [[81]] are used, and heating occurs due to energy dissipation of air being accelerated by fans.

The process of *high-temperature drying* is more intense, drying is carried out at wood temperatures of 100^{o}C and above [[3]].

Since the high-temperature treatment of wood can change its strength, color and other characteristics, the question of the quality of wood after its exposure at high temperature is one of the most debated [[19], [21], [61], [66]].

In high-temperature drying kilns, wood is heated to a temperature of 100^{o}C at a relative humidity (RH) of 100% (saturated steam) in the chamber. Then the drying agent is undergone further heating, the chamber steam becomes superheated. Sometimes this method is called *superheated steam drying* (SSD) [[28], [60]]. When the steam becomes superheated the water in the timber will start boiling. The water in the wood will be pressed out and absorbed by the overheated steam medium. This provides a short drying time without any damage to the timber because the kiln is completely closed, so there is no exchange with outside air. According to [[50]], the energy consumption at SSD is four times lower than that at hot-air drying.

Application of *vacuum drying* can reduce the temperature of treating a material, which is particularly important when temperature-sensitive materials and valuable timber are being dried. With this method, the drying rate increases due to the intensification of the process and material stresses decrease, thus improving the drying quality. For periodic vacuum drying with the use of heat, the accumulated material can achieve a uniform distribution of the moisture content in it [[49]]. Therefore, vacuum kilns are increasingly used in industry, especially for accelerated drying of hardwood and wood of large cross-section [[14], [49], [103], [104]].

Convective and conductive heat supply to the timber is mainly used in vacuum chambers. At convective heating, the timber gets the heat of hot air supplied by a fan through a radiator. After heating, the air is evacuated from the material, and this results in intense evaporation of moisture. When the wood becomes cool the hot air is again supplied to the timber and the cycle is repeated.

Conductive heating is more efficient than convective one due to a tight pressing of hot plates to the surface of the material being dried. It reduces in general the time of heating and drying. The plates are being heated by electric current or by pumped hot liquid. The tight pressing is provided by atmospheric pressure on the flexible cover (rubber membrane) at evacuation. Usually this-type dryer does not exceed the loading of 10 m^3 of timber. The

installation for heating plates poses problems in forming a timber stack before drying [[36], [80], [104]].

High-frequency drying. Wood is placed in the high-frequency a. c. field and is intensely heated due to dielectric losses in the wet material. The heating is carried out both at the material surface and inside it, which reduces several times the heating time, as compared to the convective and conductive heating method. In recent years the wood treatment has focused mainly on lumber drying in vacuum kilns at dielectric heating, often termed high-frequency/vacuum drying. For industrial wood processing with high-frequency electric current, two different frequency ranges may be distinguished: radio frequencies below 100 MHz with the use of open wire circuits and microwaves at frequencies above 500 MHz [[36], [37], [73], [80]].

The heating occurs throughout the material thickness and moisture intensely moves to the material surface. The drying time decreases many times, as compared to that in the conventional drying chamber. This method allows increasing the throughput capability and improving the quality of wood drying. The disadvantages of this method include the high cost of high-frequency equipment. Typically, this method is used for drying small timber volumes.

When wood is being dried in the alternating electromagnetic field with the industrial frequency of 50-60 Hz the heating elements (steel grates) are placed between the timber rows in the chamber (*induction wood drying).* Timber together with a ferromagnetic material is in a solenoid, steel is being heated in the alternating electromagnetic field by Foucault currents and heat is supplied to circulated air and wood [[75], [76]].

Infrared drying is a method of drying with heat infrared radiation [[21], [54]]. This radiation with wavelengths larger than 780 nanometers is provided either by special bulbs or special-type gas heaters. This drying method is not often applied to the wood. It is difficult to provide uniform heating of all parts of a stack.

Drying in liquids. For low-value species one uses the method of drying in the hot liquid by immersion, for example, in oil, petrolatum, etc. [[48], [83]]. The liquid temperature exceeds 100^{o}C, so drying goes very rapidly at rates much faster than drying in the conventional kilns. The disadvantages of this method should include timber greasing, so this method is usually used for preliminary drying of ties, piles and poles before protective impregnation.

If the wood is pre-impregnated with salt solutions (sometimes it is called *chemical drying*), then during drying this reduces internal stresses of the material that protects the surface from cracking [[80]]. One can use the following salts: magnesium chloride, potassium chloride, sodium chloride, ammonium nitrate, etc. For example, the water vapor pressure above the saturated solution of NaCl corresponds to a relative humidity of 75%. When the humidity is less than 75% the moisture is evaporating from the surface of the layers, and from the inner layers the moisture moves to the surface. The good quality of products was observed after drying of hardwood (such as apple, pear, and plum trees) pre-impregnated with the NaCl saturated solution.

The practice of protective impregnation showed that after impregnation of wood with water soluble preservatives the drying quality is improved [[100]].

Among the search works on new drying methods is the method of timber *electric-kinetic dewatering* or electroosmosis [[69], [76]]. Electroosmosis is a transfer of liquid in capillary-porous bodies under the action of an external electric field. Wood dehydration can be carried out at the electric field strength of more than 8 V/cm [[69]].

At *acoustic drying,* moisture is extracted from the dried material by the sound with appropriate characteristics. In comparison to the traditional heat method acoustic drying does not require raising a temperature of a material to be dried. In the acoustic method, energy consumption is 2-3 times lower than at conventional drying. Time expenditures according to the traditional method are by a factor of 5-10 more than those according to the acoustic one [[33]].

It seems that the method, which allows drying hardwood without the crack formation due to the water *replacement,* in the wood, of organic liquids such as methanol, ethanol, etc. [[24]], is interesting. Having combined this method with the treatment of supercritical liquids, it became possible to avoid the shrinkage problem by replacing the liquid in the wood with a high-density gas or supercritical liquid. The supercritical liquid can be removed from the wood by decompression. Supercritical drying does not damage the artifacts [[109]]. The supercritical liquid is carbon dioxide, which is cheap and safe, but will not mix with water. In consequence, the water in the artifact must first be replaced with an organic solvent – methanol. At high pressure the carbon dioxide density is similar to that of common liquids, and it can dissolve methanol.

The method of wood *drying in water is included into the unusual drying methods*. By passing an electric current in water, where the timber was placed, the author of the books [[75], [76]] was able to dry oak wood with a good quality. Electric current is selectively directed into the wet wood, which has higher electrical conductivity than water. This wood is heated and dried. Then the timber is removed from the water. In the heated state, finally it is dried quickly, giving moisture to the surrounding air.

Recently, a high-temperature heat treatment of wood with the purpose of its modification (*thermal modified wood)* has become more and more popular. Such wood in Finland is called Thermowood [[97]], Lignostone and Lignifol in Germany, and Staypak and Staybwood in the United States. These are the Thermowood process in Finland, the Plato process in Holland, the Perdure process and Retification in France [[29]].

This wood has several advantages over the usual dried wood [[96], [97]]. It absorbs less moisture and its EMC is lower than that of unmodified wood (improvements in dimensional stability). It has very good resistance to microbiological attack. Wood color becomes brown; the depth of color is determined by the treatment temperature. This material has a higher surface hardness, but is becoming more fragile. The technology of thermal modification of wood includes pre-drying in the drying kilns, then a high-temperature processing at T = 190-210^{o}C.

Removal of excess water by a conventional dryer yields good results, but requires a long time for drying. Many attempts have been made to develop methods or apparatus for wood drying in a shortened time at the lowered expense. The evaporation time of free moisture in the modern conventional drying kilns is 60-80% of the total duration of the drying process, and the rest of time is spent for the removal of hygroscopic moisture [[3]]. Therefore, there is a strong interest in the methods for mechanical removal of free moisture without the use of heating or by minimizing its use.

M. Stahl and M. Bentz applied the method of mechanical dewatering for wood drying using the *incubation decompression process (I/D-process)* [[91]]. The air introduced through the pneumatic system in the wood structure during the incubation period dissolves in the sapwood. The next stage begins with the decompression phase. Small air bubbles grow in the

liquid inside the material and mechanically push out the liquid. Combining this process with the heat treatment may improve the drying efficiency.

The *thermal mechanical method of drying* by depressurization was first used by Fleissner in 1926 for coal drying [[26], [60]]. With such a method, a wet material is preheated in a sealed chamber when pressure is increased, and then upon quick depressurization in the material bulk rapid vaporization occurs due to the accumulated heat. The hydrodynamic vapor flow captures liquid particles, as a result of which the heat expenditure in drying markedly decreases. The heat energy of the gas-vapor flow is conveyed into another chamber for preheating the material with the parallel operation of the similar devices.

More than 40 years ago A. Luikov said perspective drying by depressurization way for porous materials including the wood [[56]]. At the same time Mikhailov proposed a mathematical description of the process [[58]]. This method proved to be highly effective in experimental studies of peat drying [[89]]. Thermomechanical method gives opportunity to increase the rate of drying and reduce the power-consuming. At the same time with the drying, this method is used for the destruction of timber in wood chips production [[60]].

Centrifugal dehydration is the process where free water is removed from the porous timber volume by centrifugal forces. This occurs when the liquid pressure in the macro-capillary exceeds the capillary forces, and the inertia forces cause the liquid to leave the material. Studies have shown that the dehydration time depends on the rotation speed and lumber radius, the lumber type and length, ranging from several minutes to several tens of minutes [[51], [68], [70]]. It should be noted that due to the centrifugal forces only some amount of the free water held by the capillary forces can be removed. The bound moisture (MC $\leq$ 30%) cannot be removed mechanically. Studies have shown that according to the mechanical method the wood can be dehydrated to a final moisture content of 40-60% for 20-60 min; these values depend on the wood parameters as well as on the centrifuge parameter. Especially, the moisture can be effectively removed from the wet (flooded) wood [[45]]. After the free water removal the kiln drying can be recommended.

Combining the effects on the timber stack in a centrifugal field and convective heating enables getting wood of any moisture [[48], [67]]. Thus one can achieve significant energy savings [[45], [68]]. Rotational convection driers (of Kastmark and others) are described in the book [[67]]. In our time, such a technology of wood drying can find use in industry through designing new large centrifuges that can operate with unbalanced loads [[64]].

A combined removal of moisture from the wood can occur using other above-described drying methods, in which high-intensity transitional processes (with excess pressure in the timber) will be realized. For example, the mechanical removal of free moisture can be observed at high-intensity microwave heating, with a rapid pressure change in vacuum drying chambers [[15]], etc.

It is important to note that the high internal pressure gradient can lead to serious defects in the material even before the beginning of shrinkage (with MC above FSP). Therefore, such processes require careful study. This chapter deals with the experimental study of high-temperature drying by depressurization method with objectives to determine the conditions under which a good quality of material can be attained.

1.2. Experimental Study of High-Temperature Thermal-Mechanical Drying by Depressurization Method

To dry timber of large cross-section (large thickness, diameter) with a good quality in conventional kilns needs a lot of time. For example, for cylinder-shaped green pine with the diameter D = 0.1 m the drying time to a moisture content MC = 20% is 170–200 h.

High-temperature drying is used to accelerate the drying process. The disadvantages of high-temperature drying ($T_w > 100^oC$) include the reduction of strength due to physical and chemical changes in timber at high temperature. Usually this is caused by a long duration of the drying process and the presence of oxygen in the drying agent [[19], [61], [103]]. Wood slightly loses its strength and changes color. But the material gets a lot of useful properties after high-temperature processing. These include the reduction of water absorption, the increase in water resistance, biological stability, etc. [[66]].

The choice of the drying conditions is aimed at intensifying diffusion and molar (hydrodynamic) transfer of vapor and liquid in pores. This should ensure a low moisture gradient in the bulk of wood that determines the quality of its drying.

As previously shown in [[35], [56], [60], [89]] such conditions may provide thermal-mechanical drying by the depressurization method. The process depends on many parameters such as a temperature and a pressure of a vapor-gas medium in the chamber, a duration and number of treating cycles, a pressure release rate, properties of wood (moisture content, temperature, size, and structure), etc.

Experimental setup. The investigations were carried out on the setup schematically represented in Figure 1.2. A wood sample was placed into a sealed cylinder (chamber) 1 m in length and 0.16 m in diameter. Electric heaters were located on the cylinder body. The pressure gauge P_1 and the temperature sensors T_1 - T_3 served to control the pressure and the temperature in the cylinder and the sample. The valves made it possible to discharge vapor and draw off liquid from the cylinder. The setup incorporated a system of pressure release through a cooled condenser coil or through a sputter into a vessel with cold water. We recorded the measured temperatures of the gas medium, working cylinder body, wood, mass of the vapor-liquid flow from the chamber, and cooling water in the condenser. The experimental setup included a vacuum pump with a receiver, a steam generator and provided the following parameters: cylinder wall temperature up to 250^oC, chamber pressure 1 kPa - 1.2 MPa. The setup also allowed us to treat the material with saturated water steam at a pressure up to 0.5 MPa.

The process of thermal-mechanical drying included many stages, the main ones of which are:

1) cyclic heating of the material in the chamber (due to the radiative and convective heat transfer); in this process wood was heated in humid gas media with increasing pressure due to moisture evaporation (conditioning), which provided a decrease in wood internal stresses;
2) depressurization, at which intense release of vapor and free moisture from the wood structure occurred;
3) drying aimed at decreasing a bound moisture content from 30% to 8 - 10% by evaporation.

Vapor was condensed in the vapor collecting system where the liquid mass and the temperature were controlled. Upon completion of the drying and cooling processes the sample was weighed and then cut or split lengthwise into equal parts, and its moisture content was measured by means of an electronic MC meter.

Measurements . Experiments were conducted with cylindrical samples (D = 0.1 m, L = 0.35-1.0 m) of pine wood (*Pinus sylvestris*).

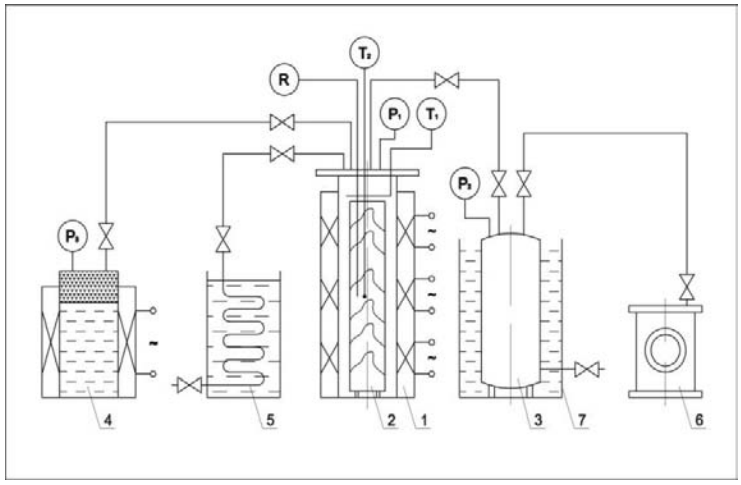

Figure 1.2. Schematic diagram of the experimental setup: 1 - working cylinder with heaters; 2 - sample of wood; 3 - vacuum receiver; 4 - steam generator; 5 - condenser; 6 - vacuum pump; 7 - jacket of cooling receiver.

Temperature sensors (thermocouples) and moisture content sensors were mounted at different depths in the sample. MC sensors – needle electrodes were installed in the holes at the surface of the cylindrical sample[2].

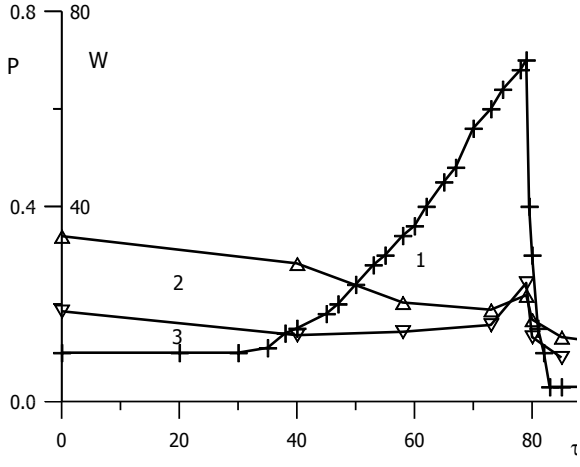

Figure 1.3. Pressure vapor in the chamber (1) and MC in the sample at a depth of 22.5mm (2) and 50mm (3). P, MPa; W, %; τ, min.

[2] Experimental work carried out jointly with K. Chizhik, N. Solntseva, B. Lovetsky

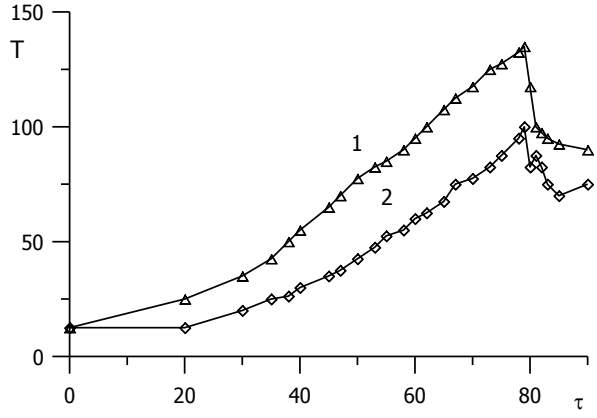

Figure 1.4. The temperature of the sample at a depth of 22.5 mm (1) and 50 mm (2). T, ^{o}C; τ, min.

The results of these measurements are shown in Figure 1.3 and Figure 1.4. As can be seen from the figures, the vapor pressure in the chamber grows with increasing temperature; the relieving pressure is accompanied by a rapid temperature drop due to the phase transition. In this case, intense drying occurs, as indicated by the MC sensors in Figure 1.3. Convergence of MC sensor readings demonstrates the reduction of the radial moisture content gradient in the timber, which is evident of a reduction of internal stresses in the material. Perhaps this is connected with a good vapor permeability of wood at high temperature.

To estimate the wood permeability we carried out an experiment on the processing of dry pine wood (L = 0.35 m, D = 0.1 m, W = 7%) by saturated water steam at a pressure of 0.3 MPa. Four cycles of treatment were performed. An increase was seen in the moisture content due to sorption of moisture in the bulk of the material. Thermocouples were placed in the timber and indicated a rapid temperature leveling over the sample cross-section. Weighing after the experiment showed that the average moisture content of the sample was MC = 24%. Therefore, we can conclude: wood at high temperatures has high vapor permeability. This confirms the data of [[75], [103]]. Perhaps there is an increase of permeability in the cross (radial) direction. It should be noted that the sample surface always has uncovered tracheids, as the sample has been processed mechanically.

Our assumption of molar (hydrodynamic) vapor transfer in the radial direction contradicts the conclusions of [[14]]. In that work the author proved the hydrodynamic motion of vapor in the axial direction of the timber and the absence of such motion in the radial direction. These results were obtained when he studied vacuum drying of oak (red and white oak), whose structure was different from the pine structure [[105]] and the drying was carried out at a temperature of 60-70^{o}C. In our experiment, the wood temperature was 110-120^{o}C.

Figure 1.5 displays the cyclic drying process of a cylindrical sample of green pine wood L= 0.9 m. The heating cycle duration was 30 min (except for the initial heating); the time of pressure relief was 5 min. The figure shows the pressure change in the chamber during the experiment, as well as the amount of moisture withdrawn from the timber in each cycle (collected in the condensing unit). It also illustrates the total mass of trapped moisture that was removed from the sample during drying (curve 3). As seen from the Figure 1.5, a

maximum vapor pressure first increases due to sample heating and then decreases. This is explained by a decrease in the wood moisture content during drying.

Drying of the sample continued for some time after cutting off the heaters. After cooling to room temperature the atmospheric pressure was set in the cylinder, the condensed liquid was discharged and the sample was removed from the chamber. Then the local moisture content was controlled by the MC meter at different points in the longitudinal section (after splitting). The data on the measured local moisture content showed that in some cases, MC changes were seen in the radial direction of the sample.

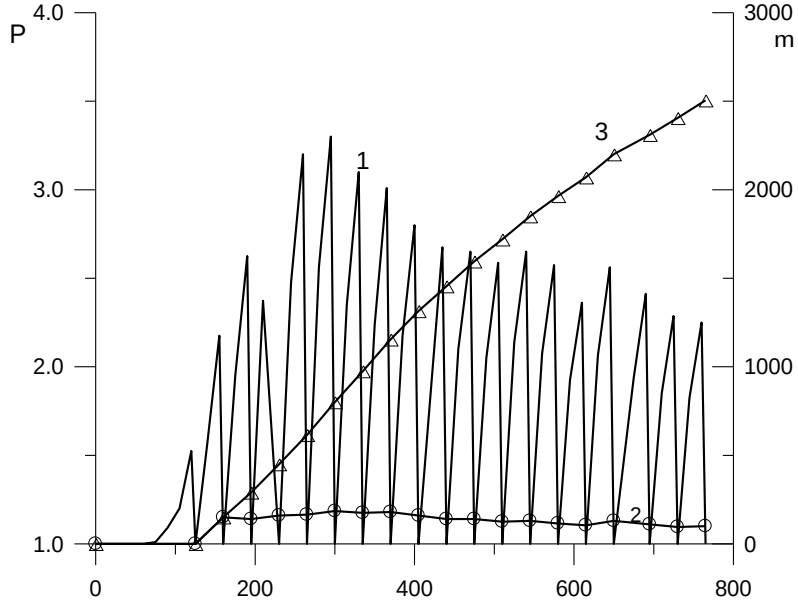

Figure 1.5. Change of pressure in the chamber and the kinetics of wood drying: 1 – pressure in the chamber; 2 - removed moisture mass in each cycle; 3 - total removed moisture mass. P, MPa; m, g; τ, min.

For example, at the surface MC = 5-8%, at a depth of 20-30 mm MC = 7-10%, in the central part of the sample (at the axis) MC = 12-16%. Noticeable internal and external cracks and other defects, often associated with accelerated drying, were absent.

The example of drying kinetics of a cylindrical sample under pressure cyclic changes is shown in Figure 1.6. In the first drying cycle the heating lasted until the readings of the temperature sensors located at different depths in the bulk of wood differed by no more than 2–3^{o}C.

The data in Figure 1.6 data illustrate the interdependence between the timber temperature and the gas pressure in the chamber. When thermocouple readings during the active vapor formation upon depressurization become much higher than 100^{o}C (at $\tau > 450$ min), this indicates that a noticeable quantity of free water in the wood is absent.

The behavior of the temperature curves confirms the fact that wood at high temperature has a high permeability.

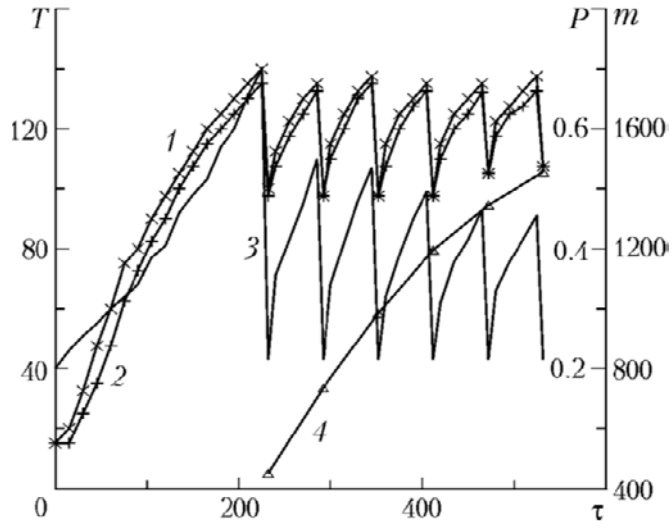

Figure 1.6. Change in the temperature inside the sample at a depth of $r/2$ (1) and at the center (2), in the chamber pressure (3), and in the removed moisture mass (4) at a periodic release of pressure (D = 0.1 m, W_0 = 69.2%, W_f = 11.3%). T, °C; P, MPa; m, g; τ, min.With kind permission from Springer Science+Business Media: <Journal of Engineering Physics and Thermophysics, Experimental study of the high-temperature thermomechanical drying of wood, vol. 82, 2009, p. 71, N.M. Gorbachev, V.P. Kozhin, Figure 3.

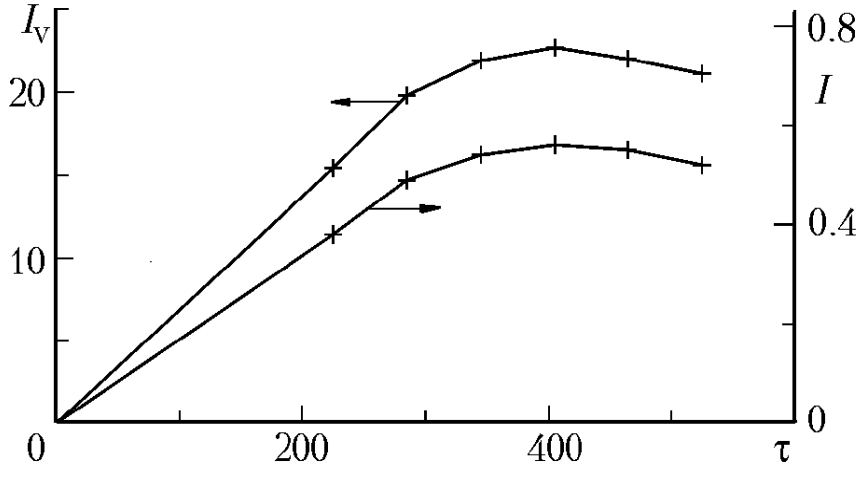

Figure 1.7. Measurement data for the volume and surface intensities of drying of cylindrical wood samples depending on the duration of the process. I_v, kg/(m^3·h); I, kg/(m^2·h); τ, min. With kind permission from Springer Science+Business Media: <Journal of Engineering Physics and Thermophysics, Experimental study of the high-temperature thermomechanical drying of wood, vol. 82, 2009, p. 72, N.M. Gorbachev, V.P. Kozhin, Figure 4.

So, according to [[103]] for pine and cedar, the highest permeability of gases is observed at the temperature T = 100-120°C, for larch 120°C, for spruce at 90-100°C, for silver fir at 110-120°C. When the wood temperature was increased to 130-140°C the permeability of all wood species decreased or stabilized.

The absence of cracks in the dried samples agrees with the data [[3], [75]]: the high temperature drying increases the plasticity and gas permeability of wood, which reduces the probability of defect formation. The plasticity occurs primarily due to softening of lignin during heating [[77]]. The glass transition temperature of lignin in the matrix is approximately 170°C. As the permeability increases the drying rate grows. In [[90]] it is shown that the permeability changes even when diffusion and capillary transport of moisture during drying can reduce the drying duration several times.

The high rate of the drying process is evidenced by curve *I* for the drying intensity versus time given in Figure 1.7. The same figure also presents the drying intensity curve I_v referred to the bulk of the material. As seen, it better describes the process of drying of wood of large cross-section (beams, poles, etc.). The intensity of the moisture removal in the experiments reached I = 0.4–0.6 kg/(m^2·h), I_v = 19–22 kg/(m^3·h), which is dozens of times higher than in conventional kilns. The maximum in the given curves points to the completion of the process of free water removal from the samples.

It should be noted that the drying rate may be even greater if there is a close contact of the timber with the hot surface such as heating plates (conduction heating) [[104]].

To evaluate the influence of mechanical removal of water from wood, in the condenser a quantity of incoming moisture and a cooling water temperature were measured simultaneously in each depressurization cycle. In the given run of measurements, a glass spherical flask filled with water was used to collect condensate; the vapor with water drops got into the water. The weight of the flask was continuously recorded by a weight meter. A water temperature was checked by means of thermocouples. A quantity of condensed vapor and droplet liquid was estimated with the use of heat balance equations with account for the loss due to the heating of the condenser case. The mass of vapor and liquid withdrawn from the timber and collected in the condenser is shown in Figure 1.8.

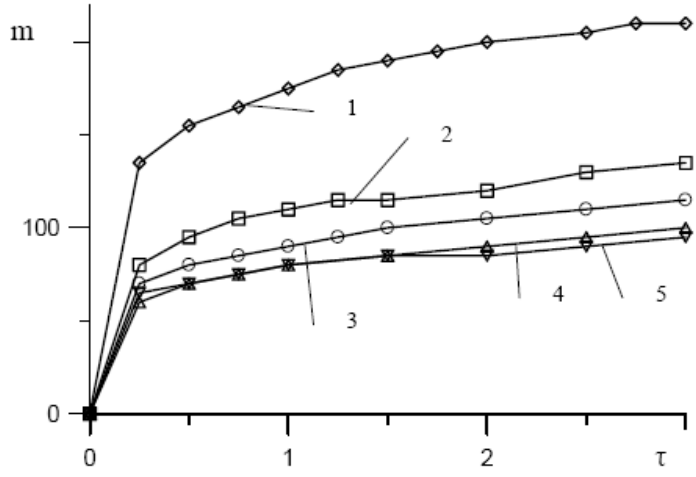

Figure 1.8. Mass collected in the water condenser during five cycles of thermal-mechanical drying of wood sample: 1-first cycle of depressurization, 2-second cycle, etc.

It follows from these data; the most intense drying process proceeds during the first minutes of pressure relief. This makes it possible to reduce the cycle duration.

The measurement data have shown that the maximum influence of thermal-mechanical release of moisture in the form of liquid was observed in the first cycle of depressurization when the wood structure contained maximum free water. In this case, the water in the liquid phase constituted up to 10% of the total mass of moisture removed from the wood. In the subsequent cycles of depressurization, the fraction of the liquid phase decreased and that of vapor increased. The estimates of the evaporated and droplet liquid removed from the wood in the first depressurization cycle for three samples with the diameter $D = 0.1$ m are given in Table 1.1.

As the wood moisture content is increased, the role of the liquid phase in the total yield grows. This is illustrated by the results of determining the coefficient of thermal-mechanical removal of moisture κ presented in Figure 1.9.

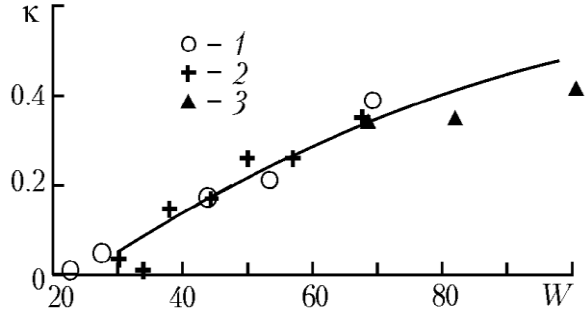

Figure 1.9 Coefficient of thermal-mechanical removal of moisture in the liquid phase versus MC of wood: 1 - $W_0 = 67.7\%$; 2 - 69.2; 3 - 100.6. W, %.With kind permission from Springer Science+Business Media: <Journal of Engineering Physics and Thermophysics, Experimental study of the high-temperature thermomechanical drying of wood, vol. 82, 2009, p. 72, N.M. Gorbachev, V.P. Kozhin, Figure 5.

These data at $W \approx 100\%$ are in good agreement with the data [[89]] obtained for thermal-mechanical drying of a peat plate with a moisture content of 1 kg/kg, where $\kappa \approx 0.5$.

It should be noted that the results presented demonstrate the influence of the removal of moisture in the form of liquid (droplets) at absolute moisture content of 30% or even less, i.e., at the values of the fiber saturation point FSP of wood. This says about the specificity of moisture transfer in wood at high temperatures.

Dissolved carbon dioxide can positively influence the dehydration process of porous material [[59]], and so we were therefore interested in studying *the_influence of carbon dioxide* in the drying process.

Before drying on the setup (Figure 1.2) the air was evacuated from wood samples, then the chamber was connected to the gas-container with CO_2 in whose atmosphere the wood was conditioned. They were then heated in the atmosphere of CO_2 and as in the previous experiment this was followed the depressurization stage. As the pressure was decreased, the solubility of carbon dioxide in water decreased. Thus, inside the material carbon dioxide was extracted in addition to evaporation [[91]].

Table 1.1. Mass of Vapor and Liquid Collected in the Condenser in the First Drying Cycle

W_0, %	Mass collected in the condenser, m, g	Temperature rise, ΔT, °C	Vapor, m_e, g	Liquid, m_l, g
67.7	400	26	260	140
69.2	450	31	275	175
100.6	575	33	335	240

Table 1.2. Experimental Data on the Carbon Dioxide Influence in the Drying Process

D, mm	T, °C (in the sample/in the chamber)	W_f, %	τ, min	Note
80	100/120	17.7	400	with CO_2
80	100/120	22.2	440	no CO_2
70	120/160	18.1	240	with CO_2
70	120/160	17.7	300	no CO_2

Inside the material, a high pressure of the gas and vapor mixture was formed under the action of which the intense blowing-through of the whole material volume with water removal. The process was cyclic.

Table 1.2 shows the experimental comparison data on the carbon dioxide influence at drying of pine cylindrical samples of length $L = 0.4$ m.

The analysis of these data allowed making several conclusions. Under the influence of CO_2 the drying time reduced. Perhaps, as expected, this occurred possibly due to additional discharge of liquid with gas (CO_2) bubbles. At the high chamber temperature (150°C) in the sample, dried in the CO_2 atmosphere, the surface was not darkened and no cracks were formed.

This series of evaluation experiments showed the significant influence of carbon dioxide in the process of wood drying. For practical recommendations to improve the drying technology with the use of CO_2, it is reasonable to continue works in this direction.

1.3. High-Temperature Vacuum-Convective Drying of Wood

It is known that the thermal energy consumption in conventional kilns decreases with increasing drying temperature. In this case, heat consumption for timber evaporation decreases and increases for timber heating [[110]]. For periodic vacuum drying, when heat accumulated by material is used, a uniform distribution of moisture in the material can be attained [[49]].

As a drying temperature is increased, coefficients of heat and mass transfer grow. The dominant role in moisture transport is played not by diffusion (molecular) but by the macroscopic (molar) transfer mechanism. The coefficients of heat and mass transfer between steam and moist material are higher than in the case when the drying agent is air. This enables

enhancing the drying process in superheated steam. Water evaporation from wood in the superheated steam is more intense than in the air at a temperature 120^{o}C and above [[60]]. The difference increases with temperature. Above T=140^{o}C the intensity increases by a factor of 2-4. A higher temperature makes the material transit to the plastic state, thereby avoiding the formation of shrinkage defects [[3]].

The present section is concerned with investigating experimentally high-temperature vacuum drying of wood at heating due to forced convection. Due to heating and convective heat and mass transfer some amount of liquid is evaporating from the material surface up to the moment of establishing equilibrium with the ambient vapor-gas medium. When the saturation pressure is attained in the chamber the moisture evaporation ceases and the heating of the material bulk continues. When the sample center reaches a given temperature a rapid pressure relief occurs from the chamber to the evacuated vessel (receiver).

As already mentioned in Section 1.1 of this Chapter, for a rapid pressure relief from the chamber to the evacuated vessel some amount of water can be removed from wood capillaries without evaporation in the form of the smallest drops. This is implemented during thermal-mechanical drying. In this case, because of vacuum, to attain low final moisture the pressure at heating can be essentially limited, which will reduce the requirements for the mechanical strength of the drying chamber.

To decrease heat losses due to the removal of the exhaust drying agent (humid air) the recuperation system can be employed, for example according to the scheme proposed in [[78]].

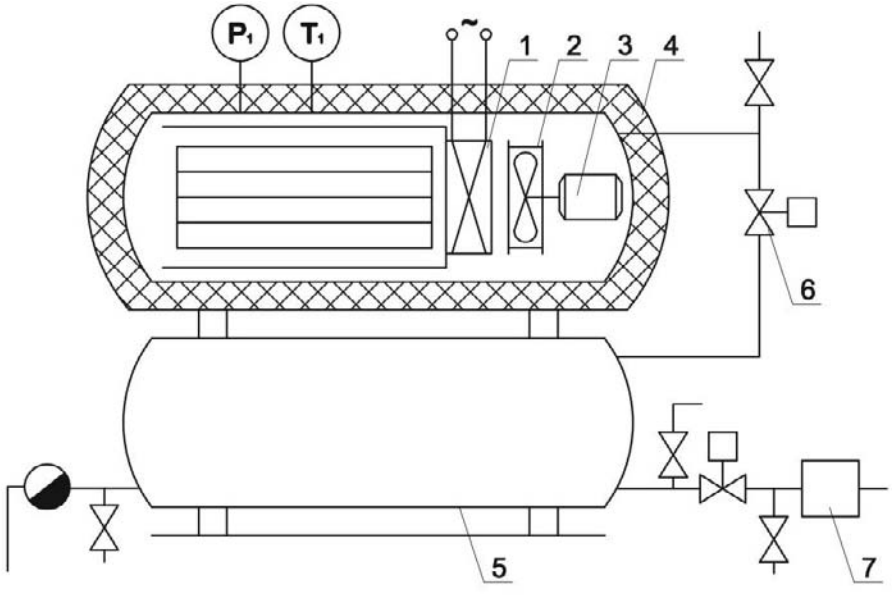

Figure 1.10. Schematic diagram of the vacuum-convective drying kiln: 1 – heater; 2 – fan; 3 - electric motor; 4 - chamber body; 5 - tank-receiver; 6 - valves; 7 - vacuum pump.

Figure 1.11. Photo of the experimental vacuum-convective drying kiln.

Vacuum-convective drying setup. To study high-temperature drying of wood an experimental vacuum drying kiln was designed, which allowed vacuum drying of a timber package in a wide temperature range. The experimental kiln is shown in Figure 1.10. It comprises the following components: a cylindrical chamber with a sealed lid, with inner diameter of 0.6 m, with length of 2.0 m; a system of heating (to 140^{o}C) incorporating a heater and a fan; a vacuum system providing a chamber pressure to 5-10 kPa. The photo of the setup is shown in Figure 1.11.

The working chamber was loaded with the packages of rounded poles. For control of specimens, temperature sensors (thermocouple) and electrodes were mounted for measuring wood MC (electric conductive method). One thermocouple was placed in the center of the wood cylinder (r = 0) at a depth of 50 mm from the surface (D =0.1 m), the second – at a depth of 0.5· r (25 mm). Similarly, the electrodes were set to control wood MC.

Samples were placed into the drying chamber and fastened on gaskets in the longitudinal direction relative to the flow of air – drying agent of the fan. The mean air blowing velocity was 2 m/s.

Drying began with timber heating to a desired temperature. The temperature was controlled by temperature sensors. The process was accompanied by increasing the chamber pressure that was recorded by a measuring system using a pressure sensor. When the sensor in the sample center showed a preset temperature, the drying process passed into the next stage – depressurization. Opening a valve connecting the chamber with a pre-evacuated receiver and within a short time (less than 30 s) sets a low pressure (vacuum) in the chamber. After wood vacuum drying during a defined time, the chamber was disconnected from the receiver and then the cycle repeated.

To determine the average MC in 6-9 hours from the beginning of the experiment the drying was stopped and the weighing was carried out (after wood cooling). These measurements of control cylindrical pine samples (L = 1.0 m, D = 0.1 m for Nos. 1-7 and D =

0.08 m for No. 8) are presented in Table 1.3. Samples Nos. 1, 3, 7 provided with the sensors were not taken from the chamber and were not weighed in the middle of the drying process.

The average duration of one cycle was not more than 90 minutes. As follows from the data, even for green wood with a high moisture content only 7-11 cycles are required to dry the timber with D = 0.1 m up to MC = 5% or less. A required time (including heating) was 15-20 h.

The comparison of drying times for samples of equal length but different diameters (0.08 and 0.1 m) showed a significant difference in the drying rate. It also demonstrates the high permeability of the specimens in the transverse direction allowing for the removal of vapor being vacuumized.

Table 1.3. Experimental Data on the Vacuum-convective Drying

No.	m_0/W_0, g/%	1-st weighing m,g/W,%	2-nd weighing m,g/W,%	3-d weighing m,g/W,%	Number of cycles
1	6800/107.3	-	3600/9.8	-	4+3=7
2	7530/66.6	5890/30.3	4950/9.5		
3	6730/92.3	-	3880/10.9	-	6+5=11
4	7430/93	4925/27.9	4200/9.1		
5	7620/82.3	5920/41.6	4570/9.3		
6	7070/89.5	5080/36.2	4230/13.4	3880/4.0	5+3+3=11
7	7640/114	-	-	3750/5.0	
8	4770/84.5	3110/20.3	2740/6.0	2630/1.7	

As expected, the drying intensity depends on the wood moisture content. These experiments confirmed that the most intense drying by depressurization occurs in the initial period when the material has the highest MC.

The experimental results presented in Figure 1.12 illustrate the drying at the chamber temperature T=120 ± 5°C. After reaching the sample center temperature T = 102-105°C, depressurization occurred. As follows from the measurement results, the pressure and the temperature change simultaneously at depressurization. Time errors between the minimum temperature values at different depths are within the measurement accuracy, which does not exceed 2 seconds. The pressure increase in the first cycle of each plot (a, b, c) is caused by air that enters the chamber during the weighing of control samples.

It should be noted that for convection to occur, after vacuum stage of the wood in the chamber it is advisable to fill up it with saturated steam. When no vapor is present in the chamber water should be injected. When heated air (T< 120°C) is supplied to the drying chamber the drying rate grows, but there is a risk for defects to form.

Figure 1.13 presents the measurement results of the moisture content of the sample after each drying cycle (measurement by MC sensors).

a

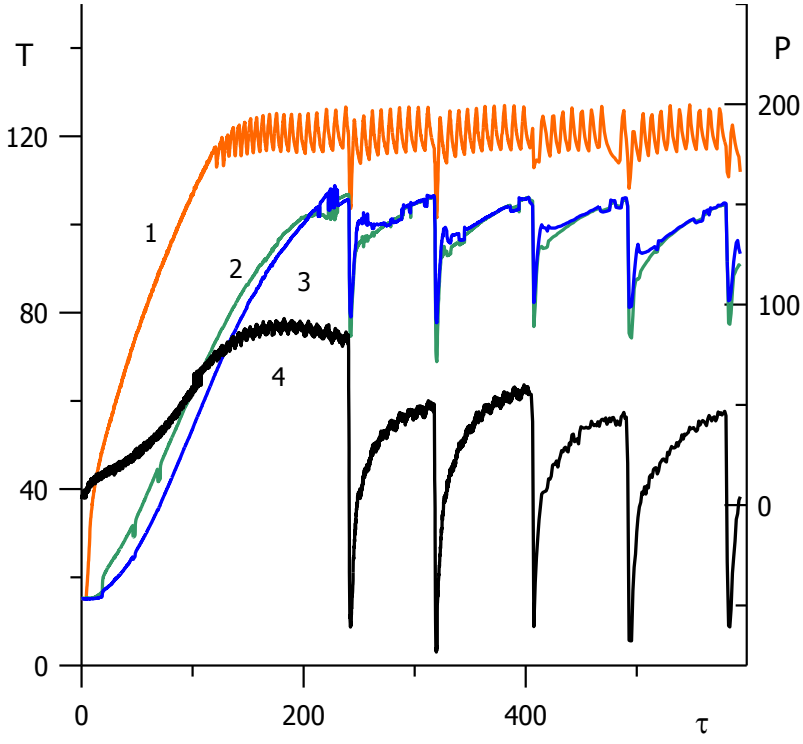

b

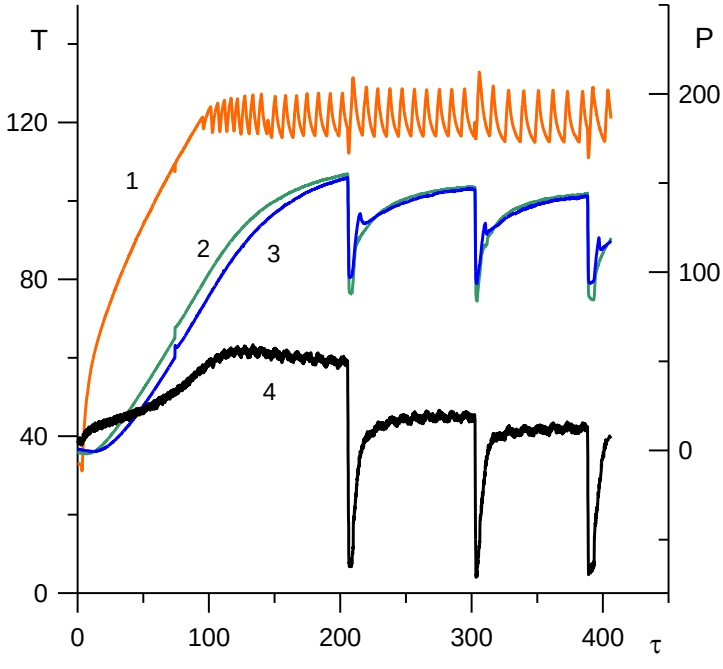

Figure 1.12. Continued on next page.

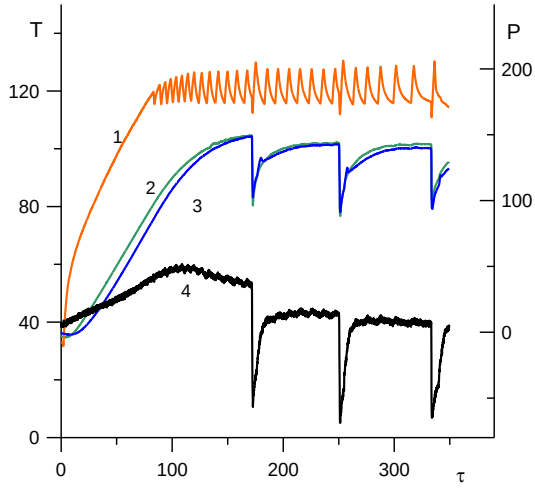

Figure 1.12. Data on the temperature and pressure in the vacuum-convective drying kiln: a - drying before the first weighing; b - second; c - third. 1 - drying agent temperature; 2 - wood temperature at a depth $r = 25$ mm; 3- in the center $r = 0$; 4 - pressure in the chamber. T, °C; P, kPa; τ, min.

It also shows the average values of a relative moisture content according to the weighting (number of points corresponds to the number of samples in Table 1.3).

During our experiment we identified the measuring features by MC sensors with metal electrodes at high temperatures. Despite the temperature corrections, the measured values had a strong scatter. This confirms the complex behavior of measurement at high MC. It is well known that the range of the moisture content that can be reliably measured is 4% to about 30% [[80], [82]].

In contrast to the traditionally used methods of measuring MC in terms electrical conductivity of quasi-stationary processes in conventional kilns, according to this drying method heat and mass transfer is substantially unsteady. In our experiments with timber heating, overestimated values of MC sensors were observed possibly due to differences in the thermophysical parameters of the electrodes and timber.

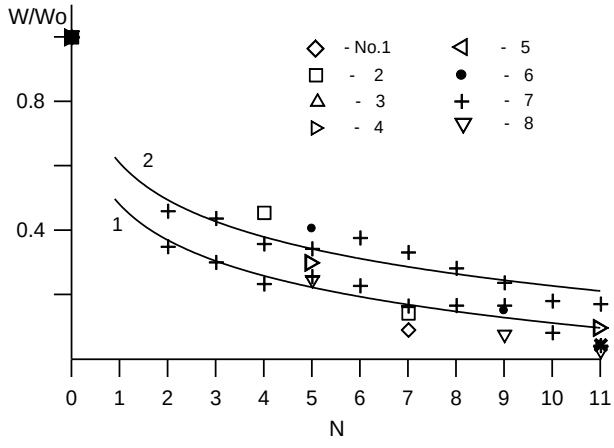

Figure 1.13 The curve of relative MC in the sample during drying; the curves - the readings of the sensors, the individual points - data of weight measurements: 1 - at a depth $r = 25$ mm; 2- $r = 0$.

Depressurization causes the vaporization in the area of the electrodes that can affect electrical conductivity of the material between the electrodes. Physical-chemical processes near the electrodes require special study.

The experimental results have revealed the high quality of the dried products and the absence of internal or external cracks. Figure 1.14 presents a photograph of dried samples. Among the disadvantages of such drying is the presence of pitch near knots at the wood surface, which is typical for high-temperature drying.

The thermal-mechanical method can be recommended for reducing a time of pre-impregnation drying of products meant for modifying impregnation. Pressure protective impregnation of wood with antiseptic in autoclaves [[10], [38], [84]] requires that the sapwood be dried to a moisture content of 20–25 %. In the method proposed, the drying time due to a pressure release to this moisture content can be reduced. So, for the wood with initial MC=62% during a drying time of 4 h the MC for the sapwood was 20-26%, in the wood core it was higher MC=35-45%. Such wood can be impregnated with aqueous solutions (e.g., antiseptic solutions). In this case, the duration of pre-impregnation drying and the drying process itself are comparable. This tells that complex modification of wood by impregnation can be arranged by performing parallel processes of drying and impregnation.

Figure 1.14. Timber samples after drying.

2. MODIFICATION OF WOOD BY IMPREGNATION

The objective in modifying wood is to change its properties and to eliminate defects of this material. This is achieved by saturating wood with substances that change wood characteristics, for example, wood begins to take on the properties of bio-and fire-resistance, water-resistance, high mechanical strength, hardness, etc. In this case, it is important that modified wood articles would not pose a threat for life and health of man and animals, including their use and utilization.

The present section deals with the impregnation of wood with liquids to modify it. A porous volume of a material is saturated due external excess pressure, capillary forces and diffusion. In some cases, liquid can enter into chemical reactions with wood substances and form new compounds.

2.1. Impregnation Methods

There are many methods of impregnation aimed at protective treatment of wood [1, [30], [38], [74] [85], [106]]. Among the most simple ones are the methods of capillary and diffusion impregnation. Wood impregnates a protective solution when contacting liquid. Before *capillary impregnation* wood must be dried and have MC≤30%. In the majority of cases, the capillary impregnation method is implemented by submerging wood into a vessel with a protective solution, by applying many times a solution on it with a brush or a roller, by spraying or washing. The rate of such a process is small. According to [[83]], the rate of capillary impregnation along fibers is 30-150 mm, across 0.2-3 mm a day. According to our data, pine wood samples had the largest absorption at MC=22-23%, in this case, the largest absorption rate is observed during the first 20-30 minutes [[5]]. Following the results [[38]], the largest depth of such impregnation is reached at MC=22-32%. To enhance absorption the method "heating-cold bath" is used, when wood after heating is being cooled in the solution, the air in pores at cooling decreases the volume and the solution is being sucked at its place [[74], [84]].

Diffusion impregnation is used for processing only raw (green) wood. This method is carried out by soaking in concentrated solutions, application of protective pastes, the use of special bandages [[30], [38]]. Usually the diffusion impregnation method takes several weeks or months.

The most common industrial method of deep impregnation of wood is the timber saturation with liquid under pressure *in sealed metal cylinders – autoclaves*. This means can be subdivided into 4 basic methods:

1) Maximum absorption method or full-cell or Bethell Process. The saturation is reached by preliminary vacuum processing of timber, its subsequent impregnation with liquid in the autoclave (cylinder) under pressure, and vacuum processing after removing the liquid from the autoclave.
2) Semi-limited absorption method or empty-cell or Lowry Process. Before impregnation, timber pores contain air under the atmospheric pressure.
3) Limited absorption method or Rueping Process. Before impregnation, there is an air overpressure in the cylinder.
4) Absorption under atmospheric pressure or VAP Method (Vacuum-Atmospheric Pressure). Wood is at first evacuated, then impregnating liquid enters the cylinder, and impregnation is accomplished at atmospheric pressure.

The possibilities of these methods of impregnation under pressure limited the need for pre-drying of wood to a moisture content MC=20-25%. If you want to impregnate wet wood, then you should apply the oscillating or cyclic impregnation methods [[74], [106]]. Wet wood can also be impregnated in centrifuges [[67], [88]].

When *a centrifugal impregnation* material is placed in a container filled with impregnating liquid that is in the centrifuge. Wood is placed so that the fibers were located along the radius of rotation. In the field of centrifugal forces the fluid pressure grows and varies along the rotation radius. Due to the heterogeneity of these forces, water in timber is replaced by impregnating liquid if its density is different from that of water.

It should be noted that the saturation of dry wood with liquids causes its swelling. Moreover, this is found not only for aqueous solutions, but also for other liquids. A magnitude of swelling is directly dependent on the liquid dielectric constant. Liquid such as kerosene almost does not cause wood swelling and its dielectric constant is 40 times smaller than that of water [[101]]. Because of the swelling one should follow the rule that after impregnation the wood should be dried before subsequent processing.

During the recent years one can observe the development of a number of other methods.

The widespread method of impregnation using *supercritical carbon dioxide* (SC-CO_2) is described elsewhere in [[2], [17], [44], [62], [72], [86], [109]]. This treatment of wood is based on the use of environmentally friendly supercritical carbon dioxide technology. Supercritical CO_2 is a carrier of an antiseptic (fungicide) in timber. Supercritical liquid treatment offers superior penetration. This allows impregnating wood that normally cannot be impregnated. After impregnation CO_2 leaves the wood that is protected by fungicide. Superior penetration adds the durability and workability to wood products. Currently, this supercritical wood treatment method has found commercial use [[31]].

The wood treatment with *vapor-boron* [[7], [99]] and the treated materials proved to be resistant to the decay of fungi and termites. No difference in the effectiveness between the vapor-boron and liquid boron treatments of wood was noted.

In [[69], [95]], the *electro-kinetic method* of impregnation was described, when the fluid motion caused by an electrical potential between the electrodes attached the wood.

Selection of Impregnating Liquid

As impregnating liquids you can use any liquid compositions: aqueous solutions, oils, melts, polymers, etc. The choice of the liquid determines the desired properties of the obtained material.

Most of the wood subjected to protective treatment is impregnated with *preservatives that* extend their use 5-10 times, as compared with non-impregnated wood. This applies mainly to products that are outside and in contact with soil or water. Only for these purposes hundreds of different products are now used: water-soluble antiseptics based on metal salts (fluoride, boron, copper, chromium, etc.), antiseptic oil (creosote, pentachlorophenol, etc.) and complex preparations. Many research works [[18], [22], [29], [30], [38], [43], [57], [74], [85], [108], [109]] are concerned with the selection of protective compositions. An important task of selecting impregnating composition and processing technology is to ensure environmental safety [[55]].

Impregnation of *polymeric structures* allows obtaining materials with new properties: increased water resistance, dimensional stability, strength, hardness, resistance to external influences. Using different compositions and the subsequent post-processing, it is possible to get materials with desired properties, for example, self-lubricating materials [[9]], wood-plastic [[29], [30], [53], [92], [93]]. After impregnation with polymers the heat or radiation treatment usual is used to produce wood-plastic. The introduction of a *dye* into the material bulk can get any color, and imitate valuable species of wood [[42]]. In the presence of liquid, particulates with the size of 1 μm or less may penetrate deeply into wood. Very promising is the introduction of protective compositions containing *nanoparticles* that can penetrate into the cell wall [[52]].

Saturation of timber with different liquids permits modifying combustion characteristics of the material produced. So, it is possible to convert a traditionally combustible material such

as dry timber into a flame-resistant and even incombustible material by impregnation with salts of phosphorus, boron, ammonium, etc. [[4], [7], [23], [40], [57]]. Because of deep wood *impregnation with a fire retardant*, the timber processed can be classified as a nonflammable material.

An opposite example of change of the timber properties due to impregnation is an increase of combustible properties. The saturation of a porous body *with a flammable liquid,* e.g., hydrocarbons, can substantially increase the calorific value of the material. For example, after impregnation with molten paraffin or wax, the volumetric calorific value increases by a factor of 3 to 4 as compared to customary firewood.

By impregnating timber *with salts of alkali metals* and then subjecting it to heat treatment in the absence of oxygen (pyrolysis) it is possible to obtain charcoal with improved fire capabilities [[40], [41]]. The comparison of charcoal obtained with and without catalyst demonstrates that in the presence of the catalyst the lower ignition point decreases from 505^{o}C to 360^{o}C. Besides, owing to the catalysis, the charcoal obtained even from pine is strong and solid. The output of charcoal with the use of catalysts will be increased by 15-50 %.

The impregnation of wood waste with *phenolic resin* and its subsequent thermolysis in vacuum allows producing wood ceramics with a wide spectrum of unique properties [[31], [94]]. Wood ceramics is a new porous carbon material that is being produced by carbonizing the wood or wood materials impregnated with phenolic resin in a vacuum furnace. During the carbonizing process in the temperature range between 573 and 2273 K, the phenolic resin is converted into glassy carbon. As wood ceramics has superior mechanical and wear properties, electric and electromagnetic shielding properties, it can find wide use in industry.

One of the main ways to preserve valuable artifacts is their impregnation. The conservation of waterlogged wood involves the introduction of material into wood which will provide mechanical strength to the wood at water removal [[16], [107], [109]]. One of these materials is *polyethylene glycol*. Often wax impregnation and sucrose (sugar) treatment are used.

One of the well-studied methods of wood modification is its *acetylating* with acetic anhydride [[29]]. The acetylated wood has a number of useful properties, including the durability, non-toxicity, resistance to UV radiation, etc. [[1]]. The ability of wood to absorb water greatly reduces, rendering stable dimensions of the wood products. The acetylated wood in small quantities is being produced in the Netherlands and Sweden.

Furfurylation has found no less development [[29], [87]]. It is the process of wood modification using furfuryl alcohol obtained from renewable resources, including vegetable residuals [[98]]. Furfuryl alcohol can penetrate into the cell wall where it undergoes polymerization. Wood furfurylation provides a high protection level against bio-degradation (fungi, bacteria and marine borers). The wood stable dimensions and hardness can be improved. Acetylation and furfurylation are the most effective modification methods for achieving wood stable dimensions and low equilibrium moisture content [[25], [39]]. The furfurylation of wood products is industrially applied in Norway [[98]].

2.2. Modelling and Experiment on the Liquid Solution Impregnation of Wood

While analyzing the quality of modifying impregnation of wood, besides the absorption of liquid by material, when it is being saturated under pressure, of no less importance is the uniformity of the distribution of an impregnating composition within the bulk of the material.

The fragment of the pine wood cross-section is shown in Figure 2.1. Tracheids are the main water transport channels in wood. The tracheid length is 2-4 mm, the transverse dimensions of tracheids are 40x40 μm for springwood and 40x20 μm for summerwood [[105]].

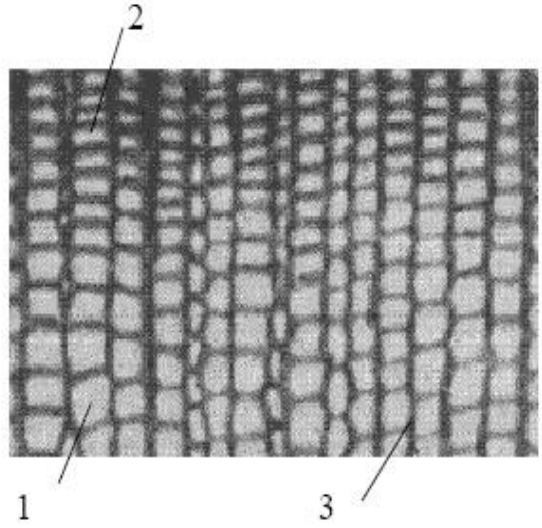

Figure 2.1. Fragment of the cross section of pine wood: 1 - springwood; 2 - summerwood, 3 - cell wall.

Tracheids are connected by numerous micropores (bordered pores) about 1 μm in size. The cell wall also has a capillary structure. A comprehensive description of dynamics of the impregnating liquid motion in wood under pressure gradient and so the calculation of determining parameters of impregnation technology present difficulties. They are first associated with the complexity of the wood internal structure and also with the choice of an adequate physical-mathematical model.

Proceeding from the general type of the wood structure as the capillary-porous one, two main types of motion of impregnating liquid can be marked out: porous and capillary. A free volume of the wood is mainly filled up through the porous structure of wood (tracheids and micropores connecting them), the cell wall (at MC less than 30%) is being saturated through microcapillaries.

Figure 2.2 illustrates the samples of birch and pine wood impregnated with dyed polymer. Impregnation was performed in half-finished products, from which these shapes were fashioned. For pine the sapwood, which is completely impregnated, and the core part, which is partially impregnated, are clearly seen.

Figure 2.2. Samples of products carved of impregnated birch (left) wood and pine (right) wood.

Having investigated the liquid impregnation depth in the timber and having treated it as a system of parallel capillaries, P. Sergovsky [[85]] proposed a formula for impregnation:

$$x = r\sqrt{\Delta P \tau / \mu},$$

where x is the impregnation depth; r is the timber capillary radius; ΔP is the differential pressure; τ is the impregnation time; μ is the viscosity of impregnating liquid.

However this formula and the proposed physical model are very approximate, do not allow for the influence of liquid and gas phases in the bulk of the wood, and are capable of describing the one-dimensional impregnation of only hardwood with long water-supplying vessels. For softwood, such a calculation model yields essential disagreement with the experimental results.

In the course of execution of the present work, the macroscopic physical-mathematical model for wood impregnation[3] [[10], [11], [12]], which allows for the motion of liquid and gas phase and the specific features of the wood structure, was proposed. This model enables calculating the kinetics of saturation of the wood with different liquids.

The model is based on the following assumption. Schematically, the softwood structure can be presented as a system of tracheids connected via micropores (Figure 2.3). Accordingly, the liquid motion in the wood involves the liquid flow along tracheids and the liquid and air

[3] Theoretical studies were carried out jointly with M. Brich.

overflow through pores connecting the adjacent tracheids. Some amount of air can remain in the tracheid and be compressed under the action of external pressure. The model enabled one to allow for the presence of the core and the sapwood as well as additional resistance in the liquid motion within the material due to the presence of meniscuses ("Jamin's beads") [[65]]. Taking into account the fact that the permeability of different wood sections can differ (e.g., the core and sapwood), the model permits calculating the liquid motion with regard to the permeability of each layer (two-layer model). The results allowed the numerical study of the saturation processes for wood samples of various length and shape, including the modeling of impregnation of large-scale objects (poles, cross ties, etc.) [[10]].

The impregnation depth and liquid absorption by timber depend on a number of factors: pressure of an impregnating solution, impregnation time, size and structure of timber, its physical-chemical properties, moisture content, characteristics of used solutions, impregnation method, etc.

These works were mainly aimed at developing procedures to enhance impregnation and attainment of maximum absorption of liquids by timber. The objective of the present work is to study a possibility of obtaining a predetermined distribution of liquid concentration within a porous body.

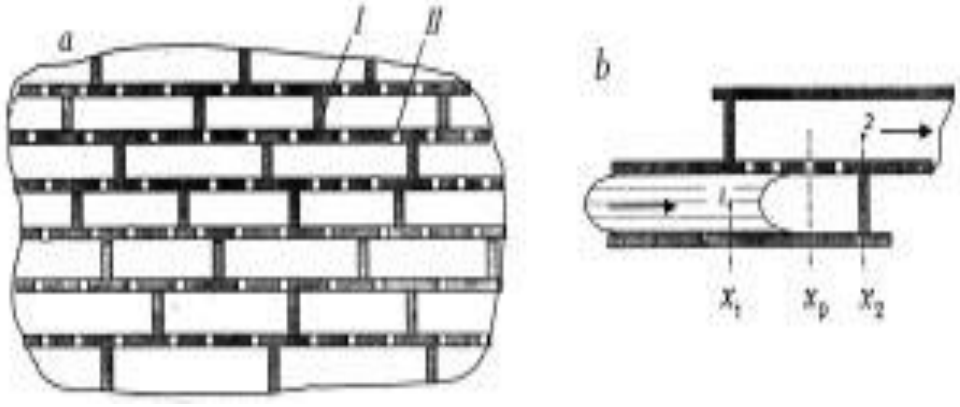

Figure 2.3. Schematic of softwood structure: a) I - cell walls, II - micropores; b) x1, x2, xp - the coordinates of the ends of tracheids and a pore, respectively. With kind permission from Springer Science+Business Media: <Journal of Engineering Physics and Thermophysics, Kinetics of the wood impregnation process. Modeling and experiment, vol. 72, 1999, p. 591, M.A. Brich, V.P. Kozhin, V.K. Shchitnikov, Figure 1.

Obviously, maximum saturation of a porous material can be achieved using the full-cell (Bethell) process. After timber impregnation it became possible to remove some part of free liquid. This occurs when the air pressure is relaxed after the removal of liquid pressure (Lowry and Ruiping processes). In certain limits, this allows one to control the saturation of a porous volume and the distribution of the liquid amount in the impregnation zone.

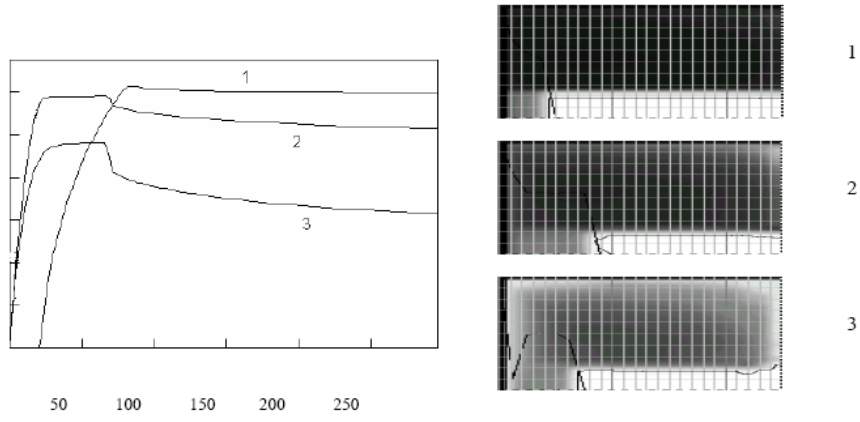

Figure 2.4.Comparison of the impregnation kinetics and concentration fields of a liquid in the cylindrical pine sample: 1 - full-cell process (Bethell); 2 - empty-cell process (Lowry); 3 - limited absorption (Ruiping method). m, kg; τ, min.

Figure 2.4 compares the calculation data on impregnation kinetics and the plot of the concentration distribution in a longitudinal section of a pine cylindrical sample obtained by different impregnation methods. A specimen is 0.5 m long is 0.2 m in dia. A maximum liquid pressure is 1.7 MPa, an exposure time of wood at this pressure is 1 hour, the time of after-impregnation vacuum processing is 15 min, and the vacuum is 20 kPa. The time shift of curve 1 relative to other saturation curves reflects the period of the previous vacuum processing of the sample. The completely colored zone belongs to sapwood and the partially colored one – to the wood core.

Figure 2.4 shows the fragments of wood samples (1/4 part of a longitudinal cut), the butt-end being on the left. Sample No. 3 was treated at an initial air overpressure P_0=0.4 MPa and the impregnating liquid pressure was 1.7 MPa. The bulk of the wood treated by this method was not less than that attained using the maximum absorption method. The increase of the initial air pressure permits a further decrease in the liquid amount in the timber without reducing the treated zone of the material.

The possibility of varying the liquid distribution throughout the timber and changing the liquid concentration in pores allows producing finished products with planned properties.

2.2.1. Experimental Setup and Study of Wood Impregnation

The choice or development of an impregnation technique and procedure and the choice of an impregnating solution must involve their testing in laboratory conditions. For this purpose, we designed and manufactured a laboratory setup providing wide possibilities for investigation of impregnation technology. A schematic diagram of the setup is shown in Figure 2.5. An inner diameter of an impregnation cylinder was 127 mm; its total capacity was 2 liters. In experiment, the amount of impregnating liquid absorbed by a sample (kinetics of the process) can be controlled both by the weight method and by a level gauge of the cylinder. Consider the operational principles of the setup for different methods of pressure impregnation of wood.

Impregnation by empty-cell Method (Lowry process). Prior to impregnation the air in wood is at atmospheric pressure (it can also be at a higher pressure); then a pressure of the

impregnating fluid is created. The wood sample is placed into impregnation cylinder 3, the cover of which is hermetically sealed. Valve 2 is opened thus connecting the pressure vessel with the impregnation tank. Simultaneously, time is recorded and the amount of the fluid absorbed by the sample is periodically measured[4].

The system for measuring the amount of the impregnating fluid and air released (returned) by the sample after pressure relief in the impregnation tank consists of two glass cylinders 6 and 7, one of which is vented to the atmosphere while the second cylinder is sealed with a rubber plug with two (inlet and outlet) pipes.

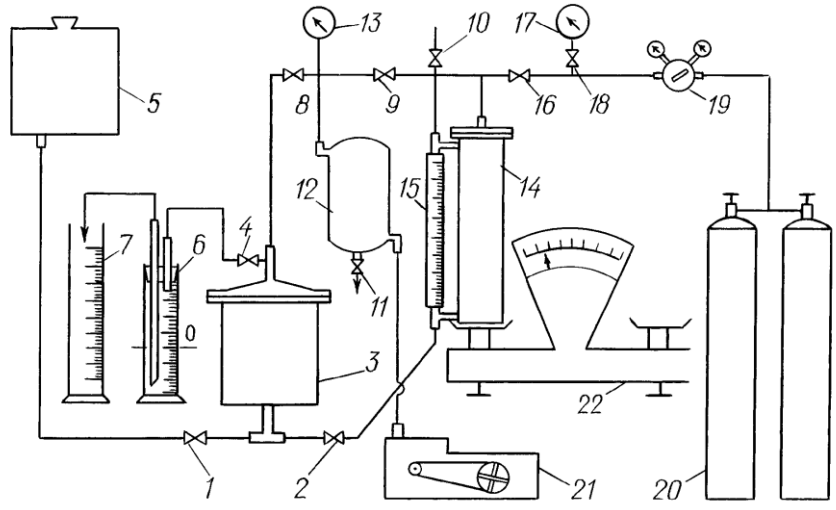

Figure 2.5. Schematic of the impregnation test setup: 1 - filling valve; 2 - connecting valve; 3 - impregnation tank; 4 - valve connecting the impregnation tank with the measuring unit; 5 - filling vessel; 6, 7 - air and fluid measuring cylinders, respectively; 8, 9 - vacuum valves; 10- valve of pressure relief in the system; 11 - atmospheric valve; 12 - vacuum receiver; 13 - vacuum gauge; 14 - pressure vessel; 15 - level gauge; 16 - pressure valve; 17 - manometer; 18 - manometer valve; 19 - pressure regulator; 20 - gas cylinders; 21 - vacuum pump; 22 - balance. With kind permission from Springer Science+Business Media: <Journal of Engineering Physics and Thermophysics, Kinetics of the wood impregnation process. Modeling and experiment, vol. 72, 1999, p. 595, M.A. Brich, V.P. Kozhin, V.K. Shchitnikov, Figure 3.>

When the fluid and the gas arrive in hermetically sealed cylinder 6, the internal pressure in the latter changes and squeezes out an equivalent volume of the fluid to cylinder 7, thus restoring the equilibrium state in cylinder 7, in which the amount of air increases and the fluid level lowers correspondingly to the volume of the air introduced.

The experimental data in Figure 2.6 (a) demonstrate the high intensity of pressure impregnation reached over small times. With pressure relief an insignificant amount of air is released. According to the measurement data for various dry wood samples for the first hour of relaxation after pressure relief 40 to 70% of the fluid absorbed by the sample is removed. The fluid remaining in the sample is retained in the porous wood skeleton by capillary forces and is due to moisture sorption by the cell walls. The preliminary experiments have shown that due to capillary impregnation the amount of fluid absorbed by the samples immersed in

[4] Experimental work carried out jointly with V.K. Schitnikov.

the liquid is from 2 to 12% of the initial mass of the sample for a period equal to the experiment time.

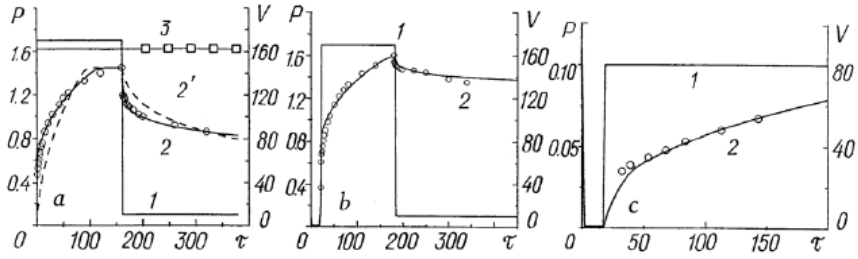

Figure 2.6. Comparison of the calculated curves and experimental data for different impregnation methods (pinewood 150 x 60 x 30 mm): a) empty-cell process (Lowry); b) full-cell process (Bethell); c) vacuum-atmospheric pressure (the VAP method): 1 - pressure of the impregnating liquid; 2 - volume of the liquid absorbed by the wood (the two-layer model); 2' - the same for the one-layer model; 3 - air volume in the wood. *P*, MPa; *V*, cm^3; τ, min. With kind permission from Springer Science+Business Media: <Journal of Engineering Physics and Thermophysics, Kinetics of the wood impregnation process. Modeling and experiment, vol. 72, 1999, p. 596, M.A. Brich, V.P. Kozhin, V.K. Shchitnikov, Figure 4.>

For the reference samples no more than 10-15 cm^3 was absorbed in this experiment owing to capillary impregnation under wood steeping conditions.

It should be noted that the property of the liquid that leaves the wood at discharge pressure can be used for extracting valuable substances from the bulk of the porous material.

Impregnation by the Maximum Absorption Method (full-cell or Bethell process). The process begins with preliminary evacuation of wood before its pressure impregnation. The vessel 3 is evacuated for 10-15 min to attain a vacuum of about 1.5-2.0 kPa. The next stages are repeated as in the previous case.

The preliminary evacuation affects the content of liquid in the wood after impregnation. A small residual amount of air in the pores after evacuation is responsible for the small amount of fluid released from the sample after pressure relief. As is seen from Figure 2.6 (b), preliminary evacuation allows an almost twofold increase of absorption of the impregnating fluid by the sample.

Impregnation by the "Vacuum-Atmospheric Pressure (VAP)" method. Wood is at first evacuated, then the impregnating fluid enters the cylinder, and impregnation is accomplished at atmospheric pressure of liquid. Experimental data for this impregnation technique are provided in Figure 2.6 (c). This method can be efficient for practical applications when penetration of an impregnating solution to great depths is not needed.

Early [[5]] it was shown that under the long action of liquid pressure even moist samples are capable of absorbing aqueous solutions. This is attributed to the fact that the wet wood always has pores filled up with air. The dependence of the free water amount on the wood initial moisture content is linear in character and is detailed in Ugolev's monograph [[101]]. The experimental laboratory data in Figure 2.7 [[5]] for the pine sapwood over the initial moisture content range 5 - 80% showed that every 1% of the initial moisture content of wood reduces its ability to absorb liquid also by 1%. These data can be governed by the following linear empirical relation:

$m_{liq}/m_{dry} = 2.18 - 0.13\ W$,

where m_{liq}, m_{dry} are the mass of absorbed liquid after impregnation of 1 m^3 of material and the mass of absolutely dry wood (for pine m_{dry} = 430 kg/m^3), respectively, and W is the initial moisture content (MC), %.

Table 2.1 gives generalized data on impregnation aimed at achieving the maximum saturation of dry pine wood with a core of 30-50% by different methods at a fluid pressure of 1.6 MPa for 160 min including evaluation for 15 min at an air pressure of 1.5 kPa. For the internal pressure of air to relax, the samples were held after impregnation for no less than two days under conditions preventing their drying. In practice, to speed up the process of internal pressure relaxation and, correspondingly, to decrease the impregnating fluid loss timbers are usually exposed to post impregnation evacuation [[5]]. The table illustrates the capabilities of each of the impregnation methods and allows the choice of the method expected to be most efficient for particular tasks.

Figure 2.8 presents the impregnation of a railway tie consisting of sapwood (20%) and a core (80%) by the full-cell (Bethell) method. Here, the measurement results obtained for industrial antiseptic impregnation of pine ties by an aqueous protective solution are presented. The data obtained in Tie-Impregnation Plant. The total amount of wood in the impregnation cylinder was about 21 m^3 (210 ties). Figure 2.8 gives experimental values of the fluid flow absorbed by the wood, obtained by measurements by a flow meter, recalculated per one tie. Solution absorption by a tie after impregnation was determined by control weighing of an arbitrarily chosen 12 ties followed by averaging the increase in weight. In terms of the volume indices this value was 18.2 ± 4.5 liters, which agrees well with the calculated results [[5], [10]].

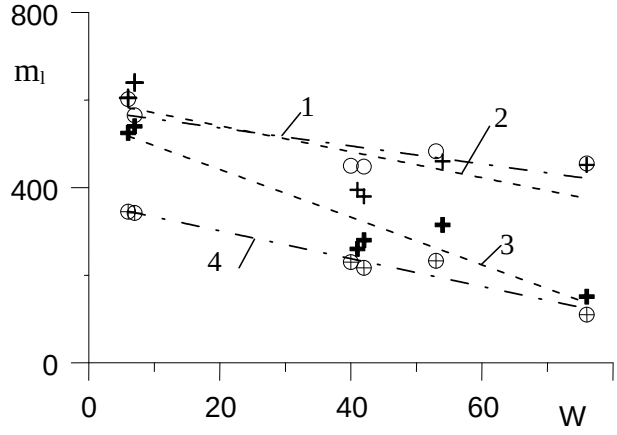

Figure 2.7. Mass of liquid absorbed by pine wood, depending on the initial moisture content: 1, 4 - impregnated by Lowry method; 2,3 - impregnated by Bethell method: 1, 2 - absorption of liquid in the process of wood impregnation; 3, 4 - a residual amount of fluid in the timber after the relaxation of internal pressure. m_l, kg/m^3; W,%.

Table 2.1. Comparison of the Absorption Volumes of the Impregnating Liquid for Different Impregnation Methods

Impregnation method	Absorption V, liter/m^3	Liquid discharge with pressure relaxation V, liter/m^3 (%)	Liquid retention V, liter/m^3 (%)
Lowry(limited absorption)	580	238 (41)	342 (59)
Bethell (maximum absorption)	645	120 (19)	525 (81)
VAP (vacuum-atmospheric pressure)	258	-	258 (100)

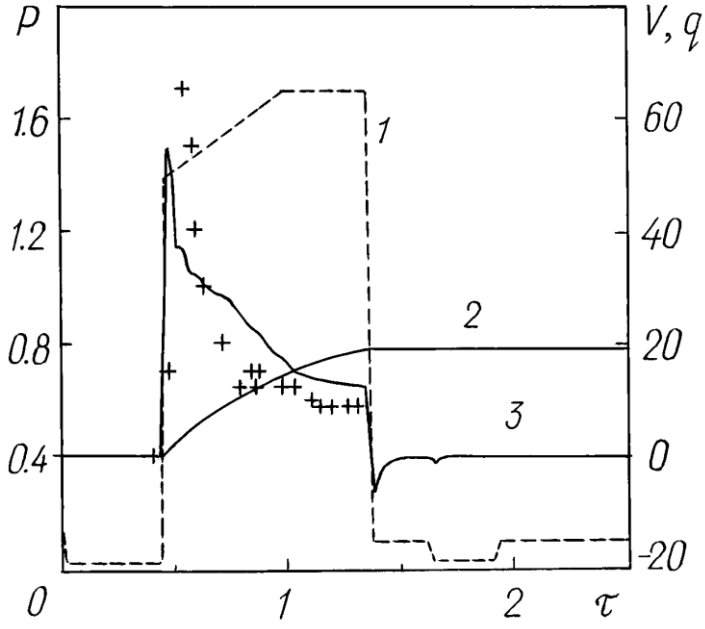

Figure 2.8. Impregnation process of the wooden tie and comparison of the calculated results and experimental data (pinewood, 2800 x 240 x 160 mm): 1 - pressure of the impregnating liquid; 2 - volume of the solution absorbed by the tie; 3 - flow rate of the liquid absorbed by the tie (curves are the calculation, the points are the experiment). V, liter; q, liter/h; τ, h. With kind permission from Springer Science+Business Media: <Journal of Engineering Physics and Thermophysics, Kinetics of the wood impregnation process. Modeling and experiment, vol. 72, 1999, p. 597, M.A. Brich, V.P. Kozhin, V.K. Shchitnikov, Figure 5.

2.2.2. Water Polymer Emulsion Impregnation

Impregnating compounds containing solid or liquid particles (suspensions, emulsions) are of undoubted interest for impregnation practice. One of the examples is represented by dyes with small particles of colors (pigments).

When wood products are being impregnated with protective solutions of water soluble salts to reduce the washing out of the solution is added with non-soluble polymer additives – synthetic resins, oils and other heavy fractions of petroleum refining. In this case, the protective composition is prepared in the form of water oil or water polymer emulsions. After impregnation and drying, water-resistant films are formed at the wood surface and within its volume, which essentially reduced the washing out of protective components. Particle sizes of the emulsion depend on its type, a manner of preparation and are 0.5 – 20 μm. Depending on this, the particles can be filtrated in the porous structure and can be kept in a thin layer or can penetrate at different depth. Consider in detail the process of impregnation with a water-emulsion bio-protective preparation containing bitumen particles.

In experiment it was found that the penetration of bitumen particles at impregnation was observed only in the wood surface layer (1-4 mm) [[6]]. At the same time a deeper penetration of a carrying protective solution into the wood volume was also seen. A bitumen layer to be formed near the wood surface protects a product from washing out because of atmospheric precipitates. Yet, the experiments as a whole have revealed the deterioration of wood impregnation in the presence of bitumen and other polymer particles. This can be explained by the deterioration of the material permeability.

The results on the impregnation of large-size products made of pine wood (2800x240x160mm ties) are plotted in Figure 2.9 [[11]]. The maximum liquid pressure was 1.8 MPa, the vacuum depth was 20 κPa. The curves illustrate a strong dependence of emulsion absorption by wood on the concentration of polymer particles in the protective preparation. The measurements of the weight increment of ties, being impregnated with bitumen emulsion, when a mean size of bitumen particles was about 10 μm, showed the adequacy of the results presented. These data illustrate the small absorption of a protective compound by wood at high concentrations of polymer particles in emulsion. Therefore, to provide a required degree of biological protection of products (ties, poles, etc.) it is recommended to increase the concentration of protective components in solution as follows. As the particle size is decreased, the concentration dependence will diminish. In the case of the particle size less than 1 μm, it should be expected that the size influence on the antiseptic absorption and distribution in the material will be inconsiderable.

For the coarse particles presented by the results in Figure 2.9, the absorption increase can be attained by the two-stage processing of wood material. At the first impregnation stage the wood absorbs a protective solution without polymer particles. At the next stage the water polymer emulsion is absorbed. The comparison with the one- stage impregnation data points to an essential increase in the absorption of the protective preparation under separate processing of wood large-sized products by two compositions [[11]].

2.2.3. Variable Pressure Impregnation of Wood

To reduce a process time and to improve a processing quality of material many attempts were made to exclude pre-impregnation drying or to suppress the influence of the initial moisture content of material on the quality of its protective treatment.

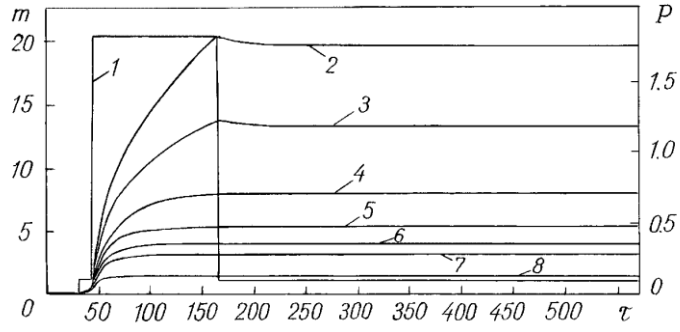

Figure 2.9. Kinetics of impregnation of railway ties with protective compositions containing polymer additives: 1 - pressure of the impregnating fluid; 2 - polymer particles are absent from the solution; 3 - polymer 2%; 4 - 4; 5 - 6; 6 - 8; 7 - 10; 8 – 20. *m*, kg; *P*, MPa; *τ*, min. With kind permission from Springer Science+Business Media: <Journal of Engineering Physics and Thermophysics, Modeling of impregnation of wood with protective solutions and emulsions, vol. 74, 2001, p. 109, M.A. Brich, V.P. Kozhin, Figure 3.

At autoclave impregnation one seeks to solve this problem by superimposing additional technological effects such as subsequent repeated alternation of vacuum and pressure actions, superposition of vibrations, ultrasound, etc. The oscillating pressure method is used, following which cyclic changes in vacuum and pressure are made [[27], [74], [106]]. Lowry modified method with changing pressure applied for processing green or non-dried wood in natural conditions also finds use. However there is no agreement on the effectiveness of the variable pressure action upon the solution absorption at impregnation [[43], [71]]. Our investigations of the cyclic impregnation of dry wood (MC=11-12%) did not reveal the effect of enhancement of the impregnation process [[5]] the present section contains the experimental results on the influence of liquid variable pressure on impregnation of pine wood samples with elevated moisture content.

The schematic of the test bench is shown in Figure 2.10. The test bench comprised an impregnation cylinder 200 litres in volume and 3 m long, a vertical graduated cylinder, a vacuum system (down to 10 кPa), and a system for providing impregnating liquid pressure (up to 1.8 MPa). The impregnation vessel was charged with pine poles 2.5 m long and 60-140 mm in dia with different initial moisture content (W=15-91%).

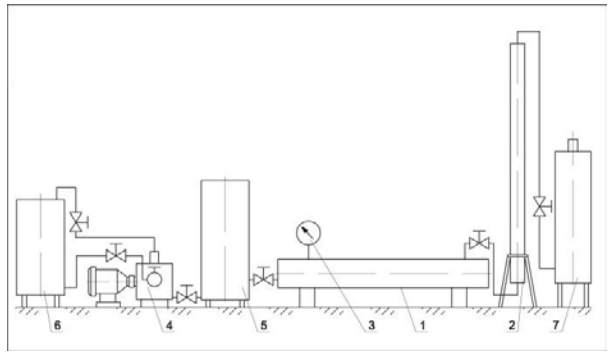

Figure 2.10. Test bench: 1 - impregnation cylinder, 2- graduated cylinder, 3 - pressure-gauger; 4 - vacuum pump; 5 – vacuum receiver; 6 – cooler of vacuum pump; 7 – tank with impregnating liquid.

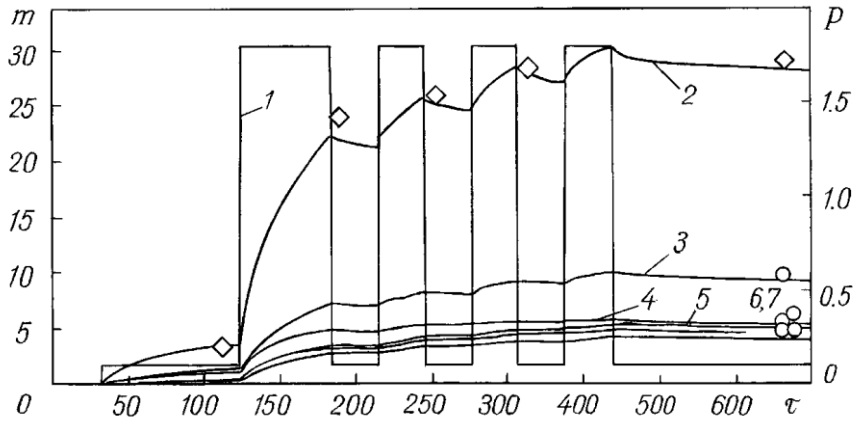

Figure 2.11. Impregnation kinetics for 2.5-m-long pine poles: 1 - pressure of the impregnating liquid; 2 - overall absorption of the liquid by the samples; 3 - absorption by an individual sample with D = 120 mm and W = 32%; 4 - 120 and 63; 5, 6 - 100 mm, 56 and 79; 7 - 80 and 59. m, kg; P, MPa; τ, min. With kind permission from Springer Science+Business Media: <Journal of Engineering Physics and Thermophysics, Modeling of impregnation of wood with protective solutions and emulsions, vol. 74, 2001, p. 107, M.A. Brich, V.P. Kozhin, Figure 1.>

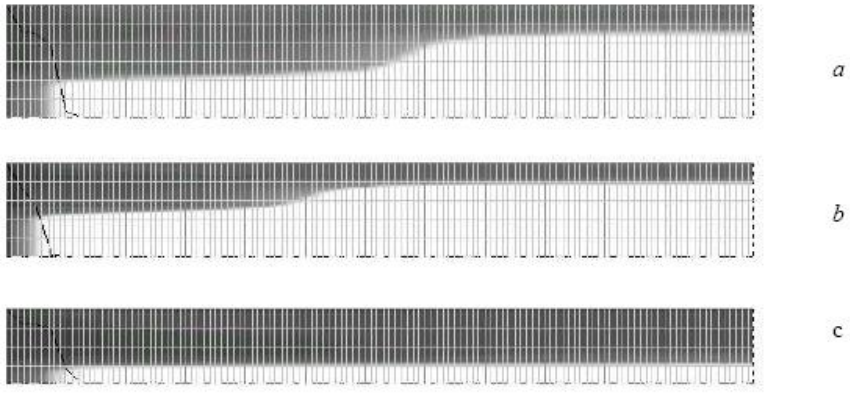

Figure 2.12. Distribution of the impregnating solution in the central longitudinal cross section of the poles: a - D = 120 mm, b - 100, c - 80. With kind permission from Springer Science+Business Media: <Journal of Engineering Physics and Thermophysics, Modeling of impregnation of wood with protective solutions and emulsions, vol. 74, 2001, p. 108, M.A. Brich, V.P. Kozhin, Figure 2.>

The liquid level was measured in the graduated cylinder after each cycle, each sample was weighed after impregnation and also the liquid distribution inside the poles was determined. The character of the liquid distribution was determined from the longitudinal sowing of poles over the diameter cross-section. Sizes of core and sapwood of poles were found using a chemical indicator.

Figure 2.11 shows the results of measuring saturation kinetics of cylindrical samples (poles with different MC) at aqueous antiseptic solution impregnation (ρ=1027 kg/m3, T = 9oC) [[47]]. As seen from the figure, the pressure during impregnation varied and was cyclic in character (curve 1). The absorbed liquid mass at impregnation was measured by controlling the level in the graduated cylinder. The vacuum depth was 10 κPa, the maximum pressure of

an impregnating solution – 1.8 MPa. As Figure 2.11 illustrates, the comparison of the experimental data with the calculation of impregnation kinetics shows a satisfactory result for practice [[11]].

The proposed low-frequency cyclic impregnation method, according to which impregnation occurs due to low-frequency pressure pulsations, was used to enhance absorption of an impregnating solution for wet wood products, when standard (one-cycle) means do not provide sufficient impregnation. The absorption enhancement at a periodic pressure change can be expected because of the reduction of the effect found by Huber and Verts [[67]]. Here the wood permeability changes when influenced by the pressure gradient due to the shift of toruses in pit membrane and by the closure of micropores connecting the water-supply path (tracheids)).

Besides a required volume of absorption of a protective solution, of no less importance is its uniform distribution over the wood bulk. In this case, the through (complete) impregnation on the sapwood is needed to attain a high degree of wood protection. Figure 2.12 presents the examples of the solution concentration distribution for the fragments of different-diameter poles (1/4 of the central longitudinal cross-section of products) that correspond to curves 4, 6, 7 in Figure 2.11. The measurements of the solution distribution in samples after longitudinal sowing showed that according to this processing method, at the initial moisture content to 48% the sapwood completely colors (Figure 2.12 c), thereby pointing to through impregnation. At the higher initial moisture content, within the chosen regimes the impregnation of sapwood is not complete (Figure 2.12 a, b).

The experiments with pine poles over a wide range of initial moisture contents of wood allowed an important conclusion to be made for practice: according to this impregnation method, when the number of cycles of the pressure action is varied from 4 to 8, high absorption of the solution is provided for wet wood (with the initial moisture content up to 90%). The oscillation methods used in practice provide more than 100 cycles [[22]], which obviously increases the depth and impregnation uniformity.

For all the wet cylindrical wood samples investigated, the impregnating solution was distributed over a greater part of the sapwood (no less than 60% of the cut area of the longitudinal cross-section and 67% of the wood). Thus, for wet pine wood it is possible to provide absorption (weight increment) according to the standard requirements on bio-and fire-protected wood. However complete dyeing (through impregnation of sapwood) at the initial moisture content of more than 45-50% was not a success in practice. Not to limit the practical application of wood impregnated by the above-described method in the medium favorable for bio-destroyers to develop, it is recommended to apply solutions of higher concentration. Due to diffusion a further penetration of antiseptic will penetrate in wet wood.

Under the industrial conditions, similar measurements made on large lots of wood products (ties) impregnated with water antiseptic revealed the noticeable effect of absorption enhancement when the pressure was varied during a number of cycles from 5 to 10 [[5]]. Also, it should be noted that the effectiveness of the cyclic process enhanced at impregnation of wet and hardly impregnated wood and the process parameters (number of cycles and duration of cyclic impregnation stages) depend on the moisture content and structure of wood, its size, pressure gradient and many other factors.

2.2.4. Impregnation with Oils and Other Liquids whose Viscosity Depends on Temperature

Impregnation of the porous material, hot melt (wax, metal), viscous oils and other high-molecular substances include pre-heating of the impregnation fluid. Traditional technology protective impregnation of wood (poles, railway ties) with oil preservatives [[38], [63]] requires heating creosote or other oily antiseptic to the temperature at which its viscosity is reduced to a value that allows to penetrate well into the wood.

Traditionally used creosote (coal or shale oil) in the technology of impregnation of crossties, poles, and others require the heating oil to a temperature of 85 – 100°C. A significant shortcoming of this technology is a high level of emissions of harmful substances into the atmosphere (phenol, anthracene, etc.). Reducing the temperature of containing creosote impregnating liquid, to 40°C we can reduce the level of harmful emissions in a few times. Promising is the use of water-oil emulsion on the basis of creosote and water.

In the last few years, in Australia and in a number of European countries ecologically safer water-oil emulsions based on the PEC (Pigment Emulsion Creosote)-type creosote have been used for such purposes. These emulsions contain a high-temperature creosote - up to 65%, oxide pigments - up to 5%, water, and other components [[18], [108]]. Such compositions permit impregnation at a temperature of 60–70°C, which is lower than in the creosote and thus reduces the danger of environmental pollution.

With the same aim, at the Heat and in Mass Transfer Institute of the National Academy of Sciences of Belarus jointly with the Belarusian State University a water-emulsion composition based on shale oil for tie impregnation has been developed [[13], [46]]. It is a water-in-oil emulsion containing 60% shale oil and about 30% water. Experimental measurements have shown that the viscosity of such a water-oil composition rapidly decreases with increasing temperature. For instance, when the temperature is increased from 10 to 40°C, it decreases from 70 to 3.5–5 cSt, which permits conducting the technological process of wood impregnation at a temperature of 40°C. Comparison of the kinetics of wood impregnation with oily and water-soluble antiseptics is given in [[46]].

The present section of the chapter is restricted to the consideration of the saturation kinetics of wood with a water-oil preservative composition with regard for the internal and external heat exchange between the timber and the hot liquid. When impregnated with oil preservatives, it is important to take into account the loss of liquid temperature due to its cooling by contact with the wood. Obviously, this depends on the mass (volume) of liquid and wood, participating in the process of heat and mass transfer during the impregnation.

By analogy with the notion of the degree of loading of the autoclave, which is determined as the ratio of the total volume of the wood (V_w) to the total working volume of the impregnation cylinder, we introduce a similar quantity for a single product:

$$K_u = V_w / (V_w + V_{ext}),$$

where V_{ext} is the external volume of the impregnating liquid per wood product. In the case of a uniform distribution of wood articles in the impregnation cylinder volume, this quantity coincides with the degree of loading of the autoclave.

Figure 2.13 presents the results of the wood impregnation kinetics and the mean temperature of the liquid contacting the specimen [[13]]. Curve 5 shows the character of the change in the external pressure of the fluid. Vacuum-treated specimens of wood with the

initial temperature T_w = 0°C are embedded with the impregnating compound with a temperature T = 40°C. In the process of compound absorption by the wood, new portions of heated liquid enter the cylinder and the total amount of the liquid external with respect to the specimen remains unchanged.

This impregnation was carried out by the method of Bethell (vacuum–pressure–vacuum). In such a method of impregnation, in the impregnating cylinder – an autoclave containing a batch of wood materials – a vacuum (P = 20 kPa) is created for 20 - 40 min and after the cylinder is filled with a heated fluid a pressure P = 1.6 MPa is maintained in it for 2 h. As wood material was a pine cylinder of L = 2.8 m and r = 0.1 m with a ratio of the core radius to the total radius of 3/5. Subsequent to the action of the pressure and the removal of the fluid from the cylinder, post-impregnation vacuum treatment is carried out, and then the wood is drawn from the cylinder.

It should be noted that when the specimen surface temperature was kept constant [[12]] (T_{ext} = 40°C = const) the value of absorption of the compound by the specimen after impregnation was m = 9.22 kg. Comparison of this result with curve 4 (see Figure 2.13) has shown that even at K_u = 0.5, i.e., at an equal volume ratio of the wood and its contacting liquid, the absorption decreased to m = 8.86 kg.

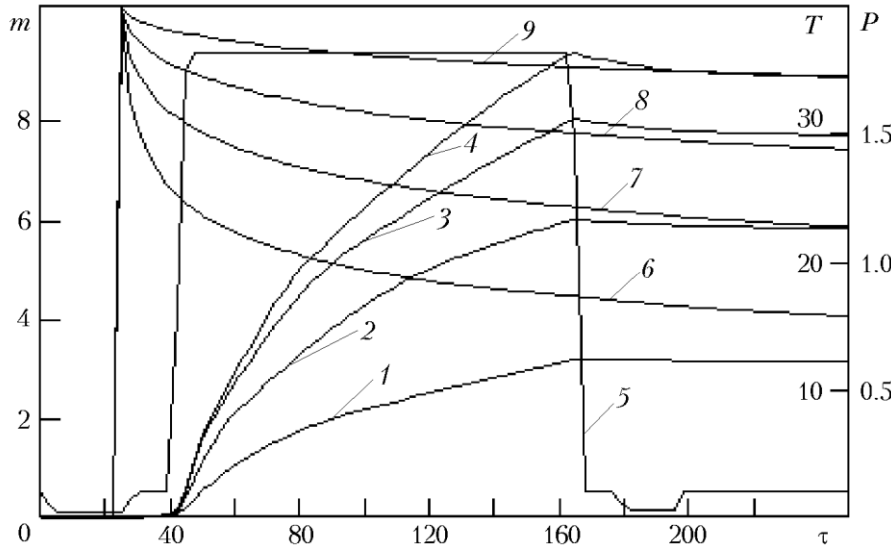

Figure 2.13. Influence of the liquid volume V_{ext} participating in the heat exchange with the wood specimen on the liquid absorption and temperature: 1, 6 - mass of the liquid absorbed by the specimen and its mean temperature at K_u = 0.9; 2, 7 - 0.75; 3, 8 - 0.6; 4, 9 - 0.5; 5 - liquid pressure. m, kg; T, °C; P, MPa; τ, min. With kind permission from Springer Science+Business Media: <Journal of Engineering Physics and Thermophysics, Influence of heat and mass transfer on wood impregnation kinetics, vol. 77, 2004, p. 40, M.A. Brich, V.P. Kozhin, Figure 1.

The results presented in Figure 2.13 demonstrate the necessity of taking into account the conditions of the heat exchange in the impregnation process: the higher the degree of loading K_u, the lower the liquid (and wood surface) temperature[5] and the smaller the absorption m.

[5] The wood-surface temperature at the end of the process before the drawing from the autoclave can be useful in practice in estimating the ecological state of the production.

This imposes certain constraints on the volume of autoclave filling and, accordingly, on the efficiency of the technological process.

There exists strong dependence of the absorption on the size of clearances between the specimens. Figure 2.14 gives the isotherms for fragments of the wood specimen (a fourth part of the longitudinal section of the pole) at the end of the impregnation process (τ = 250 min). This figure also shows the distributions of the impregnating compound concentration.

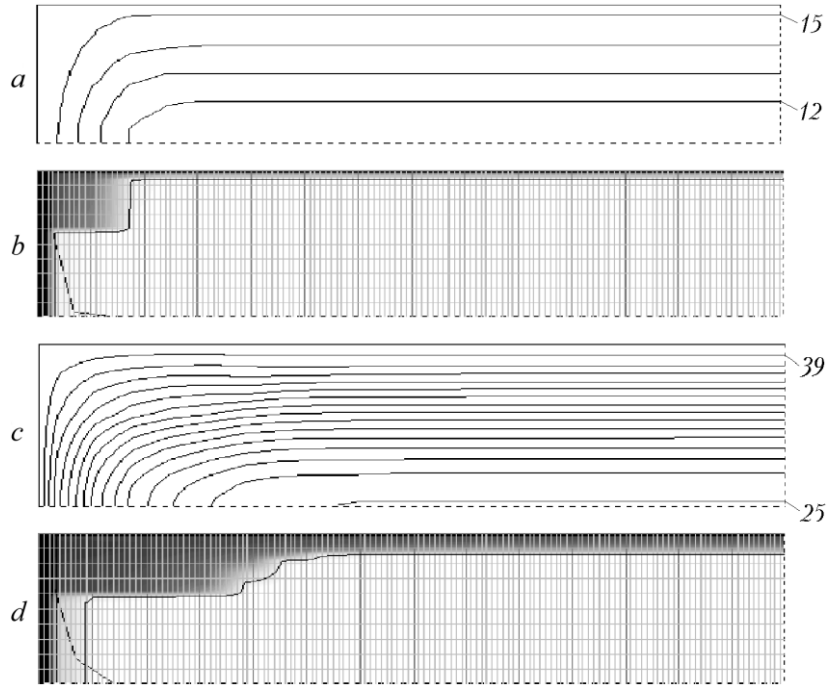

Figure 2. 14 Temperature and impregnating composition distribution in the wood specimen after impregnation: *a* and *c* - temperature levels in the specimen (isotherms have a step of 1°C); *b* and *d* - liquid mass distribution (1-cm step of the grid lines); *a* and *b* correspond to the impregnation with regard for the cooling of the liquid contacting the specimen (K_u = 0.9); *c* and *d* show the impregnation ignoring the cooling T_{ext} = 40°C. Figures show temperatures, °C. With kind permission from Springer Science+Business Media: <Journal of Engineering Physics and Thermophysics, Influence of heat and mass transfer on wood impregnation kinetics, vol. 77, 2004, p. 41, M.A. Brich, V.P. Kozhin, Figure 2.

The figure illustrates a marked difference in the heating of the wood specimen under conditions where the liquid volume interacting with the sample is approximately equal to the volume absorbed by the wood (Figure 2.14 a, b) and where this volume considerably exceeds the volume of the specimen and the liquid is practically not cooled (Figure 2.14 c, d). The distribution patterns of the impregnating composition corresponding to the given temperature fields show a direct relation between the heating depth and the impregnation depth, which corroborates the conclusion that it is necessary to take into account the heat exchange of the specimen with the liquid. The variant given in Figure 2.14 c, d at T_{ext} = 40°C corresponds to the impregnation where the volume of the liquid contacting the specimen $V_{ext} >> V_w$, which in practice can be realized only at large distances (clearances) between specimens and a low degree of loading of the autoclave.

Obviously, running of the heated liquid from the heating zone through the impregnating cylinder (liquid circulation) permits an additional heating of wood materials and makes it possible to increase the liquid absorption by the wood. The data for the impregnation kinetics of the specimen in the case where the liquid incoming from the heating zone or from the thermostatic vessel for composition storage at a temperature 40°C is run are given in Figure 2.15 [[13]]. This figure shows the case of maximum loading of the impregnation cylinder with wood (K_u = 0.9) where the liquid volume V_{ext} and its heat content are minimal. This example corresponds to the closest possible placement of cylindrical specimens in the impregnating vessel and for specimens of rectangular profile (ties, beams, boards) — to the placement with a clearance of a few millimeters. Figure 2.15 also gives the absorption data for the liquid with a fixed temperature T_{ext} = 40° (curve 5) — a perfect heating when the specimen warm-up and its saturation with the fluid are only determined by the internal heat exchange in the wood and are independent of the external fluid volume V_{ext}. We introduce the coefficient characterizing the fluid-exchange multiplicity due to the circulation during 1 h, $R_f = 3600 \cdot G/(\rho_l \cdot V_{ext})$. From Figure 2.15 it is seen that the impregnation kinetics largely depends on the liquid circulation: for instance, at R_f = 1, i.e., at a circulation of one volume V_{ext} per hour (curve 2) the liquid absorption by the wood is twice as high as than without circulation (curve 1), and at a circulation of three volumes (R_f = 3) it is higher by a factor of 2.6.

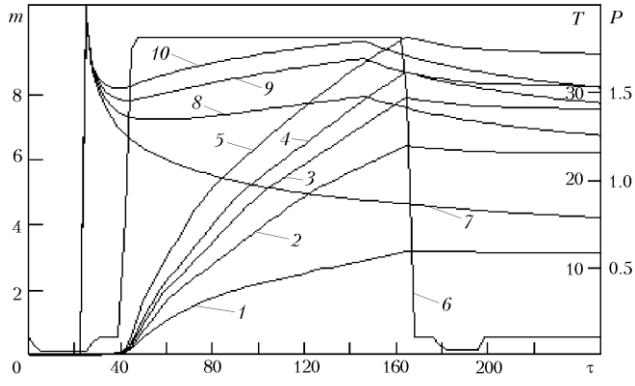

Figure 2.15 Influence of the circulation (running) on the absorption kinetics and temperature of the liquid (K_u = 0.9): 1, 7 - absorbed liquid mass and temperature T_{ext} in the absence of circulation; 2, 8 - in the presence of circulation R_f = 1; 3, 9 - 2; 4, 10 - 3; 5 - T_{ext} = 40°C; 6 - liquid pressure. *m*, kg; *T*, °C; *P*, MPa; τ, min. With kind permission from Springer Science+Business Media: <Journal of Engineering Physics and Thermophysics, Influence of heat and mass transfer on wood impregnation kinetics, vol. 77, 2004, p. 41, M.A. Brich, V.P. Kozhin, Figure 3.

Taking into account that in a real technological process it is not always possible to run the liquid in the period of impregnation at a high pressure, we consider the variant of preheating the wood loaded into the autoclave by running the heated liquid incoming from the heating zone just before the impregnation. Data on the influence of the heated compound circulation with a different flow rate in the heating period (τ = 60 min) are given in Figure 2.16. It should be noted that for the full-cell (Bethell) process wood impregnation begins simultaneously with the pouring of the impregnating liquid under the action of the liquid column and atmospheric pressure after the stage of vacuum-treatment of the wood. Presented results demonstrate a strong influence of liquid heating (circulation) on its absorption by the

specimen: for instance, with a circulation of one volume in the heating period (R_f = 1) the absorption is 1.4 times higher than without circulation, and with a circulation of three volumes it is 1.7 times higher, which is much lower than the calculation data given in Figure 2.15. Obviously, to increase these indices, it is necessary to increase the heating time.

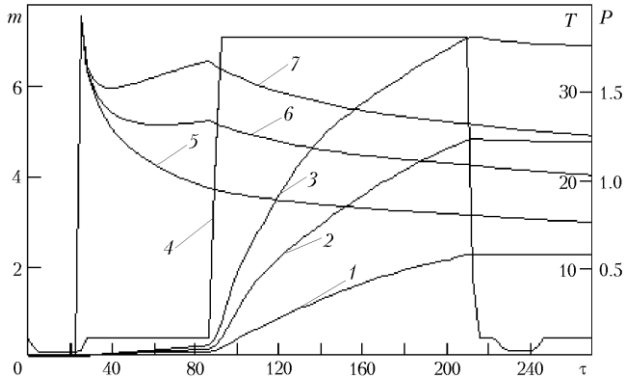

Figure 2.16. Influence of the circulation in the heating period on the absorption kinetics and temperature T_{ext} of the liquid (K_u = 0.9): 1, 5 - absorbed liquid mass and temperature in the absence of circulation; 2, 6 - in the presence of circulation R_f = 1; 3, 7 - 3; 4 - liquid pressure. *m*, kg; *T*, °C; *P*, MPa; τ, min. With kind permission from Springer Science+Business Media: <Journal of Engineering Physics and Thermophysics, Influence of heat and mass transfer on wood impregnation kinetics, vol. 77, 2004, p. 42, M.A. Brich, V.P. Kozhin, Figure 5.

The data presented show a high efficiency of the influence of the circulation (running) of the heated liquid on the impregnation process, which can ensure the required quality of wood treatment at the highest possible degree of loading of the autoclave.

The simulation of the impregnation process without vacuum pretreatment of specimens by the methods of empty-cell (Lowry) process and Rueping process has shown an analogous dependence of absorption on V_{ext} and as high an efficiency of the influence of the circulation [[13]].

It seems interesting to use the heated timber immediately after its pre-impregnation drying when it is necessary to impregnate oils, melts and other liquids whose viscosity should depend on temperature. Resting upon this idea it is possible to develop a complex technology for modifying wood products. If the heat accumulated in the wood at drying is used, then the wood is not heated during impregnation with oils, and this saves the time and energy.

A rapid method of drying by depressurization takes time close to that of impregnation. This will enable one to organize parallel processes with the intent to save production area and labor resources.

CONCLUSION

Currently, specialists in wood treatment consider wood as a raw material to produce an end product. Hydrothermal treatment first – drying and modifying impregnation – is the most important means of wood processing. Despite a limited number of parameters responsible for these processes (mainly *T*, *P*, τ, properties of the medium), both the technology of drying and

impregnation is constantly being improved. The capability of obtaining new qualitative results is shown by the example of our technology of thermal-mechanical removal of moisture under high-temperature drying. The objective evaluation of the perspectives of this development in this field can be given later.

When thermal-mechanical drying by the depressurization method, a significant amount of water is removed from wood in the form of drops. Additional water is removed from the material by hydrodynamic (vapor bulk) flow. As the wood permeability is high at $T > 100^{o}$C, low moisture content gradients are provided. Owing to this and also to the material plasticity increasing with temperature, no noticeable cracks and other defects typical of intense convective drying of wood are present. In the vacuum-convective kiln, when this method is used at heating above 100^{o}C, the drying time of pine greenwood ($D = 0.1$ m) up to a moisture content of 4–10% was equal to 7–12 h, depending on the initial moisture content of samples.

This method can also be recommended for reducing the time of pre-impregnation drying of products meant for modifying impregnation. In this case, the time of drying and the time of impregnation process itself are comparable. This says that drying and impregnation can occur simultaneously within the entire technological process.

The application of low-temperature water-oil emulsions allows the technological process of impregnation to occur at a low temperature (40^{o}C and above), which reduces harmful emissions of industrial enterprises. To ensure the maximum intensity of the process for heating liquid and wood, it is necessary to arrange for the heated liquid circulation.

The results presented can be of help for developing and implementing effective technologies of accelerated drying and modifying treatment of wood.

NOTATION

D - diameter, m; I and I_v - surface and bulk drying rate, respectively, $I = m_l / S\,\tau$, $I_v = m_l / V\,\tau$; K_u - ratio of the specimen volume to the total volume of the wood and external liquid pertaining to this specimen; L- length, m; m - mass, kg; P - pressure, Pa; q - flow rate, liter/h; r - cylindrical-sample radius, m; R_f - liquid-exchange multiplicity per hour; S - surface area; T - temperature, ^{o}C; V - volume, m^3; W-moisture content (MC),%; $\kappa = m_l / (m_l + m_e)$ - the coefficient of thermal-mechanical removal of moisture; ρ - density, kg/m^3; τ - time, min.

Subscripts: a - air; e - vapor; ext - external; f - final; l - liquid; u - unit; w - wood substance; 0 - initial value.

REFERENCES

[1] Accoya. (2009). Fine Deck. Resource Company. http://www.finewood.ru/?page=41

[2] Acda, M. N.; Morrell, J. J.; Levien, K. L. *Wood Sci. Technol.* 2001, *vol. 35*(1/2), 127-136.

[3] Anan'in, P. I.; Petry, V. N. *High-temperature Drying of Wood;* Goslesbumizdat: Moscow, 1963; 120 p.

[4] Arinkin, S. M.; Kozhin, V. P.; Luneva, N. K.; Vorobjov, V. K. In *Modern Problems of Combustion and its Applications*; II International school-seminar; ITMO NANB: Minsk, Belarus, 1997.
[5] Arinkin, S. M.; Kozhin, V. P.; Shchitnikov, V. K. *Features of the Impregnation Process and Dependence of the Absorption of Protective Solution on the Parameters of Pressure;* Preprint № 8; ITMO NANB: Minsk, 1999; 36 p.
[6] Arinkin, S. M.; Brich, M. A.; Gorbachev, N. M.; Kozhin, V. P.; Schitnikov, V. K. In *Proc. 4th Minsk Int. Forum Heat Mass Transfer. May 22-26, 2000*; 2000; Vol. 8, pp 40-48.
[7] Barnes, H. M.; Murphy, R. J. *Forest Prod. J.* 1995, *vol. 4*(5), 16.
[8] Bednarek, Z.; Kaliszuk-Wietecka, A. *J. Civil Engineer. Manage*. 2007, *vol. 13*(2), 79–85.
[9] Belyi, V. A.; Vrublevskaya, V. I.; Kupchinov, B. I. *Wood-polymer Structural Materials and Products;* Nauka i Technika: Minsk, 1980; 280 p.
[10] Britch, M. A.; Kozhin, V. P.; Schitnikov, V. K. *JEPTER.* 1999, *vol. 72*(4), 618-626.
[11] Britch, M. A.; Kozhin, V. P. *JEPTER.* 2001, *vol. 74*(1), 74-79.
[12] Britch, M. A.; Kozhin, V. P. *JEPTER*. 2002, *vol. 75*(2), 75-80.
[13] Britch, M. A.; Kozhin, V. P. *JEPTER*. 2004, *vol. 77*(1), 33-38.
[14] Chen, Z. *Primary Driving Force in Wood Vacuum Drying.* Doctoral dissertation. Virginia Polytechnic Institute, Blacksburg, VA, 1997.
[15] Choi, S. T.; Golitsyn, V. P.; Golitsyna, N. V. *Patent USA.* No. 6,640,462. 2003.
[16] Conservation of Waterlogged Wood. (2009). http://www.natmus.dk /cons/x /ww/ww2.htm
[17] Cookson, L. J.; Qader, A.; Creffield, J. W.; Scown, D. K. *J. Supercritical Fluids.* 2009, *vol. 49*(2), 203-208.
[18] Cookson, L. J.; Watkins, J. B.; Scown, D. K. In *Proc. 25th Forest Prod. Res*.; CSIRO: Clayton, 1996; pp 9-10.
[19] Craig, B. A.; Green, D. W.; Gromala, D. S. In *Proc. WTCE 2006 – 9th world conference on timber engineering*; August 6-10; Portland, OR, 2006.
[20] Danzer Services Schweliz AG. (2009). www.danzer.com
[21] Denig, J.; Wengert, E. M.; Simpson, W. T. *Drying Hardwood Lumber*. USDA, Forest Serv., Forest Prod. Lab.: Madison, WI, 2000, 138 p.
[22] *Dr. Wolman GmbH. BASF the chemical company*. (2008). http://www.wolman.de/en/wood_preservation/vacuum_pressure_impregnation/index.php?thisID=86
[23] Du Fresne, E. R.; Campbell, D. L. *Patent USA.* No. 3,306,765. 1967.
[24] Ellwood, E. L.; Ecklund, B. A.; Zavarin, E. *Forest Product J.* 1960, *vol. 10*(1), 8-21.
[25] Epmeier, H.; Westin, M.; Rapp, A. *Scandinavian J. Forest Research*. 2004, *vol. 19*(5), 31-37.
[26] Fleissner, H. *Zeitschrift Sparwirtschalt.* 1927, Wien, No. 10-11.
[27] Freeman, M. H.; Shupe, T. F.; Vlosky, R. P.; Barnes, H. M. *Forest Product J.* 2003, *vol. 53*(10), 1-15. (http://fwrc.msstate.edu/pubs/preservation.pdf)
[28] HB Group. (2009). Super Heated Steam Drying Kiln. http://www.hb-almelo.nl/en/pagina.php?id=62
[29] Hill, C. A. S. *Wood Modification. Chemical, Thermal and Other Processes.* John Wiley and Sons Ltd.: Chichester, England, 2006. 239 p.

[30] Hunt, G. M.; Garratt, G. A. *Wood Preservation*. 3-d. ed. McGraw-Hill: New York, 1967.
[31] Iizuka, H.; Fushitani, M.; Okabe, T.; Saito, K. *J. Porous Materials*. 1999, *vol. 6*, 175-184.
[32] Iversen, S. B.; Larsen, T.; Henriksen, O.; Felsvang, K. (2009). The World´s First Commercial Supercritical Wood Treatment Plant. http://www.ensic.inpl-nancy.fr/ISASF/Docs/Versailles/Papers/Pe1.pdf
[33] *Glaznev, V. N.; Koptyug, I. V.; Korobeinikov, Yu. G.* JEPTER. *1999,* vol. 72*(3), 409-411.*
[34] Gorbachev, N. M.; Dragun, V. L.; Kozhin, V. P. In *Proc. Heat Mass Transfer - 2007*. ITMO NANB: Minsk, Belarus, 2007, pp 81-88.
[35] Gorbachev, N. M; Kozhin, V. P.; Lovecky, B. K.; Solntceva, N. L.; Chizhik, K. G. In *Proc. Heat Mass Transfer - 2007*. ITMO NANB: Minsk, Belarus, 2007, pp 94-101.
[36] Goryaev, A. A. *Vacuum - dielectric Drying Kilns*; Lesnaya Prom.: Moscow, 1985, 103 p.
[37] Goryaev, A. A. *Modern Vacuum Drying Kilns. Machining Treatment of Wood*, Vol. 5, VNIIPIEIlesprom: Moscow, 1985, 32 p.
[38] Gorshin, S. N. *Wood Preservation*. Lesnaya Prom.: Moscow, 1977.
[39] Gobakken, L. R.; Westin, M. *Int.J. Biodeterior. Biodegrad*. 2008, *vol. 62*(4), 397-402.
[40] Grinchik ,N. N.; Kozhin, V. P. In *Modern Problems of Combustion and its Applications.* 3-d Int. school-seminar, ITMO NANB: Minsk, Belarus, 1999.
[41] Grinchik, N. N.; Kozhin, V. P. *Energoeffectivnost.* 1999, *vol. 5*(19), 14-17.
[42] Klupt, F. B.; Brodocky, A. I. *Deep Dyeing of Wood in Autoclaves*. Goslesbumizdat: Moscow-Leningrad, 1958.
[43] Kalninsh, A. Ya. *Preservation and Protection of Timber*. Lesnaya Prom.: Moscow, 1971, 420 p.
[44] Kim, G. H.; Morrell, J. J. *Wood Fiber Sci.* 2000, *vol. 32*(1), 29–36.
[45] Kozhin, V. P. In *Proc. Int. Science Conf. Centrifugal machines, high-tech.* NPO "Center": Minsk, Belarus, 2003, pp 52–57.
[46] Kozhin,V. P.; Britch, M. A. In *Proc. 5-th Minsk Int. Heat-Mass Transfer Forum*. Vol. 2, 2004; pp 17-26. (http://www.itmo.by /forum/mif5/S07/7.html)
[47] Kozhin, V. P.; Gorbachev, N. M. In *Proc. Heat Mass Transfer – 2005*. ITMO NANB: Minsk, Belarus, 2005; pp 82-86.
[48] Kozlik, C. J. (1959). Bibliography of Special Seasoning Methods. Forest Prod. Research Center, OR. http://ir.library.oregonstate.edu/ jspui/bitstream/1957/ 10769/1/bib_spe_sea_met_.pdf
[49] Krischer, O. *Die wissenchaftlichen Grundlagen der Trocknungstechnik*. Springer-Verlag: Berlin-Gotingen-Heidelberg, 1956, 539 p.
[50] Kudra,T.; Mujumdar, A. S. *Advanced Drying Technologies.* Marcel Dekker, Inc.: New York, 2002; 417 p.
[51] Kulimin; V. V. In *Proc. MLTI*; No.124, MLTI: Moscow, 1980.
[52] Laks, P.; Heiden, P. A. *Patent USA.* No. 6,753,035. 2004.
[53] Larnoy, E.; Westin, M.; Källander, B.; Lande, S. In *Wood Furfurylation Process Development*, Part 1, Int. Res. Group Wood Protect.: Jackson Hole, WY, 2007; pp 1-11.
[54] Lebedev, P.D. *Infrared Drying*. Gosenergoizdat: Moscow-Leningrad, 1955; 230 p.

[55] Lebow, S. In *Proc. Environmen. Impacts Preserv. Treat. Wood Conf.* Orlando, FL, 2004. (http://www.treesearch.fs.fed.us/pubs/6362)
[56] Luikov, A. V. *Theoretical Basis of Construction Thermophysics*. AN BSSR: Minsk, 1961, 340 p.
[57] Maximenko, N. A.; Gorshin, S. N. In *Questions of Wood Preservation*. VNIIDrev: Moscow, 1981; pp 3-54.
[58] Mikhailov, Yu. A. *JEPTER*. 1961, *vol. 4*(2), 33–43.
[59] Mirzadzhanzade, A. H.; Hasanov, M. M.; Bahtizin, R. N. In *Modeling of Processes of Oil and Gas Production*; ANO Inst. Computer Science: Moscow-Izhevsk, 2004; pp 245-256.
[60] Mikhailov, Yu. A. *Drying with Superheated Steam*. Energiya: Moscow, 1967; 201 p.
[61] Mohebby, B.; Sanaei, I. In *Proc. 36th Annual Meeting Bangalore, India 24 – 28 April 2005*; Int. Research Group Wood Protect. 2005.
[62] Muin, M.; Adachi, A.; Inoue, M.; Yoshimura, T.; Tsunoda, K. *J. Wood Science. vol. 49*(1), 2003.
[63] Novitsky, G. I.; Stogov, V. V. *Wood-impregnating Factories*. Gos. Transp. Zhel. Dor. Izd.: Moscow, 1959; 315 p.
[64] NPO "Center". (2009). Centrifuges. http://www.npo-center.com/other/cntrobezh_ispyt/
[65] Osnach, N. A. *Permeability and Conductivity of Wood.* Lesn. Prom.: Moscow, 1964; 182 p.
[66] Pang, S.; Simpson, I.; Haslett, T. *Wood Sci. Technol.* 2001, *vol. 35*(6), 487-502.
[67] Patyakin, V. I.; Tishin, Yu. G.; Bazarov, S. M. *Technical Hydrodynamics of Wood.* Lesnaya Prom.: Moscow, 1990.
[68] Patyakin, V.I. *Problems of Increasing the Floatation of Round Timber.* Lesnaya Prom.: Moscow, 1976; 264 p.
[69] Patyakin, V. I.; Bazarov, S. M.; Avdashkevich S. V.; Sugaipov Yu. Yu. In *Proc. IV Int. Heat-mass Transfer Forum*; 2000; Vol. 8, Minsk, pp 170-173.
[70] Polischuk, V. P.; Patyakin, V. I.; Levit, A. B.; Krutogolov, L. G.; Klevitcky, M. M. Patent RU. No. 916923, MPK F26B 3/04, 1982.
[71] Pushkin, P. S. In *Proc. Leningrad Inst. Railway Engineers*; No. 204; Leningrad, 1963.
[72] Qader, A.; Cookson, L. J. In *Proc. 6th World Chem. Eng. Congress*; CSIRO: Melburne, Australia, 2001; pp 2-156.
[73] Resch, H. *Maderas. Ciencia y tecnologia.* 2006, *vol. 8*(2), 67-82.
[74] Richardson, B. A. *Wood Preservation*. 2-nd ed. Taylor and Francis e-library, 1993; pp 85-86.
[75] Romanovsky, S. G. *The Processes of Heat Treatment and Drying in Electromagnetic Units*. Energia: Moscow, 1969; 129 p.
[76] Romanovsky, S. G. *The Processes of Thermal Treatment of Wet Materials*. Energia: Moscow, 1976; 328 p.
[77] Rowell, R. M. In *Wood Handbook—Wood as an Engineering Material*; Chapter 19; USDA Forest Service, Forest Prod. Lab.: Madison, WI, 1999; pp 19.1-19.14.
[78] Safin, R. R.; Hasanshin, R. R.; Gilmiev, R. R. In *Proc. 3-d Int. Sci. Pract. Conf. "Modern Energy-saving Heating Technology (Drying and Thermal-humidity Treatment of Materials) SETT 2008»*; Moscow; 2008; pp 209-214.

[79] Saikovsky, V. (2009). Report. Confederation of Associations and Unions for Timber, pulp and paper, woodworking and furniture industry http://www.forestconfederation.ru /site.aspx?SECTIONID=323629andIID=334224
[80] Selyugin, N. S. *Wood Drying*. 3-d ed. Goslesbumizdat: Moscow-Leningrad, 1949; 536 p.
[81] Sergeev, V. V. *Aerodynamic Wood Drying Kilns.* Lesnaya Prom.: Moscow, 1981; 72 p.
[82] Simpson, W. T. In *Wood Handbook—Wood as an Engineering Material*; Chapter 12; USDA Forest Service, Forest Prod. Lab.: Madison, WI, 1999; pp 12.1-12.20.
[83] Sergovsky, P. S. *Equipment Hydrothermal Treatment of Wood*. 2-d ed., Lesnaya Prom.: Moscow, 1981; 304 p.
[84] Sergovsky, P. S. *Hydrothermal Treatment and Preservation of Wood*. 2-d ed., Lesnaya Prom.: Moscow, 1968; 449 p.
[85] Sergovsky, P. S.; Rasev A. I. *Hydrothermal Treatment and Wood Preservation*. Lesnaya Prom.: Moscow, 1987.
[86] Schneider, P. F.; Levien, K. L.; Morrell, J. J. *Wood Fiber Sci.* 2006, *vol. 38*(4), 155-165.
[87] Schneider, M. H. ***USPTO*** *Application.* No. 20060094801, Class: 524027000 (USPTO).
[88] Shaplyko, V. I.; Kozhin, V. P.; Elets, Yu. R.; Sitko, K. K. In *Proc. All-Union Conference "Modification of wood*"; BTI: Minsk, 1990.
[89] Shteinberg, A. S.; Zeitlina, R. Z.; Sokolov, I. D. *JEPTER*. 1965, *vol. 8*(6), 730–734.
[90] Spolek, C. A.; Piroozmandi, F. In *Water Vapor Transmission Through Building Materials and System: Mechanisms and Measurement*; H. R. Trechsel and M. Bomberg, Eds.: Philadelphia, 1996; pp 114-122.
[91] Stahl M.; Bentz M. *Chem. Eng. Technol.* 2004, *vol. 27*(11), 1216-1221.
[92] Stamm, A. J. *Wood and Cellulose Science*. Ronald Press: New York, USA. 1964; 509 p.
[93] Stamm, A. J. In *Wood Technology: Chemical Aspects*, Goldstein, I.S. (Ed.). ACS Symposium Series, 43, American Chemical Society, Washington, DC, 1977; pp 141–149.
[94] Suda Toshikazu; Sanriki Kogyo; Kabushiki Kaisha. *Patent USA.* No. 6229318. 2001.
[95] Sugaipov, Yu. Yu. *Proc. Universities Forest J.* 2004, *vol. 5*, 34-36.
[96] *Test data for physical properties of thermo treated wood compared with non-treated wood (ahs, oak, poplar, pine).* Westwood Heat Treated Lumber Corp.and Keim Lumber Comp.: Charm, OH, USA, 2008.
[97] ThermoWood Handbook. (2009). Finnish Thermowood Association. http://www. thermowood.fi/data.php/200312/795460200312311156_tw_handbook.pdf
[98] Treu, A.; Pilgard, A.; Puttmann, S.; Krause A.; Westin, M. (2009). In: *Proc. 40th Annual Meeting*, Beijing, China, 2009. (http://www. skogoglandskap.no/filea rchive/irg_09-40480.pdf)
[99] Tsunoda, K. *J. Wood Sci*. 2001, *vol. 47*(2), 149-153.
[100] Thuvander, F.; Wallström, L.; Berglund, L. A.; Lindberg, K. A. H. *Wood Sci. Technol.* 2001, *vol. 34*(6), 473-480.
[101] Ugolev, B. N. *Wood study with the Fundamentals of Forestry Research*; Lesnaya Prom.: Moscow, 1986; 360 p.
[102] Using of Wood Fuels in Energy. (2009). http://www.turboblock.ru /info/drevo/

[103] Vacuum Compression Drying Chamber for Drying Wood. (2009). TERMOTEH http://www.sushilo.ru/skvk_03.htm
[104] Vacutherm. (2009).Drying Kilns. http://vacutherm.com/products.htm
[105] Vihrov, V. E. *The Diagnostic Features of the Main Timber Forest Species of the USSR.* Izd. AN SSSR: Moscow, 1959.
[106] Walker, J. C. F. *Primary Wood Processing. Principles and Practice*; 2-nd ed., Springer: London, 2006; 596 p.
[107] Waterlogged Wood Conservation. (2009). Conserv. Research Lab. Nautical Arch. Prog., Texas AandM University. http://nautarch.tamu.edu /crl/conservationmanual/ File6.htm
[108] Watkins, J. B.; Greaves, H.; Chin, Ch. W. *Patent USA.* No. 5098,472. 1992.
[109] *Wood and Cellulosic Chemistry*. Ed. Hon, D. N. S. and Shiraishi; N.-2nd ed., Marcel Dekker Inc.: New York, Basel, 2001; 923 p.
[110] *Wood Drying Handbook*. Ed. Bogdanov; E.S. Lesnaya Prom.: Moscow, 1990, 304 p.

In: Wood: Types, Properties and Uses
Editor: Lorenzo F. Botannini
ISBN 978-1-61668-837-0

Chapter 2

THE DEEP DECOMPOSITION OF WOOD: LIGHT PRODUCTS OF ELECTRON-BEAM FRAGMENTATION

A. V. Ponomarev*[1] *and B. G. Ershov
A.N.Frumkin Institute of Physical Chemistry and Electrochemistry, Russian Academy of Sciences, 119991 Moscow, Russian Federation

ANNOTATION

Productive direct conversion of lignocelluloses into liquid organic products by electron distillation of crude wood or by dry distillation of preliminarily irradiated wood is considered. Electron-beam conversion is several times more effective than ordinary hydrolytic, pyrogenous or enzymatic processing of wood. Distillation of wood by electron-beam energy yields a number of the useful reagents for heavy organic synthesis and fuel productions. In particular, this path results in high yield of furans - perspective raw materials for production of high-quality alternative fuel which is compatible to conventional engine fuel and the up-to-date types of automobile engines. Electron-beam processing of intermixtures of wood with others synthetic and natural organics (plasts, bitumen, oil, etc.) also can be perspective. An experiments have shown that the electron-beam irradiation of binary wood-bitumen or wood-polymer intermixtures is characterized by sinergistic destruction of components. Such effect can be the innovative base in the alternative fuel production, in recovery of complex polymer-cellulose waste, in processing of native bitumens and heavy petroleum residue, in practical regeneration of synthetic monomers and in synthesis of industrial inhibitors of radical polymerization.

INTRODUCTION

Wood is the important reproducible resource which can play important role in the future strategy of energy safety and a sustainable development. Transformation of wood into liquid

[1] E-mail: ponomarev@ipc.rssi.ru.

and/or gas organic products is considered as a perspective path of raw materials supply for the alternative macroenergetics and for a heavy chemical industry. Reorientation from an oil stock to wood raw materials is caused by a lot of reasons - the accelerated rates of oil and gas consumption; adverse dynamics of the prices; politicization and instability of the hydrocarbons market; non-uniform hydrocarbons deposition; etc. The tendency of the basic economic and ecological coefficients indicates that it is impossible to satisfy future energy and material needs by conserving today's structure of fuel and energy balance.

Fodder grain was used as raw materials for production of firstgeneration biofuel (bioethanol and biosolar oil). Previous experience has shown that one-way orientation to production of biofuel from grain crops is fraught with both a deficit of the foodstuffs and essential dependence on soil fertility, agricultural productivity, weather and climatic parameters. Besides, initially developed processes of cultivation, a harvesting and conversion of grain into biofuel are burdensome enough for environment.

It is supposed that second generation biofuel (grassoline) will be manufactured by ecologically safe methods from wide assortment of inedible raw materials including wood and wood residue. Today's global consumption of oil is about 30 billion barrels per year. Five times more equivalent energy resources can be obtained due to annual global self-increment of inedible cellulose biomass. In-depth research of direct biomass conversion into convenient fuel or into fuel chemicals is the important global problem.

Products of a wood origin are widely used in a daily life. There are many technological processes when wood components are exposed to radiation processing [1-3]. The most known among them are sterilization of medicines and dressing materials; destruction of wood raw materials for the purpose of an intensification of the hydrolytic processing and production of edible, fodder and technical products (blasting powders, lacquers, viscose, various monosaccharoses and agricultural feedstuff from wood); pretreatment of wood for the subsequent manufacturing of various ethers (nitrates, xanthogenates, etc.). The specified aspects stimulate interest to studying of radiolysis of wood and its components, in particular, to detailing of the radiolytic transformations mechanism. At the same time wood components are convenient modelling objects for studying of radiation effects in biological structures.

Electron-beam technologies can play the important role in formation of alternative energy resources from wood. Earlier effects of the accelerated electrons on wood components were investigated widely enough. The ionizing radiation provokes deep chain destruction of wood, changing a molecular-mass distribution and the physicochemical properties (structure, mechanical strength, solubility, reactivity and other.) [3]. The radiation-induced changes facilitate the subsequent mechanical grinding and hydrolysis of wood. These effects are interesting from the point of view of perfection of conventional technologies of wood processing - diminutions of number of technological operations, decrease in power consumption, replacements of ecologically hazardous chemical stages on electrophysical processing without reagents. Previous radiolytic studies have played a key role in determination of the destruction mechanism in lignocelluloses, thereby having accelerated progress of vegetative macromolecules chemistry.

Wood destruction can be intensified by combination of radiation processing with heat processing. Electron accelerators are the basic radiation sources in the modern radiation-chemical technologies. As a rule generated radiation is characterized by high beam current density ~100 $\mu A/cm^2$. Processing by such beam results in an effective heating of a material being irradiated (radiation heating). Accordingly, the combination of radiolysis and the fast

heating, being the most productive mode of radiation-thermal degradation, can be created by means of only electron accelerator without additional heat sources. The up-to-date accelerators are capable to generate high power electron beams - ≥ 500 kW. It allows to regard the accelerators as the perspective equipment for a large-capacity process industry.

The present work views destruction of wood and its main components (cellulose and lignine) at high dose rate of electron beam radiation when radiolysis is accompanied by fast increase of feedstock temperature, initiating distillation (electron-beam distillation) [4-7].

Electron-beam distillation is the updated and advanced modification of a conventional method of dry distillation. The routine dry distillation method (high-temperature airless transformation into volatile products) [2, 8] as well as the enzymatic processing of phytogenous substances are well known long since. Dry distillation of biomass yields both high-quality wood charcoal for metallurgy and a number of valuable chemical reagents - acetone, methanol, acetic acid, phenols, etc. Low molecular weight products of wood distillation can serve as prospective raw materials for synthesis of new polymers. Dominating products of pyrolitic distillation of wood are water (~1/3), carbon oxides (~1/6) and wood charcoal (~2/5) [2, 6]. The total yield of liquid organic products is ≤11 wt %. Condensation of vaporous products results in two immiscible liquids - the transparent light water-organic solution and a dark heavy concentrate of compounds slightly soluble or insoluble in water (tar). High viscosity, density and refraction index of tar are caused by aromatic and furan components. An average molecular weight of tar is ≤ 150. The light water-organic solution contains a small amount of carbonyl compounds and methanol. Slightly yellow color of the solution is induced by furans inclusion. Interest to dry distillation development has weakened owing to both low efficiency of the method and reorientation of metallurgy from charcoal to coke.

EXPERIMENTAL

Anhydrous and airless vegetative samples were used for the experimental electron-beam distillation. Linac U-10-10T (energy, 8 MeV; pulse duration, 6 μs; pulse repetition frequency, 300 Hz; maximal beam current, 800 μA; scan width, 245 mm; and scan frequency, 1 Hz) served as an irradiator (radiation heater).

Experimental electron-beam distillation can be executed by means of the simple equipment. The universal schema of laboratory installation is shown on Figure 1. The electron beam ***1*** is oriented to the quartz reactor ***2*** containing a plant material (3-80 grams). Vaporous products are condensed by air condenser ***3*** (at 17±2°C) and by water cooler ***4*** (at 15±2°C) outside of irradiation area. Liquid products separate from gases in the collector flask ***5***. Gaseous products can be returned again into a reactor ***2*** or removed from installation by pump ***8***. Inner gas composition in installation can be adjusted using a gas bottle ***7*** (for example, by hydrogen or by light alkanes).

Absorbed dose rate was estimated using aqueous bichromate dosimeter and standard film dosimeter with a phenazine dye-doped copolymer.

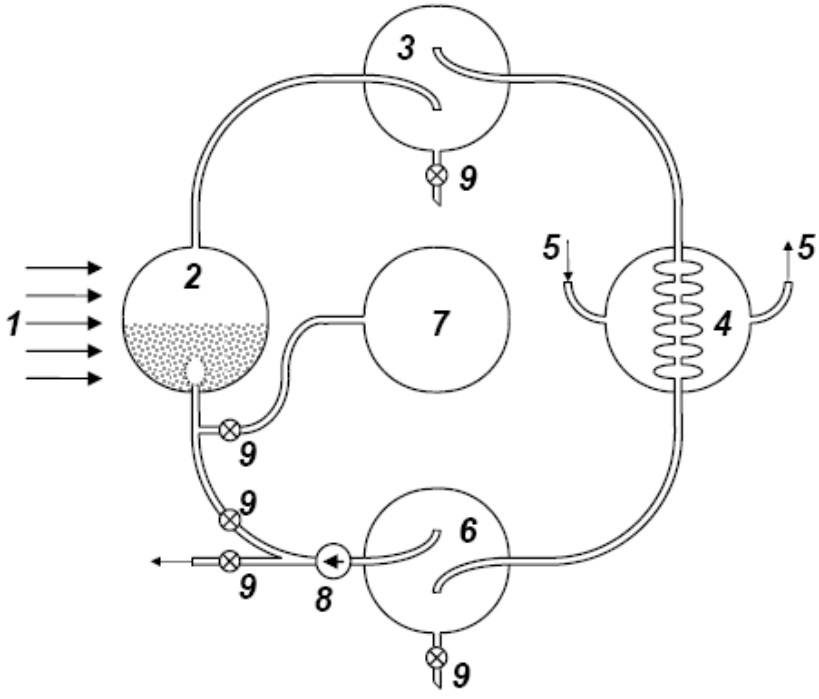

Figure 1. Schematic diagram of electron-beam distillation: (1) electron beam, (2) quartz reactor, (3) air condenser, (4) water cooler, (5) cooling water, (6) collector flask, (7) gas bottle, (8) gas pump and (9) valve.

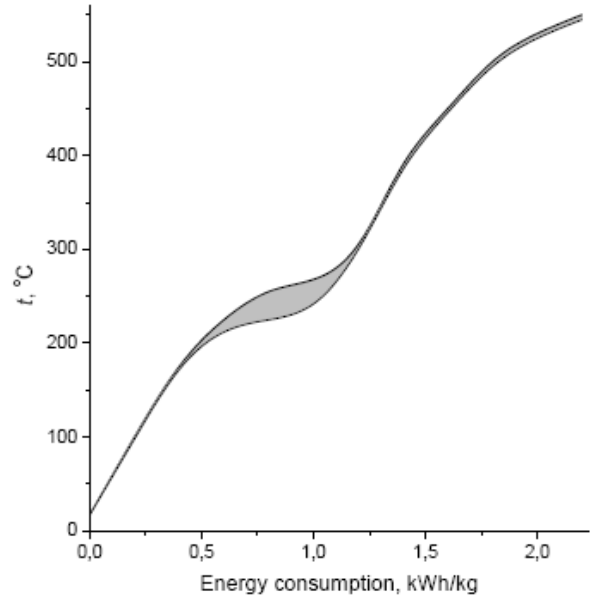

Figure 2. Typical dynamics of electron-beam heating. Data observed at distillation of several wood types are placed between curves (feedstock specific surface Z=105 cm^2/g and bulk density 150 g/dm^3).

The average dose rate was 2 kGy/s. It is necessary to mention that absorbed dose rate was not a stationary value owing to transformation of a feed stock to charcoal. Radiation use factor was 5-25 %. Distillation products (sampled from ***3*** and ***6***) were analyzed chromatographicly (Q-Mass, Perkin Elmer AutoSystem XL; helium as the carrier gas, capillary glass column 60 m long 0.25 mm in inner diameter).

Typical dynamics of an electron-beam heating of wood at dose rate 2 kGy/s is shown on Figure 2. The most intensive condensation of vapours inside coolers is observed after 3 minutes whereas after 6 minutes the vaporization is terminated. Intensive vaporization testifies to the chain mechanism of wood destruction. Observed yield of condensation is ≥ 15 μmol/J. Only wood charcoal remains in a reactor at beam heating above 400°C.

At atmospheric pressure wood pyrolysis could take place at temperature above 270°C [2]. However the sample under beam irradiation does not reach such temperature a long time (see Figure 2). A fast chain formation and transpiration of radiolytic products preclude an excessive heating in a reactor - the heating curve has sag. Thus the probability of the adverse "pyrogenic" destruction mechanism is minimized. So the self-organization effect (self-preservation mechanism) takes place in electron-beam destruction process. In temperature range 220-260°C the beam irradiation does not provide a fast feedstock heating. Heating rate is retarded testifying to initiation of effective endothermic process. The majority of liquid radiolytic products have boiling points in the range 100-250°C. Their specific evaporation heats are 30-46 kJ/mole. Warmth saved up at initial radiation heating is ~10 times less. Main part of beam energy is used for feedstock fragmentation and evaporation of radiolytic products, not yielding the further heating. On the other hand, apparently, the temperature ≤260°C degrees is sufficient for chain cleavage of instable radiolytic intermediates. Significant rise of temperature is being renewed after wood charcoal formation.

The accelerated electron loses energy by small portions (~20 eV on the average), forming 2-5 nm spurs - the isolated zones of ionization and excitation [1, 9]. The typical distance between spurs is hundreds nanometers. Recombination of the ionic and radical pairs in a spur results in the energy liberation (equivalent to local fast rise in temperature). Thus the sequence of the high-temperature nano-reactors isolated from each other is promptly being shaped along an electron trajectory. In contrast to pyrolysis the electron-beam radiolysis preferentially produces the excited and super-excited molecules preceding the splitting of skeletal bonds. Usually a singlet excitations decay by forming the molecular products whereas triplet states dissociate into the radicals [1]. Excess energy is being dissipated along cold macromolecular chains, supporting further cleavage of instable intermediates.

DISTILLATION OF VARIOUS WOOD

The influence of the wood type on the phase composition of electron-beam distillation products is shown in Table 1. Softwood yields a somewhat greater amount of charcoal as compared to hardwood. At the same time, the relative amount of charcoal remaining after radiation heating is lower than that upon the conventional pyrogenic treatment. The conventional dry distillation of pine, spruce, alder, and birch produces about 33–36 wt % charcoal and 15–17 wt % incondensable gases; almost a half of the liquid condensate is water [2].

Table 1. Phase composition (wt %) of the products of electron-beam distillation of various wood feedstock (in *i*-butane at atmospheric pressure; feedstock specific surface Z=40±5 cm^2/g and bulk density 150 g/dm^3)

Wood feedstock	Charcoal	Gas	Liquid
Alder (*Alnus*)	25.4	18.0	56.6
Aspen (*Populys tremula*)	25.4	16.7	57.9
Birch (*Betula*)	23.7	14.7	61.6
Larch (*Larix*)	28.9	14.5	56.6
Linden (*Tilia*)	23.5	15.1	61.4
Mespilus (*Amelanchier*)	25.0	17.1	57.9
Messmate (*Eucalyptus*)	28.5	14.0	57.5
Pine (*Pinus*)	29.6	13.3	57.1
Poplar (*Populus*)	25.5	16.5	58.0
Spruce (*Picea*)	29.5	15.9	54.6

Table 2. Component composition (wt %), average density ρ (at 18°C), and average molecular mass M of condensates from wood feedstock (in *i*-butane at atmospheric pressure; feedstock specific surface Z=90±5 cm^2/g and bulk density 150 g/dm^3)

	Wood feedstock				
Main components	Birch	Aspen	Alder	Spruce	Pine
Methanol + Methylformiat	10.1	10.9	13.9	12.7	9.8
Acetone + propenal	4.3	2.4	3.4	3.4	2.3
2,3-Butanedione	5.9	9.9	7.2	3.8	4.5
2-Oxopropanal	3.0	3.7	4.9	1.2	1.2
Acetic acid	26.1	28.0	23.5	15.1	10.6
1-Hydroxy-2-propanon	6.1	6.2	4.9	9.7	8.6
2-Furaldehyde (furfural)	13.1	11.1	11.2	15.6	16.1
3-Furaldehyde	9.5	2.9	4.8	0.3	0.1
Furanmethanols	1.6	9.0	6.7	3.3	3.1
5-Methyl-2-furaldehyde	0.5	0.3	0.8	0.8	2.0
4-Methylphenol	≤0.1	0.6	0.2	≤0.1	0.3
	Wood feedstock				
Main components	Birch	Aspen	Alder	Spruce	Pine
2-Methoxyphenol	≤0.1	0.1	1.5	3.7	6.1
2-Methoxy-4-methylphenol	≤0.1	0.1	0.2	0.7	4.0
Total furans	24.7±2.1	24.9±2.3	24.8±2.9	24.9±3.9	28.4±5.1
Total aromatics	≤0.3	2.2±0.9	2.6±1.0	13.9±3.0	18.4±6.2
Density ρ, kg/m^3	1141	1122	1119	1138	1125
Mole mass M, kg/mol	73.8±1.1	73.6±0.7	75.8±1.4	79.4±1.6	81.2±1.4

Differences between wood species are manifested already at the step of condensation of the vapors distilled off in the radiation heating mode. Approximately half of vapor produced

from the soft wood and less third part from foliar wood are condensed in an air condenser. The fresh condensate contains a small amount of water (≤8 wt %). The water fraction is incremented during storage of the condensate, especially, upon heating which accelerates the water formation. The instability of the condensate assumes necessity to dilute and to process (stabilize) the low-molecular-mass products of distillation already at the vapor withdrawal step [6].

The component composition of the condensable products of electron-beam distillation substantially depends on the type of wood used (Table 2). The condensate obtained upon the destructive distillation of softwoods is enriched in phenolic compounds. Their precursors are lignin and other aromatic wood macromolecules [2]. Aromatic compounds exhibit radioprotector and antioxidant properties [1, 10]; therefore, their increased concentration predetermines a number of significant specific features of degradation of softwood. Softwood condensates contain a smaller amount of low-molecular-mass components composed of 1–3 carbon atoms. This is an indication of less severe fragmentation of wood enriched in aromatic components. Correspondingly, the average molecular mass of pine and spruce condensates is higher than that of hardwood condensates (Table 2). The liquid mixtures of softwood electron-beam distillation products are substantially more stable upon storage and heating. At the same time, a higher yield of charcoal is probably also due to an increased concentration of aromatic components in the softwood feedstock.

Radiation-induced degradation of both softwood and hardwood results in a considerable amount of the furan fraction (Table 2). The main source of furans is cellulose [5]. Among furan derivatives, furaldehydes prevail. Radiation heating of hardwood yields 3-furaldehyde along with 2-furaldehyde (furfural). Furfural becomes a dominating representative of furaldehydes in the case of decomposition of softwood material. Aspen and alder condensates are characterized by a higher proportion of furanmethanols, whereas the condensate from pine contains 5-methyl-2-furaldehyde in a relatively greater amount. However, the variety of furans produced from softwoods is greater as compared to hardwoods. For example, the pine condensate additionally contains furan, 2-methylfuran, 2,5-dihydrofuran, 2,5-dimethylfuran, 2,5-dihydro-3-methylfuran, and 5-methyl-2(3H)-furanone.

Table 3. Distribution of components in the oxygenate fraction of condensates, wt % (in *i*-butane at atmospheric pressure; feedstock specific surface Z=40±5 cm^2/g and bulk density 150 g/dm^3)

Functional group (compound)	Wood feedstock				
	Birch	Aspen	Alder	Spruce	Pine
-OH (alcohols, phenols)	13.8	12.3	8.4	20.2	28.1
-COOH (acids)	41.3	35.8	35.6	22.4	17.8
-C=O (ketones)	11.6	23.1	18.5	19.5	17.0
-C=O (aldehydes)	17.6	16.2	21.3	18.1	22.4
-O- (ethers)	10.5	10.7	12.9	15.1	22.2
-O- (esters)	5.2	1.9	3.3	4.7	0.4

The wide variety of furans and their higher total yield can also be due to a reduction in the severity of cellulose fragmentation in the presence of softwood aromatic components.

The most representative fractions in condensates are low-molecular-mass oxygenated compounds. Oxygen atoms appear in various functional groups, forming acids, aldehydes, ketones, alcohols, ethers, and esters. The relative distribution of compounds bearing different oxygen-containing groups in the total oxygenated components is shown in Table 3. Carbonyl compounds occupy almost 3/4 of the total mass of hardwood condensates, but their fraction in softwood condensates is noticeably lower.

Ambient isobutane too participates in radiolysis, being in particular the predecessor of liquid alkanes. The fraction of liquid alkanes in the condensates is relatively small (≤ 2 wt %) and includes C_8 isomers. On the other hand, there are butanols and some ethers untypical of the products of electron-beam distillation of the wood itself among the oxygen-containing components. It is evident that the formation of these products is associated with radiolytic transformations of the isobutane, the carrier gas. It is interesting that the mode of electron-beam distillation of wood in a light alkane medium provides the yield of the gas alkane fixation on order of magnitude above than radiolysis of dry or watered gas without wood additives [11, 12]. This effect can result from the processes of charge and energy transfer from lower products of chain fragmentation of wood to light alkane molecules. As a consequence, more effective degradation of the gas increases the probability of participation of its intermediates in the formation of liquid alkanes, alcohols, and ethers.

Natural rotting processes have an effect on the product composition of electron-beam distillation of wood [13]. The condensate contains a lesser amount of light products resulting from cellulose fragmentation whereas the fraction of aromatic fragments and furans increases. For example, in the case of electron-beam distillation of rotten pine dust, the relative amount of aromatics and furans in the condensate reaches 65–70 wt %. The total condensate yield decreases to 40 wt % and the yields of charcoal and gas increase to 42 and 18 wt %, respectively, in this case. These changes indicate that aromatic compounds are more stable during natural biochemical wood aging processes.

LOW-TEMPERATURE DESTRUCTION OF CELLULOSE AT MODERATE DOSE RATES

Cellulose forms vegetative cellular walls, it is a main structural component of natural phytogenous matters. Radiation-chemical yield of cellulose destruction at room temperature is G^0=6.0 ± 1.0 [3]. Both dose rate and initial polymerization degree and microcrystallinity of cellulose do not practically influence a destruction yield. The dense crystalline structure results in low gas permeability of cellulose fibrils. Therefore the vacuum, ambient inert gases and air also feebly influence cellulose radiolysis. Oxygen promotes only superficial radiolytic oxidizing, forming carbonyl and carboxyl groups on a cellulose surface. Cellulose destruction is a little inhibited by a moisture [14, 15].

Dependence of cellulose polymerization degree P on a dose D at doses <200 kGy is linear, being well featured by the equation (1).

$$\frac{1}{P}+\frac{1}{P^0}=\frac{1.62G^0D}{N_Ak} \qquad (1)$$

where P^0 – initial polymerization degree of cellulose, k - auxiliary coefficient, N_A - Avogadro number. Decomposition rate decreases at higher doses. This effect is caused by formation and accumulation of fragmentation products. These intermediates and final products retard the further destruction of cellulose, being scavengers of electron, radical and excitations. Cellulose destruction at very high doses (> 1 MGy) can be featured by empirical equation (1) in which D should be substituted on D^q where q is equal 0.83 [16, 17] or 0.73 [18].

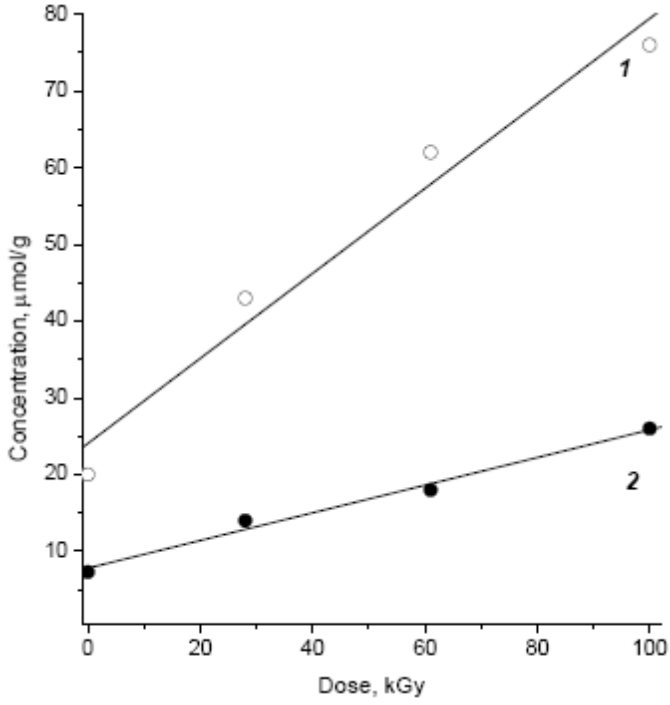

Figure 3. Accumulation of carbonyl (*1*) and carboxyl (*2*) groups in a cotton cellulose [23].

The irradiation at low temperature and at low dose rate results in the deep chemical transformations of cellulose [19-23] Among the water-soluble products the cellobiose, glucose, arabinose, glyoxal, 2-ketogluconic acid and some other acids are found out. Hydrolysis of the water-soluble fraction results in formation of xylose, arabinose, glucuronic and formic acids, malonic dialdehyde, etc. Figure 3 illustrates influence of an irradiation on the content of >C=O and –COOH groups in a cotton cellulose at room temperature.

Preferentially carbonyl compounds are formed via cellulose destruction. Yield of carbonyl groups formation is 6.5 ± 0.5. Yields of carboxyl groups are from 0.9 to 1.8 [18, 24-29]. Radiolytic formation of carbonyl and carboxyl practically does not depend on the initial content of these groups in raw cellulose (see Table 2). About 3 mmoles >C=O and 1 mmole -COOH are formed in 100 g of cellulose at an absorbed dose 50 kGy.

Both carbonyl and carboxyl concentrations at high doses are featured by non-linear dependence $c = BD^q$. The coefficient B is $6.8 \cdot 10^{-7}$ for carbonyl and $1.8 \cdot 10^{-7}$carboxyl groups [16]. The exponent q for both groups is 0.50-0.69 [18, 24]. Apparently this effect at high doses is due to an involving of carbonyls and carboxyls into radiolytic transformations.

Hydrogen, dioxide carbon and monoxide carbon are main light-end products of cellulose radiolysis [21, 23, 25, 31-34]. Their yields in vacuum at doses ≤ 300 kGy are 6.0, 3.2 and 0.9 respectively. Methane also has been detected among light-end products.

The conventional view on the nature of the free radicals in irradiated cellulose has been formulated after the publication [15, 35-50]. Predominating radical states in the irradiated cellulose are localized on endgroups of polymeric chain.

Probabilities of C(1)-H and C(4)-H bonds cleavage in glucopyranose at nitrogen boiling point are similar. The irradiated samples of the frozen cellulose have the dark blue colour due to optical absorption of trapped electrons. Colouring is intensified in the moist samples.

Radiolytic destruction of cellulose is initiated by ionization, ion-electron pair neutralization and decay of excited states:

$$RH \rightarrow RH^+ + e^- \quad , \tag{2}$$

$$RH^+ + e^- \rightarrow RH^* \quad , \tag{3}$$

$$RH^* \rightarrow R\cdot + \cdot H \quad . \tag{4}$$

Excited states decay preferentially by cleavage of C(1)-H or C(4)-H bond in glucopyranose ring (radicals RO· in the irradiated cellulose are not detected). H· atoms eliminate hydrogen from glucopyranose, forming the same radicals R·

$$RH + \cdot H \rightarrow R\cdot + H_2 \quad . \tag{5}$$

Primary R· radicals, apparently, are instable as a result of the considerable strains induced by discrepancy between electronic configurations of radical centre (sp^2-hybridization) and initial molecular unit (sp^3-hybridization). Already at room temperature R· radicals degrade by glucosidic bond cleavage [3]:

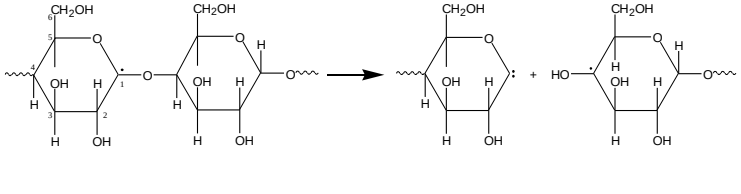

(6)

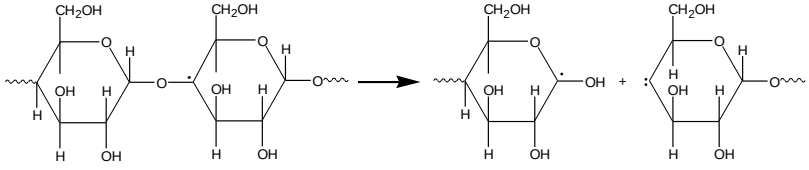

(7)

The fragments from (6) and (7) reactions decay to form further stable low-molecular-weight products. The yield of carbonyl groups formation is enough close to a yield of destruction of cellulose and a yield of CO_2 formation; i.e. each cleavage of cellulose polymeric chains results in formation of one molecule CO_2 and one carbonyl group.

Change of temperature from 300 to 77 K results in almost double decrease of cellulose destruction yield, as well as formation yields of carbonyl compounds, CO_2 and CO. In the same conditions the H_2 formation yield is invariable. It indicates that C-H cleavage not depends on temperature, whereas cleavage of glucopyranose units can be retarded by a cooling. Process of radiation destruction of cellulose can be stimulated by a heating [19]. The temperature is more, the degree of polymerization is lower. Temperature effect on cellulose destruction is shown on Figure 4. There are two temperature ranges differing by efficiency of radiation destruction in cellulose. Destruction yields vary slightly at temperatures below 110°C. Higher temperatures result in appreciable increase of the destruction yields.

Activation energy of destruction in high-temperature range (110-190°C) is 23.4 ± 1.6 kJ/mol. Such value is characteristic for diffusion of radicals in the polymer and corresponds to energy of conformational oscillations of glucopyranose unit [51]. The destruction yield coincides with a yield of carbonyl groups formation (see Figure 4). High-temperature destruction of cellulose is also accompanied by increased yield of hydrogen and carbon dioxide.

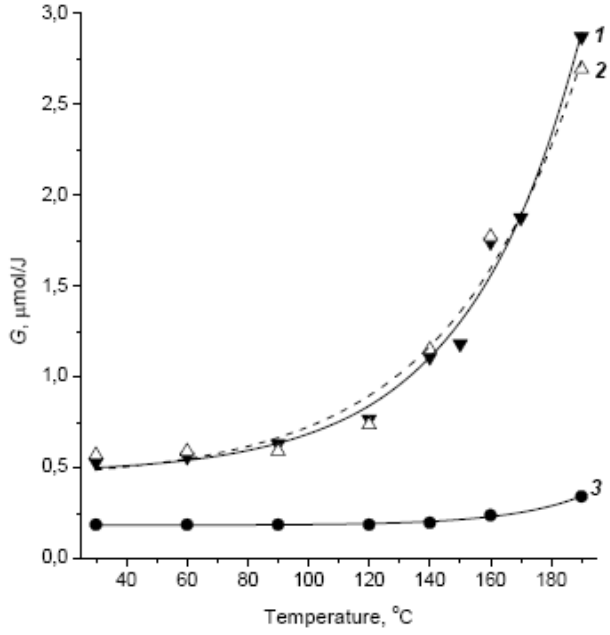

Figure 4. Temperature dependence of destruction yield of cellulose (*1*) and formation of carbonyl (*2*) and carboxyl groups (*3*) [19].

The radical-chain mechanism of radiation-chemical destruction of cellulose takes place at temperature above 110°C. At the same time ratios of main products yields do not depend on temperature. Hence there is a likeness of processes of a radiolytic fragmentation of cellulose in different temperature ranges - decay of each glucopyranose unit is accompanied by formation of carbonyl compound and CO_2 molecule [3].

Cellulose destruction depends significantly on operational sequence of an irradiation and heating [52]. Both the irradiation and thermal processing result in decrease in cellulose polymerization degree and in increase of a yield of hydrolytic formation of reducing sugar.

Bond breaking in a cellulose macromolecule at sequence "heating→irradiation" corresponds to the equation:

$$S_{(T\rightarrow R)} = S_T + S_R \quad (8)$$

where $S_{(T\rightarrow R)}$ - number of cleavages via the consecutive two-stage processing; S_R - number of cleavages via single-stage radiolysis; S_T - number of cleavages via single-stage thermal processing. That is, the sequence "heating→irradiation" yields the additive effect. The sequence "irradiation→heating" yields the superadditive number of cleavages [21, 53, 54]:

$$S_{(R\rightarrow T)} = S_R + S_T + \beta D \quad , \quad (9)$$

where β - the coefficient corresponding to a rise of efficiency of thermal destruction of irradiated cellulose at dose D. The sequence "irradiation→heating" gives also the superadditive influence on a yield of hydrolytic formation of reducing sugar from the treated cellulose [52].

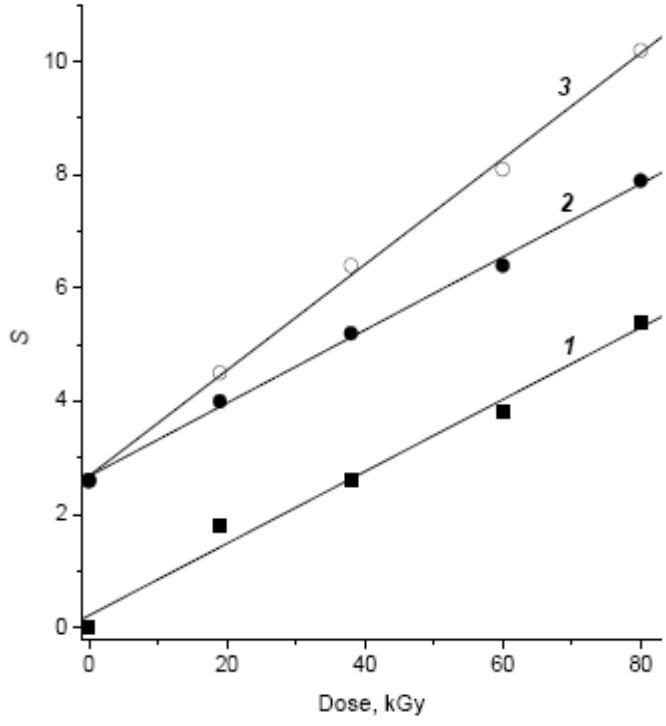

Figure 5. Dose dependences of bond cleavage number (S) in wood cellulose at various combinations of an irradiation and a heating (3 h at 190 °C): 1 – irradiation; 2 - heating→irradiation; 3 - irradiation→heating.

Dose dependences of bond cleavage number in wood cellulose are shown on Figure 5 at various combinations of an irradiation and a heating. The slope of linear dependences *1* and *2* is identical, confirming that pre-award thermal processing does not influence efficiency of the

subsequent radiation destruction. At the same time, larger slope of a line *3* displays more effective destruction of cellulose at sequence "irradiation-heating". The coefficient β correlates with slopes variance of dose dependences at specified treatment temperature. At 150, 170 and 190°C β-values are 0.004, 0.02 and 0.038 bond cleavages per 1 kGy [21, 54].

ELECTRON-BEAM DISTILLATION OF CELLULOSE

We studied the efficiency of electron-beam conversion of cellulose into liquid organic compounds depending on initial temperature, dispersion degree (specific surface *Z*) and feedstock type. Three cellulose types were tested: a cotton cellulose (C1), the unbleached pine sulphate cellulose (C2) and the bleached pine sulphite cellulose (C3).

Telemetry does not reveal any significant distinctions in dynamics of electron-beam distillation of C1, C2 and C3 samples in airless medium at 730-740 mm Hg pressure. Absorption of dose ~250 kGy is accompanied by formation of the heavy fog gradually flowing from a reactor into condensers. Vapours colour changes from initial white to brightly yellow.

The condensate accumulates in a collector flask. Its amount increases during an irradiation. Formation of vapours and build-up of the condensate level are terminated at a dose ~500 kGy. The condensate represents the homogeneous odorous brown liquid; yield of a condensate formation ~60 wt % (see Table 5). The dry black residue (charcoal) remains inside a reactor after distillation. Volume of charcoal is less than initial volume of a feedstock. Charcoal yield is approximately 20 % of initial dry weight of cellulose.

The content of the main components in the condensates formed from C1, C2 and C3 is shown in Table 6. Condensates originated from all three samples have similar compositions and include over 40 organic compounds of molecular weight 32-128. Main liquid products are furans among which 2-furaldegid (furfural), 2-furanmetanol, 5-metil-2-furaldegid and 3-furaldegid predominate. Water content in a condensate is ≤ 8 wt %. Similar results have been revealed earlier [55] by examination of electron-beam distillation of cotton wool and sulphate pulp in a gaseous alkanes flow.

Table 4. Initial concentrations and radiation-chemical yields of the oxidized groups in cellulose (γ-radiolysis) [30]

Cellulose type	Concentration, mmoles/100 g		Yield, mmoles/100 eV	
	-CHO	-COOH	-CHO	-COOH
Wood sulphite cellulose	0.13	0.24	6.0	2.0
Wood sulphite high-viscosity	0.53	3.16	5.4	1.8
cellulose	0.10	0.45	5.9	2.5
Cotton cellulose				

Table 5. Yield *G* (in % from dry weight of cellulose), index of refraction n_D^{18}, density ρ^{18}, and viscosity η_0 of condensates (Z=104 cm^2/g)

Feedstock	G, wt %	n_D^{18}	ρ, kg/dm^3	η_0, mPa·s
C1	63	1.4479	1.1639	5.96
C2	58	1.4449	1.1560	5.67
C3	60	1.4455	1.1594	5.79

Table 6. The average content of the main components in condensates (wt %)

Component	Feedstock (Z=104 g/cm^3)		
	C1	C2	C3
Methyl formiate	0.9	0.8	1.3
Acetone	4.9	2.7	3.4
Formic acid	5.0	5.2	3.6
2,3-Butandione	1.6	3.5	1.7
2-Oxopropanal	3.4	0.6	0.8
Acetic acid	7.3	6.0	3.1
1-Hydroxy-2-propanone	7.3	10.7	1.5
1-Methylpropylacetate	1.8	0.9	2.0
Furaldehydes	42.5	44.3	51.0
Furanmethanols	2.0	2.8	4.7
Methylfuraldehydes	9.4	13.3	17.3
Total Furans	72.5	64.4	79.0

Crushing of C2 does almost not influence duration and intensity of electron-beam distillation. The condensate yield does not change - 58±1 wt %. However the light tendency to decrease of a chared residue yield and increase of a volatile products yield (about 2-3 wt %) is observed for more crushed C2 samples. At the same time, composition of a condensate varies - the finer crushing of a feedstock, the more both density, viscosity, average molar mass, refraction index, and optical density of a condensate (see Figures 6 and 7). Following correlations are being detected by means of comparison of the condensates forming from cellulose via a specific surface *Z* magnification:

- the fraction of the furan-derivatives representing large fragments of a glucopyranose (such as furaldehydes, furanmethanols, furanones) increases;
- the fraction of small fragments of a glucopyranose (such as 1-hydroxy-2-propanone, acetic and formic acids) decreases;
- the fraction of the heavy products forming in the secondary interactions between main primary products (such as furanmethanolacetates) decreases also.

Undoubtedly, products of a radiolytic fragmentation of cellulose form both on a surface and in volume of solid particles. Migration of fragments from volume to a surface (into the mobile vaporous phase) demands a time. That delay increments probability of additional

radiolytic destruction of primary fragments or their reactions with other products (formation of "hybrid" compounds). Apparently, such effects result in distinction of composition of the condensates received at distillation of samples with various crushing.

Influence of a preliminary heating on electron-beam distillation was studied at temperature ≤250°C to prevent cellulose pyrogenic decomposition before an irradiation [2]. Insignificant temperature effect on a condensate yield was observed. According to telemetry the observed time of the vapors emersion in the preheated samples has decreased a little, however end time of distillation did not depend on initial temperature. It specifies that dynamics of the electron-beam distillation is controlled by radiolysis and radiation heating, instead of feedstock temperature. The condensate yield at initial feedstock temperature 16-250°C was 58.0±1.5 wt %.

As a rule, cellulose pyrolysis is initiated at ~270°C. It would seem that radiation heating of hotter samples should result in to more prompt distillation. However it does not occur.

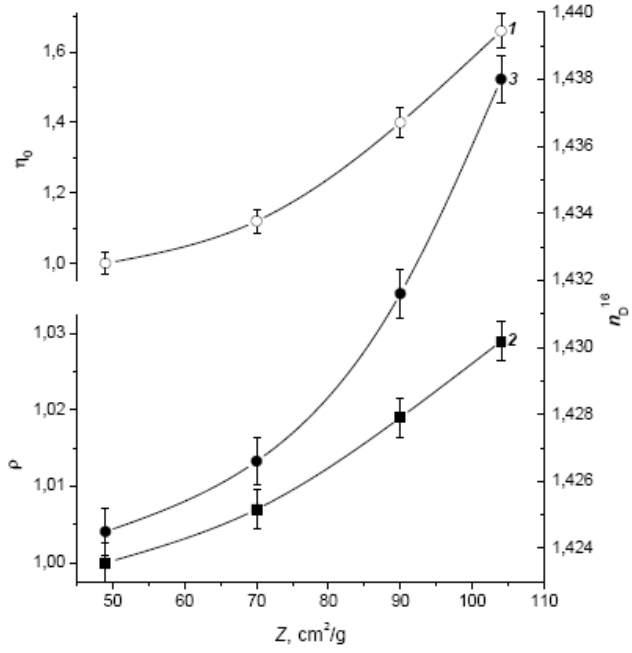

Figure 6. Influence of specific surface *Z* of samples C2 on the relative values of density ρ (*1*), viscosity η_0 (*2*) and refraction index n_D^{16} (*3*) of condensate.

Figures 7 and 8 testify that the preliminary heating promotes formation of heavier condensate - while raising an initial feedstock temperature, an increase of density, viscosity and index of refraction of a condensate are observed. The molar mass of a condensate continuously grows from ~87 to ~94 g/mol. Optical density at λ_{max}=275 nm (typical of furans) increases. Furans-derivatives fraction in a condensate expands from 60 to 72 wt %. The furan fraction is introduced preferentially by furaldehydes (furfural content about ¾). Influence of a preliminary heating is most significant at the radiolysis initial stage - more prompt migration and volatilizing of primary products of a fragmentation takes place, as well as decomposition of thermally astable fragments. It prevents participation of primary products in the subsequent radiolytic transformations. Preheating experiments reveal dominating value

of radiolytic processes in formation of final products of distillation. Rough chain formation of the carbonic gas and other radiolytic products massive attenuates excessive overheat of a cellulose feedstock, thereby preventing development of destruction and distillation via the adverse "pyrogenous" mechanism.

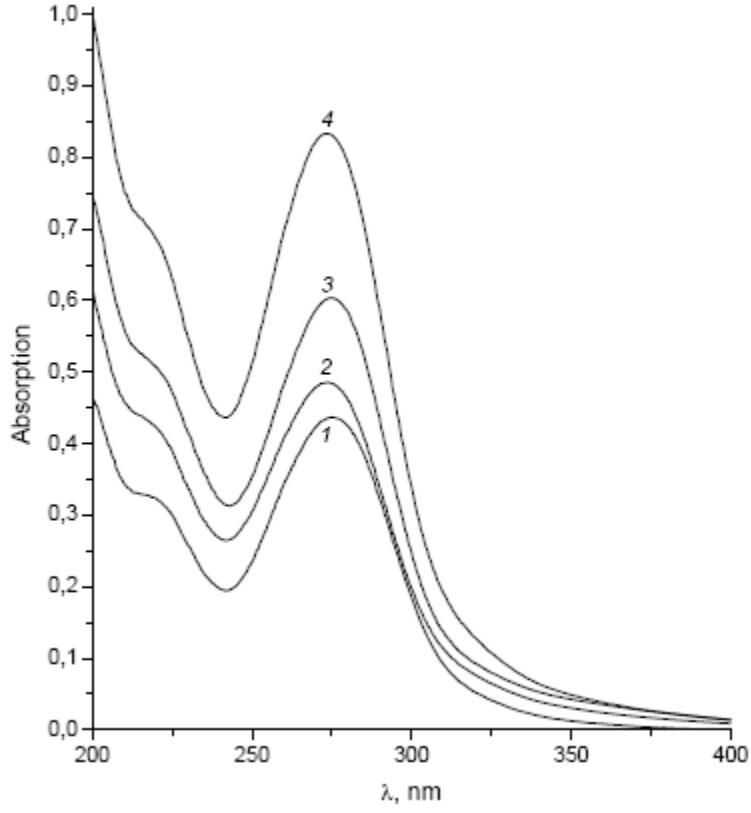

Figure 7. Optical absorption spectra of condensates originating from C2 at initial temperature 16°C (*1* - *Z*=49, *2* - *Z*=70, *3* - *Z*=104 cm^2/g) and 230°C (*4* - *Z*=104 cm^2/g).

The basic gaseous products of destruction are CO_2, H_2 and CO. Equimolar formation of carbonic gas and hydrogen is observed whereas CO yield is less by an order of magnitude. Stoichiometrically the -O-C-O- fraction (CO_2 predecessors) in $C_6H_{10}O_5$ glucopyranose unit is about 27 wt %. At the same time the experimentally observed total CO_2 + CO yield is 1/5 from dry mass of cotton feedstock. Undoubtedly that distinction between stoichiometric and experimental yields can be caused by incomplete decomposition of a feed stock, or by discrepancy between real feedstock composition and the classical formula of cellulose. For example, the microelement analysis of C3 sample testifies that a real atomic ratio C/O=1.8 whereas stoichiometric value should be C/O=1.2. Besides, real C3 contained mineral components about 2.0 wt %. Thus, the oxygen atoms deficit took place in explored C3 feedstock.

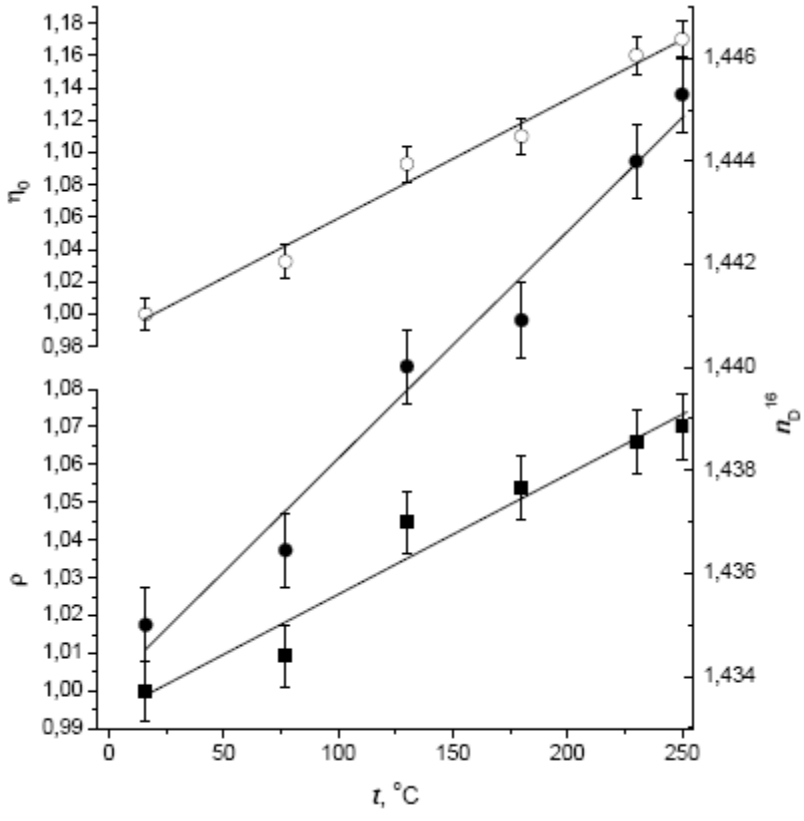

Figure 8. Influence of initial temperature of C2 samples (Z=104 cm^2/g) on the relative values of density ρ (*1*), viscosity η_0 (*2*) and refraction index n_D^{16} (*3*) of condensate.

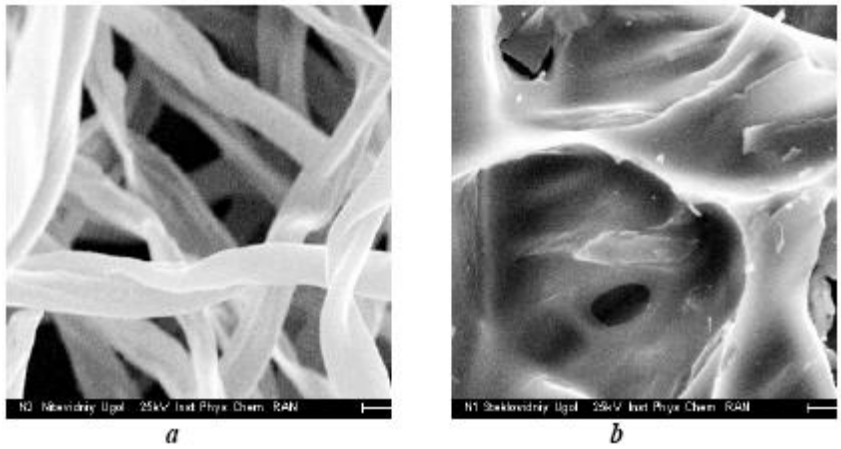

Figure 9. Two structures of charcoal (105×80 μm).

Components impoverished by oxygen, possibly, were one of basic predecessors of the wood charcoal remaining in the end of distillation. At the same time, the wood charcoal part could be formed by means of condensation of destruction products into the higher-boiling

compounds whose volatilization from a reaction area is complicated. The charred residue in samples C1-C3 consisted of two fractions - long fibers (structure, similar to an initial cellulose; atomic ratio C/O≈8.4; see Figure 9a) and the frothed inclusions (in the form of blobs and films; the atomic relation C/O≈6.4; see Figure 9b). The second fraction meets on surface of a charcoal and, apparently, is formed by condensation processes. In particular, condensation processes are characteristic for furfural and some its derivatives at the dry distillation conditions [2]

$$2C_5H_4O_2 \rightarrow C_{10}H_6O_3 + H_2O \quad . \qquad (10)$$

It has been shown in [56], that furfural promptly decays in acidic medium, yielding both formic acid and humic substances (formic acid 50 g and humic substances 41.5 g are formed from furfural 100 g). Formation of high-molecular products by an interaction of furfural with other intermediate compounds [56] can also contribute to additional carbonization of feedstock. Apparently the fastest removal of vapours from irradiation area is the main method to reduce a yield of high-molecular products and to minimize losses of furfural homologues.

In practice furfural can be manufactured by acid hydrolysis of pentosans which are a part of easily hydrolyzable vegetative hemicelluloses [56]

$$C_5H_{10}O_5 - 3H_2O \rightarrow C_5H_4O_2 \qquad (11)$$

In contrast to hemicelluloses, both hydrolysis and pyrolysis of cellulose are characterized by low probability of furfural formation [2, 6, 56]. The present study dealt with hemicelluloses-deficient feedstock. Hence high yield of furfural is caused just by the cellulose destruction. Taking into account real composition of samples, experimentally observed yield of CO_2 specifies that the overwhelming majority of normal glucopyranose rings decomposes during electron-beam distillation.

The Mechanism of Cellulose Destruction Via Electron-Beam Distillation

Most likely, a radiolytic destruction of cellulose at high dose rate (electron-beam distillation) is initiated by the same reactions, as at low dose rate. However a fast beam-heating changes both decomposition paths and stabilization paths of intermediates.

Absolute majority of low-molecular-weight products of distillation contain from 1 to 6 C atoms. The composition analysis of products specifies that all of them have one predecessor - a glucopyranose ring ~($C_6H_{10}O_5$)~. Besides, the fragmentation of a glucopyranose unit can include the set of reactions - dehydration, dehydrogenation, decarboxylation, single bond cleavage, isomerization, and some other.

Reactions (2)-(7) including C-H bond cleavage on glucopyranose ring are the main ways of radiolytic formation of primary organic radicals ·R. Primary R· radicals, apparently, are instable as a result of the considerable strains induced by discrepancy between electronic configurations of radical centre (sp^2-hybridization) and initial molecular unit (sp^3-hybridization) [3]. Less stable C(1) radical easily breaks already at low temperature whereas C(4) radical decay is initiated by a heating [15].

Primary radical ·R takes allyl structure via thermostimulated dehydration, for example:

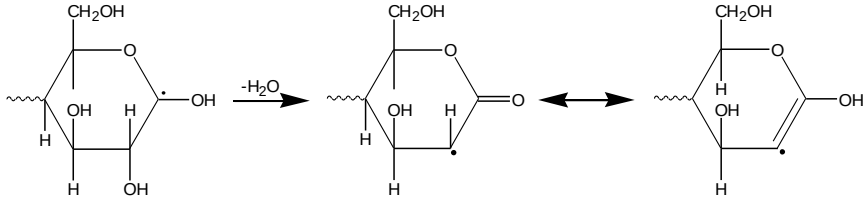

(12)

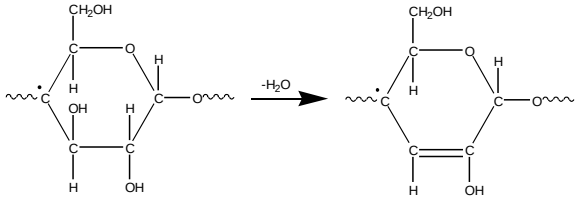

(13)

This process is detected by ESR method [3, 15, 57]. In turn, -C=C- conjugation destabilizes C-O bonds. That can also result in isolation and removal of an organic fragment or disclosing of pyranose ring. For example, the C(4) radical via reaction (7) and subsequent dehydration and decarboxylation can be transformed to a short-lived fragment which in turn can be the predecessor of furfuryl alcohol and furfural:

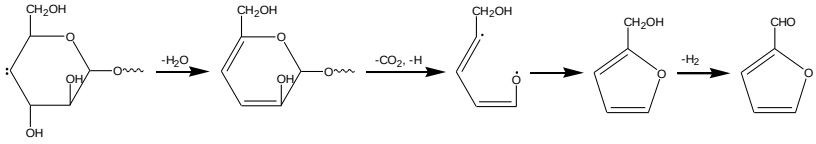

(14)

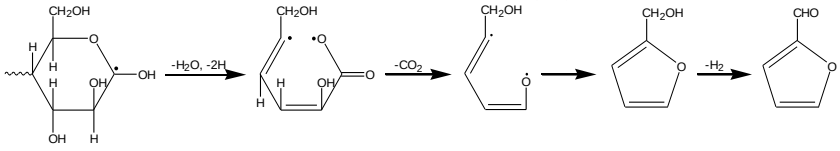

(15)

The organic fragment liberated from glucopyranose unit can have several configurations depending on following factors: a place of C-H bond cleavage and localization position of unpaired electron in ·R radical; a position of the olefinic bond arising via dehydration or dehydrogenation; excess energy and local temperature; content and configuration of hydrogen bridges system; the steric factor controlling a removal of fragmentation products from the origin place; and some other. Presence of several shapes of the liberated fragment predetermines several paths of its stabilization.

Cleavage of C-C bonds can precede dehydration and decarboxylation of radicals. It is shown, in particular, by a low yield of water and high yield of carboxylic acids and saturated $-CH_3$ or $-CH_2-$ derivatives. Hence, the wide assortment of the final products resulting from splitting of C-C bond in the liberated fragment is observed, for example

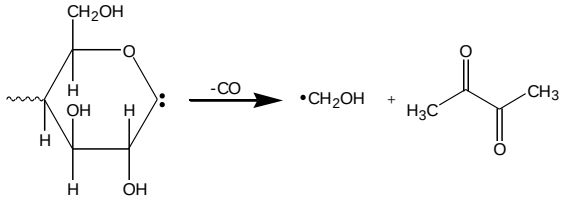

(16)

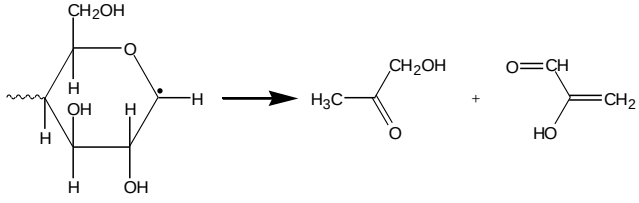

(17)

Chain propagation of cellulose destruction is caused by transformation of large primary radicals ·R into shorter secondary ones being also thermally astable. The rigid fixing of fragments by ambient molecules can interfere with their removal. In this case allyl radicals can be transformed into polyene radicals, which are more stable and precede to a charcoal formation.

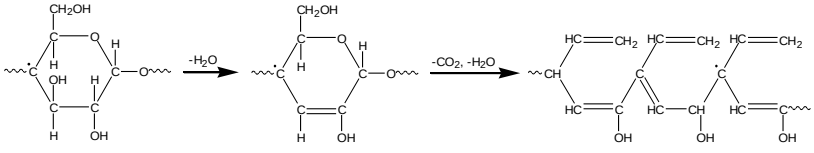

(18)

Being an effective scavengers of radicals and excess energy, a part of organic fragments (for example, furfural) participates in fast reactions with other fragmentation products or decomposes - it results in expansion of assortment of final products.

Cellulose conserves a hard state and is turning yellow at low dose rate (~0.15 kGy/s) insufficient for effective heating and a distilling initiation. A condensate and charcoal yields at post-radiation (dose ~500 kGy) dry distillation are about 47 and 32 wt %, respectively. Significant decrease of a condensate yield in comparison with electron-beam distillation testifies to the important role of the reactions proceeding directly at radiolysis. Post-radiation dry distillation deals exclusively with thermal degradation of stable molecular fragments of the cellulose having reduced degree of polymerization. Probably, the intermediates participating in pyrolitic destruction process differ from products of radiolytic reactions (6) and (7). Accordingly, yields of electron-beam destruction differ from post-radiation destruction yields.

Apparently, electron-beam distillation of C2 and C3 pine cellulose samples yields different effects owing to distinction of methods of chemical pine treatment applied at cellulose production. The remaining content of lignin and hemicelluloses in cellulose depends on an applied technique of digestion and bleaching of wood feedstock [2].

Thus, the main effect of electron-beam distillation of various type of cellulose is formation of a liquid organic condensate. Furfural and its derivatives dominate among liquid products. Both crushing and a preliminary heating of a feedstock promote an increase of furans fraction in condensate. The explored mode of electron-beam distillation can become a

key to development of perspective methods of furans production from widespread plant materials (including a wastage).

ELECTRON-BEAM DISTILLATION OF LIGNIN AND BINARY MIXTURES

Radiolytic destruction of cellulose as a part of wood (in situ) is less productive, than destruction of the purified cellulose fiber [58-60]. Apparently, cellulose protection in the bulk of irradiated wood is caused by an excitation energy transfer from cellulose to more stable aromatic groups of lignin [61,62].

Lignin is the second widespread vegetative polymer, however it is one of the most difficult for studying. It is polyphenolic branched polymer without regular alteration of repeating units, unlike cellulose and proteins. The primary structural units of lignin are *p*-hydroxycinnamic alcohols (Figure 10): p-coumaryl ($R_1 = R_2 = H$), coniferyl ($R_1 = H$, $R_2 = OCH_3$), and sinapyl ($R_1 = R_2 = OCH_3$) alcohols. The molecular chain of lignin is a combination of largely 4 types of phenoxyl radicals, of which the radical with the unpaired electron localized on the phenolic oxygen is the most significant [2]. Lignin is a waste of cellulose production and has smaller application. At the same time, annual world output of lignin exceeds 50 million tons [2, 63].

Protective action of lignin in wood was revealed via studying of the quantitative and qualitative content of radiolytic radicals [62, 64]. The irradiated wood contains both cellulose origin radicals (as in the purified cellulose fiber) and phenoxy radicals originated from lignin. In ESR spectrum of the foliar wood irradiated at 60 kGy and 77 K the signal of lignin radicals dominates in spite of the fact that about 70 % of wood mass consist of carbohydrates (cellulose and hemicellulose). In an aspen wood an yield of lignin type radicals is 1.7, whereas a yield of cellulose origin radicals is 0.8. In turn, a yield of cellulose radicals in the purified aspen cellulose is 2.7.

Hydrolytic lignin containing 10 wt % cellulose was studied under electron-beam distillation.

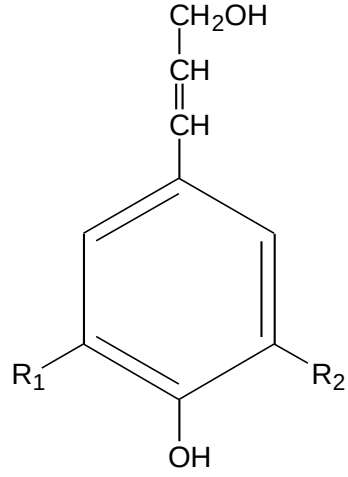

Figure 10. A primary structural unit of lignin.

The composition of the tar obtained via conventional dry distillation and electron-beam distillation of the lignin is given in the Table 7. In the case of thermal treatment, the tar consists of a wide variety of aromatic compounds with a relatively high mass fraction: the chromatogram contains about 50 peaks. The most significant components are toluene, xylenes, phenol, guaiacol, and creosol. The dry distillation products also include furfural, furanmethanols, and 5-methylfurfural. Their formation is presumably due to the cellulose admixed to the initial lignin samples.

The range of products narrows in the case of electron-beam degradation of lignin: the chromatogram of the tar contain 35 peaks, of which only 27 coincide with those of the dry distillation products [4, 5]. The base of the radiolytic tar is formed mainly by two compounds, guaiacol and creosol. However, the total yield of tar during electron-beam distillation is almost three times higher.

It is important to note that the fraction of alkylbenzols among products of radiolysis is lowered. The phenols and alkoxyphenols are the predominant liquid radiolytic products. Methane prevails among gaseous products. The formation of stable products of radiolytic fragmentation of aromatic macromolecules is determined mainly by radical processes [1, 2]. Radiolysis results primarily in the abstraction of hydrogen atoms from saturated substituents in the lignin molecule Lig.

Table 7. Main products of ordinary dry distillation (mode T) and electron-beam distillation (mode R) of lignin, wt %

Products	Mode		
	T	R (4.8 kGy/s)	R (3.6 kGy/s)
Chared residue	56.1	48.8	46.8
Gas	20.5	15.8	18.9
Aqueous distillate fraction	16.2	16.8	15.3
Tar: total	7.2	18.6	19.0
including (wt % of tar):			
Methanol + Ethanol	0.5	1.0	0.4
Benzene	0.8	-	-
Methylbenzene (toluene)	8.7	0.2	0.2
Furfural	0.5	0.1	0.2
Furanmethanols (*total*)	0.8	0.2	0.1
Ethylbenzene	0,6	0.1	0.1
Dimethylbenzenes (*total*)	9.7	0.1	0.1
(1-Methylethyl)-benzene	1.1	-	-
Phenol	12.4	3.6	2.9
Ethyl-methylbenzenes (*total*)	2.2	0.1	0.1
4-Methyl-1-methoxybenzene	0.3	0.1	0.1
2-Ethyl-1,3-dimethyl-benzene	1.1	0.1	0.1
Methylphenols (*total*)	2.7	1.1	0.9
Methoxyphenols (*total, including guaiacol*)	38.6	57.7	60.2
Dimethylphenols (*total*)	2.5	2.2	1.8
4-Methyl-3-methoxyphenol	0.4	3.9	2.8
Dimethoxyphenols (*total*)	0.5	3.9	2.3
4-Methyl-2-methoxyphenol (creosol)	5.8	19.8	21.3
4-Ethyl-2-Methoxyphenol (4-ethylguaiacol)	0.8	3.0	3.8

A substantial part of H atoms is produced via the dissociation of hydroxyl groups yielding phenoxyl radicals ArO· [1, 2]

$$\text{Lig (ArOH)} \rightarrow \text{ArO}\cdot + \cdot\text{H} \quad . \tag{19}$$

Similar phenoxyl radicals ArO· can be formed via the rupture of ether bonds

$$\text{Lig (Ar-O-Ar)} \rightarrow \text{ArO}\cdot + \cdot\text{Ar} \tag{20}$$

The H atom easily reacting with an aromatic ring is being transformed into H-adduct [1, 2, 65]. Probably, an aromatic H-adducts have a low thermal stability. The decay of H-adduct takes place via cleavage of lateral C-C bond. The stable aromatic ArH molecule and the secondary R· radical are formed as a result

$$\text{Lig (ArR)} + \text{H}\cdot \rightarrow \text{LigH}\cdot \rightarrow \text{ArH} + \text{R}\cdot \tag{21}$$

Such an effect was reported for toluene [65]: alkylcyclohexadienyl radicals at elevated temperatures (<500°C) readily dissociate yielding benzene and the alkyl radical. Furthermore, it is known [1] that dealkylation products are formed with a higher yield than alkylation products in the radiolysis of alkylbenzenes.

The recombination of methyl and phenoxyl radicals gives a methoxy-derivants

$$\text{CH}_3 + \text{ArO}\cdot \rightarrow \text{ArOCH}_3 \quad . \tag{22}$$

In turn, the $\cdot\text{CH}_3$ radical is being transformed into methane by eliminating hydrogen from lignin

$$\cdot\text{CH}_3 + \text{Lig} \rightarrow \text{CH}_4 + \text{Lig}\cdot \quad , \tag{23}$$

or forms larger hydrocarbon by radical recombination

$$\cdot\text{CH}_3 + \cdot\text{CH}_3 \rightarrow \text{C}_2\text{H}_6. \tag{24}$$

The tar distilled off via electron-beam heating is distinguished by high antioxidizing ability, in particular, in processes of inhibition of styrene thermopolymerization. The Figure 11 collates the formation kinetics of the styrene thermopolymer in the presence of 0.025 wt % various inhibitors.

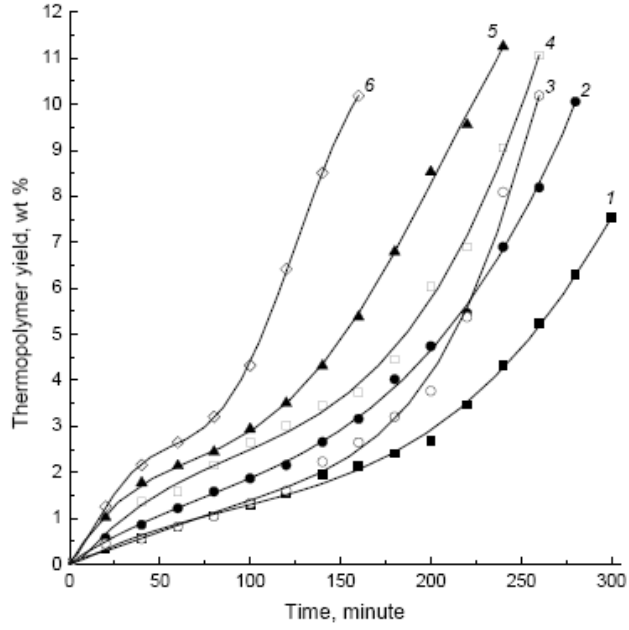

Figure 11. Polystyrene formation at 120 °C in the presence of 0.025 wt % various inhibitors: *1* - 4-dimethylaminomethyl-2,6-di-*tert*-butilfenol; *2* - tar; *3* - di(methylbenzyl)-phenols; *4* - bis-(2-oxy-5-methyl-3-*tert*-butylphenyl)-methan (Agidol-2); *5*- 2,6-di-*tert*-butyl-4-methylphenol (Agidol-1); *6* - (methylbenzyl)-phenols.

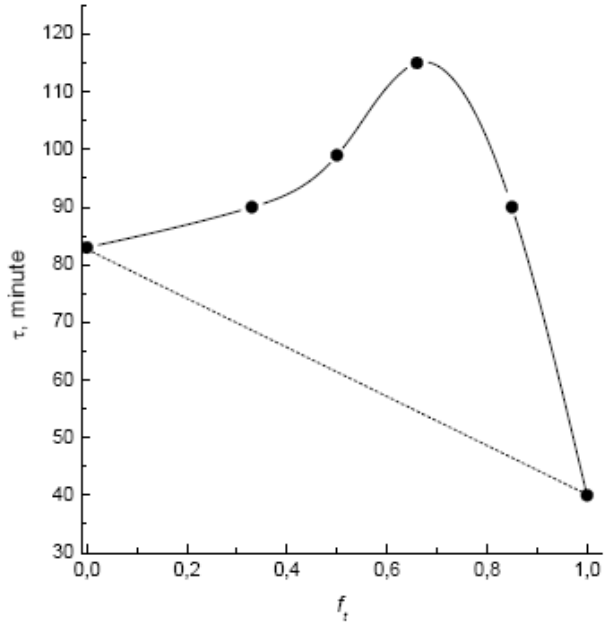

Figure 12. Induction periods τ of styrene thermopolymerization at 120°C in the presence of 0.05 wt % the mixed inhibitor consisting of tar and Mannich base (f_t - the tar fraction in the mixed inhibitor).

It is seen that all tested phenolic inhibitors are inferior in efficiency to the reference stabilizer Mannich base - 4-dimethylaminomethyl-2,6-di-*tert*-butilfenol (the curve *1*). Note that the structure of phenolic compounds has a considerable effect on their inhibiting activity. For example, monosubstituted phenols - methylbenzylphenols - are less effective than their disubstituted counterparts - di(methylbenzyl)phenols. The kinetic curves for the case of the di(methylbenzyl)phenol mixture (curve *3*) and for the case of the unpurified tar obtained via electron-beam distillation from lignine (curve *2*) are closer to the reference curve 1 than other curves. The inhibitory effect of commercial stabilizers Agidol-1 (2,6-di-*tert*-butyl-4-methylphenol) and Agidol-2 (bis-(2-oxy-5-methyl-3-*tert*-butylphenyl)-methan) was noticeably weaker than that of the tar. Moreover, the intermixture of tar with the Mannich base demonstrates a synergistic magnification of the inhibition ability (see Figure 12).

High inhibitory effect can testify to presence of polyhydroxy phenols in tar composition. Such components dominate in the fraction boiling at $t \geq 235$ °C. Thus, the tar generated by electron-beam distillation of wood or lignin can be applicable for practical production of polymerization retarders.

Lignin or lignocellulose affects productivity of electron-beam distillation of binary mixtures containing a synthetic polymer or a heavy oil hydrocarbon as the second component. Effective cracking of heavy hydrocarbons can be initiated by radiation [1], in particular, by electron-beam radiation [66]. At a temperature of $T \geq 300$°C, the radiolytic cleavage of bonds in hydrocarbon macromolecules is accompanied by the thermally stimulated chain destruction of generated radicals. The advantage of the radiation-initiated thermal cracking is the effective formation of radicals at temperatures below those required for conventional thermal cracking [1, 66]. Electron-beam destruction of wood components is controlled also by the chain mechanism. It is of interest to trace the simultaneous occurrence of two radiation-initiated chain processes using wood–bitumen mixtures as an example.

The electron-beam distillation of one-component samples differs in the rate — lignocellulose feedstock is distilled several times faster than the natural bitumen. In the study of bitumen and binary samples, the yields of distillation products were measured at a dose D= 300 kGy; i.e., within the dose sufficient to complete the distillation of lignocellulose, but insufficient to complete the distillation of individual bitumen. Irradiation was conducted at initial temperatures T_0 of 18 and 200°C. The observed dependences of the yield of liquid products of distillation on the feedstock composition are presented in the Figure 13.

At D = 300 kGy and T_0 = 18°C , about 60 and 28 wt % of organic liquid is distilled from pine wood and lignin, respectively. In turn, the yield of low-molecular condensate from the bitumen is 37 wt %. If the distillation of degradation products from binary mixtures of bitumen and wood sawdust obeyed additive rule, the total yield of distilled products G_Σ would decrease with an increase in the proportion of bitumen in the mixture (as shown by dotted line). However, the data in the Figure 10 show that G_Σ is higher than it should be expected from the additive rule. A similar effect is observed in mixtures of bitumen and lignin. At an initial temperature of the mixtures of T_0= 200°C, the dependence of G_Σ on the composition also indicates the presence of a synergistic effect.

The propagation step of the chain degradation process for bitumen hydrocarbons $R\dot{C}_nH_{2n-1}R'$ can be conventionally represented as a set [1] of radical reactions of hydrogen abstraction (25) and β-cleavage (26)

$$\dot{C}_mH_{2m}R + RC_nH_{2n}R' \rightarrow RC_mH_{2m+1} + R_i\dot{C}_nH_{2n-1}R' \quad (25)$$

$$R\dot{C}_nH_{2n-1}R' \rightarrow R\dot{C}_kH_{2k} + R'C_{n-k}H_{2(n-k)-1} \quad (26)$$

in which small radicals abstract hydrogen from a heavy hydrocarbon, and large radicals dissociate to alkenes and a small radical. The termination of the chain process is caused by dimerization or disproportionation of radicals.

It is quite likely that small intermediates of wood origin can be converted into final low-molecular products via the abstraction of hydrogen from bitumen components (similar to reaction (25)), thus contributing to the development of the thermally stimulated chain decomposition of hydrocarbons.

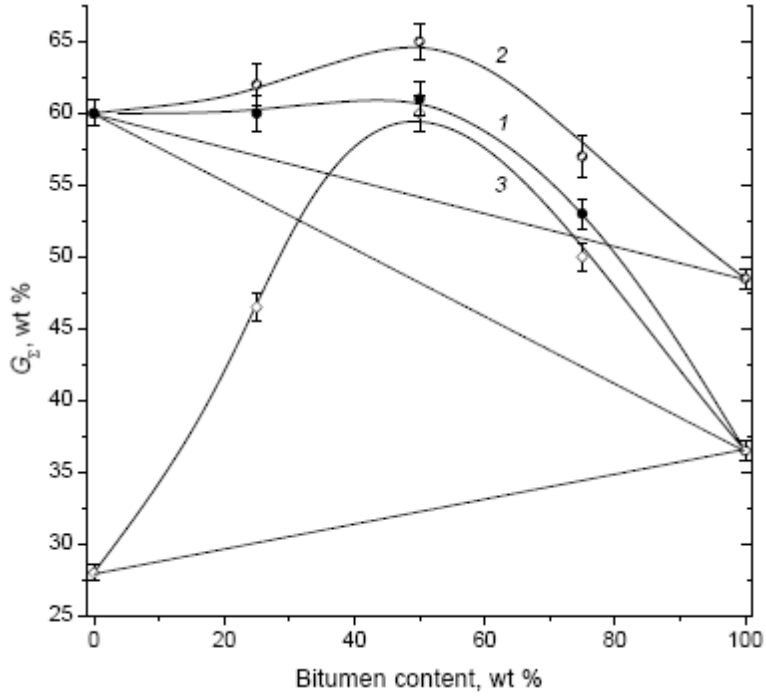

Figure 13. The dependence of the total yield of condensate G_Σ on the bitumen content in mixtures with (*1, 2*) pine sawdust and (*3*) lignin at initial feedstock temperature (*1, 3*) 18 and (*2*) 200°C.

The composition of products derived from the binary mixtures indicates the formation of compounds, the origin of which can be explained by cross combination of intermediates of wood and bitumen origin - alkyl acetates, phenyl acetates, alkylfurans, benzofurans, etc. The yield of these “hybrid” products makes up to 15% of the total yield of condensate.

Along with the participation in the chain transfer reaction, wood components can play a more sophisticated role. In particular, the starting binary mixtures have loose consistency, which could facilitate the distillation of bitumen degradation products from the irradiation area. In addition, light products of wood degradation can facilitate the distillation of heavy hydrocarbons owing to the “steam distillation” effect. Charcoal produced from the binary mixtures is crumbly, does not stick together, and is easy to withdraw from the reactor,

properties that compare it favorably with conventional coke produced by the cracking of bitumen.

It is important that wood and lignin degradation products act as inhibitors of radical polymerization [10]. They impede tarring in the bitumen fraction. For example, upon the distillation of binary mixtures, in which bitumen was replaced with polystyrene, we observed an almost complete recovery of styrene, which is usually easy to polymerize by heating. Increase of radiolytic destruction yield of synthetic polymers was observed also in the wood-polymer mixtures containing polyethylene-terephthalate, polyvinyl-acetate, polyethylene, polypropylene and some other.

Thus, under the conditions of electron-beam heating and distillation of binary mixtures of natural bitumen or synthetic polymer with wood, the synergistic increase in the yield of condensable products of their degradation has been revealed. The effect is due to an increase in the efficiency of the decomposition of mainly the non-wood fraction.

CONCLUSION

Thus direct productive conversion of wood into valuable chemicals can be implemented by means of the electron-beam distillation. Technical application of this method can be considered as reasonable prospect because electron-beam distillation is characterized by valuable performances: the chain mechanism, high yield of a organic condensate, selectivity, low enough energy consumption, and uniprocessing. Electron-beam conversion of wood into organic liquid can be interesting as initial stage for subsequent formation of various products in industry: effective polymerization retarders; monomers and reagents for polymeric production; the alternative liquid fuel; special types of wood charcoal; and some others.

Polymerization retarders. Phenolic retarders of polymerization are applied for a long time in the industry, in particular at styrene processing. Phenols of a coke-chemical and petrochemical origin are used more often in the today's polymeric industry. Vegetative lignin is the major reproducible source for phenols production. Conventional dry distillation of lignin or wood yields a mixture of benzenes and phenols whereas electron-beam distillation produces exclusively phenols (including dibasic phenols). It has been shown above that the crude tar obtained by distillation of lignin has higher inhibiting effect in comparison with many other industrial inhibitors. The same tar immixed with 4-dimethylaminomethyl-2,6-di-*tert*-butilphenol yields synergetic inhibiting effect in styrene. High yield of the active aromatic tar allows to regard the electron-beam distillation of lignin and coniferous wood as one of competitive paths for production of industrial polymerization retarders, antioxidants and stabilizers of monomers.

Monomers. Many household plastics easily decompose under the influence of electron-beam processing in the presence of lignocelluloses. Monomers or the low-molecular-weight oligomers formed as a result can be distilled off at stable state. Lignocelluloses destruction products react as inhibitors interfering with backward polymerization reactions. Such effect can be applied to processing of a complex domestic wastes (paperstock and plastics) for the purpose of regeneration of low-molecular-weight chemical raw materials. At the same time, the condensates forming by electron-beam distillation of lignocelluloses consist also of the molecules having olefin bonds and the active carbonyl groups. Similar substances are widely

used both as monomers and as auxiliary reagents in various polymerization processes [67]. In the present work effective formation of polymers was observed at a heating or boiling of the condensates originated from purified cellulose. As the yield of condensates from woods is more than 50 wt % the electron-beam distillation attracts attention as a productive mode for prospective formation of useful monomers and reagents.

The alternative fuel. Liquid products from electron-beam distillation cannot be used directly as fuel. Presence of nonsaturated bonds and the active functional groups promotes undesirable chemical interaction (dehydration, polyfunctional condensation, etc.) between components in condensates. Alkanes, benzenes, aliphatic alcohols, ethers and esters are usually perceived as suitable components for liquid fuel [68]. Tetrahydrofuran derivatives are also considered as a proper component for high-octane engine fuels [69].

Our experiments indicate that hydrogenation and/or alkylation of organic vapors from electro-beam distillation of wood feedstock can yield stable fuels (motor, diesel, reactive or boiler fuels). The radiolytic variant of such transformation follows from observed influence of gas flow rate on condensate composition [6]. Participation of gaseous alkanes or hydrogen in radiolytic destruction of a vegetative feedstock results in several effects. Gas flow facilitates removal of fragmentation products from feedstock being irradiated. High dilution of vapour by the gas prevents both secondary processes of vapour fragmentation and undesirable reactions between vapour components. Hydrogenous containing molecules RH used as carrier gas contribute to the radiolytic formation of ·H atoms and alkyl radicals ·R [1, 70]

$$RH^* \rightarrow \cdot R + \cdot H \qquad (4)$$

initiating both chain decomposition of feedstock and processes of hydrogenation and alkylation of the fragmentation products

$$=C=C= + \cdot R \rightarrow =CR–\dot{C}= \quad , \qquad (27)$$

$$=C=O + \cdot R \rightarrow =\dot{C}–OR \quad . \qquad (28)$$

As a consequence the hydrocarbonaceous part in vapour molecules elongates but the vapour unsaturation degree (instability) is being decreased. At last, radiolysis of the gas results in a condensates enrichment by valuable fuel components - branched alkanes [71]. The intermediates formed from carrier gas react preferentially with unsaturated vaporous as scavengers therefore the utilization yield of gas also increases due to prevention of its regeneration.

Earlier we have shown [6] that the birchwood in a methane flow can be transformed to the liquid engine fuel having proper fractional composition and octane value > 90. High dose rate (to prevent synthesis of high-molecular compounds) and low concentration of vapours in a vapour-gas mixture (to preclude polycondensation) are the important parameters needed to formation of qualitative fuel.

As it has been shown above, electron-beam processing of native bitumen or high-viscosity oil in the presence of lignocellulose can be used too in fuel production. Destruction of lignocelluloses influences comprehensively the destruction of heavy hydrocarbons, incrementing a yield of easy fragments at rather small heating.

Wood charcoal. Conventional dry distillation yields the wood charcoal essentially differing on composition and structure from the chared residue formed by electron-beam distillation [5]. Carbonification is incomplete in both modes. But electron-beam mode produces wood charcoal, conserving an ordered structure of initial cellulose fibers and lignin aggregates. In turn, conventional dry distillation results in charcoal deformations and a sintering. The structural distinctions of wood charcoals can appear interesting from the point of view of development of new sorbents and catalytic agents.

Thus, the present work demonstrates possibility of effective transformation of lignocellulose matters into liquid organic products by electron-beam distillation. Conventional dry distillation results in large amount of both water and charcoal whereas the electron-beam heating produces much more organic liquid. Fermentative formation of bioethanol and biosolar oil is also less productive than electron-beam conversion of a vegetative feedstock into organic liquid. Besides, both enzymatic and hydrolytic processes result in large volume of wastewater, its handling is extremely labour-consuming and expensive [1]. A residual product of the discussed electron-beam conversion is wood charcoal - ordinary and convenient hard fuel or a sorbent.

High efficiency of electron-beam distillation can be a key to development of wasteless methods for plant materials transformation into the useful products, such as polymerization retarders, monomers or the alternative fuel.

ACKNOWLEDGMENT

This work was supported within the Program "Fundamental Problems in Power Industry" (principals - academician Moiseev I.I. and academician Myasoedov B.F.) of the Presidium of the Russian Academy of Sciences. Authors express gratitude to academician Tsivadze A.Yu. for the help and support.

REFERENCES

[1] Woods, R. J. and Pikaev, A. K. Applied Radiation Chemistry: Radiation Processing; Willey Interscience: New York, 1994.
[2] Fengel, D.; and Wegener, G. Wood (Chemistry, Ultrastructure, Reactions); Walter de Gruyter: New York. 1984.
[3] Ershov, B. G. Russ. Chem. Rev. 1998, 67, 315.
[4] Chulkov, V. N.; Bludenko, A. V.; Ponomarev, A. V. High Energy Chem. 2007, 41, 470.
[5] Ponomarev, A. V.; Bludenko, A. V.; Chulkov, V. N.; Liakumovich, A. G.; Yakushev I. A.; Yarullin, R. S. Mendeleev Commun. 2008, 18, 156.
[6] Ponomarev, A. V.; Tsivadze, A. Yu. Doklady Phys. Chem. 2009, 424, 57.
[7] Ponomarev A. V. Radiat. Phys. Chem. 2009, 78, 345.
[8] Obryadchikov, S. N. Production of Motor Fuels; Gostoptechizdat: Moskow. 1949 (in Russian).
[9] Byakov, V. M.; Nichiporov, F. G. Intratrack chemical processes; Energoatomizdat: Moscow. 1985 (in Russian).

[10] Shalyminova, D.P.; Cherezova, E.N.; Ponomarev, A.V.; Tananaev, I.G. High Energy Chemistry. 2008, 42, 342.
[11] Ponomarev, A. V.; Makarov, I. E.; Ershov, B. G.; Tsivadze, A. Yu. Doklady Phys. Chem. 2007, 416 (part 2), 271.
[12] Ponomarev, A.V.; Makarov, I. E.; Saifullin, N. R.; Syrtlanov, A. Sh.; Pikaev, A. K. Radiat. Phys. Chem. 2002, 65, 71.
[13] Bludenko, A.V.; Ponomarev, A. V.; Chulkov V. N. High Energy Chem. 2009, 43, 83.
[14] Kusama, Y.; Kageyama, E.; Shimada, M.; Nakamura Y. J. Appl. Polym. Sci. 1976, 20, 1679.
[15] Kuzina S.I., Mikhailov A.I. Russ. J. Phys. Chem. A. 2006, 80, 1874.
[16] R.Imamura, T.Uena, K.Murukami. Bull. Inst. Res. Kyoto Univ. 1972, 50, 51.
[17] Sultanov, K.; Azizov, U. A.; Usmanov H. U. Doklady Phys. Chem. 1989, 309, 907.
[18] Sakurada, I.; Okada, T.; Kaji, K. J. Polym. Sci., Part C, Polym. Lett. 1972, 37, 1.
[19] Ershov, B. G.; Samuilova, S. D.; Petropavlovskii, G. A.; Vasileva, G. G. Doklady Phys. Chem. 1984, 274, 102.
[20] Ershov, B. G.; Isakova, O. V.; Matyushkina, E. P.; Samuilova, S. D. Cellul. Chem. Technol. 1987, 21, 331.
[21] Ershov, B. G.; Komarov, V. B.; Samuilova, S. D. Cellul. Chem. Technol. 1987, 21, 457-.
[22] Klimentov, A. S.; Petropavlovskii, G. A.; Kotelnikov, N. E.; Skvortsov, S. V.; Volkova, L. A. Cellul. Chem. Technol. 1985, 19, 251.
[23] Ershov, B. G.; Isakova, O. V.; Matyushkina, E. P.; Samuilova, S. D. High Energy Chem. 1986, 20, 142.
[24] Blouin, F. A.; Arthur, J. C. Textile Res. J. 1958, 29, 198.
[25] Arthur, J.; Blouin, F. A.; Demint, R. J. Am. Dyes Rep. 1960, 49, 383.
[26] Burczak, K.; Pekala, W.; Rosiak, J. Wiad. Chem. 1983, 37, 193.
[27] Bludovsky, B.; Duchacek, V. J. Radiochem. Radioanal. Lett. 1979, 38, 21.
[28] Duchacek, V.; Bludovsky, R. J. Radiochem. Radioanal. Lett., 1979, 38, 31.
[29] Bludovsky, R.; Prochazka, M.; Kopoldova, J. J. Radioanal. Nucl. Chem. 1984, 87, 69.
[30] Komarov, V. B.; Samuilova, S. D.; Kirsanova, L. S.; Morozov, V. A.; Kuleshova, T. M.; Smirnov, A. G.; Ershov, B. G. Russ. J. of Appl. Chem. 1993, 66, 393.
[31] Horio, M.; Imamura, R.; Murukami, K. Butt. Inst. Res. Kyoto Univ. 1965, 43, 117.
[32] Dilli, S.; Garnet, J. L. Chem. Ind. (London). 1963, 409.
[33] Nekhaichuk, A. D.; Evdokimov, A. M.; Kitaev, S. Kh.; Moskaleva, V. E.; Yatsenko-Khmelevskii, A. A. Chem. of Wood (Russian). 1974, (1), 32.
[34] Freidin, A. S. Action of ionizing radiation on wood and its components; Nauka: Moscow, 1961; 75.
[35] Florin, R.; Wall, L.; Brown, D. Trans. Faraday Soc. 1960, 56, 1304.
[36] Makatun, V. N.; Potapovich, A. K.; Ermolenko, N. N. Polymer Science. 1963, 5A, 467.
[37] Baugh, P. J.; Hinojosa, O.; Arthur, J. J. Appl. Polym. Sci. 1967, 11, 1139.
[38] Arthur, J.; Hinojosa, O.; Tripp, V. W. J. Appl. Polym. Sci. 1969, 13, 1497.
[39] Arthur, J. C.; Mares, T.; Hinojosa, O. Textile Res. J. 1966, 36, 630.
[40] Dilly, S.; Ernst, J. T.; Garnet, J. Aust. J. Chem. 1967, 20, 911.
[41] Worlungton, K.; Baugh, P. Cellul. Chem. Technol. 1971, 5, 23.
[42] Hinojosa, O.; Nakaraura, Y.; Arthur, J. J. Polym. Sci., Pan C. Polym. Lett. 1972, 37, 27.
[43] Siraionescu, Cr.; Butnaru, R.; Rosmarin, Gh. Cellul. Chem. Technol. 1973, 7, 153.

[44] Khamidov, D. S.; Azizov, U. A.; Milinchuk, V. K.; Usmanov, H. U. Polymer Science. 1972, 14A, 838.
[45] Shimada, M.; Nakamura, Y.; Kusama, T.; Matsuda, O.; Kageyama, E. J. Appl. Polym. Sci. 1974, 18, 3387.
[46] Gaponova, I. S.; Pariiskii, G. P.; Toptygin, D. Ya. Polymer Science. 1977, 19B, 706.
[47] Ershov, B. G.; Klimentov, A. S. Polymer Science. 1977, 19A, 808.
[48] Klimentov, A. S.; Ershov, B. G.; Bykov, A. E. Chem. of Wood (Russian). 1977, (2), 74.
[49] Plotnikov, O. V.; Mikhailov, A. I.; Payavee, E. L. Polymer Science. 1977, 19A, 25.
[50] Hon, N.-S. J. Macromol. Sci. Chem., 1976, A10, 1175.
[51] Golova, O. P. Russ. Chem. Rev. 1975, 44, 687.
[52] Takeshi, S.; Shosaki, K. Nucl. Eng. (Jpn.), 1977, 23, 41.
[53] Ershov, B. G.; Komarov, V. B. Polymer Science. 1985, 27B, 132.
[54] Ershov, B. G.; Komarov, V. B.; Samuilova, S. D. Polymer Science. 1985, 27B, 430.
[55] Ponomarev, A. V.; Bludenko, A. V.; Chulkov, V. N.; Tananaev, I. G.; Myasoedov, B. F.; Tsivadze, A. Yu. High energy Chem. 2009, 43, 350.
[56] Scherbakov, A. A. Furfural; Kiev: Gos. Izd-vo Tekhn. Lit-ry USSR, 1962 (in Russian).
[57] Kuzina, S. I.; Mikhailov, A. I. Russ. J. of Phys. Chem. A. 2005, 79, 1115.
[58] Arnapalskii, I. N.; Skrigan, A. I.; Kuprina, N. S. Chem. of Wood (Russian), 1975, (1), 126.
[59] Sergeeva, V. N.; Kreitsberg, Z. N.; Yakobsone, M. Ya. Chem. of Wood (Russian). 1976, (5), 58.
[60] Ficher, K.; Goldberg, W.; Wilke, M. Lenzinger Ber. 1985, 33.
[61] Campbell, F.J. Radial. Phys. Chem. 1981, 18, 109.
[62] Ershov, B. G.; Isakova, O. V.; Komarov, V. B.; Matyushkina, E. P. Chem. of Wood (Russian). 1986, (1), 6.
[63] Zakis, G.F. Functional Analysis of Lignins and Their Derivatives. Zinatne: Riga, 1987 (in Russian).
[64] Kuzina, S. I.; Demidov, S. V.; Brezgunov, A. Yu.; Poluektov, O. P.; Grinberg, O. Ya.; Dubinskii, A. A.; Mikhailov, A. I.; Lebedev, Ya. S. Physics and chemistry of the elemental chemical processes. Reports of 5th All-Russia Conference. Chernogolovka. 1997, 310 (in Russian).
[65] Amano, A.; Horie, O.; Hanh, N.H. Int. J. Chem. Kinet. 1975, 8, 321-340.
[66] Bludenko, A.V.; Ponomarev, A.V.; Chulkov, V.N.; Yakushev, I.A.; Yarullin, R.S. Mendeleev Commun., 2007, 17, 227.
[67] Sykes, P. A guidebook to mechanism in organic chemistry, Longman: London. 1971.
[68] Ponomarev, A.V. Mendeleev Commun. 2006, 5, 256.
[69] Paul, S. F. Alternative Fuel, US Pat. No. 5,697,987; 1997.
[70] Cserep, G.; Gyorgy, I.; Roder, M.; and Wojnarovits; L. Radiation Chemistry of Hydrocarbons, Akademiai Kiado: Budapest. 1981.
[71] Ponomnarev, A. V.; Tsivadze, A. Yu. Dokl. Phys. Chem. 2006, 411 (part 2), 345.

In: Wood: Types, Properties and Uses
Editor: Lorenzo F. Botannini
ISBN 978-1-61668-837-0

Chapter 3

BIOMASS FOR DOMESTIC AND AGRO INDUSTRIAL APPLICATIONS

N.L. Panwar [1]
Department of Renewable Energy Sources,
College of Technology and Engineering, Maharana Pratap
University of Agriculture and Technology, Udaipur,
313 001 Rajasthan, India

ABSTRACT

Biomass in a holistic view produces food, fodder, fuel, fiber and fertilizer. There are a number of simple, efficient and convenient biomass-based systems for different domestic, agro-industrial and agricultural applications. The replacement of conventional fossil fuels with biomass for thermal energy production results both in a net reduction of greenhouse gas emissions and in the replacement of conventional energy sources. Biomass energy accounts for about 11% of the global primary energy supply, and about 2 billion people worldwide depend on biomass for their energy needs. Modern applications of biomass cover not only industrial thermal application and electricity production, but also include domestic applications through improved cookstoves, wood gas stoves and gasifier. Combustible producer gas extracted from gasifier is effectively and economically converted from low value solid biomass fuel to a gaseous mixture. This gaseous mixture can be used to generate processing heat for thermal application. In this chapter, various biomass conversion routes such as thermo chemical, bio-chemical and agro chemical conversion have been covered, which includes improved cookstoves and biomass gasifier. The thermo chemical conversion process starts from a direct combustion process to more efficient gasification process, which includes pyrolysis, gasification and improved cookstoves. A gasification system to generate processing heat for baking bakery items and drying of phosphoric acid through open core down draft type; durable biomass cookstove for domestic, agro industrial and community applications; and a gasification-based wood stove for cooking application are discussed. The natural draft gasifier to generate thermal heat to extract chemical components from

[1] Email- nlpanwar@rediffmail.com.

medicinal plants, fuel replacement and greenhouse gas mitigation potential through installation of biomass gasifier and cookstoves are also discussed in this chapter.

1. INTRODUCTION

A comprehensive thrust on use and application of renewable-energy-based appliances at the domestic, commercial and industrial level has been strongly impacted by global warming. The environmental impact from the use of fossil fuel has induced the Europian Union (EU) to take action in order to increase the share of renewable energy sources (RES) on the energy market [1]. The "White Paper on Renewable Energy" [2] set the target of doubling the share of renewable energy from the (1997) level of 6% to 12% by 2012. Biomass is the most common form of renewable energy, widely used in the developing countries as the primary source of domestic energy. Biomass usually had been considered as a low status fuel, associated with poverty and the past. This is reflected in the poor quality of official statistics relating to biomass energy although this is now improving. [3]. It is accepted both for thermal application and power generation at the industrial level. Combustion of biomass in a controlled manner cut CO_2 emission because whatever CO_2 is released during combustion, is consumed by the growing agriculture crops. Hence it is a carbon neutral source of energy. However, the CO_2 released during its transportation needs to be considered to find out the net emission.

2. BIOMASS

2.1. Introduction

The term "biomass" generally refers to renewable organic matter generated by plants through photosynthesis. Materials having organic combustible matter are also referred to under the term biomass. [4-5]. It is an important fuel source in our overall energy scenario. Biomass is produced through chemical storage of solar energy in plants and other organic matter as a result of photosynthesis. During this process, conversion of solar energy into sugar and starch, which are energy-rich compounds, takes place. The chemical reaction of photosynthesis can be written as:

$$6CO_2 + 6H_2O + \text{sun light} \rightarrow C_6H_{12}O_6 + 6O_2 + 2.66MJ$$

It indicates that the storage of 2.66 MJ is associated with the transfer of 72 gm carbon into organic matter. Biomass can be directly utilized as fuel or can be converted through different routes into useful forms of fuel. In fact, biomass is a source of five useful agents, which start with "F" like food, fodder, fuel, fiber and fertilizer. Further, biomass has many advantages such as the following:

1) It is widely available
2) Its technology for production and conversion is well understood.

3) It is suitable for small or large applications
4) Its production and utilization require only low light intensity and low temperature (5–35°C)
5) It incorporates advantage of storage and transportation
6) Comparatively, it is associated with low or negligible pollution.

2.2. Biomass Classification

Biomass includes plantation that produces energy crops, natural vegetable growth and organic wastes and residues. The biomass classification is illustrated in Figure 1. It can be grouped as:

1) Agricultural and Forestry Residues: Silviculture Crops.
2) Herbaceous Crops: Weeds, Napier grass.
3) Aquatic and marine biomass: Algae, water hyacinth, aquatic weeds, plants, sea grass beds, kelp and coral reefs, etc.
4) Wastes: Municipal solid waste, municipal sewage sludge, animal waste and industrial waste, etc.

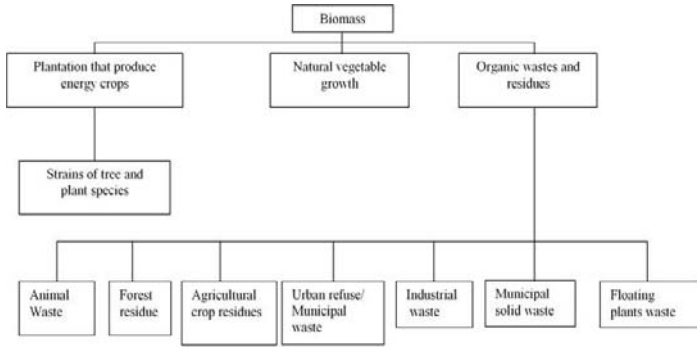

Figure 1. Biomass Classification.

2.2. Biomass of properties

Proximate analysis few biomasses were presented in Table 1. This biomass is suitable to convert to useful fuel through thermo chemical conversion route [6].

Thermal behaviour of few biomass including devolatisation temperature, weight losses and volatile yield is as follows:

Tuwar and Urad **(***Vigna radiata)*

This fuel has low ash content and high ash deformation and fusion temperature is apparently suitable for gasification. The devolatisation initiates at 290^{o}C and approaches completion by 650 ^{o}C with the maximum occurring at about 390^{o}C at a rate of 0.48% weight loss per ^{o}C. The total volatiles yield is as high as 84%

Groundnut Shell (Vigna mungo L)

High fixed carbon content, medium range ash content and ash fusion temperature make this fuel apparently suitable for gasification. The devolatilisation starts at 300°C and approaches completion by 720°C, the maximum occurring at 505°C , at a rate of 0.67% wt loss per °C. The total volatiles yield on pyrolysis is 68%

Rape and Mustard shell (Brassica napus and Sisymbrium officinale)

It is high ash content fuel coupled with high ash deformation temperature. It is apparently suitable for gasification. The devolatilisation starts at about 300 ^{o}C and completes by 550 ^{o}C. The maximum pyrolysis rate of 0.67% wt loss per ^{o}C is at 370 ^{o}C. The total volatiles yield during pyrolysis is about 62%.

Soya bean Shell (*Glycine max)*

The fuel is having medium ash content and high ash fusion temperature, it is apparently suitable for gasification. The high calorific value adds to its advantages. The devolatilisation initiates at about 280 ^{o}C and approaches completion by 510 ^{o}C with a maximum occurring at 385 ^{o}C wt during pyrolysis is about 69%

Cotton Stalk (*Gossypium spp.)*

Cotton Stalks have high fixed carbon, low ash content with high fusion temperature. It is suitable for gasification. The devolatilisation starts at 280 ^{o}C and reaches to near completion by 520 ^{o}C, the maximum occurs at 390 ^{o}C with a rate of 0.70% at loss per ^{o}C. The total volatiles yield on pyrolysis is 64%.

Gram Shell (Vigna mungo L)

This biomass is having low ash content but very low ash deformation and fusion temperature. Possibility of clinker formation is high. The maximum is at 375 ^{0}C with a rate of 0.45% at loss per ^{0}C. The total volatiles yield on pyrolysis is 80%.

2.3. Energy Potential

To mitigate climatic change caused by greenhouse gas emissions, the developed nations are working to substitute fossil fuels with renewable energy sources. To stabilise the atmospheric concentration of CO_2, global emissions must be reduced by at least 60% from the current levels [7]. It is estimated that there are 3870 (10^6) ha of forest worldwide or 30% of the earth's land area, of which about 95% are natural forests and 5% are plantations. Tropical and subtropical forests comprise 56% of the world's forests, while temperate and boreal forests account for 44% [8].

The potential of biomass energy derived from forest and agricultural residues world-wide is estimated at about 30 EJ/yr, compared to an annual world-wide energy demand of over 400 EJ [4]. Nevertheless, about 10–15% (or 45±10 EJ) of this demand is covered by biomass resources, making biomass by far the most important renewable energy source used to date. On average, in the developed nations biomass contributes some 9–13% to the total energy supplies, but in developing countries the proportion is as high as a fifth to one third. In quite a number of under developed countries biomass covers even over 50–90% of the total energy demand. A large part of this biomass use is however non-commercial and used for cooking and space heating, generally by the poorer part of the population [9].

Table 1. Proximate analysis of biomass

S.No.	Properties	Saw dust	Rice straw *(Oryza sativa L)*	Tuwar and Urad *(Vigna radiata)*	Groundnut shell *(Arachis hypogaea)*	Rape and Mustard shell *(Brassica napus and Sisymbrium officinale)*	Soya bean Shell *(Glycine max)*	Cotton Stalk *(Gossypium spp.)*	Gram shell *(Vigna mungo L)*
1.	Fixed carbon (FC), %	16.35	5.70	14.8	25	14.5	16.7	22.4	17.1
2.	Volatile Matter (VM), %	70.55	69.11	83.5	68.1	70.1	75.1	70.9	80.3
3.	Ash %	0.83	15.23	8	6.9	15.4	3.0	6.7	2.7
4.	C, %	45.66	33.96	46.75	44.78	46.2	45.71	43.64	56.45
5.	H, %	4.86	5.01	6.55	6.08	6.21	5.89	5.81	8.99
6.	Calorific Value (CV) MJ kg^{-1}	18.06	15.17	15	17.2	17.61	16.1	18.26	19.64
Ash Characteristics									
7.	Deformation Temperature (^oC)	1370-1400	1380-1400	1250-1300	1180-1200	1350-1400	1300-1350	1320-1380	800
8.	Fusion Temperature (^oC)	1435-1475	1430-1500	1460-1500	1220-1250	1400-1450	1420-1450	1400-1450	800-900

In 1992 at the Rio United Nations Conference on environment and development, the renewable intensive global energy scenario (RIGES) suggested that, by 2050, approximately half the world's current primary energy consumption of about 400 EJ/yr, could be met by biomass and that 60% of the world's electricity market could be supplied by renewable, of which biomass is a significant component [10].

3. BIOMASS CONVERSION

Basically there are three different routes for producing energy from biomass in different form i.e., heat, electricity and liquid fuel for transportation. These routes are thermo chemical conversion of biomass where the biomass convert into fuel at elevated temperature and controlled combustion conditions. Direct combustion, gasification and pyrolysis considered as thermo chemical conversion routes. Second conversion routes is biochemical conversion, in this routes digestion and fermentation processes taking into account. Third one is extraction of transportation oil through esterification of non edible oil. Conversion of biomass into fuel through different routes were illustrated in Figure 2

3.1. Direct Combustion of Biomass

Domestic energy requirement for cooking and space heating leads to direct combustion of biomass with energy efficient combustion devices. Further, electrical power generation is quite possible through dendro thermal route. It is basically involves combustion of biomass externally. The thermal energy is converted into shaft power either directly or through various inter-mediate stages of conversion, involving steam or the organic fluid etc.

Basically it consists of the following components:

a) Dryer
b) Boiler
c) Steam Turbine
d) Condenser
e) Generator

The dryer is used to reduce the dampness of the uneven wood to a lower level. In the dryer a part of the flue gas from the boiler, supplies the drying energy. The dried wood is fed into the boiler. It is then burnt in suspension in the boiler to raise a high-pressure steam.

As far as power generation from dendro thermal based power generation is concerned it makes use three commonly available thermodynamic cycles i.e. Brayton, Stirling or Rankine cycles.

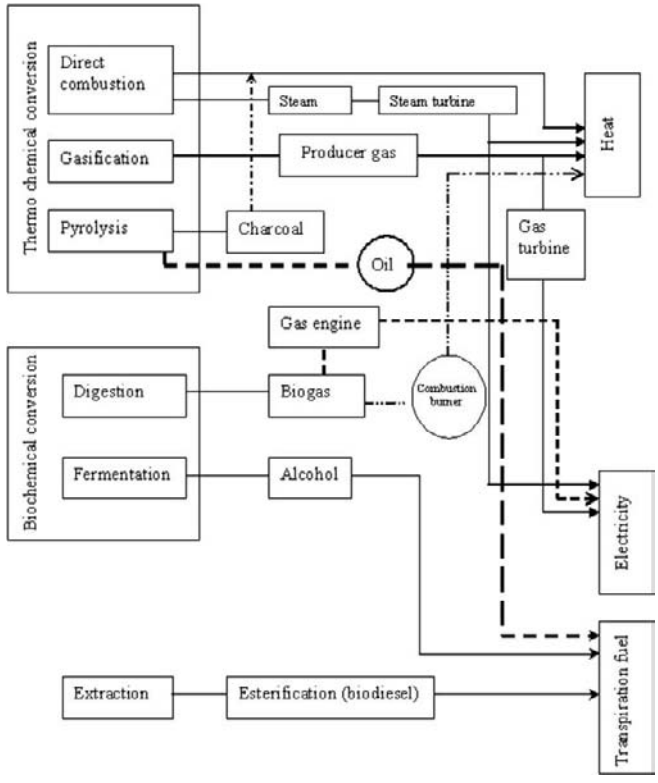

Figure.2. Biomass conversion routes.

In simple fashion, heat of combustion gases can be used to run gas turbine for power generation through Brayton cycle or alternately it can pass through heat exchanges for exciting a working fluid and finally to run a gas engine through a Stirling cycle. The heat of combustion gases can be used to generate steam vapour and to use it in steam/vapour engine or steam/vapour engine through Rankine cycle as illustrated in Fig 3.

The high-pressure steam is turn drives a steam turbine in Rankine cycle route. The steam turbine can be one, two or three state units. The steam turbine drives the alternator or generator [11].

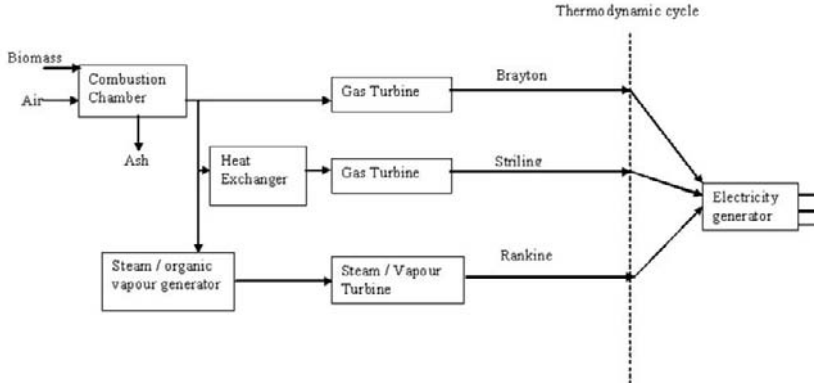

Figure 3. Dendro thermal power generation route.

3.2. Thermo Chemical Conversion

Gasification and pyrolysis is two main thermo chemical conversion route of biomass.

3.2.1. Gasification

Gasification as a means to convert a diversity of solid fuels to combustible gas at elevated temperature. Complete combustion of biomass required about 6 kg of air. But in gasification process restrict air entry for complete combustion hence it leads to partial combustion. In gasification 2 -2.5 kg of air per kg of biomass is required to produce combustible gaseous mixture, is called producer gas. Producer gas is the mixture of combustible and non-combustible gases. The constituents of producer gas depend upon the type of fuel and operating condition. Typical properties of producer gas from gasifier are shown in Table 2.

Table 2. Constituent of Producer Gas

Compound	Symbol	Gas (vol. %)	Dry Gas (vol. %)
Carbon monoxide	CO	21.0	22.1
Carbon dioxide	CO_2	9.7	10.2
Hydrogen	H_2	14.5	15.2
Water vapour	H_2O	4.8	--
Methane	CH_4	1.6	1.7
Nitrogen	N_2	48.4	50.8
Gas High heating value:			
Generator gas (wet basis)		5506 kJ Nm^{-3}	
Generator gas (dry basis)		5800 kJ/Nm^{-3}	
Air ratio required for gasification		2.38 kg wood (kg air)$^{-1}$	
Air ratio required for gas combustion		1.15 kg wood (kg air)$^{-1}$	

3.2.2. Gasification Process

Gasification process is completed in four different stages [12], such as:

a) Drying
b) Pyrolysis
c) Oxidation
d) Reduction

a) Drying

Biomass is fed at the top of the gasifier hopper and it moves down as the process proceeds. As a result moisture is removed from the biomass. Usually, air dried biomass contains moisture in the range of 13-15%. The heat radiations from the oxidation zone, evaporates the moisture of biomass in the upper most layers. The temperature of this zone remains less than 120°C.

b) Pyrolysis

As the dried biomass moves down, it is subjected to stronger heating from the oxidation zone. At temperatures above 200°C, the material starts loosing its volatilies. No air is admitted until then. Once temperature reaches 400oC, a self sustaining exothermic reaction takes place, in which the material structure of wood or other organic solids breaks down. Water vapour, methane, acetic acid and a considerable quantity of heavy hydrocarbon tars are evolved. The remaining of biomass is only charge i.e. fixed carbon. This zone in which biomass loses all its volatile and gets converted into two parts such as:

I. Primary pyrolysis zone: the normal temperature in this zone is 200°C - 600°C
II. Secondary pyrolysis zone: the temperature range is 300-800°C.

c) Oxidation

The actual combustion of char, pyrolysed gases and tars takes place in this zone. A calculated quantity of air is supplied through tuyres/air nozzles provided for the purpose. Combustion similar to normal stove/furnace takes place. This raises temperature to 900-1200°C. The principal reaction is

$$C + O_2 \rightarrow CO_2 + Heat$$
$$CH_x + O_2 \rightarrow CO_2 + H_2O + Heat$$

The tar is cracked in the high temperatures. The products of oxidation zone are high temperature gases containing products and water vapour.

(d) Reduction

The products of oxidation zone passes through reduction zone. It is the packed bed of charcoal. This charcoal is initially supplied from external sources. Later, reduction reactions are being simultaneously replenished by the char produced in the pyrolysis zone. The zone is maintained within close temperature limits of 900°c to 800°c, the highest temperature being nearest to the oxidation zone.

$$CO_2 + C \rightarrow 2CO - 173\,MJ\,(kg\,mole)^{-1}$$
$$C + H_2O \rightarrow CO + H_2 - 132MJ\,(kg\,mole)^{-1}$$
$$C + 2H_2O \rightarrow CO_2 + 2H_2 - 88\,MJ\,(kg\,mole)^{-1}$$
$$C + H_2 \rightarrow CH_4 + 75MJ\,(kg\,mole)^{-1}$$

Carbon monoxide (CO) production is the principal reaction in the reduction zone. The products are combustible. Most of the hydrogen (H2) produced in the reduction zone remains free. Only some of it combines with carbon to form methane. In addition to these, the gas contains measurable amounts of particulate and tars. The gas drawn is at about 400°C.

3.2.3. Pyrolysis

A good solution for technical application of biomass energy is conversion of biomass by a pyrolysis process [13-15]. Pyrolysis is the basic thermochemical process for converting solid biomass to a more useful liquid fuel. Sometime this process called as destructive distillation of biomass. Biomass is heated in the absence of oxygen, or partially combusted in a limited oxygen supply, to produce a hydrocarbon rich gas mixture, an oil-like liquid and a carbon rich solid residue. The flash pyrolysis technology has been considered as a good solution to convert biomass only to liquid fuel, not to gaseous fuel. The reasons that strongly support this approach are that the gas yield from conventional pyrolysis technology is very low, normally below 40 wt. % [16-17] and the accompanying corrosion is serious to downstream equipment, like a gas turbine/engine, caused by the high content of tar vapour contained in the gas phase [18].

Traditionally in developing countries, the solid residue produced is charcoal, which has a higher energy density than the original fuel, and is smokeless and thus ideal for domestic use. The traditional charcoal kilns are simply mounds of wood covered with earth, or pits in the ground. However, the process of carbonisation is very slow and inefficient in these kilns, and more sophisticated kilns are replacing the traditional ones. The pyrolytic or "bio-oil" produced can be easily transported and refined into a series of products similar to refining crude oil.

3.3. Bio Chemical Conversion

Digestion and fermentation of biomass in controlled conditions come under bio chemical conversion process. From biochemical conversion route it is quite possible to produce bio fuel for application in both domestic and transportation sector. Biofuels as replacements for oil and gasoline is gaining attention around the world as issues of climate change, apparent declines in oil reserves, and insecure oil sources intensify. In the USA, corn-based ethanol leads biofuel production. In 2006, more than 45 billion kilograms of corn grain produced 18.5 billion liters of ethanol. However, corn grain alone cannot meet the US government’s goal of replacing 30% of gasoline use by 2030 [19].

3.3.1. Fermentation

This process basically used for ethanol production and, it is well established technology to convert biomass in to ethanol. Ethanol can be produced from certain biomass materials that contain sugars, starch or cellulose. The best-known feedstock for ethanol production is sugar cane, but other materials can be used, including wheat and other cereals, sugar beet, Jerusalem artichoke, and wood. The choice of biomass is important, as feedstock costs typically make up 55 - 80% of the final alcohol selling price [20]. Starch-based biomass is usually cheaper than sugar-based materials, but requires additional processing. Similarly, cellulose materials, such as wood and straw, are readily available but require expensive preparation. The lignin by-product, which is around 50% of the material, can be combusted to provide the energy to drive the process.

Typically, sugar is extracted from the biomass crop by crushing, mixing with water and yeast, and then kept warm in large tanks called fermenters. The yeast breaks down the sugar

and converts it to ethanol. A distillation process is required to remove the water and other impurities from the dilute alcohol product which is generally about 10%-15% ethanol. The concentrated ethanol (95% by volume with a single step distillation process) is drawn off and condensed back to a liquid form, which can be used as a supplement or substitute for petrol in spark ignition engines.

The remaining crop residues (such as straw or bagasse) that are not suitable for producing ethanol is can used to supply the external heat required for the process. In ethanol production there is a significant energy loss in the distillation stage, particularly the complex secondary distillation process required to achieve ethanol concentrations of 99% or better. This may be acceptable, however, due to the convenience of a liquid fuel, and the relatively low cost and maturity of the technology. The process of producing ethanol can be schematized in Figure 4

Two methods are currently used to produce ethanol from grain: wet milling and dry milling.

Dry mills produce ethanol, distillers' grain and carbon dioxide (Figure 5). The carbon dioxide is a co-product of the fermentation, and the distillers' dried grain with solubles (DDGS) is a non-animal based, high protein livestock feed supplement, produced from the distillation and dehydration process. If distillers' grains are not dried, they are referred to as distillers' wet grain (DWG).

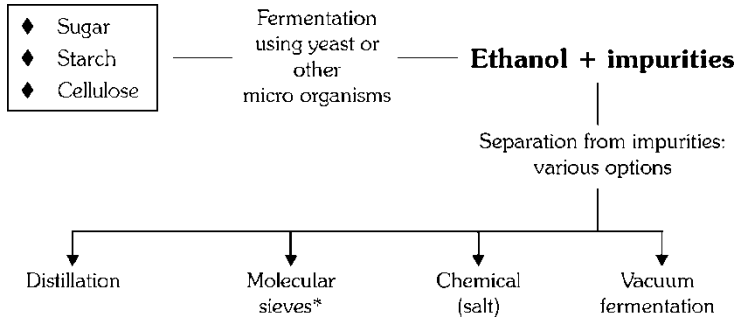

*Today, almost all ethanol plants use molecular sieves for dehydration. The technology alone reduces energy use by 10 per cent per liter of ethanol produced.

Figure 4. Ethanol production process.

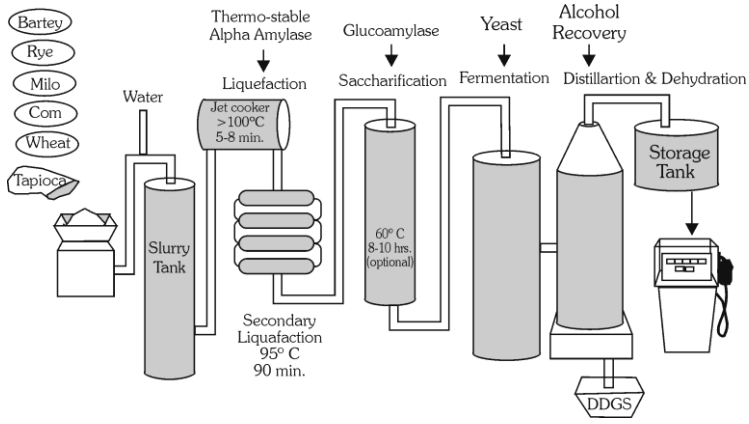

Figure 5. Conventional dry mill ethanol production process.

Wet mill facilities are 'bio-refineries' producing a host of high-values products (Figure 6). Wet mill processing plants produce more valuable by-products than the dry mill process. For example, in wet mill plants, using corn as feedstock, they produce:

- ethanol;
- corn gluten meat (which can be used as a natural herbicide or as a high protein supplement in animal feeds);
- corn gluten feed (also used as animal feed);
- corn germ meal;
- corn starch;
- corn oil; and
- corn syrup and high fructose corn syrups.

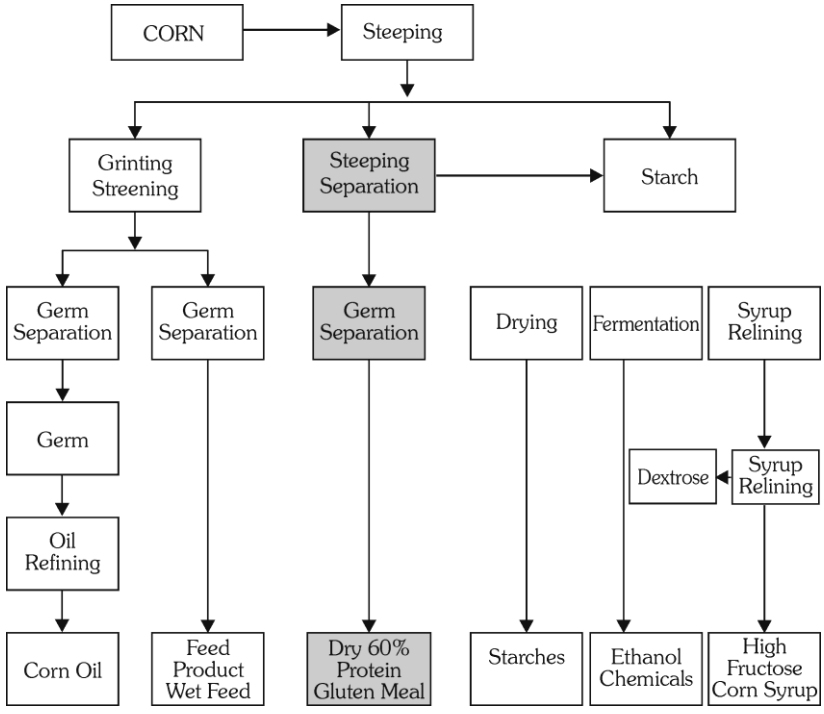

Figure 6. Conventional wet mill ethanol production process. [21].

3.3.2. Digestion

Anaerobic digestion, the reduction by bacteria of organic matter to a gas composed of methane and carbon dioxide, is neither a new process, nor a manmade process [22]. The gas produce through anaerobic digestion is called biogas. Biogas production technology is not only meant for production of combustible gas but also manure producing factory, has a very significant role to play in integrated agricultural operations, rural sanitation, large-scale dairy farms and sewage disposal (which otherwise creating pollution and destroying natural environment) etc.

Biogas generation is a biological process in which biomass or organic matter, is converted into methane and carbon dioxide. It is characterized by low nutrient requirement, and high degree of waste stabilization process where biogas is one of the two useful products; the other being enriched organic manure in the form of digested slurry. It is essentially a three stage process involving following reactions:

1) Hydrolysis
2) Acid formation
3) Methane generation.

For all practical purposes the first two steps are often defined as a single stage, i.e. hydrolysis and acid formation stages are grouped as acid formation stage. Micro-organisms taking part in this phase are termed as acid formers. As a group, these organisms are rapidly growing and are not much dependent upon surroundings. Products of first two stages serve as the raw material for the third stage where organic acids are utilized as carbon source by methane forming micro-organisms, which are also known as methanogens. These methanogens are more susceptible to their surroundings. The tolerated pH range is 6.8 to 7.5 with optimum 7.0. Any departure from this range is inhibitory. Atmospheric oxygen is extremely toxic for methanogens, as they are strict anaerobes. It means there should not be any entry of oxygen during methane formation [12].

Biogas release depends largely on the composition of the organic material, the process conditions, and other factors. There are two ways to produce biogas: by synthesis of carbonic acid and hydrogen, and by breakdown of acetic acid and other organic acids and alcohols. In the course of anaerobic processing of the biomass, 70% to 75% of the methane is generated in decomposition of the fatty acids, and only 25% to 30% is generated by synthesis of carbonic acid and hydrogen [23].

The biogas consists of approximately 60% methane (CH_4, a useful fuel), 40% carbon dioxide (CO_2, a diluting gas), and a small-but-potent dose of hydrogen sulfide (H_2S, a corrosive gas). It is also saturated with water vapor [24-25]. Pure methane at standard temperature and pressure has a lower heating value of approximately 34.30 MJm^{-3}. Biogas, however, is typically only 40-80% CH_4 and, therefore, has a heating value of approximately 13.72-27.44 MJm^{-3}. Obviously, this and other physical and chemical properties of biogas affect the choice of technology used for combustion (and clean-up), and a knowledge of these properties is essential to system design and operation [26].

4. BIOMASS-BASED TECHNOLOGY AT DOMESTIC LEVEL

4.1. Wood Gas Stove

Wood gasification is the process of converting wood fuel into combustible carbon monoxide by thermo-chemical reaction of the oxygen in the air and the carbon available in biomass during combustion. In complete combustion of fuel, the process takes place with excess air. In gasification process, on the other hand, it is accomplished with excess carbon. In order to gasify woods, about 30 to 40% of the stoichiometric air (6.0 kg of air per kg of

wood) is needed [27]. Commercially viable gasification has long been understood and used in industry and even in transportation, but not for small applications such as a household stove. Gasification of wood (or other biomass) offers the possibility of cleaner, better controlled gas cooking for developing countries. Wood gas stove offers the advantages of "cooking with gas" while using a wide variety of biomass fuels. The emissions from the close coupled gasifier-burner are quite low and the stove can be operated indoors [28]. The system was developed which is suitable for Indian conditions. The inexpensive wood-gas stoves which can bring the "joy of cooking with gas" to everyone while using a wide variety of renewable biomass fuels or coal [29-31].

4.1.1. Design of Wood Gas Stove:

The fabrication of stove after designing parameter is to construction with inexpensive local materials by village artisans and efficient applications make the renewable energy devices user's friendly and sustainable in the rural society. The system was designed in following manner [32].

a. Energy Needed - The amount of energy needed to cook food in one hour for a family of six members.

Q_n =15.8 MJ per hour

b. Energy Input – This refers to the amount of energy needed in terms of fuel having calorific value 15.5 $MJkg^{-1}$ to be fed into the stove. This can be computed using the formula,

$$FCR = \frac{Qn}{C.V. \times \eta_g}$$

c. Reactor Diameter –

$$D = \left[\frac{1.27FCR}{SGR}\right]^{\frac{1}{2}}$$

d. Height of the Reactor –

$$H = \frac{SGR \times T}{\rho_{wood}}$$

The height of designed gas stove was found 31.5 cm. The actual height of the system was kept 41.5 cm to accumulate the proper mixing of secondary air for proper combustion of the producer gas. The schematic line diagram of designed stove were presented in the Figure7

The insulation done inside the stove to minimize heat loss, MS anchor was welded inside reactor to retain the insulation material. The insulyte 11 U was used for insulation. Proper queering was done before actual use.

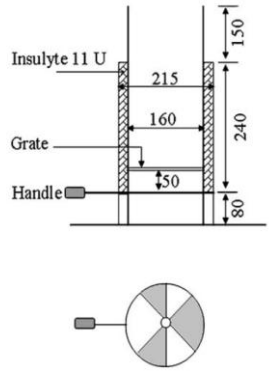

Figure 7. Line diagram of wood gas stove.

4.1.2. Fuels for Testing

The stove was tested with four different types of biomass i.e. babul wood (*Prosopis julliflora*), groundnut (*Arachis hypogaea*) shell briquettes, saw dust briquettes and Cashew nut (*Anacardium occidentale*) shell. Proximate analysis was conducted to analyze the feed stock characteristics. The parameters studied were, moisture content (ASTM D317373), volatile matter (ASTM D3175-73) and ash content (ASTM D3174-73). Fixed carbon (FC) was determined using material balance [33-35]. The physical and thermal properties of feed stock used for testing purposes are given in Table 3

Table 3. Physical and thermal properties of different biomass fuels

Characteristics	Biomass fuel			
	Babul wood *(Prosopis julliflora)*	Groundnut *(Arachis hypogaea)* shell briquettes made from groundnut shell powder	Saw dust briquettes made of saw dust powder	Cashew nut *(Anacardium occidentale)* shell
Diameter (mm)	22-38	52	52	Not measured
Length (mm)	30-60	20-40	20-40	Not measured
Bulk density (kg m^{-3})	410	620	650	481.83
Angle of repose (deg)	19.2	Not measured	Not measured	18.85
Moisture content (% wb)	9.2	9.6	8.2	7.2
Volatile matter (% db)	82.92	81.2	83.53	79.6
Ash content (% db)	1.1	7.95	1.27	1.66
Fixed carbon (%db)	15.98	10.85	15.2	18.74
Calorific value (MJ kg^{-1})	16.79	17.20	16.3	17.90
Oil content	Not measured	Not measured	Not measured	8.2

4.1.3. Stove performance

The water boiling test was carried out as per the protocol of the Ministry of New and Renewable Energy, Government of India, to evaluate the thermal performance of the stove. The thermal efficiency of biomass stove was calculated as 35%, which is close to 37% as reported by Dixit et al. [36] and it is almost 10% higher than earlier studies reported by Panwar and Rathore [32] and Bhattacharya et al. [37]. The fire hole of stove was filled with fuel within 5 cm of the top. It is desirable to have the uniform spread of fire laterally across the surface to provide heat over the whole area. This was accomplished by spreading kerosene oil initially on top of the fuel bed. Once it ignited from top, it gave combustible gas (producer gas) and a blue flame was established within 5 min of ignition. The use of kerosene oil was limited for experimental purpose only. For actual operation loose biomass which catches fire easily can be used to ignite the cookstove. The ignition time and flame temperature of stove with different fuel is given in Table 4.

Table 4. Performance result of stove with different fuels

S.No.	Fuel	Ignition time (min)	Flame temperature, ^{o}C	Thermal efficiency (%)	Power rating (kW)
1.	Babul wood *Prosopis julliflora)*	2-3 min	735	34.8	1.62
2.	Groundnut (Arachis hypogaea) shell briquette	5-6 min	742	35.2	1.68
3.	Sawdust briquettes	5-6 min	741	33.9	1.53
4.	Cashew nut *(Anacardium occidentale)* shell	1-2 min	763	35.4	1.76

It has been observed that the stove burns continuously for 41 and 35 min when it operates with Babul wood (Prosopis julliflora) and Cashew nut (Anacardium occidentale) shell respectively. Whereas it gave gas continuously for 62 min duration in both groundnut (Arachis hypogaea) shell and sawdust made briquettes. The ash was collected from bottom end when it operated with Babul wood (Prosopis julliflora) and briquettes but no ash was recorded when it operated on Cashew nut (Anacardium occidentale) shell. The shell remains in their actual shape with dark black colour. The burnt shell has to be removed from the stove, if second operation of stove is needed. During the testing, temperature of the outer surface of stove was recorded as about 95°C. The power rating of the stove varies in the range of 1.53 to 1.76 kW. The production cost of each unit is about $21.2 (Rs. 49.85 (INR) US^{-1}, February 18, 2009) and it increases with capacity. A variety of biomass including densified fuel can be used in this stove [38].

4.1.4. Safety during Operation

The out side temperature of the stove during testing was recorded as 95°C, which can accidentally burn users, so it is recommended to use a handle when moving or handling a hot stove. During the operation of the stove, carbon monoxide was obtained, which is toxic in nature. Therefore, it is recommended not to use the stove in an enclosed area, i.e. in a tent, camper or in a house. Subsequently after completion of the burning period some charcoal is obtained as unburnt fuel. If the stove is closed before charcoal is fully consumed, there are chances that the charcoal remains a fire hazard. Disposal of the charcoal in a safe place where it does not produce a fire, or waiting until it cools to a safe temperature as mentioned on wood camp stove [39], is also an important requirement in operating a stove.

4.2. Improved Cookstove

4.2.1 Single Pot Improved Cookstove (Chetak)

This cookstove is suitable for firewood, agro waste and dung cakes. Bigger sized wood can also be used in this cookstove at the fuel burning rate of 1.00 kg h^{-1}. The passage between the firebox chamber and the inlet of the chimney pipe is horizontal, which flow smoky gases outside the kitchen. A mixture of cement and sand is used to fix up the bricks and to enhance the life of the structure. The single pot improved cookstove in working is illustrated by Figure 8. The overall size of this improved cookstove is 55 x 45x 22 cm. This model is suitable for those who prefer one cooking at a time.

Figure 8. Single pot improved cookstove (Chetak).

4.2.2. Double Pot Cookstove (Udairaj)

The “Udairaj” model having two pot holding places is specially designed for those who prefer two cooking at a time. This stove is sufficient to cook the meal of a family of 6-12 persons and is of permanent nature. The special feature of this improved biomass cookstove is

bigger size of fire box, which is suitable for big size firewood and light agro-waste type of fuel.

The diameter of the 1st pot is 17 cm, which is suitable for households for baking of wheat flour made bread named as "Chapatti". The diameter of 2nd pot is 15 cm and suitable for cooking vegetables and boiling of milk etc. The burning of wood is very efficient without back fire. The overall size of this improved cookstove is 85 x 40 x 25 cm. The construction procedure is the same as of Chetak model. Modified double pot Udairaj improved cookstove in actual use is illustrated in Figure 9.

4.2.3 Performance of improved cookstove

a) Thermal efficiency

Performance of Chetak (Single-pot) and Udairaj (Double-pot) have been carried out as per the standard water boiling test approved through Ministry of New and Renewable Energy, Government of India. The sun dried fuel wood of Desi Babool (*Acacia nilotica*) was used for test. Proximate analysis of fuel was carried out before the test by using the method suggested by ASTM [33]. Fifteen trails were taken in different conditions to carry out the thermal efficiency test of the both cookstoves. Calorific value of fuel wood was calculated by Digital bomb calorimeter (Advance Research Instrument Company). Physical and thermal properties of fuel wood were presented in Table-5. Test result of water boiling test is given in Table- 6.

Figure 9. Double pot improved cookstove (Udairaj).

Table 5. Physical and thermal properties of fuel wood

Characteristic		Biomass (Desi Babul wood) *(Acacia nilotica)*
Size (mm)	:	25-40
Length (mm)	:	35-75
Bulk density (kg m^{-3})	:	405
Angle of repose (deg)	:	16
Moisture content (% wb)	:	9.6
Volatile matter (% db)	:	82.52
Ash content (%db)	:	1.05
Fixed carbon (%db)	:	16.43
Calorific value (kcal kg^{-1})	:	3965

Table 6. Thermal Efficiency of Durable Improved Cook Stoves

Model	Type of fuel used for testing	Burning rate (kg h^{-1}.)	Power rating kW	Thermal efficiency (%)
Chetak (Single pot)	Desi Babul *(Acacia nilotica)*	1.00	1.87	21.0
Udairaj (Double pot)		1.00	2.46	25.0

b) Cost of construction

Chetak and Udairaj improved biomass cookstoves are made of materials of permanent nature and having at least five years life. Estimate for construction of these durable improved biomass cookstoves including materials and labour is presented in Table 7.

Table 7. Cost estimates of Chetak and Udairaj (Rs. 49.85 (INR) US^{-1}, February 18, 2009)

c)

Model	Cost in US $
Chetak (single pot)	9.00
Udairaj (double pot)	122.00

d) Indoor air quality

The direct combustion of biomass is the simplest and easiest method of converting chemically stored energy into heat. When biomass is heated its first thermal decomposition or pyrolysis is initiated. The heating at first stage results in elimination of water vapour and oxygenated gases mainly CO_2. On further increasing the temperature the volatile gets combustible and constituents such as CO and hydrocarbons are produced as reported by Rathore et al. [40]. Well designed improved cookstoves can significantly reduce particulate matter and CO emissions [40]. CO_2 and CO was recorded by a gas analyzer (AFRISO EURO INDEX, Multilyzer Industries). There were found in the range of 10-15 ppm and 0.9-1.3 ppm respectively, which is with permissible limit as recommended by world health organisation [32]. An improved biomass cookstove is in position to save the 700 kg of fuelwood per year

[42]. Hence an improved cookstove can save 161 kg of CO_2 emission annually as by Online Emission Calculator [43]. It shows that an improved biomass cookstove is eco-friendly [44].

5. BIOMASS-BASED TECHNOLOGY AT INDUSTRIAL LEVEL

Gasifier can classify on the bases of type of fuel used and air introduces in fuel column. There are many commercially approved design of gasifier is available. The most commonly available gasifier are classified as-

a) Updraft gasifier
b) Downdraft gasifier

5.1. Updraft Gasifier

An updraft gasifier has four different zones for drying of biomass, partial combustion, reduction, and pyrolysis. Primary air for partial combustion is introduced at the bottom and act as countercurrent to fuel flow. The gas is drawn at upper end. The updraft gasifier achieves the highest efficiency as the hot gas passes through fuel bed and leaves the gasifier at low temperature. The sensible heat given by gas is used to preheat and dry fuel. Disadvantages of updraft gas gasifier are excessive amount of tar in raw gas and poor loading capability. Hence it is not suitable for running vehicle or for electric power generation it found most suitable for thermal application.

An updraft gasifier was designed for an industry which produces herbal medicine and process heat is prime requirement to extract required chemical component from medicinal plants. Prior to this the industry was burning 3 liter of light diesel oil through burner for getting process heat. The burner efficiency was assumed as 65% and *CV* of LDO was taken about 43.5 MJ kg^{-1}, hence total heat requirement is 84 MJ h^{-1}. On this basis, the system was designed and its performance was evaluated.

5.1.1. System Description

This gasifier is of updraft type and made in four parts, namely, hopper, reactor, air distribution unit and ash pit. Various parameters like specific gasification rate, gas outlet position, shape of the biomass hopper and minimum tar condensation in the gasifier were taken into consideration while designing the gasifier. Suitable open space was provided below the stationary grate so as to maintain the air velocity of 6 ms^{-1} to 8 ms^{-1} recommended for the updraft gasifier. A manually operated grate scrapper (comb type) was provided above the grate to remove the ash from the reactor to ash pit. A gas outlet was provided near the top of the reactor (Fig 10) [45].

5.1.2. Performance of Updraft Gasifier

The thermal efficiency of the system was calculated by following formulae (water boiling test),

$$\eta_g = \frac{Energy\,Output}{Energy\,Input} \times 100$$

The thermal capacity of the gasifier was calculated by following formulae,

$$Thermal\,Capacity = \frac{Calorific\,Value\,of\,Fuel \times \eta_g}{860 \times 100}$$

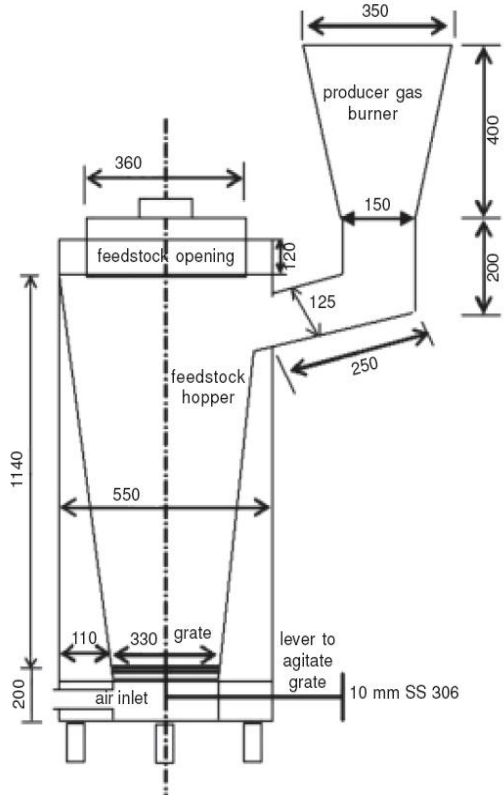

Figure10. Schematic of designed updraft gasifier.

The overall efficiency of the gasifier cum burner system was found to be 39.53% (by water boiling test) and the power rating was worked out to be nearly 14.54 kW. The cost economics indicated that the total operating cost was 0.80 US \$ h^{-1}. The net present worth of investment made on commercial natural draft biomass gasifier cum burner system in a year was 88.66.33 US \$. The benefit cost ratio came as 2.1 and the pay back period was 3.5 years.

5.2. Downdraft Gasifier

In downdraft type gasifier, air is introduced into downward flowing packed bed or solid fuels and gas is drawn off at the bottom side. The time (20-30 minutes) needed to ignite and bring plant to working temperature with combustible gas quality is shorter than updraft gas producer. This gasifier produces low tar gas and preferred for internal combustion engines.

5.2.1 Experimental Study

An experiment was conducted on open core downdraft gasifier at M/s Suman Food Product, a franchise of internationally recognized, Hindustan Lever Limited is situated in Udaipur [46]. Fig 11 shows the view of open core downdraft gasifier during experimental trail at laboratory level. It produces bread, biscuits, toast etc. for the consumption in local market. The industry had one rotary oven for processing the products. One batch of 60 kg dough (one trolley) required 20–25 min at 230–280°C for backing by burning Liquefied Petroleum Gas (LPG). Oven consumed 6.5 kg of LPG per hour earlier. Now industry switched over to gasifier which was operated nearly 15–18 h per day. The technical specification of gasifier system is given in Table 8.

5.2.2. System Performance

The system operated for a cumulative period of more than 3000 hours with individual test run of 15-18 hours and babul wood *(Prosopis juliflora)* with diagonal length 20-100 mm was used as feed stock. No problem was found in the operation of gasifier and combustible producer gas was recorded after 10 minutes of flaring. The required temperature was attained at an average gas flow rate of 95-115 $Nm^3 h^{-1}$. The calorific value of producer gas varied in the range of 4.2 - 4.6 $MJNm^{-3}$ and cold gas efficiency in the range of 70-74% as shown in Table 9, it is very closed to result addresses by Dasappa et al. [47].

Table 8. Technical specifications of the gasifier system

Type	Down draft open core
Biomass	Babul wood (*Prosopis juliflora*)
Biomass consumption rate	60 kg h^{-1}
Capacity	180 kW_{th}
Ash removal unit	Manual rotating type
Fuel feeding	Manual
Fuel properties	Moisture less than 15% (wb). The fuel size should not be more than 1/10th of the reactor diameter in length, and between 1 and 3 in diameter or thickness

Figure 11. Open core down draft gasifier.

The variation in the temperature of different zones of gasifier with respect to time is illustrated in Figure12. No load testing was carried out and it was found that oven temperature 367 ^{o}C maximum was attained in 130 min as graphically presented in Figure 13. After attaining temperature of about 367 ^{o}C during no load conditions, the loaded trolley having 60 kg of product for baking was placed in the oven which was baked in 8 minute, and the temperature drop by 24 ^{o}C was recorded. Afterwards two more loaded trolleys were placed successively for baking period of 8 minutes each. The total temperature dropped during these three baking batches was found to be 82 ^{o}C. Its graphical variation is illustrated in Figure 14. Table 10 reveals the chemical constituent of producer gas obtained in different samples during operation. The higher heating value of producer gas varies in the range of 4 -5 MJ Nm^{-3}. Similar heating value of producer gas was presented by Bhoi et al. [48] for thermal application.

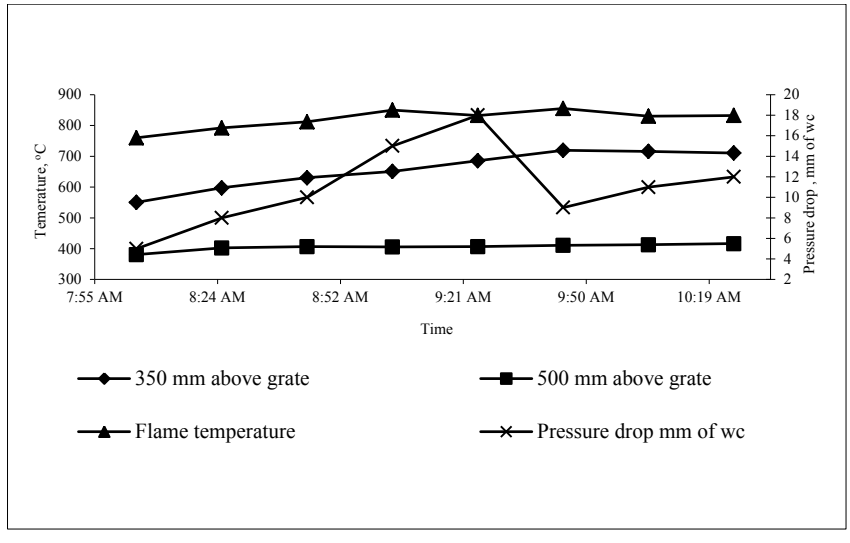

Figure12. Variation in temperature and pressure drop across the gasifier.

Table 9. Performance of gasifier at M/s Suman Food Product

S. No.	Parameters	Babul wood *(Prosopis juliflora)*
1.	Fuel consumption rate, kg h^{-1}	38.0
2.	Producer gas flow rate, $Nm^3 h^{-1}$	100.7
3.	Calorific value of producer gas, $MJNm^{-3}$	4.27 – 5.07
4.	Cold gas efficiency, %	70-74
5.	Gas production, $m^3 kg^{-1}$	2.65

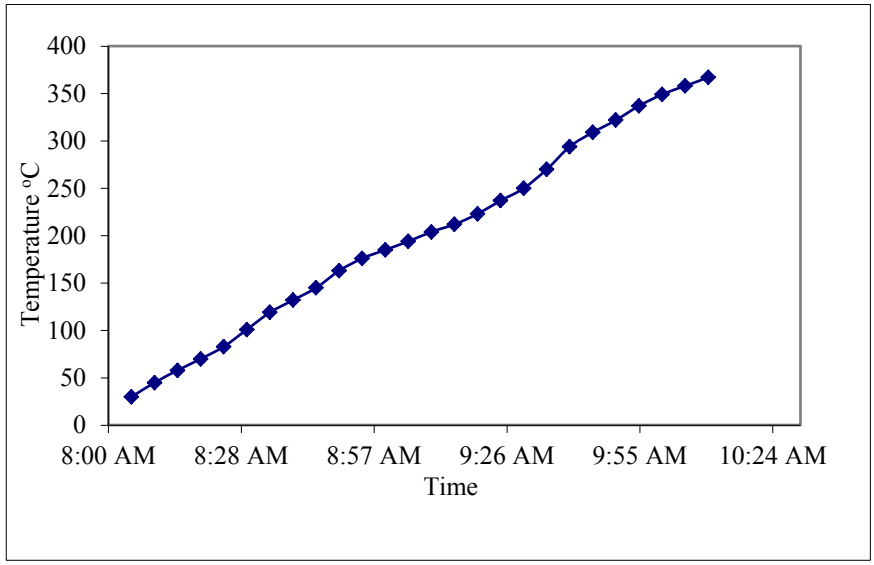

Figure 13. Temperature profile during no load testing.

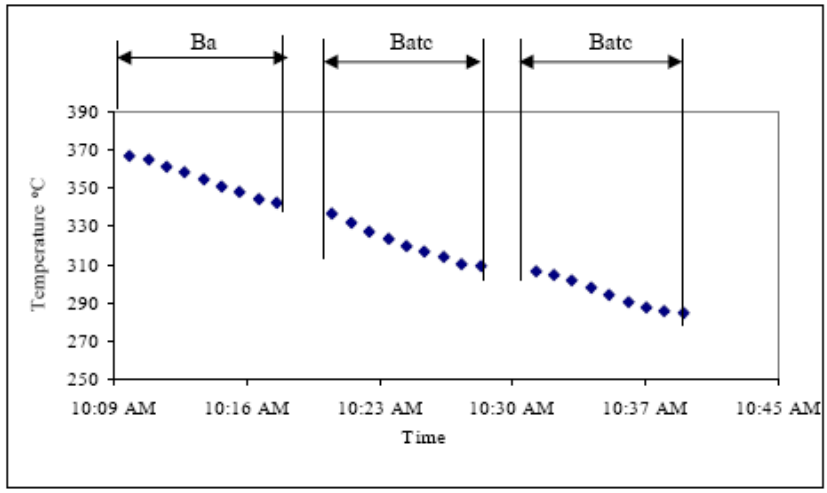

Figure 14. Temperature profile during full load testing.

Table 10. Gas composition of producer gas during operation

	CO %	H_2%	CH_4%	CO_2%	N_2%	Calorific Value MJ Nm^{-3}
Sample 1	18.2	13.5	1.66	10.1	56.54	4.84
Sample 2	19.3	15.1	1.35	8.5	55.75	5.07
Sample 3	17.12	11	1.42	7.9	62.56	4.27

5.2.3. Economics of Gasifier

Earlier, one oven was consuming 6.5 kg of LPG per hour, for 3,000 h of operation 19.5 tons of LPG is required which costing about 17,994 US $. It was replaced by 110 tons of wood which costing about 6,619US $. The system is in position to save about US $. 11,375 at 3,000 h of operation as compared to LPG (Table 11). The result of fuel cost economics is given in Table 11. Over 3,000 h of operation this system has resulted in a saving of about 19.5 tons of LPG, implying a saving of about 33 tons of CO_2 [43], thus a promising candidate for clean development mechanism.

Table 11. Comparison of operating cost with different fuel

Fuel per hour	Cost per kg	Fuel required per hour (kg)	Operating cost per day (US $)	Operation cost for 3,000 h (US $)
LPG	0.92	6.5	89.7	17994
Wood (sized)	0.06	38	34.2	6619
Saving				11,375

Similar gasifier was designed by Rathore et al. [49] and evaluated its performance at M/S Phosphate India Pvt. Limited, Udaipur for heating and concentrating Phosphoric Acid. The biomass consumption rate of the gasifier was found to vary from 100-120 kg h^{-1}. The average air and gas flow rate was 92.69-99.20 and 204-210.26 m^3 h^{-1} respectively. The temperature at 20mm above the grate varied from 800-1143°C. The gas outlet and flame temperature varied during the test from 380-440°C and 690-740°C, respectively. The quality of gas samples were analysed and heat value of the producer gas was observed 4.35 $MJNm^{-3}$.The system works satisfactory and to save about 20 liter of light diesel oil per hour [50].

6. CONCLUSION

Biomass is one of the renewable energy sources that have high potential to contribute to energy needs of modern society worldwide. Although the actual role of bioenergy will depend on its competitiveness with fossil fuels and on agricultural policies worldwide, it seems realistic to expect that the current contribution of bio-energy of 40–55 EJ per year will increase considerably. A range from 200–300 EJ may be observed looking well into this century, making biomass a more important energy supply option than mineral oil today [9]. It can play a pivotal role in helping the developed world reduce the environmental impact of

burning fossil fuels to produce energy but only if significant areas of replanting are created immediately. There are many routes to convert biomass to a useable from of fuel. Direct combustion of biomass is the traditional one, and now it has been improved to several means to enhance combustion efficiency and fuel economics. Solid biomass can be converted into gaseous form through the thermo chemical conversion route. No doubt biomass is low grade fuel and this can be converted into high grade fuel through pyrolysis and carbonization where biomass is converted into charcoal. Further in anaerobic digestion, biomass can be converted into biogas.

Biogas is one of the successful proven technologies at the global level. It yields multiple benefits to the households, community and the country. Health, environmental and agriculture benefits are some of the important local benefits. The use of biogas as an energy source reduces the chance of possible emission of two greenhouse gases, CH_4 and CO_2, into the atmosphere at the same time. Pyrolysis is a rapidly developing technology with great potential but the process is inherently better suited to producing a fuel oil, more suited to use in diesel engines and gas turbines. [51].

Improved biomass stoves were developed and found suitable for Indian rural kitchen. They performed with a better fuel economy, better indoor air environment and clean kitchen. Households with biomass-burning stoves potentially can gain three kinds of benefits: (1) reduced fuel demand, with economic and time saving benefits to the household and increased sustainability of the natural resources base; (2) reduced human exposure to health damaging air pollutants; and (3) reduced emission of the greenhouse gases that are thought to increase the probability of global climate change [52]. Single double pot improved biomass cookstove can save about 700 kg of fuel wood per year and at the same time it reduces the CO_2 emission by 161 kg per year. It helps to improve health standard of women and child, also reduces the burden of fuel collection.

An experimental study reveals that a downdraft gasifier provides a clean gas, i.e., low tar gas, and has been found suitable for thermal application. The gas exerted from downdraft type gasifier can be used to run engines after cooling and cleaning of producer gas whereas for thermal application no cooling and cleaning is required. An updraft gasifier is recommended only for thermal applications. A key issue for bio-energy is that its use should be modernized to fit into a sustainable development path.

REFERENCES

[1] Berggren, M.; Lijunggren, E.; Johnsson, F. Biomass co-firing potentials for electricity generation in Poland- Matching supply and co-firing opportunities. *Biomass and Bioenergy*. 2008, 32, 865-879.

[2] European Commission White Paper for community Strategy and action Plan COM(97)599 final(26/11/1997)

[3] Hall, D.O.; Scrase, J.I. Will biomass be the environmentally friendly fuel of the future? *Biomass and Bioenergy.* 1998, 15, 357-367.

[4] McKendry, P. Energy production from biomass (part 1): overview of biomass. *Bioresource Technology.* 2002, 83, 37–46.

[5] Rathore, N.S.; Panwar, N.L.; Kothari, S. *Biomass Production and Utilization Technology*. Himanshu Publication, Udaipur (Rajasthan) India.2007

[6] Rathore, N.S.; Panwar, N.L. Biomass Assessment in the District of Mandsaur and Neemach of Madhya Pradesh. A report submitted to M/s Vikram Cement Limited, Khor, Tehsil- Jawad, District: Neemach (MP), India. 2009

[7] Parikka, M. Global biomass fuel resources. *Biomass and Bioenergy.* 2004 27, 613–620.

[8] FAO. State of the World's Forests—2001, www.fao.org, 2001.

[9] Faaji, A. Modern biomass conversion technologies. *Mitigation and Adaptation Strategies for Global Change.* 2006, 11, 343–375.

[10] Price, B. Electricity from Biomass. *Financial Times Business Limited*. 1998, ISBN 1 84083 0735.

[11] Rathore, N.S. New and Renewable Energy sources for Environmental Protection and Sustainable Development for Industrial Sector. *XIX National Convention of Environmental Engineers.* 2003,243-250.

[12] Rathore, N.S.; Panwar, N.L.; Kurchania, A.K. *Renewable Energy: Theory and Practices*. Himanshu Publication, Udaipur (Raajasthan) India. 2008

[13] Chen, G.; Fang, M.; Luo, Z.; Yu, Ch.; Li, X.; Ni, M.; Cen, K. Study on Combustion Characteristics of Rice Husk-Fired Fluidized Bed Boiler. *Journal of Combustion Science and Technology*. 1998, 4(2), 193-198

[14] Demirbas, A. Mechanisms of liquefaction and pyrolysis reactions of biomass. *Energy Conversion and Management*. 2000,41,633-646.

[15] Vriesman, P.; Heginuz, E.; Sjostrom, K Biomass gasification in a laboratory-scale AFBG: influence of the location of the feeding point on the fuel-N conversion. *Fuel*. 2000,79,1371-1378.

[16] Scott, D.S; Piskor, Z. The flash pyrolysis of aspen-poplar wood. *Canadian Journal of Chemical Engineering*. 1982; 60, 666-674.

[17] Bingyan, X.; Chuangzhi, W.; Zhengfen, L.; Xi guang, Z. Kinetic study on biomass gasification (A 1991 ISES Solar World Congress honors paper. *Solar Energy.* 1992, 49,199-204

[18] Chen, G.; Andries, J.; Luo, Z.; Spliethoff, H. Biomass pyrolysis/gasification for product gas production: the overall investigation of parametric effects. *Energy Conversion and Management.* 2003, 44 ,1875–1884.

[19] Perlack, R.D.; Wright, L.L.; Turhollow, A.F.; Graham, R.L.; Stokes, B; Erbach, D.C. 2005. Biomass as feedstock for a bioenergy and bioproducts industry: the technical feasibility of a billion-ton annual supply. Available via http://www.ornl.gov/~webworks/cppr/y2001 /rpt/123021.pdf. Cited 14 September 2007

[20] World Energy Council 1994. http://www.rise.org.au/info/Applic /Ethanol/index.html (Online, Accessed 15 October 2009)

[21] Image taken from; www.ethanolrfa.org/objects/images/wetmill_2.jpg

[22] Hobson, P.N.; Feilden, E.H. Pproduction and use of biogas in agriculture *Prog. Energy Combust. Sci.,* 1982, 8,135-158.

[23] Asankulova, A. Analysis of Factors Influencing Biogas Release. *Applied Solar Energy.* 2008, 44(3), 229–231.

[24] Darrell, T.M. Biogas Applications for Large Dairy Operations: Alternatives to Conventional Engine-Generators Cornell Cooperative Extension Association of Wyoming County, 2001

[25] Meena, M.; Sharma, M.; Panwar, N.L. Performance Evaluation of Dual Fuel Engine with Scrubbed Biogas for Power Generation. Institution Engineers (India), Journal (MC), January, 2008, 88,37-41.

[26] Walsh, J.L.; Ross, C.C.; Smith, M.S.; Harper, S.R. Utilization of biogas. Biomass. 1989, 20,277-290.

[27] Kaupp, A. Gasification of Rice Hull: Theory and Praxix. Federal Republic of Germany: GATE/GTZ. 1984; 303

[28] Reed, T.B.; Larson R. A wood-gas stove for developing countries. *Energy for Sustainable Development*. 1996,3,34-37.

[29] La Fontaine, H;.Reed, T. B. An Inverted Downdraft Wood-Gas Stove and Charcoal Producer, in Energy from Biomass and Wastes XV, D. Klass, Ed., Washington, D. C., 1993.

[30] Reed, T. B.; Larson, R., A wood-Gas Stove for Developing Countries, in Developments in Thermochemical Biomass Conversion, Ed. A. V. Bridgwater, Blackie Academic Press, 1996.

[31] Reed, T. B.; Walt, R. The "Turbo" Wood-Gas Stove, in Biomass: Proceedings of the 4th biomass Conference of the Americas in Oakland, Ca, Ed R. P. Overend and E. Chornet, Pergamon Press, 1999.

[32] Panwar, N.L.; Rathore, N.S. Design and performance evaluation of a 5kW producer gas stove. Biomass and Bioenergy. 2008, 32, 1349-1352.

[33] ASTM (1983). Annual Book of ASTM Standard, American Society for Testing of Materials, Philadelphia, pp 19103.

[34] Singh, R.N.; Patil, K.N.; Ramana, P.V. Performance evaluation of biomass gasifier based thermal back up for solar dryer. *SESI Journal.*1999, 9(2),115–122.

[35] Singh, R.N.; Patil, K.N. SPRERI method for quick measurement of moisture content of biomass fuels. *SESI Journal*.2001, 11(1), 25–28.

[36] Dixit, C.S.B.; Paul, P.J.; Mukunda, H.S. Experimental studies on a pulverised fuel stove: part I. *Biomass Bioenergy.* 2006, 30, 673–683.

[37] Bhattacharya, S.C.; Attalage, R.A.; Augustus, M. Potential of biomass fuel conservation in selected Asian country. *Energy Conversion and Management.* 2001, 40,1141–1162.

[38] Panwar, N.L. Design and performance evaluation of energy efficient biomass gasifier based cookstove on multi fuels. *Mitigation and Adaptation Strategies for Global Change.* 2009,14,627–633.

[39] Wood gas camp stove (2009) http://www.woodgascampstove. com/Safety.htmlS (accessed on 15.03.2009).

[40] Rathore, N.S.; Panwar, N.L.; Kothari, S. Biomass rpduction and utilization technology. Himanshu publication, Udaipur (Rajasthna) India. 2007

[41] Roden, C.A.; Bond, T.C.; Conway, S.; Pinel, A.B.O.; MacCarty, N.; Still, D. Laboratory and field investigations of particulate and carbon monoxide emissions from traditional and improved cookstoves. *Atmospheric Environment.* 2009, 43, 1170–1181.

[42] Kishore, V.V.N.; Ramana, P.V. Improved cookstoves in rural India: how improved are they? A critique of the perceive benefit from the national programme on improved chulhas (NIPC). Energy. 2002, 27, 47-63.

[43] Online Emission Calculator http://www.abc.net.au/tv /carboncops/ calculator.htm (accessed on May, 7, 2009)

[44] Panwar, N.L.; Kurchania, A.K.; Rathore, N.S. Mitigation of greenhouse gases by adoption of improved biomass cookstoves. *Mitigation and Adaptation Strategies for Global Change.* 2009,14,569–578.

[45] Sharma, D.; Panwar, N.L. Performance Evaluation of Biomass based Natural Draft Gasifier System for Thermal Application. *Institution Engineers (India), Journal* (AG), June 2009, 90,34-38.

[46] Panwar, N.L.; Rathore, N.S.; Kurchania, A.K. Experimental investigation of open core downdraft biomass gasifier for food processing industry Mitigation and Adaptation Strategies for Global Change.2009, 14, 547–556.

[47] Dasappa, S.; Paul, P.J.; Mukunda, H.S.; Rajan, N.K.S.; Sridhar, G.; Sridhar, .H.V. Biomass gasification technology – a route to meet energy needs. *Current Science*. 2004, 87(7),908-916.

[48] Bhoi, P.R.; Singh, R.N.; Sharma, A.M.; Patel, S.R. Performance evaluation of open core gasifier on multi-fuels. *Biomass and Bioenergy.* 2006, 30, 575-579

[49] Rathore, N.S.; Panwar, N.L.; Chiplinkar, V.Y. Industrial Application of Biomass Based Gasification System. *World Applied Sciences Journal.* 2008, 5(4), 406-409.

[50] Rathore, N.S.; Panwar, N.L.; Chiplinkar, V.Y. Design and techno economic evaluation of biomass gasifier for industrial thermal applications. *African Journal of Environmental Science and Technology.* 2009, 1, 006-012.

[51] McKendry, P. Energy production from biomass (part 3): gasification technologies. Bioresource Technology. 2002, 83, 55–63.

[52] Smith, K.R. Health, energy, and greenhouse-gas impact of biomass combustion in household stoves. *Energy for sustainable development.* 2004, I(4), 23–29.

In: Wood: Types, Properties and Uses
Editor: Lorenzo F. Botannini
ISBN 978-1-61668-837-0

Chapter 4

ABOVEGROUND WOOD BIOMASS AND NUTRIENTS IN BRAZILIAN WOODY SPECIES AND EUCALYPTUS PLANTATIONS

Marcela C. Pagano
Federal University of Ceará, Fortaleza, Ceará, Brazil.

ABSTRACT

The aboveground biomass and nutrient content are important measures of the characteristics and individual requirements of the plant species. Also, a previous evaluation of the areas to be planted is essential to a successful establishment of forests with native or exotic species. The aim of this review is to explore the current information on the total aboveground biomass, nutrient content and the benefit of symbiosis in some native woody species and exotic *Eucalyptus* plantations in Brazil. The methodology for native and exotic plant species used for agroforestry is illustrated. The *Eucalyptus* species presented an aboveground wood biomass (AWB) of 26.9 to 44.4 Mg ha^{-1}, and the aboveground wood volume varied for 42.8 to 75.9 m^3ha^{-1}. The biomass of the stem wood, leaves, branches, and stem bark accounted for 64–66%, 16–19%, 15–17%, and 0.2–0.6% of the total biomass, respectively. The wood localized in superior parts of the trunk presented a higher concentration of P and bark containing significant amounts of nutrients. On the other hand, the native species evaluated, presented a higher total aboveground biomass when inoculated with arbuscular mycorrhizal fungi and *Rhizobium* bacteria. Leguminous trees showed greater height and diameter growth, as well as, higher dry matter and nutrient concentration when inoculated. The AWB varied for 0.48 to 0.76 Mg ha^{-1} for *Anadenanthera peregrina*. The agroforestry trees exhibited mycorrhizal mycotrophy. The potential of agroforestry as a carbon sequestration strategy (carbon storage potential in its multiple plant species and soil) as well as its applicability in agricultural lands and in reforestation must be more exploited. Research directions that are needed to increase understanding of mycorrhizal associations in tropical cropping systems and to increase mycorrhizal benefit are indicated. The benefits and problems encountered are discussed in this chapter, in order to highlight the need for a continual study of the forestry species.

INTRODUCTION

Eucalyptus species present characteristics suitable for commercial use, such as fast growth, high cellulose production and resistance to environmental stress and diseases (Santos et al. 2001). In Brazil, Gonçalves (1995) reported the nutrient accumulation in 5–6 year-old *Eucalyptus grandis* plantations and observed that during harvesting part of the nutrients remain in the ecosystem accumulated in leaves, branches and litter when these are not removed from the site. Nevertheless, 30% of nitrogen (N), phosphorus (P) and calcium (Ca), and 43% of potassium (K) are removed when wood is extracted. The loss of N, P, K and Ca increases 40%, 60%, 65%, and 48%, respectively, when bark is extracted with wood. Mineral fertilization is a common practice to improve productivity; however, management policies need further study. Most biomass and nutrients accumulated by planted *E. grandis* occurred between two and five years of age, when the leaf area is expanding. *E. camaldulensis* is a fast growing tree species that can tolerate moderate salinity, alkalinity, extended dry seasons and waterlogging, and is extensively planted throughout the world for purposes such as shade, shelter, agroforestry, furniture and industrial wood production (Midgley et al. 1989; Marques Júnior et al. 1996). The rotation length is about 3–5 years for *E. camaldulensis* and 7 years for *E. grandis* (Campinhos 1999).

Eucalyptus has the capacity to form two types of mycorrhizas, arbuscular (AM) and ectomycorrhiza (ECM) (Zambolim and Barros 1982). The benefits of AM symbiosis in *Eucalyptus* have proved commercially relevant (reviewed by Carrenho et al. 2008). Studies of AM inoculation on eucalypt are increasing (Standish et al. 2007) and the AM genus *Glomus* is a promising inoculum (Arriagada et al. 2007, Pagano et al. 2009). As regards ECM, Molina et al. (1992) and Thomson et al. (1996)'s studies suggest that the majority of fungi, selected for their enhancement of seedling growth, may persist only for short periods in the field, where they are replaced by wild populations. However, Pampolina et al. (2002) showed the significance of ECM in immobilizing P and other nutrients as well as the impact of P fertilization, as well as, Chen et al. (2000) and Mason et al. (2000) recommended the inoculation with tested ECM. It is important then to know the mycorrhizal condition of the plant species in order to allow for research on seedlings production and technologies. Arbuscular mycorrhiza are substantially involved in the vegetative state of the mycotrophic plants, defining their ecologic niches, influencing vegetal communities composition, maintenance and soil fertility, plant fitness, and nutrient turnover (Jeffries et al. 2003).

The study of plant nutrient content and mycorrhizal status, aiming at increasing the possible ways of forest management with the objective of mixed plantations is essential to identify methods for sustainable management. Moreover, agroforestry has been recognized to be of special importance as a carbon sequestration strategy because of its applicability in agricultural lands as well as in reforestation (Montagnini and Nair 2004).

Valuable trees such as *Acer*, *Araucaria*, *Podocarpus*, as well as Cupressaceae, Taxodiaceae, Taxaceae, and the majority of tropical hardwoods present mycorrhizal symbiosis (Smith and Read 2008), and this association is used at present.

Little work has been done with native plants of Brazil, including valuable wood species with differing exigencies for soil fertility (Totola and Borges 2000). The relative scarcity of scientific papers on native species may be attributed to the high predation without replacement of trees extracted from native forests. Moreover, due to the great genetic

variability and longer cycle, research on those species is time consuming and does not bring technological return in the short term (Resende et al. 2005).

Native trees such as *Tabebuia heptaphylla* (Vell.) Tol., *Schinopsis brasiliensis* Engl., *Anadenanthera peregrina* (L.) Spegazzini, *Plathymenia reticulata* Benth and *Enterolobium contortisiliquum*, one of them (*S. brasiliensis*) classified within the threatened category of the official Brazilian endangered species list, were mixed with a second non legume species, and with two timber *Eucalyptus* species (Table 1, Figure 1), considered of good adaptation for the semi arid region of Brazil.

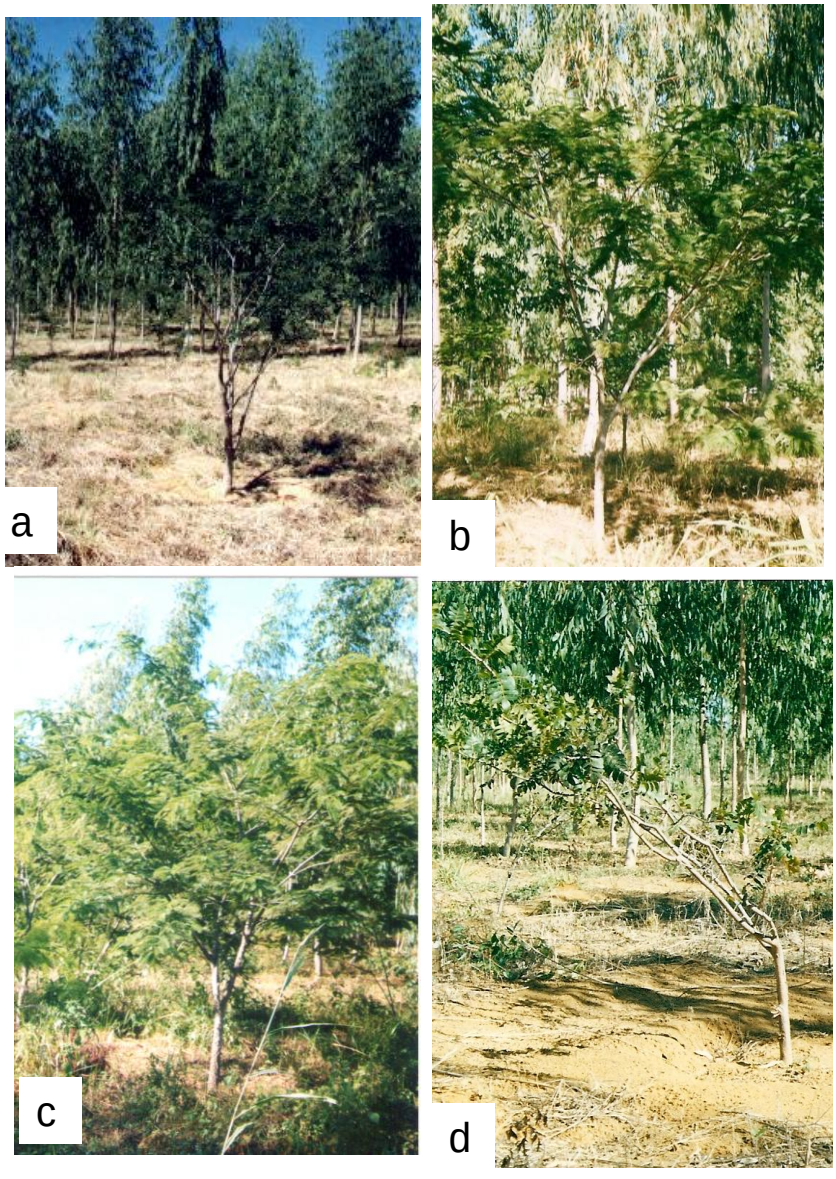

Figure 1 Native and *Eucalyptus* species at the experimental site at Jaíba in the state of Minas Gerais, Brazil.

Table 1. Trees used for agroforestry in Brazil (listed per family names and species) after two years of growth

Family	Plantation species	Common uses of the wood	Wood density	Reference
Bignoniaceae	*Tabebuia heptaphylla*	Ship, posts, pillars, railroad ties, heavy construction, parquet flooring, wheels.	0.87 g/cm³	2
Mimosaceae	*Anadenanthera peregrina*†	The wood very hard, it is good for making furniture.	0.86 g/cm³	4
	Enterolobium contortisiliquum †	Boat building, canoes, plywood, cases, toys, handicrafts, canoes, roof.	0.49 - 0.54 g/cm³	4
Leguminosae	*Plathymenia reticulata*†	Boat building, cabinetmaking, canoes, construction, door, flooring, flooring: industrial heavy traffic, furniture, heavy construction, interior trim, joinery, light construction, moldings, parquet flooring, plywood, railroad ties, tables, turnery, vehicle parts, veneer.	-	*
Anacardiaceae	*Schinopsis brasiliensis*	Posts, structural work, railroad ties, furniture, heavy construction, carpentry	1.23 g/cm^3	1
Mirtaceae	*Eucalyptus camaldulensis*	Important timber, firewood, shelter belt, and honey tree. In the Sudan, it is planted to protect crops from blowing sands. Widely used in Australia for strong durable construction, interior finish, flooring, cabinetry, furniture, fenceposts, cross-ties,	0.68 g/cm^3	own study
Family	Plantation species	Common uses of the wood	Wood density	Reference
		sometimes pulpwood. Australian aborigines made canoes from the bark.		
	Eucalyptus	Agricultural	624	3

Family	Plantation species	Common uses of the wood	Wood density	Reference
	grandis	implements, boat building (general), cabinetmaking, flooring, fuelwood, furniture, handles: general, heavy construction, joinery, ladders, light construction, mine timbers, paneling, particleboard, piling, plywood, poles, pulp/paper products, railroad ties, shingles, sporting goods, toys, turnery, veneer, wheel spokes, wheels	kg/m3	

†Legume tree. The different plant species were inoculated or not with AMF and rhizobia (legumes). Source: The wood explorer, NewCROP (New Crops Resource Online Program). References used for wood density values: 1 – Lorenzi (1992); 2 – Wittmann et al. (2008); 3 – Wood density database (http://worldsagroforestrycentre.org/sea/Products/AFDbases/WD/); 4 – other sources; * – no data available in literature.

The noduliferous leguminous (inoculated with specific rhizobia), as well as non leguminous trees, can be inoculated with a defined AM cocktail (spores of *Gigaspora* sp., *Scutellospora* sp., and *Glomus* sp.), isolated from pot cultures with *Brachiaria decumbens* Stapf, applied in a 5 cm furrow and mixed with soil at planting, to find out which AM species persist and the effects of inoculation.

Anadenanthera peregrina is a species commonly used in the revegetation of degraded sites, due to its good adaptation to soils of low fertility and poor physical characteristics. On the other hand, other species (*S. brasiliensis*) have a valuable timber wood and could be variable in soil fertility exigencies. However, the fertilization recommendation has been based upon the requirements of the most demanding species, aiming to assure a satisfactory growth of all species. Thus, in order to warrant an adequate initial seedling establishment under field conditions, the fertilization with NPK is recommendable, in spite of the unknown species demand (Siqueira et al. 1995). Common uses of the wood of the surveyed trees are present in table 1.

This chapter reports relevant research data on wood biomass, nutrition and the response of tree species to mycorrhizal inoculation, and shows management strategies. I present here an overview necessary to place in perspective the findings from the present chapter. If further detail is required on any subject covered by this paper, the references by the author should be consulted.

DETERMINATION OF BIOMASS AND NUTRIENT QUANTIFICATION

Mean diameter at breast height (1.3 m) over bark (D) (BHD, cm) and mean height of the plant species were calculated for each treatment (inoculated or not). Studies include the selection of three tree species at random. They were chainsawed and sampled for subsequent nutrient analysis. Branches were separated from the trunk and all the leaves were collected at field (Figure 2a,d). Then, total fresh weight of leaves, branches, bark and trunk wood of the sampled trees were determined at a local Laboratory. Native *A. peregrina* plants were sampled from monocultures with and without inoculation for an estimate of leaf, branch and stem dry matter. The branches were separated from the trunk, all the leaves were collected and fresh weight was recorded. The samples were dried in a chamber with air circulation at 60°C until constant weight was achieved. Finally, the samples were weighed in order to determine dry weight. Composite samples (100 g) of different physiological states (young, mature and old) were used to estimate total dry weight.

Dry mass production and nutrient concentration of *Eucalypus* cultivated in monoculture were evaluated at 28 months. The growth model was based on individual trees. Trunk samples consisted in 3.0 cm thick discs removed at each trunk (Figure 2b,c), at base and 25%, 50%, 75% and 100% of height, including BHD, as proposed by Shimoyama (1990). For each disc (Figure 2e), the bark was separated from the wood. This measurement served as a reference for wood density (wd) determination. These samples (weighed after immersion) were dried in a circulation oven at temperatures ranging from 65°C, until constant weight.

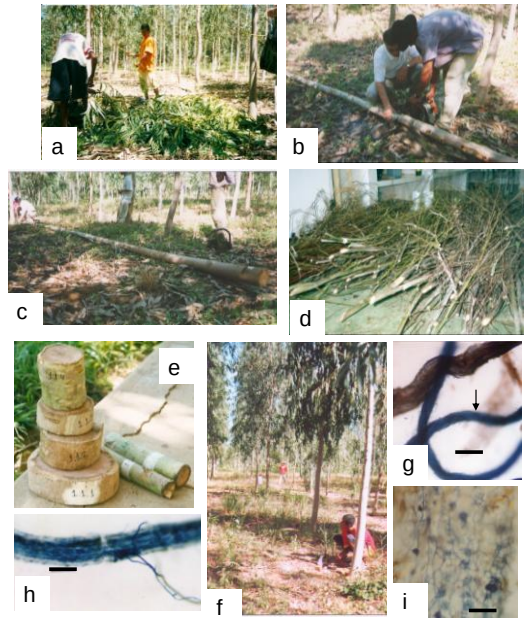

Figure 2. Methodology for native and exotic plant species used for agroforestry at Jaíba, Minas Gerais, Brazil: (a) collected fresh leaves, (b-c) chainsawed trunk for measures, (d) collected branches to estimate their weight, (e) *Eucalyptus* disks sampled for subsequent nutrient analysis, (f) root sampling, (g) ECM (arrow) in roots of eucalypt, and AM colonization in *P. reticulata* fine root (h) and *S. brasiliensis* fine root (i). Bars for figures g, h = 100 µm and i =10 µm.

Finally, samples were weighed with an analytical balance in order to obtain dry weight (dw) and the dry biomass of the components in each tree was calculated proportionally.

Total dry weight of leaves was obtained against composite samples of fresh weight, by using the following equation:

$$TDW = (TFW \times SDW) / SFW$$

where, *TDW* is the total dry weight (g), *TFW* the total fresh weight (g), *SDW* the sample dry weight (g), and *SFW* is the sample fresh weight (g).

Discs were used to calculate wood density of each subcompartment (bark and trunk wood), in each section of trunk, by the hydrostatic balance method, according to Bellote (1990).

$$bd = DW / (FW - IW)$$

where *bd* is the basic density (g cm^{-3}), *DW* the dry weight, *FW* the saturated fresh weight (g), and *IW* is the immersed weight (g).

Bark was removed from stem sections used to determine wood density. Dry mass of the sample was determined after oven drying for 48 h at 105°C.

Samples were taken of BHD, D5 (disc 5) and D6 sections for determination of mineral nutrient levels at a Soil Analyses Laboratory. Samples were dried at 75°C, digested in nitric-perchloric mixture and analyzed for macronutrients. Phosphorus was analyzed by the ammonium phosphomolybdate method. Calcium, potassium and magnesium were analyzed by atomic absorption and potassium by flame photometry.

After sulfuric digestion, Nitrogen (N) was determined by Kjeldahl method. These procedures are in according with Sarruge and Haag's methodology (1974). Nutrient concentrations of D2 sample were used to calculate wood (under bark) and bark nutrient concentrations (Young and Carpenter 1976).

Total tree volume (bark and trunk wood) was calculated by the Smalian equation which expressed the sum of segments of length calculated, which make up the trunk

$$V = 1/2 \times (\pi D^2 / 4 + \pi d^2 / 4) \times h$$

where *V* is the log volume (m^3), *D* the log major diameter (cm), *d* the log minor diameter (cm), and *h* is the log height (m).

Based on basic density and volume, total dry weight (W) was determined by using the following equation:

$$W = bd \times V \text{ (for bark and trunk wood)}$$

where *W* is the weight (g), *bd* the basic density (g·cm^{-3}), and *V* the log volume (m^3).

The mean biomass (wood and branches) was used to estimate the aboveground wood biomass (AWB) (Mg ha^{-1}) multiplying by 10,000 m^2 (one hectare) and dividing by 9 m^2 (area occupied by one tree, with spacement of 3 x 3 m).

To find out tree nutrient content, the model considered differences in concentration in stem compartment, that is, in bark and wood and also in leaves and branches. Bark volume was obtained through the difference between volumes with bark and without bark. The sum of leave and branches provided 12 samples, which yielded 12 determinations of nutrient levels. Discs (18 samples) provided 16 density determinations (2 samples were contaminated), besides allowing for calculating nutrient content in each tree log and each compartment analyzed.

Macronutrient stock ($kg \cdot ha^{-1}$) in the aboveground biomass was calculated on the basis of the dry mass estimation ($kg \cdot ha^{-1}$) and the macronutrient concentrations ($g \cdot kg^{-1}$) obtained in the present study. The sum of the values for each component provided the total nutrient content ($kg \cdot ha^{-1}$) of aboveground dry mass.

EVALUATION OF ROOT COLONIZATION BY FUNGI

Roots of *Eucalyptus* spp. were collected by excavating from the trunk to the lateral root system of each tree. Four root samples were harvested around the tree, and mixed together. Samples were collected from three trees at each block and were fixed in FAA solution (formalin:alcohol:acetic acid) until samples could be processed. Roots were stained (Pagano et al. 2009) and assessed for mycorrhizal colonization according to McGonigle et al. (1990), and results were expressed as percentage of colonized segments. Roots colonized by ECM (presence of Hartig net) were included when calculating the percentage of root length colonized by ECM. Dual mycorrhizae (AM and ECM) were observed and individually recorded for calculation. These data were arcsin (x/100)1/2 transformed. The data were subjected to one-way ANOVA using MINITAB software version 13.2 and means were compared by Tukey test ($P < 0.05$).

ABOVEGROUND BIOMASS AND NUTRIENTS IN EUCALYPTUS

The height of *E. camaldulensis* observed was higher than that previously reported by Bernardo et al. (1998) in southeastern Brazil, and the mean diameter was bigger than that in conventional fertilization plantation. The aboveground biomass was 33.6 $Mg \cdot ha^{-1}$ for *E. camaldulensis* and 53.1 $Mg \cdot ha^{-1}$ for *E. grandis.* Of the total aboveground biomass of *E. camaldulens*is, the stem wood, leaves, branches, and stem bark account for 64.4%, 19.6%, 15.4%, and 0.6%, respectively (Table 2), and, a similar partition of the total aboveground biomass was also found for *E. grandis* (66.6%, 16.1%, 17.1%, and 0.2% spread in the stem wood, leaves, branches, and stem bark, respectively). The aboveground biomass of *E. grandis* was higher than that reported by Faria et al. (2002) at 80 months-old stands of this species in a Cerrado region of Brazil, whereas the stem volume was lower than that observed. Biomass distribution in descending order was: wood> leaves> branches> bark, for *E. camaldulensis* and, wood> branch> leaves> bark for *E. grandis.*

The aboveground wood biomass (AWB) of tropical forests plays an important role in the carbon sequestration, and AWB estimates provide essential data that enable the extrapolation of biomass stocks (Wittmann et al. 2008) to agroforestry system carbon cycle modeling.

Therefore, the potential of agroforestry as a carbon sequestration strategy (carbon storage potential in its multiple plant species) must be more explored.

The content, average amount and ratio (percentage) of micro- and macronutrients immobilized in each component of the aboveground biomass of *E. camaldulensis* and *E. grandis* can be estimated.

E. camaldulensis accumulated 33.2% of nutrients in leaves, 6.2% in wood, 21.6% in branches, and 38.8% in stem bark (Pagano et al. 2009). For *E. camaldulensis*, the contents of N, P, K, Ca, Mg, and S in the total biomass were 122.7, 6.4, 99.8, 208.9, 16.1, and 11.2 kg·ha-1, respectively. The dry matter of leaves and branches accounted for 35% of the total biomass, and the contents of N, P, K, Ca, Mg, and S in leaves and branches accounted for 15.5%, 0.7%, 12.3%, 22.6%, 1.9%, and 1.4% of those in total above-ground biomass, respectively. In the trunk (bark and wood), which represents the remaining 65% of the total above-ground biomass, 4.5% of N, 0.28% of P, 7.4% of K, 31.3% of Ca, 1.1% of Mg, and 0.6% of S were accumulated (Pagano et al. 2009). Thus the canopy (leaves and branches) concentrates 54.73% nutrients of total aboveground biomass. Leaves have most tree living cells that tend to accumulate larger quantities of nutrients, due to respiration and photosynthesis (Kramer and Koslowski 1979).

For *E. grandis*, the contents of N, P, K, Ca, Mg, and S in the total biomass were 224.4, 10.7, 103.1, 225.4, 26.5, and 12.6 kg·ha-1, and the contents of N, P, K, Ca, Mg, and S in leaves and branches accounted for 23.6%, 1.1% , 10.5%, 20.9%, 2.6%, and 1.1% of those in total aboveground biomass (Table 3). In the trunk (bark and wood), which represents the remaining 66.8% of the total aboveground biomass, 6.3% of N, 0.34% of P, 4.7% of K, 26.4% of Ca, 1.8% of Mg, and 0.6% of S were accumulated (Pagano et al. 2009b).

The contents of N observed in our study corroborate the results obtained by Hunter (2001), who reported an average N content of 16 mg/g for E. grandis at 37 months and 14 mg/g for *E. camaldulensis* in a mixed plantation with 2m×2 m spacing. In general, the concentrations for N varied as foliage > branches, bole bark, roots > bole wood. Harrison et al. (2000) showed a higher N concentration in leaf and bark in *E. camaldulensis* in Cerrado soils, but the same concentrations in branches and wood. Schumacher and Poggiani (1993) reported higher N, P and K concentrations in leaves and highest concentrations of Ca and Mg in bark in *E. camaldulensis* and *E. grandis*. However, Dell et al. (1995) suggested that N leave concentrations for Eucalyptus grandis × Eucalyptus urophylla must be between 18 to 29 $g \cdot kg^{-1}$.

Phosphorus accumulation observed in that study (Pagano et al. 2009b) was similar to the results obtained by Hunter (2001). The concentration of P in branches was somewhat higher than the results showed by Hunter (2001). By other hand, Harrison et al. (2000) showed higher levels of P for this species, which varied as foliage > branches, bole bark, small roots > taproot, coarse roots, bole wood. Moreover, calcium concentration in *E. grandis* was similar to results showed by Hunter (2001), whereas Ca and Mg contents in *E. camaldulensis* were lower than the data showed.

Sulfur (an essential element found in plants mostly in its reduced form in amino acids cysteine and methionine) contents of the leaves were slightly lower than usual values (1.9 to 3.2 $g \cdot kg^{-1}$) reported by Dell et al. (1995). Silveira et al. (2003) also found a lower S concentration compared to that proposed in *E. grandis* seedlings leaves. The sulfur content in the total biomass (11 to 12.5 $kg \cdot ha^{-1}$) was higher than that reported by Caldeira et al. (2002) for other leguminous tree. Most of the nutrients were concentrated in the leaves and bark.

Nutrient concentration in leaves is influenced by diverse factors such as site conditions, age, position of leaves and season (Van der Driessche 1984). Bellote (1990) observed that nutrient concentration in leaves of E. grandis in Brazil varies with stand age and with the season. For all components, E. camaldulensis had the highest K concentration (33% higher). An exploitation system that preserves these tree components in the site would mean that approx. 403 $kg \cdot ha^{-1}$ of these nutrients could remain in the soil system.

In terms of aboveground dry mass, *E. grandis* performed better than E. camaldulensis. The two species show a difference in biomass partitioning and accumulation and differ in their concentrations of macronutrients (Pagano et al. 2009b). To assess nutrient content in trees during sampling, an age of three years old must be chosen since at this age *E. grandis* shows larger biomass accumulation per time unit. This is due to three-year-old trees' bigger capacity to absorb soil nutrients and according to Bellote (1990) to the fact that nutrient content in three-year-old *E. grandis* mature leaves shows the highest values.

The inner variability of trees species in longitudinal sense has more drastic effect on the chemical composition of bark than on that of wood. Wood of basal log of the two Eucalyptus species presented higher levels of N than the others logs. More apical logs present the highest N and P in the bark, and the highest P in the wood. *E. camaldulensis* showed the highest levels of Ca, Mg and S, at the basal log, and for K, the highest content was in the bark of basal log and wood of apical logs. *E. grandis* showed also more Ca, Mg and S content in basal log wood but, in contrast, bark of apical logs and wood of basal log presents more K (Pagano et al. 2009b). Potassium and Ca are nutrients that could limit productivity in the next cycle of plantation, and this limitation can be reduced, if only wood is harvested. To support the optimum soil calcium levels is, therefore, of increasing interest due to the lower levels of this nutrient present in soils cultivated with eucalypt, and to the fact that about 58% of total calcium absorbed is exported by bark removal (Pagano et al. 2009b).

COLONIZATION OF EUCALYPTUS ROOTS BY FUNGI

Mycorrhizal colonization varied with *Eucalyptus* species. Assessments of percentage AM and ECM root length for *E. camaldulensis* and *E. grandis* are shown in Table 2. The *E. camaldulensis* AM root colonization was 15%. Structures observed suggest a Glomeraceae AM colonization (Sieverding 1991), *Glomus* sp. being relevant for this species (Pagano et al. 2008). These results are in accordance with those obtained by Santos et al. (2001) where *E. camaldulensis* presented the highest values of percent AM mycorrhizal colonization among several *Eucalyptus* species and with Adjoud-Sadadu and Halli-Hargas (2000) who reported a <50% AM colonization by this same species. By other hand, *Eucalyptus* presented a Hartig net (ECM) confined to epidermal cells (Brundrett 2004). *Eucalyptus grandis* did not show AM root colonization (Table 2). This may depend on the time of sampling, but ECM was preferentially related with this species. The dual colonization by ECM and AM fungi in *E. camaldulensis* support the predominance of ECMs (Chen et al. 2000). ECM colonization of *E. grandis* was similarly to the results presented by Chen *et al*. (2006) for *E. urophylla*. Sustained levels of root colonization above 50% have been mentioned as necessary to ensure high survival and productivity of plantation (Marx et al. 1989) accessing sufficient N and P.

Ectomycorrhizal fungi are common in eucalypt plantations, being ecologically important in nutrient cycling (Högberg and Högberg 2002, Read and Perez–Moreno 2003). Observations of abundant basidiocarps (probably *Pisolithus*), especially in *E. grandis* plots, suggest that ECM may enable uptake of immobile phosphorus and other nutrients as has been reported by other references (Smith and Read 2008) reflecting this in plant nutrient content. Thus, the higher nutrient content (especially N and P) in *E. grandis* biomass may be explained by the presence of ECM. On the other hand, AM have an ecological and agronomic importance in the tropics and their presence can be influenced by environmental factors such as: climate conditions, physical proprieties, soil chemical and physical proprieties, host vegetal species and their age and variety (Cardoso and Kuyper 2006).

Moreover, *E. camaldulensis* showed a lower colonization during the rainy season. However, during the rainy season, ECM increased. This may be explained by the periodical death of ECM when water is limited and the demand by the trees is high, which have to form again when drought ends before being able to resume nutrient uptake (Courty et al. 2006). This suggests that Eucalyptus could obtain nutrients mainly from litter decomposition through ECM effect during the rainy season, corroborating results from Santos et al. (2001), who observed an increase in ECM colonization and AMF reduction in this species. These findings support the hypothesis that ECM develop more intensively in the organic residues of their autotrophic partners (Read 1991) and degrade the recalcitrant litter. The composition and properties of plant litter are essential controlling factors for organic matter formation and soil humification (Kögel–Knabner 2002).

ABOVEGROUND BIOMASS AND NUTRIENTS IN NATIVE WOODY SPECIES

The role of wood is to provide mechanical support and to supply water to the canopy, structural requirements that impact on wood density (Thomas et al 2004)**.** The high wood density of plants (c. 1.0 g cm^3), suggests, according to Borchert (1994), a lower stem water storage capacity in comparison with plants which have a lower wood density (<0.5 g cm^{-3}).

Under field conditions, the double inoculation of trees can improve height and diameter growth. Pagano (2008) has showed the benefit of the inoculation of *Rhizobium* in a native legume. Pagano et al. (2008) also showed that *A. peregrina* dry matter production and nutrient content, especially N and P, was improved. The productivity of the inoculated stand was greater than that of the uninoculated stands, especially regarding aboveground biomass. Most of the nutrients were concentrated in the leaves, stem, and in the bark (Figure 3) especially in inoculated plants. Nutrient concentrations in uninoculated *A. peregrina* plants followed the order: N>K>Ca>P>S>Mg, while in inoculated plants P content was higher (Figure 3).

When inoculated with *Rhizobium* and AM, the legume *P. reticulata* showed higher height growth than non-inoculated plants (Table 2). With respect to diameter growth, the inoculated plants in monoculture differed from uninoculated mixed plantation. Thus, after 2 years of cultivation, there was an effect of inoculation on *P. reticulata* height growth, both in monoculture and mixed plantation (Pagano et al. 2009a).

Therefore, the inoculation of both *P. reticulata* and *A. peregrina* with AMF resulted in an overall highly positive effect on the plant growth and nutrient absorption suggesting the efficiency with which the absorbed nutrients were used to produce plant biomass. The AM fungi colonized the roots of both species. Enhancing this hypothesis, a high number of AMF spores in soil under inoculated plantations was observed. Interestingly, inoculation increased the AM spore recovery of *P. reticulata* by *Gigaspora* sp.

In accordance with other authors (Manjunath et al. 1984, Faria et al. 1995, Marques et al. 2001, Gross et al. 2004, Pagano et al. 2007) who reported that dual inoculation generally increases plant growth to a greater extent than inoculation with only one symbiont (Chalk et al. 2006), the plant species *Anadenanthera peregrina and P. reticulata* plants grew better when inoculated with *Rhizobium* and AM as reported by for other trees.

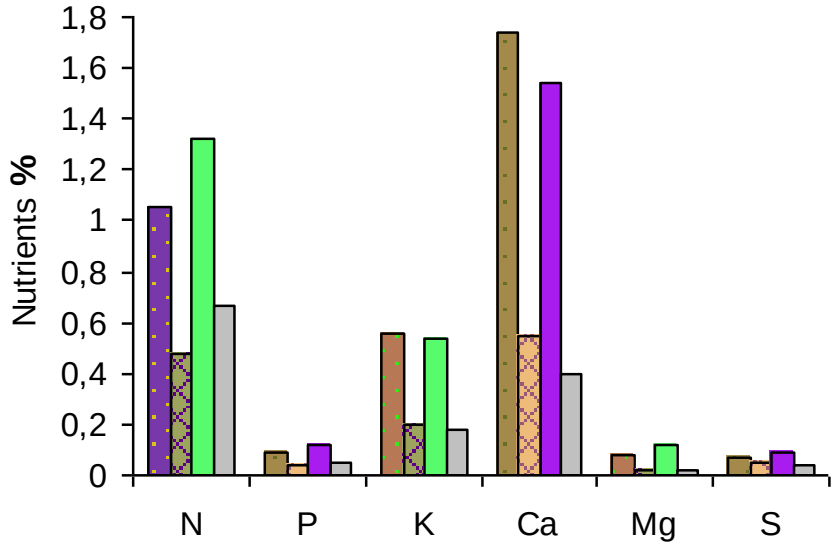

Figure 3 Percentage of nutrients (g/100 g) in the bark and wood of inoculated and uninoculated plants of *A. peregrina* in Brazil. Bark inoculated (*black*), wood inoculated (*hatched*), bark uninoculated (*white*), wood uninoculated (*gray*). Modified from Pagano et al. (2008).

COLONIZATION OF NATIVE TREE ROOTS BY FUNGI

AM are the most frequent fungi supported by legumes trees, enhancing the uptake of phosphorus, nitrogen and others nutrients, consequently being of high interest for agroforestry. AM form a mycelium in soil, and the hyphal proliferation occurs in response to several types of organic material and near potential host roots, improving physical soil quality (reviewed by Cardoso and Kuyper 2006). The use of the AM symbioses provides an alternative for decrease the high inputs of fertilizers and pesticides in sustainable plant production systems; however, AM inoculation technology is limited by the lack of production of commercial inocula, because AMF cannot be multiplied on artificial growth media without a host (Sieverding 1991).

This indicates that, similarly to what is recommended for forest formation with exotic trees, a best knowledge of characteristics and individual requirements of the utilized species, as well as, a good previous evaluation of the areas to be planted, are essential to a successful establishment of native species. Some tropical trees benefit from AM inoculation, while others do not (Bâ et al. 2000) because plant response to inoculation with AMF differs (Siqueira et al. 1998, Siqueira and Saggin Júnior 2001).

Plathymenia reticulata exhibited the highest values for root colonization. Carrenho et al. (2002) also found higher AM colonization in legumes than in non-legumes.

Studies of AM colonization are important for seedling production and preparation of technologies for successful afforestation, because of the fact that vegetal species exhibit different AM dependency (Siqueira and Saggin–Junior 2001).

BENEFITS AND PROBLEMS ENCOUNTERED IN THE STUDY

In order to maximize the benefits of mycorrhizas for soil fertility more research should be directed towards: (i) understanding the occurrence of benefic soil microorganisms and survival in soil, particularly field studies under different management conditions; (ii) the impact of fertilizers on soil microbiota; (iii) the possible role of legumes in transmitting nutrients to non-legumes through mycorrhizal pathway; (iv) the presence and effects of alellophatic substances on soil biota; and (v) developing relevant indicators for assessing soil biological quality and plant nutrient requirements. Sometimes, unnecessary nutrient supply is given to less demanding species, which results in waste of inputs (Faria 1999).

The presence of the commonly *Glomus* spores in both, native trees and eucalypt rhizospheres suggest that this AM genus could be a potential inoculum for the trees.

Mycorrhizal management through agroforestry is often a better option than mycorrhizal inoculation, considering the problems and costs of large-scale inoculum production. However, leguminous tree as *Anadenanthera peregrina* and *Plathymenia reticulata* showed greater height and diameter growth, as well as, higher dry matter and nutrient concentration (in *A. peregrina* plants) when inoculated.

Eucalyptus is very important in Brazil as an energy source and to produce pulp/paper and charcoal; however, large-scale plantations cause environmental impacts. *Eucalyptus* monoculture may reduce the fungal species found in the soil after several years of continuous culture as well as arbuscular mycorrhizal (AM) colonization percentage, number of spores and arbuscular mycorrhizal fungi (AMF) infectivity and a decrease in bioavailable nutrients (Carrenho et al. 2008). However, *Eucalyptus* spp. have the capacity to form two types of mycorrhizas, arbuscular (AM) and ectomycorrhiza (EM) and the potential uses of microbiological inoculants may be more studied. *Pisolithus tinctorius* is the most important ECM fungus for forestation and has been used to increase the growth of plantations of eucalypts (Garbaye et al. 1988); however, functional diversity of ECM is nowadays more studied (Garbaye 2009). Thus, a complete understanding of plant life histories should include traits related to AM formation.

The main problems facing woody forestation studies in Brazil are low financial support, long distances between the study site and the laboratory and the detrimental state of the highways. What is lacking is a suitable body of research that can be used to undertake more

as well as continuous field studies. Some techniques can be applied from other areas. The survey of ectomycorrhizas fruitbodies is essential in the *Eucalyptus* stands and some new methods derived from the woody evaluation are also relevant. Complications due to the short time of the field surveys and little technical support provide extra problems. Moreover, a conditioned sample is critical, because some samples must be processed rapidly in order to do not be detrimental by fungal action.

It may be that more nursery experiments need to be developed to prevent seedling development under different conditions, and there is a lack of greenhouse or nursery availability for these purposes. More detailed studies involving responses to nutrient addition in the field are needed for most native species used in reforestation. Also, more studies including molecular identification directly in host plant roots are important to select efficient AM isolates. Moreover, sampling in the rainy and dry periods would be required to conclude more information on mycorrhizal characterization in the plantations.

CONCLUSION

In the introduction to this chapter, the need for reforestation with native species and the significant benefits of mycorrhizal symbioses enhancing mineral nutrition, tolerance to drought stress, and soil fertility, were briefly described.

Throughout the chapter, I have shown that intercropping inoculated native and exotic trees maintain high root colonization and spore numbers, confirming the benefic role of AMF, and highlighting the importance of mycorrrhizae as an essential component for sustainability of artificial forests. All these results indicate that the tree species evaluated are dependent on mycorrhizas. Total productivity was of the order *E. grandis* > *E. camaldulensis* and these species did not reduce growth and aboveground biomass production when cultivated at this site, showing nutrient concentrations similar to that informed in the literature. The highest nutrient concentrations were found in the leaves and the lowest concentrations of N, P, K, Ca and Mg were found in the stem wood, those of S being in the stem wood and bark; wood localized in superior parts of trunk presented higher concentration of P and bark contained significant amounts of nutrients. Most of the nutrients were concentrated in the leaves and bark, and the methodology for native and exotic plant species used for agroforestry was also illustrated.

Also, the results indicate the need for selecting species to be used in programs to attain maximum benefit from mycorrhizal association. Nonetheless, further studies are required to achieve benefits from highly dependent tree hosts (native and exotic) in Brazil, especially regarding litter accumulation, below-ground biomass, nutrient dynamics and mycorrhizal symbiosis.

Finally, this chapter argues for an optimality view of agroforestry by showing how the complementary distribution of nutrients and symbioses are related.

Table 2. Characteristics of the Trees

Plantation species	Inoculation *	Height (m)	Diameter (cm)	Branches (g)	Bark (g)	Stem (g)	Wood (g)	AC (%)	EC (%)
T. heptaphylla	-	1.16	1.5	NE	NE	NE	NE	58.7	-
A. peregrina	-	2.38	3.7	191.04	NE	291.06	261.96‡	NE	-
	+	2.76	2.8	299.57	NE	467.87	421.09‡	NE	-
E. contortisiliquum	-	1.40	1.4	NE	NE	NE	NE	35	-
	+	1.53	1.4	NE	NE	NE	NE	30.1	-
P. reticulata	-	1.70	2.8	NE	NE	NE	NE	60	-
	+	2.35	4.5	NE	NE	NE	NE	65	-
S. brasiliensis	-	0.69	7.2	NE	NE	NE	NE	45	-
	+	0.80	7.8	NE	NE	NE	NE	60	-
E. camaldulensis	-	5.52	4.7	NE	NE	NE	NE	45	23.3
	+	12.2	10.5	4645.5	179.7	NE	19475.5	15	26.6
E. grandis	-	5.59	4.8	NE	NE	NE	NE	-	50
	+	12.9	11.8	8180.2	87.3	NE	31834.1	-	50

*The different plantations were inoculated or not with AMF and rhizobia (legumes). AC – arbuscular mycorrhizal colonization, EC: ectomycorrhizal colonization. Source: Pagano et al. 2008, Pagano et al. 2009 a,b, Pagano and Scotti 2009, Pagano et al. (in press). ‡Measure includes bark. AC – arbuscular mycorrhizal colonization, EC – ectomycorrhizal colonization of roots. NE – non-evaluated.

ACKNOWLEDGMENTS

The author is grateful to the Council for the Development of Higher Education at Graduate Level, Brazil (CAPES).

REFERENCES

Adjoud, D; Plenchette, C; Halli-Hargas, R. Response of 11 *Eucalyptus* species to inoculation with three arbuscular mycorrhizal fungi. *Mycorrhiza* 1996 6, 129–135.

Adjoud-Sadadou, D; Halli-Hargas, R. Occurrence of arbuscular mycorrhiza on aged *Eucalyptus*. *Mycorrhiza* 2000 9, 287–290.

Allen, EB; Rincón E; Allen MF; Pérez-Jimenez A; Huante P. Disturbance and seasonal dynamics of mycorrhizae in a tropical deciduous forest in Mexico. *Biotropica* 1998 30,261–274.

Bâ, AM; Plenchette, C; Danthu, P; Duponnois, R; Guissou, T. Functional compatibility of two arbuscular mycorrhizae with thirteen fruit trees in Senegal *Agroforestry Systems* 2000 50, 95–105.

Becerra, A; Cabello, M; Chiarini, F. Arbuscular mycorrhizal colonization of vascular plants from the Yungas forests, Argentina. *Ann. For. Sci.* 2007 64, 765–772.

Bhadalung, NN; Suwanarit, A; Dell, B; Nopamornbodi, O; Thamchaipenet, A; Rungchuang, J. Effects of long-term NP-fertilization on abundance and diversity of arbuscular mycorrhizal fungi under a maize cropping system. *Plant Soil* 2005 270, 371–382.

Borchert, R. Soil and stem water storage determine phenology and distribution of tropical dry forest trees. *Ecology* 1994 75, 1437–1449.

Brundrett, M; Kendrick, B. The roots and mycorrhizas of herbaceous woodland plants. I. Quantitative aspects of morphology. *New Phytol.* 1990 114, 457–468.

Cardoso, IM; Boddington, C; Janssen, BH et al. Distribution of mycorrhizal fungal spores in soils under agroforestry and monocultural coffee systems in Brazil. *Agrofor. Syst.* 2003 58, 33–43.

Cardoso, IM; Guijt, I; Franco, FS; Carvalho, AF; Ferreira Neto, PS. Continual learning for agroforestry system design: university, NGO and farmer partnership in Minas Gerais, Brazil. *Agricultural Systems* 2001 69, 235–257.

Cardoso, IM; Kuyper, TW. Mycorrhizas and tropical soil fertility. *Agric. Ecosyst. Environ.* 2006 116:72–84.

Carneiro, MAC; Siqueira, JO; Moreira, FMS; Carvalho D de; Botelho AS; Junior OJS. Micorriza arbuscular em espécies arbóreas e arbustivas nativas de ocorrência no Sudeste do Brasil. *Cerne* 1998 4, 129–145.

Carrenho, R; Barbosa, FF; Araújo, CVM; Alves, LJ; Santos, OM. Mycorrhizal Associations in *Eucalyptus* spp.: Status and Needs. *Tree and Forestry Science and Biotechnology* 2008 2, 1.

Carrenho, R; Trufem, SFB; Bononi, VLR. Effects of using different host plants on the detected biodiversity of arbuscular mycorrhizal fungi from an agroecosystem. *Rev. Bras. Bot.* 2002 25, 93–101.

Cavagnaro, TR; Gao, LL; Smith, FA; Smith, SE. Morphology of arbuscular mycorrhizas is influenced by fungal identity. *New Phytol.* 2001 151, 469–475.

Ceccon, E. *Eucalyptus* agroforestry system for small farms: 2-year experiment with rice and beans in Minas Gerais, Brazil. *New For.* 2005 29, 261–272.

Chen, YL; Brundrett, MC; Dell, B. Effects of ectomycorrhizas and vesicular-arbuscular mycorrhizas, alone or in competition, on root colonization and growth of *Eucalyptus globulus* and *E. urophylla*. *New Phytol.* 2000 146, 545–556.

Chilvers, GA; Lapeyrie, FF; Horan, DP. Ectomycorrhizal vs. endomycorrhizal fungi within the same root system. New Phytol. 1987 107, 441–448.

Coelho, FB; Borges, AC; Neves, JCL; Barros, NF; Muchovej, RM. Characterization and occurrence of mycorrhizal fungi in stands of *Eucalyptus grandis* and *Eucalyptus saligna*, in Botucatu, São José dos Campos and São Miguel Arcanjo, São Paulo State (in Portuguese). *Rev. Árvore* 1997 21, 563–573.

Colozzi, A; Cardoso, EJBN. Detection of arbuscular mycorrhizal fungi in roots of coffee plants and *Crotalaria* cultivated between rows. *Pesq. Agropec. Bras.* 2000 35, 2033–2042.

DeBell, D; Whitesell, CD; Schubert, TH. Mixed plantation of Eucalyptus and leguminous tree enhance biomass production. Pacific Southwest forest and Range Experiment Station Forest Service. US Department of Agriculture, Res Paper PSW-175. 1985 Berkeley, CA.

Denison, RF; Kiers, ET. Why are most rhizobia beneficial to their plant hosts, rather than parasitic? *Microbes and Infection* 2004 6, 1235–1239.

Dhar, PP; Mridha MAU. Biodiversity of arbuscular mycorrhizal fungi in different trees of madhupur forest, Bangladesh. *J. For. Res.* 2006 17, 201–205.

Dickson, S. The *Arum–Paris* continuum of mycorrhizal symbioses. *New Phytologist* 2004 163, 187–200.

Dickson, S; Smith, FA; Smith, SE. Structural differences in arbuscular mycorrhizal symbioses: more than 100 years after Gallaud, where next? *Mycorrhiza* 2007 17, 375–393.

Eom, AH; Hartnett, DC; Wilson, GWT. Host plant species effects on arbuscular mycorrhizal fungal communities in tallgrass prairie. *Oecologia* 2000 122, 435–444.

Frioni, L; Minasian, H; Volfovicz, R. Arbuscular mycorrhizae and ectomycorrhizae in native tree legumes in Uruguay. *For. Ecol. Manage*. 1999 115, 41–47.

Garbaye, J; Delwaulle, JC; Diangana, D. Growth responses of eucalypts in the Congo to ectomycorrhizal inoculation. *For. Ecol. Manage.* 1988 24, 151–157.

Garbaye, J. Structure and function of ectomycorrhizal communities in response to soil mechanical and chemical disturbances. In: Abstracts ICOM 6, Belo Horizonte, Brazil. 2009 19–20.

Giachini, AJ; Souza, LAB; Oliveira, VL. Species richness and seasonal abundance of ectomycorrhizal fungi in plantations of *Eucalyptus dunnii* and *Pinus taeda* in southern Brazil. *Mycorrhiza* 2004 14, 375–381.

Gianinazzi, S; Schüepp, H. Impact of Arbuscular Mycorrhizas on Sustainable Agriculture and Natural Ecosystems, Birkhauser-Verlag, Basel 1994.

Gomes, SP; Trufem, SFB. Arbuscular mycorrhizal fungi (Glomales, Zygomycota) in Ilha dos Eucaliptos, Represa do Guarapiranga, São Paulo State, SP. *Acta Bot. Brás.* 1998 12, 393–401.

Govindarajulu, M; Pfeffer, PE; Jin, H; Abubaker, J; Douds, DD; Allen, JW; Bücking, H; Lammers, PJ; Shachar-Hill, Y. Nitrogen transfer in the arbuscular mycorrhizal symbiosis. *Nature* 2005 435, 819–823.

Grazziotti, PH; Barros, NF; Borges, AC; Neves, JC; Fonseca S. Seasonal variation of root colonization by mycorrhizal fungi in hybrid eucalypt clones in Espírito Santo State. *Rev. Bras. Ciênc. Solo* 1998 22, 613–619.

Guillemin, JP; Gianinazzi, S; Trouvelot, A. Screening of arbuscular endomycorrhizal fungi for establishment of micropropagated pineapple plants. *Agronomie* 1992 12, 831–836.

Haselwandter, K; Bowen, GD. Mycorrhizal relations in trees for agroforestry and land rehabilitation. *Forest Ecology and Management* 1996 81, 1–17.

Hokka, V; Mikola, J; Vestberg, M; Setälä, H. Interactive effects of defoliation and an AM fungus on plants and soil organisms in experimental legume-grass communities. *Oikos* 2004 106, 73–84.

Jakobsen, I; Smith, SE; Smith, FA. Function and diversity of Arbuscular mycorrhizae in carbon and mineral nutrition. In: van der Heijden MGA and Sanders IR, editors. *Mycorrhizal Ecology*. Berlin: Springer; 2003, 75–92.

Jefwa, JM; Sinclair, R; Maghembe, JA. Diversity of glomale mycorrhizal fungi in maize/sesbania intercrops and maize monocrop systems in southern Malawi. *Agroforestry Systems* 2006 67, 107–114.

Jesus, EC; Schiavo, JÁ; Faria, SM. Dependência de micorrizas para a nodulação de leguminosas arbóreas tropicais. *Rev. Arvore* 2005 29, 545–552.

Johnson, NC; Gehring, CA. Mycorrhizas: symbiotic mediators of rhizosphere and ecosystem processes. In: Cardon ZG and Whitbeck JL, editors. *The rhizosphere: an ecological perspective*. London: Elsevier Academic Press; 2007; 31–56.

Jones, MD; Durall, DM; Tinker, PB. Phosphorus relationships and production of extramatrical hyphae by two types of willow ectomycorrhizas at different soil phosphorus levels. *New Phytologist* 1990 115, 259–267.

Khanna, PK. Nutrient cycling under mixed-species tree systems in southeast Asia. *Agrofor. Syst.* 1997 38, 99–120.

Koide, RT; Schreiner, RP. Regulation of the vesicular-arbuscular mycorrhizal symbiosis. *Annu. Rev. Plant Physiol. Plant Mol. Biol.* 1992 43, 557–81.

Landeweert, R; Hoffl, E; Finlay, RD; Kuyper, TW; Breemen, N. Linking plants to rocks: ectomycorrhizal fungi mobilize nutrients from minerals. *Trends Ecol. Evol.* 2001 16, 248–254.

Lorenzi H (1992) Árvores Brasileiras. Nova Odessa: Editora Plantarum.

Maia, SMF; Xavier, FAS; Oliveira, TS, Mendonça, ES, Araújo Filho, JA. The impact of agroforestry and conventional systems on the soil quality from cearense semi-ard region. *Rev. Árvore* 2006 30, 837–848.

Malajczuk, N; Linderman, RG; Kough, J; Trappe, JM. Presence of vesicular-arbuscular mycorrhizae in *Eucalyptus* sp. and *Acacia* sp., and their absence in *Banksia* sp. after inoculation with *Glomus fasciculatus*. *New Phytologist.* 1981 87, 567–57

Marcar, NE; Zohar, Y; Guo, J; Crawford DF. Effect of NaCl and high pH on seedling growth of 15 *Eucalyptus camaldulensis* Dehnh. provenances *New Forests* 2002 23:193–206.

Marques Júnior, OG; Andrade, HB; Ramalho, MAP. Avaliação de procedências de *Eucalyptus cloeziana* F. Muell e estimação de parâmetros genéticos e fenótipos na região noroeste do estado de Minas Gerais. *Cerne* 1996 2, 12–19.

Martensson, AM; Rydberg, I; Vestberg, M. Potential to improve transfer of N in inter-cropped systems by optimizing host-endophyte combinations. *Plant and Soil* 1998 205, 57–66.

Mason, PA; Ingleby, K; Munro, RC; Wilson, J; Ibrahim, K. The effect of reduced phosphorus concentration on mycorrhizal development and growth of *Eucalyptus globulus* Labill. seedlings inoculated with 10 different fungi, *For. Ecol. Manage.* 2000 128, 249–258.

May, BM; Attiwill, PM. Nitrogen-fixation by Acacia dealbata and changes in soil properties 5 years after mechanical disturbance or slash-burning following timber harvest. *For. Ecol. Manage.* 2003 181, 339–355.

Molina, R; Massicotte, H; Trappe, JM. Specificity phenomena in mycorrhizal symbioses: community-ecological consequences and practical implications. In: Allen MJ, editor. *Mycorrhizal Functioning*. New York: Chapman and Hall; 1992; 357–423.

Muleta, D; Assefa, F; Nemomissa, S; Granhall, U. Distribution of arbuscular mycorrhizal fungi spores in soils of smallholder agroforestry and monocultural coffee systems in southwestern Ethiopia. *Biol Fertil Soils* 2008 44,653–659.

Olsson, PA; Jakobsen, I; Wallander, H. Foraging and resource allocation strategies of mycorrhizalfungi in a patchy environment. In: van der Heijden MGA and Sanders IR, editors. *Mycorrhizal Ecology*. Berlin: Springer; 2003, 93–115.

Pagano, MC. Characterization of Glomalean mycorrhizal fungi and its benefits on plant growth in a semi-arid region of Minas Gerais (Jaíba Project), Brazil. PhD thesis. Belo Horizonte: Federal University of Minas Gerais; 2007.

Pagano, MC; Cabello, MN; Scotti, MR. Phosphorus response of three native Brazilian trees to inoculation with four arbuscular mycorrhizal fungi. *J. Agric. Technol.* 2007 3, 231–240.

Pagano, MC. Rhizobia associated with neotropical tree Cenrolobium tomentosum used in riparian restoration. *Plant Soil Environment* 2008 54, 498–508.

Pagano, MC; Cabello, MN; Bellote, AF; Sa, NM; Scotti, MR. Intercropping system of tropical leguminous species and *Eucalyptus camaldulensis*, inoculated with rhizobia and/or mycorrhizal fungi in semiarid Brazil. *Agrofor. Syst*. 2008 74, 231–242.

Pagano, MC; Scotti, MR. Arbuscular and ectomycorrhizal colonization of two Eucalyptus species in semiarid Brazil. *Mycoscience* 2008 49, 379–384.

Pagano, MC; Scotti, MR; Cabello, MN. Effect of the inoculation and distribution of mycorrhizae in *Plathymenia reticulata* Benth under monoculture and mixed plantation in Brazil. *New Forests* 2009 38, 197–214.

Pagano, MC; Bellote, AF; Scotti, MR. Aboveground nutrient components of *Eucalyptus camaldulensis* and *E. grandis* in semiarid Brazil under the nature and the mycorrhizal inoculation conditions. J. For. Res. 2009 20, 15-22.

Pagano, MC; Cabello, MN; Scotti, MR. Agroforestry In Dry Forest, Brazil: Mycorrhizal Fungi Potential. In:. Kellimore LR, editor. *Handbook on Agroforestry: Management Practices and Environmental Impact*. New York: Nova Publishers, 2010 Chapter 14 ISBN 9781608763597.

Patreze, CM; Cordeiro, L. Nodulation, arbuscular mycorrhizal colonization and growth of some legumes native from Brazil. *Acta Bot. Bras*. 2005. 19, 527–537.

Plenchette, C; Clermont-Dauphin, C; Meynard, JM; Fortin, JA. Managing arbuscular mycorrhizal fungi in cropping systems. *Can. J. Plant. Sci.* 2005 85, 31–40.

Prado, DE. As Caatingas de América do Sul. In: Leal IR, Tabarelli M and Silva JMC, editors *Ecologia e Conservação da Caatinga*. Recife: Ed. Universitária da UFPE; 2003; 1–74.

Read, DJ. The structure and function of the vegetative mycelium of mycorrhizal roots. In: Jennings DH and Rayner ADM, editors. *The ecology and Physiology of the fungal Mycelium*. Cambridge University Press; 1984; 215–240.

Read, DJ. Mycorrhizas in ecosystems. *Experientia* 1991 47:376–391.

Read, DJ. Towards Ecological Relevance – Progress and Pitfalls in the Path Towards an understanding of mycorrhizal functions in nature. In: van der Heijden MGA and Sanders IR, editors. *Mycorrhizal Ecology*. Berlin: Springer; 2003; 3–29.

Reis, MF; Krügner, TL. Evaluation of VA mycorrhizal fungi in development of *Eucalyptus grandis* in greenhouse conditions. IPEF *Instituto de Pesquisas e Estudos Florestais* 1990 43/44, 79–83.

Rizzini, CT. Tratado de fitogeografia do Brasil: aspectos ecológicos, sociológicos e florísticos. 2nd Edition. Rio de Janeiro: Âmbito Cultural Edições Ltda.; 1997.

Santos, VL; Muchovej, RM; Borges, AC; Neves, JCL; Kasuya, MCM. Vesicular–arbuscular ectomycorrhiza succession in seedlings of *Eucalyptus* spp. *Braz. J. Microbiol.* 2001 32, 81–86.

Sieverding, E. Vesicular-arbuscular mycorrhiza management in tropical agrosystems. Eschborn: Deutsche Gesellschaft für Technische Zusammenarbeit. (GTZ) GmnBH, Esch boran; 1991.

Siqueira, JO; Saggin–Júnior, OJ; Flores-Ayles, WW; Guimaraes, PTG. Arbuscular mycorrhizal inoculation and superphosphate application influence plant development and yield of coffee in Brazil. *Mycorrhiza* 1998 7, 293–300.

Siqueira, JO; Saggin–Júnior, OJ. Dependency on arbuscular mycorrhizal fungi and responsiveness of some Brazilian native woody species. *Mycorrhiza* 2001 11, 245–255.

Silva Junior, JP; Cardoso, EJBN. Arbuscular mycorrhiza in cupuaçu and peach palm cultivated in agroforestry and monoculture systems in the Central Amazon region *Pesq. Agropec. Bras*. 2006 41, 819–825.

Sinclair, FL. A general classification of agroforestry practice. *Agroforestry Systems* 1999 46, 161–180.

Smith SE, Read DJ. 2008. Mycorrhizal symbiosis. 3rd ed. Academic Press.

Soares, ACF; Garrido, MS; Azevedo, RL; Mendes, LN; Grazziotti, PH. Produção de mudas de ipê roxo inoculadas com fungos micorrízicos arbusculares. *Magistra* 2003 15, 2.

Somasegaran, P; Hoben, HJ. Handbook for rhizobia: methods in legume-*Rhizobium* technology. New York: Springer-Verlag; 1994.

Tabarelli, M; Silva, JMC. Áreas e ações prioritárias para a conservação da biodiversidade da Caatinga In: Leal I.R., Tabarelli M and Silva JMC, editors. *Ecologia e Conservação da Caatinga.* Recife: Ed. Universitária da UFPE; 2003; 777–796.

Thomasa, DS; Montagub, KD; Conroy JP. Changes in wood density of *Eucalyptus camaldulensis* due to temperature—the physiological link between water viscosity and wood anatomy. *Forest Ecology and Management* 2004 193, 157–165.

Thomson, BD; Grove, TS; Malajczuk, N; Hardy, GEStJ. The effectiveness of ectomycorrhizal fungi in increasing the growth of *Eucalyptus globulus* Labill. in relation to root colonisation and hyphal development in soil. *New Phytol.* 1994 126, 517–524.

Tótola, MR; Borges, AC. Growth and nutritional status of Brazilian Wood species *Cedrella Fissilis* and *Anadenanthera Peregrina* in bauxite spoil in response to arbuscular mycorrhizal inoculation and substrate amendment. *Brazilian Journal of Microbiology* 2000 31, 257–265.

Trouvelot, A; Kough, JL; Gianinazzi-Pearson, V. Mesure de taux de mycorhization VA d'un système radiculaire. Recherche de méthodes d'estimation ayant une signification fonctionnelle. In: Gianinazzi-Pearson V, Gianinazzi S, editors. *Physiological and Genetical Aspects of Mycorrhizae*. Paris: INRA Press; 1986; 217–221.

Verchot, LV; Noordwijk, MV; Kandji, S; Tomich, T; Ong, C; Albrecht, A; Mackensen, J; Bantilan, C; Anupama, KV; Palm, C. Climate change: linking adaptation and mitigation through agroforestry. *Mitig. Adapt. Strat. Glob. Change* 2007 12, 901–918.

Wang, B; Qiu, YL. Phylogenetic distribution and evolution of mycorrhizas in land plants. *Mycorrhiza* 2006 16, 299–363.

Wittmann F., Zorzi B T,Tizianel F A T,Urquiza MVS,Faria R R, Sousa NM, Módena É S, Gamarra R M, Rosa A L M. 2008. Tree Species Composition, Structure, and Aboveground Wood Biomass of a Riparian Forest of the Lower Miranda River, Southern Pantanal, Brazil. *Folia Geobot.* 2008 43, 397–411.

Wubet, T; Kottke, I; Teketay, D; Oberwinkler, F. Mycorrhizal status of indigenous trees in dry Afromontane forests of Ethiopia. *For. Ecol. Manage.* 2003 179, 387–399.

Zambolim, L; Barros, NF. Vesicular-arbuscular mycorrhiza ocurrence in *Eucalyptus* spp. in Viçosa region, Minas Gerais. *Rev. Árvore* 1982 6, 95–97.

Zangaro, W; Nisizaki, SMA; Domingos JCB; Nakano EM. Micorriza arbuscular em espécies arbóreas nativas da Bacia Do Rio Tibagi, Paraná. *Cerne* 2002 8, 077–087.

Zhao, X; Yu, T; Wang, Y; Yan, X. Effect of arbuscular mycorrhiza on the growth of *Camptotheca acuminate* seedlings *Journal of Forestry Research* 2006 17, 121–123.

In: Wood: Types, Properties and Uses
Editor: Lorenzo F. Botannini
ISBN 978-1-61668-837-0

Chapter 5

FUNGAL DECOMPOSITION OF BEECH COARSE WOODY DEBRIS IN A TEMPERATE FOREST ECOSYSTEM

Yu Fukasawa[1], Takashi Osono[2] and Hiroshi Takeda[3]

1.Totoro Fund, Kotesashi 4-20-2-101, Tokorozawa, Saitama 359-1141, Japan
2.Center for Ecological Research, Kyoto University, 2-509-3, Hirano, Otsu, Shiga 520-2113, Japan
3.Wildlife Preservation Laboratory, Faculty of Science and Engineering, Doshisha University, Miyakodani 1-3, Tatara, Kyotanabe, Kyoto 610-0321, Japan

ABSTRACT

Decomposition of coarse woody debris (CWD) is an important component of the carbon cycle and biodiversity of forest ecosystems. Dynamics of organic chemicals, nutrients and occurrence of fungi during CWD decomposition have been studied intensively in coniferous boreal forests. However, little attention has been paid to the CWD of angiosperms that dominate temperate areas and to the relation between the organic chemical dynamics and fungal succession during CWD decomposition. Thus, the purpose of the present study is to clarify the mechanism of fungal decomposition of CWD of an angiosperm tree, Japanese beech (*Fagus crenata* Blume).

First, the dynamics of the physicochemical properties of beech CWD during decomposition were estimated. A chronosequence method with a five decay class system was used to estimates the decay process of CWD. Second, a mycological survey was conducted for macrofungi fruiting on CWD and microfungi isolated from CWD, and the relationships between fungal succession and physicochemical changes during CWD decomposition were detected. In light of the results, fungal decomposition of beech CWD and the implication for soil humus accumulation were discussed.

1. INTRODUCTION

Coarse woody debris (CWD) is a major component of forest ecosystems accounting for about one-third of the total annual aboveground litterfall in temperate areas (e.g., Nishioka and Kirita 1978). CWD is characterised by low nutrient content (Vogt et al. 1986; Laiho and Prescott 2004) and high content of cell wall components such as acid-unhydrolyzable residue (AUR, also known as the acid-insoluble residue or "Klason lignin" fraction) and holocellulose (Eriksson et al. 1990; Eaton and Hale 1993). These properties make CWD an important sink of nutrients and carbon pools accumulating on the forest floor (Harmon et al. 1986). The study of decomposition of CWD is important for understanding the mechanisms of accumulation and turnover of carbon and nutrients in forest ecosystems.

Fungi play a central role in transformation and mineralization of CWD since their mycelial form and enzymatic capacities are especially suitable for invasion of CWD (Eriksson et al. 1990; Boddy 1991). Wood decay fungi cause three types of decay according to the color changes in decayed wood, the changes in microscopic features, and the relative loss of AUR and holocellulose. White-rot fungi attack both AUR and holocellulose, and white-rotted wood becomes white and fibrous texture. Brown-rot fungi preferentially attack holocellulose with a slight or negligible loss of AUR, and brown-rotted wood becomes brown in appearance and shows cubically cracked texture. Soft-rot fungi actively utilize holocellulose under water-saturated and fluctuating conditions, and soft-rotted wood becomes cheesy soft and considerably darkened (Eriksson et al. 1990; Boddy 1991; Eaton and Hale 1993). The decomposition of CWD on the forest floor proceeds through a sequential colonisation by fungal species with different decay types and their interspecific interactions, which leads to a fungal succession during decomposition (Rayner and Boddy 1988).

Because of the slow decomposition rate, the long-term pattern of CWD decomposition has been estimated by means of chronosequence methods in which logs and snags decaying on the forest floor are classified into decay classes based on a combination of visual and physical properties (Table 1). Differences in CWD properties observed between decay classes are regarded as changes during the decay process. Using chronosequence methods, several studies have described CWD decomposition on the forest floor, but mostly in boreal coniferous forests (e.g., Lambert et al. 1980; Hope 1987; Preston et al. 1990, 1998; Means et al. 1992; Ganjegunte et al. 2004; Bütler et al. 2007). These studies revealed that chemical changes in decomposing conifer CWD followed a general two-phase pattern with different classes of organic components dominating in each phase. A simultaneous loss of AUR and holocellulose occurs in the first phase (decay class 1–3). In the second phase (decay class 4–5), holocellulose is decomposed selectively and AUR accumulates in the remaining CWD. Means et al. (1992) reported that the dominant decay types of Douglas-fir logs changed from white-rot to brown-rot during log decomposition. These results suggested that, in conifers, the selective decomposition of holocellulose in the brown-rot process, after the simultaneous decomposition of AUR and holocellulose in the white-rot process, causes AUR accumulation in well-decayed CWD. This explanation was also supported by the succession patterns of fungal fruit bodies during conifer CWD decomposition, that start from white-rot fungi to brown-rot fungi (Bader et al. 1995; Renvall 1995; Temnuhin 1996; Høiland and Bendiksen 1997; Lindblad 1998; Kruys et al. 1999; Sippola and Renvall 1999; Sippola et al. 2001; Jankovský et al. 2002).

On the other hand, few studies have revealed the whole decay process of angiosperm CWD, although fungal community development has been studied intensively (Boddy and Heilmann-Clausen 2008). The composition of angiosperm wood is very different from that of gymnosperm, and that may affect their decay processes. Thus, more studies are necessary to follow the decomposition of angiosperm CWD (Hatcher 1987; Schowalter 1992; Schowalter et al. 1998; Idol et al. 2001) to obtain a general picture of CWD decomposition in forests.

This chapter considers the pattern of changes in organic chemical components (AUR and holocellulose) and nitrogen in decomposing logs and snags of an angiosperm tree, Japanese beech (*Fagus crenata* Blume).

Table 1. Characteristics used for the classification of beech CWD in decay classes (modified from Heilmann-Clausen 2001)

Decay class	Characteristics
1	Wood hard, a knife (with a thin blade) penetrates only a few mm into the wood, bark intact, twigs (diam < 1 cm) intact.
2	Wood rather hard, a knife penetrates less than 1 cm into the wood, bark starting to break up, twigs±lost, branches (diam 1-4 cm) intact.
3	Wood distinctly softened, knife penetrates ca. 1-4 cm into the wood, except for parts colonized by certain pyrenomycetes (in particular *Eutypa spinosa*, *Kretzschmaria deusta* and *Biscogniauxia capnodes*), bark partly lost, branches±lost, original log circumference intact.
4	Wood strongly decayed, knife penetrates ca. 5-10 cm into the wood, except for parts colonized by certain pyrenomycetes (see above), bark lost in most places, original log circumference disintegrating.
5	Wood very strongly decayed, either to very soft crumbly substance, or being flaky and fragile with numerous remnants of pseudosclerotial plates, these defining the log surface, knife penetrates in most places more than 10 cm into the wood, original log circumference not or hardly recognizable.

The pattern of fungal succession on the logs and snags are investigated simultaneously by means of chronosequence method. Based on these results, possible roles of fungal communities in decomposition of beech CWD are discussed with reference to previous works on the decay ability of fungal species examined under pure culture conditions (e.g. Tanaka et al. 1988; Tanesaka et al. 1993; Worrall et al. 1997; Fukasawa et al. 2005a).

2. STUDY SITE AND CWD MATERIALS

All field surveys were conducted in a cool temperate deciduous forest dominated by *F. crenata* and *Quercus crispula* in Ashiu Experimental Forest of Kyoto University (35˚ 18'N, 135˚ 43'E, asl. 640–810m) about 40 km north of Kyoto, central Japan. Vegetation detail of the study site was described in Tateno and Takeda (2003). Mean annual temperature was about 10 ˚C and mean monthly temperature range from 0.4 ˚C in January to 25.5 ˚C in August. The mean annual precipitation over 56-year was 2495 mm. The study area was located in the Sea of Japan coastal regions where heavy snow covered the ground (over 2 m depth in max) in the winter period from December to April.

In the study site, snags and logs of beech (diameter > 10 cm) were investigated. In the present study, we defined snags as "standing dead stems over 2 m in height". We assigned each log of beech to one of five decay classes, using visual criteria applicable to angiosperms (Heilmann-Clausen 2001; Table 1). Snags were assigned a decay class of 1 through 4. To eliminate the within-stem variation of decay class (Pyle and Brown 1999), a part (about 2 m along the stem) where decay class is uniform was selected for each CWD and used for investigation. Snags and logs of beech were identified by bark texture and xylem ray distribution of wood tissues using the keys in Shimaji et al. (1980). A total of 47 snags and 66 logs of beech were marked along a 3-km walkway that included the ridge and bottom of a slope. The range of the diameter of the CWD was 13–73 cm.

3. DYNAMICS OF WOOD CHEMICAL PROPERTIES DURING BEECH CWD DECOMPOSITION

Wood chemical properties (contents of AUR, holocellulose and nitrogen) were analysed for both snags and logs. Details of the chemical analysis were described in Fukasawa et al. (2009a).

Decomposition processes of beech CWD showed two phases characterised by different dominant organic chemical constituents (Figure 1). The first phase corresponded to decay class 1 to 3, which was characterised by the simultaneous decomposition of AUR and holocellulose. Net retention of nitrogen (decay class 1–2), followed by net release (decay class 2–3) occurred in this phase. The second phase corresponded to decay class 3 to 5, which was characterised by selective decomposition of holocellulose and concomitant AUR accumulation. Immobilisation of N occurred in this phase. The first phase is a typical white-rot process as reported previously (Schowalter 1992; Schowalter et al. 1998; Kawase 1962).

Net retention and subsequent release of N in the first phase may due to relatively high initial N concentration of beech CWD among tree species (Laiho and Prescott 2004) and may be caused by accumulation in the fungal biomass and subsequent loss by fruiting body formation, respectively (Merrill and Cowling 1966; Frankland 1982; Matsumoto and Tokimoto 1992; Harmon et al. 1994).

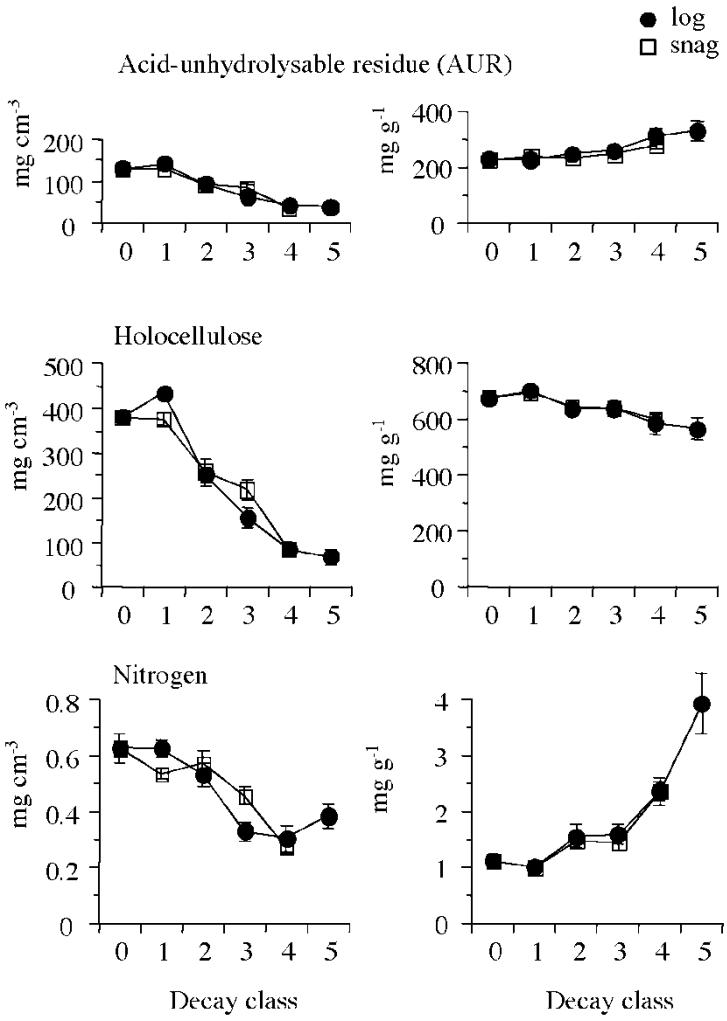

Figure 1. Changes in mass per volume (left) and concentration (right) of AUR, holocellulose and nitrogen during decomposition. Bars indicate standard errors. Bars indicate standard errors. Symbols, *closed circle* log; *open square* snag.This figure is published in Dynamics of physicochemical properties and occurrence of fungal fruit bodies during decomposition of coarse woody debris of *Fagus crenata* by Yu Fukasawa, Takashi Osono, and Hiroshi Takeda (2009). Journal of Forest Research, 14, 20-29. The original figure includes alphabets showing significant difference between decay classes.

On the other hand, in the second phase, holocellulose was decayed selectively and AUR accumulated. Nitrogen concentration increased in this phase. High N concentrations in much decayed wood are a combination of (1) active transport of N from soil to wood by basidiomycetes with mycelial cords (Tlalka et al. 2008), (2) a general up-concentration of N as carbon is released as CO_2 (Laiho and Prescott 2004) and (3) a high animal biomass (Boddy and Jones 2008).

The AUR accumulation in decay class 4 to 5 observed in the present study was similar to that of boreal gymnosperm (Lambert et al. 1980; Hope 1987; Preston et al. 1990; Means et al. 1992; Preston et al. 1998; Bütler et al. 2007). These studies suggested that brown-rot processes due to brown-rot fungi, after the primary white-rot process, caused AUR

accumulation in well-decayed CWD of gymnosperm (Renvall 1995; Niemelä et al. 1995). Brown-rotted wood was characterised by brown discoloration and a friable, cubically cracked texture (Eriksson et al. 1990). However, such characteristics were seldom observed in beech CWD in the present study (Fukasawa Y personal observation). Thus, it is expected that the AUR accumulation processes observed in the present study may be different from the brown-rot process. The soft, humus-like texture of beech wood in decay class 5 in the present study resembled soft-rotted wood.

4. FUNGAL SUCCESSION DURING BEECH CWD DECOMPOSITION

4.1. Succession of Macrofungi

Fungi forming large (> 1 mm) sporocarps are called macrofungi, including Basidiomycota and xylariaceous Ascomycota. They have been regarded as functional decomposers of CWD (Rayner and Boddy 1988). Appearance of fruiting bodies of macrofungi was recorded for both snags and logs in this study. The occurrence of fungal taxa on a CWD was scored as a single record regardless of the number of fruiting bodies that developed on the CWD. Frequency of each taxon on snags and logs was represented as percentage of the number of records of a taxon in the total number of CWD. Although, recently developing molecular technique allow identification of fungal species directly from colonized wood tissues (Vainio and Hantula 2000), it is still obvious that recording fruit bodies is an easy and actual way to recognize fungal colonization.

Among a total of 69 taxa of basidiomycetes and 24 species of ascomycetes were recorded on the logs and snags, ten taxa frequently encountered with a frequency of occurrence more than 10% on the logs and/or snags are: *Omphalotus guepiniformis*, *Biscogniauxia capnodes*, *Eutypa spinosa*, *Trichaptum biforme*, *Fomes fomentarius*, *Pluteus* spp., *Ganoderma tsunodae*, *Mycena haematopus*, *Steccherinum rhois* and *Oudemansiella venosolamellata* (Figure 2). *Oud. venosolamellata*, *G. tsunodae* and *F. fomentarius* occurred more frequently on snags than on logs, whereas the other 7 taxa occurred on both snags and logs. The ten frequent taxa were divided into early and late colonisers according to their occurrence during CWD decomposition. Eight species (*Oud. venosolamellata*, *S. rhois*, *G. tsunodae*, *T. biforme*, *Omp. guepiniformis*, *F. fomentarius*, *B. capnodes* and *E. spinosa*) were more frequent on CWD at decay class 1 to 3 than those at decay class 4 and 5, and thus were regarded as early colonisers. The frequencies of the other 2 taxa (*Pluteus* spp. and *M. haematopus*) increased as decay progressed and became frequent at decay class 4 and 5. These two species thus were regarded as late colonisers. Community structure of macrofungi was significantly related with decay class, water content and type of CWD (log or snag) (Fukasawa et al. 2009a).

Succession of macrofungi on decomposing CWD of beech followed a similar pattern to previous studies (Ueyama 1966; Lange 1992; Allen et al. 2000; Ódor et al. 2004; Takahashi and Kagaya 2005). Species in the genera *Biscogniauxia* and *Eutypa* are known to be latent inhabitants of live stems of angiosperms and to act as primary decomposers of dead woody tissue (Hendry et al. 1998). Recalcitrant sporocarps of *B. capnodes* and *E. spinosa* were resident until the late phase of decomposition. *Omphalotus guepiniformis*, *Fomes fomentarius* and species in the genus *Trichaptum* are known to be early colonisers (Ueyama 1966;

Niemelä et al. 1995; Renvall 1995; Temnuhin 1996; Lindblad 1998; Sippola et al. 2001; Lindhe et al. 2004). *Mycena haematopus* and *Pluteus* spp. are known to be late colonisers (Lange 1992; Allen et al. 2000; Takahashi and Kagaya 2005).

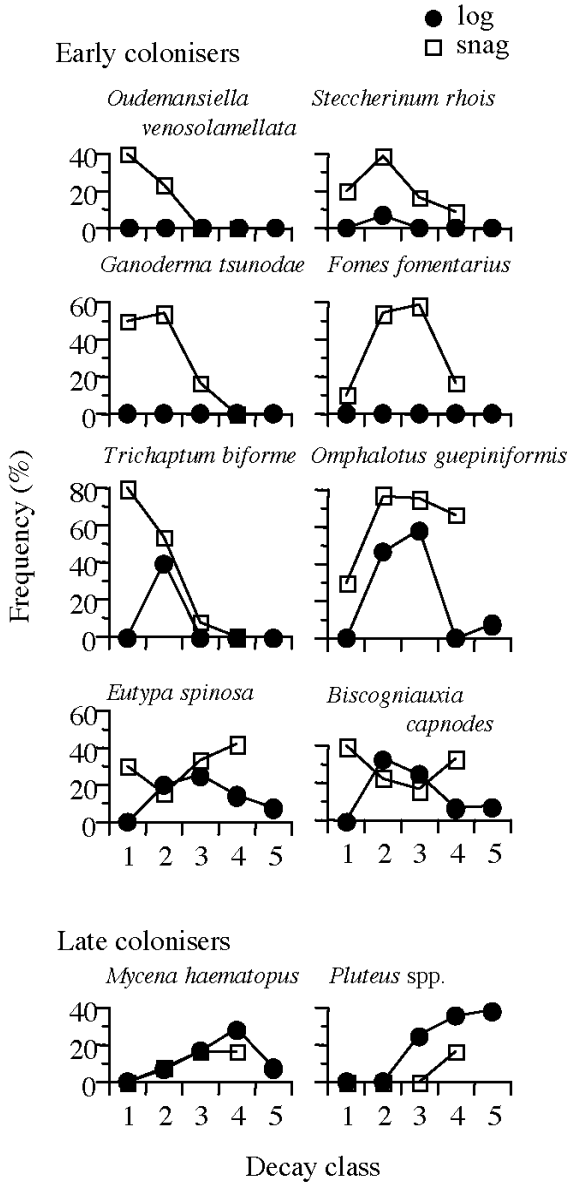

Figure 2. Changes in frequency of 10 taxa of macrofungi (frequency ≥ 10%) during decomposition. Symbols as in Figure 1. This figure is published in Dynamics of physicochemical properties and occurrence of fungal fruit bodies during decomposition of coarse woody debris of *Fagus crenata* by Yu Fukasawa, Takashi Osono, and Hiroshi Takeda (2009). Journal of Forest Research, 14, 20-29.

The preference of *Pluteus* spp. for well-decayed wood may be due to its high water content. In general, the water content of CWD increases along with wood decomposition and

has an important effect on the fungal community structure (Allen et al. 2000; Lumley et al. 2001).

4.2. Succession of Microfungi

Fungi forming microscopic (< 1 mm) sporocarps are called microfungi, including Zygomycota and anamorphic Ascomycota that could not be detected by fruit body survey of macrofungi. Although the wood decaying abilities of microfungi are relatively small as compared with those of macrofungi, some species of microfungi, known as soft-rot fungi, have the ability to decompose wood holocellulose especially under high water-stress conditions, and thus play a role on the decomposition of wood (Eriksson et al. 1990). Colonization of microfungi can influence the activities of basidiomycetes and consequently affect the rate of wood decay (Cox et al. 2001). Moreover, melanin production by some microfungi has been reported to play an important role in soil humus formation (Stevenson 1982; Knicker et al. 1995). Thus, an understanding of the diversity and dynamics of microfungus communities in relation to the decomposition of wood is essential to understand the decomposition dynamics of woody debris and soil humus formation in forest floor. In this study, microfungi were isolated from logs to isolation media by cutting out small wood chips. Details of fungal isolation were described in Fukasawa et al. (2009b). The occurrence of fungal species in samples from a single log was scored as a binary variable regardless of the number of colonies that developed in the isolation media. The frequency of each species in the logs was represented as percentage of the number of records of a species in the total number of logs.

From 674 beech wood chips (average 13.5 chips per log), 1490 isolations were made. Of the isolations, 1394 (93.6%) yielded fungal isolates; the remaining 6.4% of isolations were contaminated with bacteria or were sterile. We identified 96 fungal species from the fungal isolates, including 16 zygomycetes and 80 anamorphic Ascomycetes. Isolates of basidiomycetes (26.7% of isolates) and sterile non-basidiomycetes (11.7%) were not identified to species or genus and are not discussed here.

Eighteen species were isolated with a frequency of occurrence ≥10% of the logs sampled: *Trichoderma viride* (42%), *Gliocladium viride* (30%), *Scytalidium lignicola* (30%), *Tr. hamatum* (26%), *Sesquicillium candelabrum* (24%), *Tr. harzianum* (24%), *Tr. koningii* (22%), *Colletotrichum* sp. (14%), *Fusarium solani* (14%), *Leptographium* sp. (14%), *Mucor hiemalis* (14%), *Aureobasidium* sp. (10%), *Mortierella parvispora* (12%), *Tolypocladium cylindrosporum* (10%), *Torula* sp. (12%), *Tr. piluliferum* (10%), *Tr. virens* (10%), and Zygomycete sp.2 (10%).

Four large groups were identified by cluster analysis of their occurrence patterns (Figure 3). Fungi in group A are early colonizers, fungi in groups B and C are intermediate colonizers, and fungi in group D are late colonizers during the decay process in beech logs. Three fungi in group A (*Colletotrichum* sp., *Aureobasidium* sp., *Fusarium* sp.) are well known endophytes inhabiting cambium or sapwood of alive stem, and have tolerance against high CO_2 stress in alive wood tissue (Boddy and Griffith 1989). These fungi act as primary saprophytes of dead wood tissue, but are immediately replaced by secondary colonizers such as basidiomycetes. In decay class 2-4, fungi in groups B and C colonize into CWD instead of group A. Decrease in wood relative density along CWD decomposition is associated with a

reduction in the high CO_2 stress inside CWD and is creating a passageway for colonizing hyphae (Hintikka and Korhonen 1970; Rayner and Boddy 1988), and thus allows colonization of microfungi in groups B and C that are not high CO_2 stress tolerant. In decay class 5, fungi in group D colonize into CWD instead of group C. *Trichoderma hamatum* and *Mucor hiemalis* were reported from leaf litter in the study site (Osono and Takeda 2001; Osono 2005), and are expected to broadly distributed in the litter layer. In late stages of wood decomposition, such "soil-born" microfungi are dominant (Tokumasu et al. 1987). Occurrence of fungi in group D were positively correlated with water content and nitrogen concentration of wood, both of which have been reported to be important factors affecting wood-inhabiting fungal communities (Levy 1982; Lumley et al. 2001).

5. Relationships between Wood Decomposition and Fungal Succession

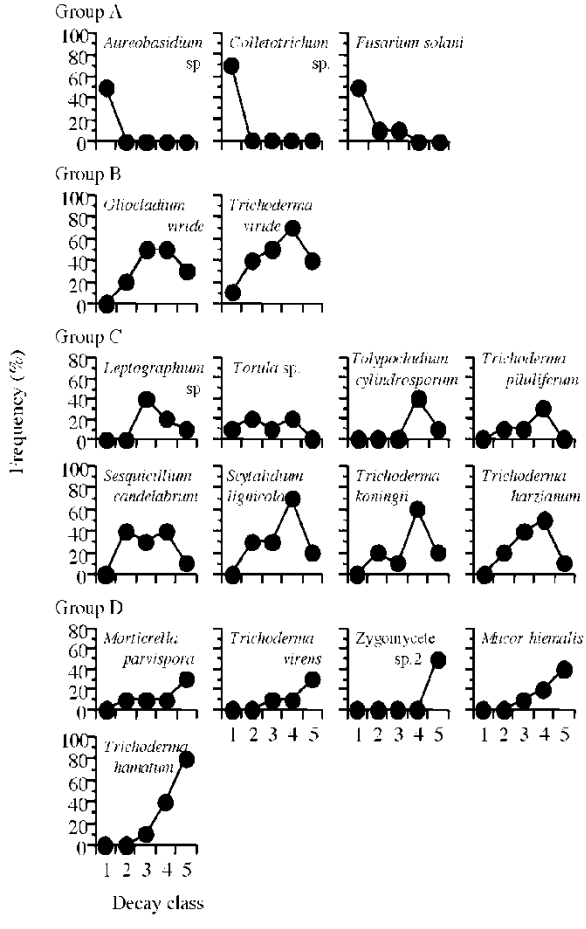

Figure 3. Changes in frequency of frequent 18 microfungi (frequency ≥ 10%) during decomposition of beech log. This figure is published in Microfungus communities of Japanese beech logs at different stages of decay in a cool temperate deciduous forest by Yu Fukasawa, Takashi Osono, and Hiroshi Takeda (2009). Canadian Journal of Forest Research, 39, 1606-1614.

The present study demonstrates a clear relationship between chemical changes and fungal succession (Figure 4). Immediately after a tree died, endophytic microfungi (group A) quickly colonize wood tissue, and utilize soluble sugar but could not decay holocellulose guarded by lignin (AUR).

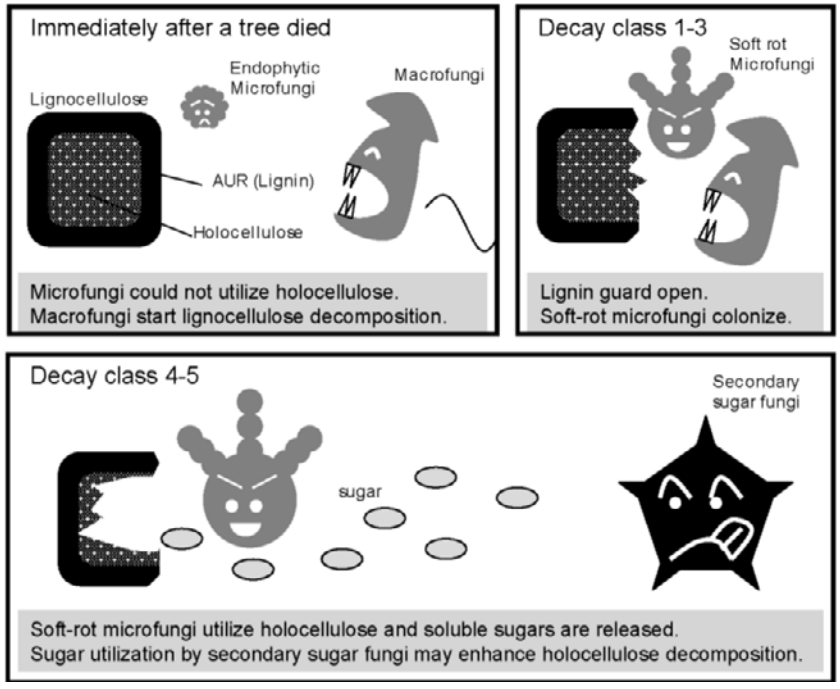

Figure 4. Illustrated schema showing functional roles of macro- and microfungi during lignocellulose decay process of beech CWD.

The early colonisers of macrofungi also start to colonize, replace endophytic microfungi, and become dominant at decay class 1–3 where the simultaneous decomposition of AUR and holocellulose occurred. We previously reported that the early colonisers *Omphalotus guepiniformis* (formerly denoted as *Lampteromyces japonicus*), *Steccherinum rhois*, *Ganoderma tsunodae* and *Trichaptum biforme* were capable of decaying both AUR and holocellulose simultaneously (Fukasawa et al. 2005a). *Oudemansiella venosolamellata* and *Fomes fomentarius* are also known as simultaneous white-rot fungi (Tanesaka et al. 1993; Schmidt 2006). Although the AUR decay ability of *Biscogniauxia capnodes* has not been tested yet, previous studies suggested that this genus degrades AUR and causes white-rot (Abe 1989; Hendry et al. 1998). Only *Eutypa spinosa*, among the early colonisers, was expected to have a low ability to decompose AUR, because a species in the same genus *E. lata* was reported to have low ability for AUR decomposition (Elghazali et al. 1992). These results suggest that the early colonisers of macrofungi observed in the present study have an important role in the simultaneous decay of AUR and holocellulose in the first phase of decomposition of beech CWD in the study area. Especially, *Omp. guepiniformis*, the most frequent species in the present study, dominated in terms of not only the frequency of fruiting bodies, but also in the wood volume occupied in beech CWD (Fukasawa et al. 2005b), and may have a central role in lignocellulose decomposition in the first phase.

Wood decomposition by macrofungi reduces high CO_2 stress inside CWD and raises wood water content. Those change in wood properties allow colonization of microfungi in group B and C in decay class 4-5. Species in the genus *Trichoderma* are known as soft-rot microfungi and have the ability to decay wood holocellulose (Nilsson 1973; Fukuda et al. 1984; Kim et al. 2005). High water and nitrogen contents in the late stages of log decomposition are suitable for soft-rot fungal activity (Fukuda et al. 1985; Worrall and Wang 1991). Interestingly, wood decomposition by soft-rot microfungi were previously shown to be promoted by primary delignification by white-rot fungi (Tanaka et al. 1988). This phenomenon may be due to improvement of holocellulose accessibility of microfungi. High water and nitrogen condition stimulates colonization of group D microfungi. Species in the genus *Mortierella* have no ability to decompose holocellulose (Nilsson 1973), and are called "secondary sugar fungi" because they utilize simple sugars produced by holocellulose decomposers (Hudson 1968; Osono and Takeda 2001). Secondary sugar fungi can enhance holocellulose breakdown by the holocellulose decomposers by utilizing sugars that would otherwise slow the rate of holocellulose decomposition (Deacon 1985). Although it is difficult to determine the cause and effect of certain relationship, it is thought that holocellulose decomposition by soft-rot microfungi enhances the colonization of secondary sugar fungi, and resource consumption of these fungi consequently stimulates holocellulose decomposition. Osono and Takeda (2001) reported that many species of secondary sugar fungi colonize in the late phase of litter decomposition.

Since high water and nitrogen conditions are not suitable for the majority of macrofungi, only a few species are related with well-decayed wood, and their roles in wood decomposition are not clear. Our previous study reported that *Mycena haematopus* has a low ability to decompose beech wood (Fukasawa et al. 2005a). The wood decay abilities of *Pluteus* spp. have not been revealed yet. Ecological function of macrofungi inhabiting well-decayed wood is a research field in the future.

6. IMPLICATIONS FOR SOIL HUMUS ACCUMULATION

The present study clearly shows AUR accumulation process during beech CWD decomposition. Residual AUR after CWD decomposition is an important precursor of soil humus (Stevenson 1982). Although AUR accumulation in CWD decay process is a well-known phenomenon in gymnosperm (e.g. Preston et al. 1998), concentration of AUR accumulated in decay class 5 CWD is tend to be low in angiosperm compare to gymnosperm (Table 2).

Difference in recalcitrance between lignin of gymnosperm and angiosperm (Eriksson et al. 1990) may be an inherit reason causing such difference in AUR accumulation. Furthermore, difference in fungal decay agents may also be a part of the reason. Different from conifer CWD where brown-rot fungi are the main agents of holocellulose selective decomposition, soft-rot microfungi are suggested to be the main agents of holocellulose selective decompoisition and of consequent AUR accumulation in beech CWD.

Table 2. Relative density (g cm^{-3}) and AUR concentration (%) of wood at decay class 5

Tree species	Relative density	AUR	References
Angiosperm			
Fagus crenata	0.12	33	Fukasawa et al. (2009a)
Quercus alba	–	23	Idol et al. (2001)
Gymnosperm			
Abies amabilis	0.18	58	Hope (1987)
Abies balsamea	0.10	47	Lambert et al. (1980)
Picea abies	0.31	41	Bütler et al. (2007)
Pinus radiata	0.16	37	Ganjegunte et al. (2004)
Pseudotsuga menziesii	0.19	67	Means et al. (1992)
Pseudotsuga menziesii	0.20	90	Preston et al. (1998)
Thuja plicata	0.11	80	Preston et al. (1998)

In this process, primary delignification by white-rot basidiomycetes is necessary for effective holocellulose decomposition. Since brown-rot fungi decay holocellulose more selectively than soft-rot fungi (Eaton and Hale 1993), whether brown- or soft-rot occur after the primary white-rot process and the timing of fungal succession may be crucial for AUR accumulation. Further studies are needed to reveal the effects of the relative importance of fungal decay agents (brown-, white- and soft-rot fungi) during the CWD decay process of humus accumulation on the forest floor.

CONCLUSION

Decomposition processes of beech CWD shows two phases characterised by different dominant organic chemical constituents, and have a close relationship with fungal succession. Simultaneous decomposition of AUR and holocellulose in the early phase of decomposition was mainly caused by white-rot fungi such as *Omphalotus guepiniformis*. The mass of remaining nitrogen within CWD and its successive release that occurred in this phase may have been caused by nitrogen recycling in the fungal mycelium and the successive formation of fruit bodies and spore production by these fungi. On the other hand, it was suggested that selective decomposition of holocellulose in the late phase of CWD decomposition was caused by soft-rot fungi. This decay pattern of beech CWD was different from that of boreal gymnosperm CWD where brown-rot fungi caused holocellulose decomposition in the late phase. The difference in relative importance of fungal decay agents (brown-, white- and soft-rot fungi) between angiosperm and gymnosperm CWD may cause a difference in chemical properties of the final decay residue accumulated on the forest floor.

REFERENCES

Abe, Y. (1989). Effect of moisture on decay of wood by xylariaceous and diatrypaceous fungi and quantitative changes in the chemical components of decayed wood. *Transactions of Mycological Society of Japan, 30,* 169-181.

Allen, R.B., Buchanan, P.K., Clinton, P.W. and Cone, A.J. (2000). Composition and diversity of fungi on decaying logs in a New Zealand temperate beech (*Nothofagus*) forest. *Canadian Journal of Forest Research, 30,* 1025-1033.

Bader, P., Jansson, S. and Jonsson, B. G. (1995). Wood-inhabiting fungi and substratum decline in selectively logged boreal spruce forests. *Biological Conservation, 72,* 355-362.

Boddy, L. (1991). Importance of wood decay fungi in forest ecosystems. In D. K. Arora, B. Rai, K. G. Mukerji, G. R. Knudsen (Eds.), *Handbook of applied mycology. Vol. 1: Soil and plants* (pp. 507–539). New York: Marcel Dekker.

Boddy, L. and Griffith, G. S. (1989). Role of endophytes and latent invasion in the development of decay communities in sapwood of angiospermous trees. *Sydowia, 41,* 41-73.

Boddy, L. and Heilmann-Clausen, J. (2008). Basidiomycete community development in temperate angiosperm wood. In L. Boddy, J. Frankland and P. van West (Eds.), *Ecology of saprotrophic basidiomycetes* (pp. 211-237). London: Academic Press.

Boddy, L. and Jones, T. H. (2008). Interactions between basidiomycota and invertebrates. In L. Boddy, J. Frankland, and P. van West (Eds.), *Ecology of saprotrophic basidiomycetes* (pp. 155-179). London: Academic Press.

Bütler, R., Patty, L., Bayon, R-C. L., Guenat, C. and Schlaepfer, R. (2007). Log decay of *Picea abies* in the Swiss Jura Mountains of central Europe. *Forest Ecology and Management, 242,* 791-799.

Cox, P., Wilkinson S. P., and Anderson, J. M. (2001). Effects of fungal inocula on the decomposition of lignin and structural polysaccharides in *Pinus sylvestris* litter. *Biology and Fertility of Soils, 33,* 246-251.

Deacon, J. W. (1985). Decomposition of filter paper cellulose by thermophilic fungi acting singly, in combination, and in sequence. *Transactions of the British Mycological Society, 85,* 663-669.

Eaton, R. A. and Hale, M. D. C. (1993). *Wood: Decay, pests and protection*. London: Chapman and Hall.

Elghazali, B., Gas, G. and Fallot, J. (1992). Biodegradation of lignocelluloses in grapevine (*Vitis vinifera* cv. Cabernet Sauvignon) by *Eutypa lata* (Pers. Fr.) Tul. *Vitis, 31,* 95-103 (in French with English abstract).

Eriksson, K-E. L., Blanchette, R. A. and Ander, P. (1990). *Microbial and enzymatic degradation of wood and wood components*. Berlin Heidelberg: Springer.

Frankland, J. C. (1982). Biomass and nutrient cycling by decomposer basidiomycetes. In J. C. Frankland, J. N. Hedger and M. J. Swift (Eds.), *Decomposer basidiomycetes: their biology and ecology* (pp. 241–261). Cambridge: Cambridge University Press.

Fukasawa, Y., Osono, T. and Takeda, H. (2005a). Decomposition of Japanese beech wood by diverse fungi isolated from a cool temperate deciduous forest. *Mycoscience, 46,* 97-101.

Fukasawa, Y., Osono, T. and Takeda, H. (2005b). Small-scale variation in chemical properties within logs of Japanese beech in relation to spatial distribution and decay ability of fungi. *Mycoscience, 46,* 209-214.

Fukasawa, Y., Osono, T. and Takeda, H. (2009a). Dynamics of physicochemical properties and occurrence of fungal fruit bodies during decomposition of coarse woody debris of *Fagus crenata*. *Journal of Forest Research, 14,* 20-29.

Fukasawa, Y., Osono, T. and Takeda, H. (2009b). Microfungus communities of Japanese beech logs at different stages of decay in a cool temperate deciduous forest. *Canadian Journal of Forest Research, 39,* 1606-1614.

Fukuda, K., Onodera, H., Watanabe, M., Tubaki, K., and Haraguchi, T. (1984). Action of microfungi on wood (Part 4) Wood decay by fungi isolated from buna wood. *Journal of Antibacterial and Antifungal Agents, 12,* 595-601 (in Japanese with English abstract).

Fukuda, K., Mizutani, S., and Haraguchi, T. (1985). Action of microfungi on wood VI. Nitrogen requirments of fungi for wood decay. *Mokuzai Gakkaishi, 31,* 294-300.

Ganjegunte, G. K., Condron, L. M., Clinton, P. W., Davis, M. R. and Mahieu, N. (2004). Decomposition and nutrient release from radiata pine (*Pinus radiata*) coarse woody debris. *Forest Ecology and Management, 187,* 197-211.

Harmon, M. E., Franklin, J. F., Swanson, F. J., Sollins, P., Gregory, S. V., Lattin, J. D., Anderson, N. H., Cline, S. P., Aumen, N. G., Sedell, J. R., Lienkaemper, G. W., Cromack, K. and Cummins, K. W. (1986). Ecology of coarse woody debris in temperate ecosystems. *Advances in Ecological Research, 15,* 133-302.

Harmon, M. E., Sexton, J., Caldwell, B. A. and Carpenter, S. E. (1994). Fungal sporocarp mediated losses of Ca, Fe, K, Mg, Mn, N, P, and Zn from conifer logs in the early stages of decomposition. *Canadian Journal of Forest Research, 24,* 1883-1893.

Hatcher, P. G. (1987). Chemical structure studies of natural lignin by dipolar dephasing solid-state ^{13}C nuclear magnetic resonance. *Organic Geochemistry, 11,* 31-39.

Heilmann-Clausen, J. (2001). A gradient analysis of communities of macrofungi and slime moulds on decaying beech logs. *Mycological Research, 105,* 575-596.

Hendry, S. J., Lonsdale, D. and Boddy, L. (1998). Strip-cankering of beech (*Fagus sylvatica*): Pathology and distribution of symptomatic trees. *New Phytologist, 140,* 549-565.

Hintikka, V. and Korhonen, K. (1970). Effects of carbon dioxide on the growth of lignicolous and soil-inhabiting Hymenomycetes. *Communicationes Instituti Forestalis Fenniae, 62,* 1-22.

Høiland, K. and Bendiksen, E. (1997). Biodiversity of wood-inhabiting fungi in a boreal coniferous forest in Sør-Trøndelag County, Central Norway. *Nordic Journal of Botany, 16,* 643-659.

Hope, S. M. (1987). Classification of decayed *Abies amabilis* logs. *Canadian Journal of Forest Research, 17,* 559-564.

Hudson, H. J. (1968). The ecology of fungi on plant remains above the soil. *New Phytologist, 67,* 837-874.

Idol, Characterization of coarse woody debris across a 100 year chronosequence of upland oak-hickory forests. *Forest Ecology and Management, 149,* 153-161.

Jankovský, L., Vágner, A. and Apltauer, J. (2002). The decomposition of wood mass under conditions of climax spruce stands and related mycoflora in the Krkonoše Mountains. *Journal of Forest Science, 48,* 70-79.

Kawase, K. (1962). Chemical components of wood decayed under natural condition and their properties. *Journal of Faculty of Agriculture Hokkaido University, 52,* 186-345.

Kim, G.-H., Son, D.-S. and Kim, J.-J. (2005). Fungi colonizing douglas-fir in cooling towers: Identification and their decay capabilities. *Wood and Fiber Science, 37,* 638-642.

Knicker, H., Almendros, G., González-Vila, F. J., Lüdemann, H.-D. and Martin, F. (1995). ^{13}C and ^{15}N NMR analysis of some fungal melanins in comparison with soil organic matter. *Organic Geochemisrly, 23,* 1023-1028.

Kruys, N., Fries, C., Jonsson, B. G., Lämås, T. and Ståhl, G. (1999). Wood-inhabiting cryptogams on dead Norway spruce (*Picea abies*) trees in managed Swedish boreal forests. *Canadian Journal of Forest Research, 29,* 178-186.

Laiho, R. and Prescott, C. (2004). Decay and nutrient dynamics of coarse woody debris in northern coniferous forests: a synthesis. *Canadian Journal of Forest Research, 34,*763-777.

Lambert, R. L., Lang, G. E. and Reiners, W. A. (1980). Loss of mass and chemical change in decaying boles of a subalpine balsam fir forest. *Ecology, 61,* 1460-1473.

Lange, M. (1992). Sequences of macromycetes on decaying beech logs. *Persoonia, 14,* 449-456.

Levy, J. F. (1982). The place of basidiomycetes in the decay of wood in contact with the ground. In J. C. Frankland, J. N. Hedger and M. J. Swift (Eds.), *Decomposer basidiomycetes* (pp. 161-178). Cambridge: Cambridge University Press.

Lindblad, I. (1998). Wood-inhabiting fungi on fallen logs of Norway spruce: relations to forest management and substrate quality. *Nordic Journal of Botany, 18,* 243-255.

Lindhe, A., Åsenblad, N. and Toresson, H.-G. (2004). Cut logs and high stumps of spruce, birch, aspen and oak: nine years of saproxylic fungi succession. *Biological Conservation, 119,* 443-454.

Lumley, T. C., Gignac, L. D. and Currah, R. S. (2001). Microfungus communities of white spruce and trembling aspen logs at different stages of decay in disturbed and undisturbed sites in the boreal mixedwood region of Alberta. *Canadian Journal of Botany, 79,* 76-92.

Matsumoto, T. and Tokimoto, K. (1992). Quantitative changes of mineral elements in bedlogs of *Lentinula edodes* during fruiting body development. *Reports of the Tottori Mycological Institute, 30,* 75-82 (in Japanese with English abstract).

Means, J. E., MacMillan, P. C. and Cromack, K. (1992). Biomass and nutrient content of Douglas-fir logs and other detrital pools in an old-growth forest, Oregon, U.S.A. *Canadian Journal of Forest Research, 22,* 1536-1546.

Merrill, W. and Cowling, E. B. (1966). Role of nitrogen in wood deterioration: Amount and distribution of nitrogen in fungi. *Phytopathology, 56,* 1083-1090.

Niemelä, T., Renvall, P. and Penttilä, R. (1995). Interactions of fungi at late stages of wood decomposition. *Annales Botanici Fennici, 32,* 141-152.

Nilsson, T. (1973). Studies on wood degradation and cellulolytic activity of microfungi. *Studia Forestalia Suecica, 104,* 1-40.

Nishioka, M. and Kirita, H. (1978). Litterfall. In T. Kira, Y. Ono and T. Hosokawa (Eds.), *JIBP Synthesis 18. Biological production in a warm-temperate evergreen oak forest of Japan* (pp. 231–238). Tokyo: University of Tokyo Press.

Ódor, P., van Hees, A. F. M., Heilmann-Clausen, J., Christensen, M., Aude, E., van Dort, K. W., Piltaver, A., Siller, I., Veerkamp, M. T., Grebenc, T., Kutnar, L., Standovar, T., Kosec, J., Matoèec, N. and Kraigher, H. (2004). Ecological succession of bryophytes,

vascular plants, and fungi on beech coarse woody debris in Europe. Nat-Man Working Report, 50 [http://www.flec.kvl.dk/natman/html/menu.asp?id=124]

Osono, T. (2005). Colonization and succession of fungi during decomposition of *Swida controversa* leaf litter. *Mycologia, 97,* 589-597.

Osono, T., and Takeda, H. (2001). Organic chemical and nutrient dynamics in decomposing beech leaf litter in relation to fungal ingrowth and succession during 3-year decomposition processes in a cool temperate deciduous forest in Japan. *Ecological Research, 16,* 649-670.

Preston, C. M., Sollins, P. and Sayer, B. G. (1990). Changes in organic components of fallen logs in old-growth Douglas-fir forests monitored by ^{13}C nuclear magnetic resonance spectroscopy. *Canadian Journal of Forest Research, 20,* 1382-1391.

Preston, C. M., Trofymow, J. A., Niu, J. and Fyfe, C. A. (1998). ^{13}CPMAS-NMR spectroscopy and chemical analysis of coarse woody debris in coastal forests of Vancouver Island. *Forest Ecology and Management, 111,* 51-68.

Pyle, C. and Brown, M. M. (1999). Heterogeneity of wood decay classes within hardwood logs. *Forest Ecology and Management, 114,* 253-259.

Rayner, A. D. M. and Boddy, L. (1988). *Fungal decomposition of wood: its biology and ecology*. New York: Willey.

Renvall, P. (1995). Community structure and dynamics of wood-rotting Basidiomycetes on decomposing conifer trunks northern Finland. *Karstenia, 35,* 1-51.

Schmidt, O. (2006). *Wood and tree fungi: biology, damage, protection, and use*. Berlin Heidelberg: Springer.

Schowalter, T. D. (1992). Heterogeneity of decomposition and nutrient dynamics of oak (*Quercus*) logs during the first 2 years of decomposition. *Canadian Journal of Forest Research, 22,* 161-166.

Schowalter, T. D., Zhang, Y. L. and Sabin, T. E. (1998). Decomposition and nutrient dynamics of oak *Quercus* spp. logs after five years of decomposition. *Ecography, 21,* 2-10.

Shimaji, K., Sudou, S. and Harada, H. (1980). *Mokuzai no soshiki*. Tokyo: Morikita Publishing (in Japanese).

Sippola, A.-L. and Renvall, P. (1999). Wood-decomposing fungi and seed-tree cutting: A 40-year perspective. *Forest Ecology and Management, 115,* 183-201.

Shippola, A.-L., Lehesvirta, T. and Renvall P (2001). Effects of selective logging on coarse woody debris and diversity of wood-decaying polypores in eastern Finland. *Ecological Bulletins, 49,* 243-254.

Stevenson, F.J. (1982). *Humus chemistry: genesis, composition, reactions*. New York: Willey.

Takahashi, K. H. and Kagaya, T. (2005). Guild structure of wood-inhabiting fungi based on volume and decay stage of coarse woody debris. *Ecological Research, 20,* 215-222.

Tanaka, H., Enoki, A., Fuse, G., and Nishimoto, K. (1988). Interactions in successive exposure of wood to varying wood-inhabiting fungi. *Holzforschung, 42,* 29-35.

Tanesaka, E., Masuda, H. and Kinugawa, K. (1993). Wood degrading ability of basidiomycetes that are wood decomposers, litter decomposers, or mycorrhizal symbionts. *Mycologia, 85,* 347-354.

Tateno, R. and Takeda, H. (2003). Forest structure and tree species distribution in relation to topography-mediated heterogeneity of soil nitrogen and light at the forest floor. *Ecological Research, 18,* 559-571.

Temnuhin, V. B. (1996). Preliminary quantitative estimation of wood decomposition by fungi in a Russian temperate pine forest. *Forest Ecology and Management, 81,* 249-257.

Tlalka, M., Bebber, D., Darrah, P.R., and Watkinson, S.C. (2008). Mycelial networks: nutrient uptake, translocation and role in ecosystems. In L. Boddy, J.C. Frankland, and P. van West (Eds.), *Ecology of saprotrophic basidiomycetes* (pp. 43-62). New York: Academic Press.

Tokumasu, S., Okada, G., and Tubaki, K. (1987). Late stages of fungal succession on small beech sapwood stripes in a beech forest litter. *Bulletins of Sugadaira Montane Research Center, 8,* 9-15.

Ueyama, A. (1966). Studies on the succession of higher fungi on felled beech logs (*Fagus crenata*) in Japan. *Materials und Organismen, 1,* 325-332.

Vainio, E. J. and Hantula, J. (2000). Direct analysis of wood-inhabiting fungi using denaturing gradient gel electrophoresis of amplified ribosomal DNA. *Mycological Research, 104,* 927-936.

Vogt, K. A., Grier, C. C. and Vogt, D. J. (1986). Production, turnover, and nutrient dynamics of above- and belowground detritus of world forests. *Advances in Ecological Research, 15,* 303-377.

Worrall, J. J., Anagnost, S. E. and Zabel, R. A. (1997). Comparison of wood decay among diverse lignicolous fungi. *Mycologia, 89,* 199-219.

Worrall, J. J. and Wang, C. J. K. (1991). Importance and mobilization of nutrients in soft rot of wood. *Canadian Journal of Microbiology, 37,* 864-868.

In: Wood: Types, Properties and Uses
Editor: Lorenzo F. Botannini
ISBN 978-1-61668-837-0

Chapter 6

EFFECTIVE RAINFALL SEASONS FOR EARLY AND LATE WOOD FORMATION OF CHINESE PINE AND BLACK LOCUST IN THE LOESS PLATEAU, CHINA

Satomi Koretsune[1], Kenji Fukuda[1], Zhaoyang Chang[2], Fuchen Shi[3], and Atsushi Ishida[4]

1. Department of Natural Environmental Studies, Graduate School of Frontier Sciences, The University of Tokyo, 5-1-5, Kashiwanoha, Kashiwa City, Chiba, 277-8563, Japan
2. College of Life Sciences, Northwest Sci-Tech University of Agriculture and Forestry,Yangling, Shaanxi, 712100, China
3.College of Life Sciences, Nankai University, Tianjin, 300071, China
4.Department of Plant Ecology, Forestry and Forest Products Research Institute (FFPRI), 1 Matsuno-sato,Tsukuba City, Ibaraki, 305-8687, Japan

ABSTRACT

The stable-carbon-isotope ratio ($\delta^{13}C$) of plants is strongly related to the ratio of CO_2 assimilation rate and stomatal conductance, and water use efficiency (WUE), and thus $\delta^{13}C$ analysis of tree rings gives long-term records on carbon gain and water use associated with wood formation. To identify the effective rainfall seasons for early and late wood formation of Chinese pine (*Pinus tabulaeformis* Carr.) and black locust (*Robinia pseudoacacia* L.) in the Loess Plateau, China, we examined correlations of seasonal precipitation with annual values of $\delta^{13}C$ and tree-ring width for early and late wood. The correlations with precipitation were examined for each month and for periods of all possible lengths from 2 to 22 months starting from January of the previous year to October of the current year. The period with the highest correlation was adopted as the most effective rainfall season for interannual variations in tree-ring $\delta^{13}C$ and width. In early wood, precipitation during the dry season (October to May) before the growing season was negatively correlated with $\delta^{13}C$ of pine trees and positively correlated with ring width of pine and locust trees. In late wood, rainfall during the growing season in the current year was negatively correlated with $\delta^{13}C$ of pine and locust trees, and positively

correlated with ring width of locust trees. Our results demonstrated the different water use strategies between pine and locust trees. The lower $\delta^{13}C$ of pine trees indicated higher WUE and more conservative water use compared to locust trees. Precipitation during the dry season affected the interannual variation in tree-ring $\delta^{13}C$ and width of pine and locust trees, indicating that the rainfall during the dry season before the growing season is important for wood formation in the Loess Plateau.

INTRODUCTION

The stable carbon isotope ratio ($\delta^{13}C$) is often used for estimating water use efficiency (WUE) in C_3 plants, because it is strongly related to the ratio of CO_2 assimilation rate and stomatal conductance (Francey and Farquhar 1982). The $\delta^{13}C$ in tree rings provides a long-term record on water use associated with wood formation, as it fluctuates with seasonal variations in water balance (Livingston and Spittlehouse 1996; Schleser et al. 1999; Porte and Loustau 2001; Li et al. 2005; Skomarkova et al. 2006). At the same time, tree-ring growth is sensitive to seasonal variation in important environmental factors such as temperature and precipitation (Gagen et al. 2004; Liu et al. 2004b). Hence, parallel analyses of the relationships between seasonal precipitation and $\delta^{13}C$ or width of early and late wood can provide crucial information on the effects of precipitation on water use and tree growth.

The Loess Plateau of China, located in the middle of the Yellow River basin, experiences serious soil erosion problems caused by overgrazing and improper cultivation (Fang and Xie 1994; Shi and Shao 2000; He et al. 2006; Li et al. 2006). Chinese pine (*Pinus tabulaeformis*), black locust (*Robinia pseudoacacia*), poplars (*Populus* spp.), willows (*Salix* spp.), and Chinese arborvitae (*Platycladus orientalis*), etc., have been widely planted on the denuded lands to restore forests and reduce soil erosion. However, black locust and poplar do not grow well and often suffer from repeated treetop dieback because of drought stress, especially in drier areas (Han and Hou 1996). Thus, it is important to clarify water use and growth traits of tree species for selecting species suitable for the afforestation of dry zones.

Among other tree species, Chinese pine and black locust are the most frequently used for afforestation and commercial use in the Loess Plateau. Chinese pine, an evergreen coniferous tree, has low water consumption with slow growth (Han et al. 1994). It is a species native to the area and is used for construction of houses, bridges, railway ties, and for resin collection (Guo et al. 2008). Black locust, a deciduous broad-leaved tree, grows fast and supplies nitrogen to the soil due to its nitrogen-fixing ability (Rice et al. 2004), although it consumes water intensively (Han et al. 1994). It was introduced from North America, but local people use its flowers as a food and for medicinal purposes (Xie et al. 2006). On the Loess Plateau, interannual variation in precipitation is high, with most rainfall occurring during the rainy season from June to September. However, little is known about the effects of interannual rainfall variation on the water use and growth of these two species in this area. Here we studied the importance of effective rainfall seasons for interannual variation in WUE and tree-ring growth of Chinese pine and black locust. We calculated correlations of precipitation for various periods with the annual $\delta^{13}C$ values and ring widths in early and late wood, and analyzed the water use strategies and growth traits of the two species in an arid area.

STABLE-CARBON-ISOTOPE RATIO OF C_3 PLANTS

The $\delta^{13}C$ is expressed by next formula (Farquhar et al. 1982).

$$\delta^{13}C_{sample} = \{(^{13}C/^{12}C)_{sample}/(^{13}C/^{12}C)_{standard} - 1\} \times 1000\ [‰] \quad (1)$$

The $^{13}C/^{12}C$ is mass ratio of carbon isotope. The $\delta^{13}C$ of C_3 plants is approximated as follows (Francey and Farquhar 1982).

$$\delta^{13}C_{plant} \cong \delta^{13}C_{air} - a - (b - a)(c_i/c_a) \quad (2)$$

$$c_i = c_a - A/g \quad (3)$$

$\delta^{13}C_{plant}$: $\delta^{13}C$ of C_3 plants, $\delta^{13}C_{air}$: $\delta^{13}C$ of air, c_i: CO_2 concentration in leaf intercellular spaces, c_a: CO_2 concentration in external atmosphere, A: CO_2 assimilation rate, g: stomatal conductance, a: fractionation coefficient due to diffusion in air (4.4‰), b: fractionation coefficient due to carboxylation (~30‰). When a plant widely opens stomata, A/g, which is proportionate to WUE, decreases, and c_i increases, and the value of $\delta^{13}C_{plant}$ decreases. When a plant closes stomata, A/g (i.e. WUE) increases, c_i decreases, and $\delta^{13}C_{plant}$ increases. Thus, $\delta^{13}C$ of C_3 plants is useful to estimate WUE and water stress to plants especially in arid areas.

MATERIALS AND METHODS

Study Site

Tree-ring samples were taken from trees in Zhifanggou village, Ansai County, Shaanxi Province, in the central part of the Loess Plateau, China (Figure 1). Mean annual temperature and precipitation are 9.4°C and 465.2 mm, respectively (1992-2002 data recorded at the Ansai meteorological observatory, 36°52'43" N, 109°18'41" E, 1068 m above sea level [a.s.l.]). Typical for the Loess Plateau, the interannual variation in annual precipitation was relatively large (275.0–622.1 mm), and precipitation was concentrated during the rainy season from June to September (55.6–86.1% of total annual rainfall; Figure 2). The dry season lasted from October to May as distinguished from the rainy season by a precipitation threshold of 50 mm per month.

Plant Materials

Samples were taken at breast height (1.2 m) from 12–20-year-old planted forests of Chinese pine and black locust located at 36°44' 51" N, 109°15' 15" E, 1140 m a.s.l. (Table 1). The trees were planted at intervals of 1.5 m. All canopy leaves were relatively well exposed because the canopy layer had not yet closed (maximum height of the canopy was less than 10 m).

Figure 1. Location of the study site (Ansai County, Shaanxi Province, China).

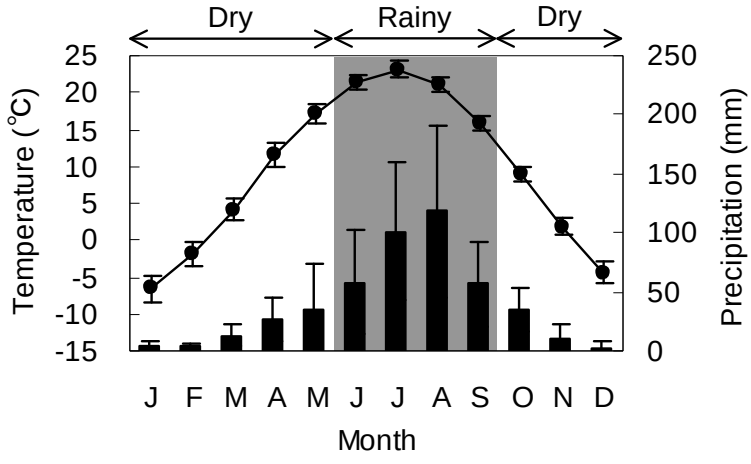

Figure 2. Mean monthly temperature (symbols) and monthly precipitation (bars) for 1992–2002, recorded at the Ansai meteorological observatory located 16 km northeast of the study site. Error bars indicate standard deviation. Dry and rainy seasons are shown with arrows, rainy season highlighted with dark color.

Wood disks were taken from felled trees, and 5 mm diameter wood cores were taken through the trunk from north to south of standing trees; that is, each core showed the growth of trees both in north and south directions. We obtained disk or core samples from four pine trees and four locust trees in the same mountain area in Zhifanggou village in 1999 and 2003. Two wood disks of pine and one of locust were taken in 1999 (P1, P2 and L1 in Table 1), and two wood cores of pine and three of locust were taken in 2003 (P3, P4, and L2–L4 in Table 1).

Table 1. Sample no., DBH and age of tree-ring samples

Species	Sample no.	DBH (cm)	Tree age (year)
Pinus tabulaeformis	P1	6.2	12
	P2	9.2	16
	P3	8.0	18
	P4	7.5	20
Robinia pseudoacacia	L1	12.5	16
	L2	10.5	17
	L3	9.5	17
	L4	18.0	20

The phenology of pine and locust trees is shown in Figure 9. In pine trees, the leaf primordia for the current-year needles form from the middle of May to September of the previous year (Sucoff 1971), while the period of shoot elongation lasts from April to May (ZY Chang, pers. obs.). Early wood formation starts in the middle of May, and late wood forms from late July to the middle of September (Vaganov et al. 2006). In locust trees, the leaf buds for the next spring form before dormancy (in September); the period of shoot growth is from the middle of April to May (ZY Chang, pers. obs.). After the shoot stops growing, additional buds form and burst in May followed by renewed growing of shoots (intermittent flush phenology; Khosla et al. 1992). Early wood formation starts in early April before bud break as in other ring-porous trees (Hill et al. 1995; Hauch and Magel 1998; Helle and Schleser 2004), while late wood is formed from July to September (Schmitt et al. 2000).

Measurement of Tree-Ring Width

Early and late wood widths of each annual ring were measured. We distinguished early and late wood by the difference in color and size of cells or vessels using a stereomicroscope (SMZ645, Nikon, Tokyo, Japan; Figure 3). The surfaces of wood samples were smoothed using sandpaper (in the case of disks) or a knife (in case of cores) and then scanned on a flatbed scanner. When it was difficult to scan the narrow rings clearly, photographs of tree rings were taken using a stereomicroscope.

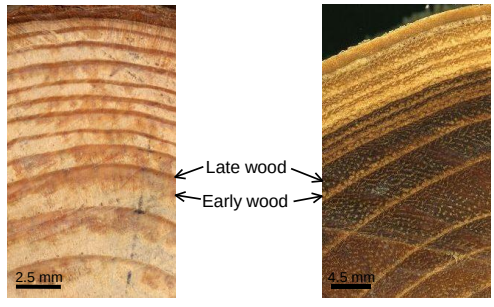

Figure 3. Tree-ring sample images of pine (left) and locust (right) trees. Sample no. P2 and L1 in Table 1, respectively, are shown.

These images were analyzed using tree-ring analysis software (WinDENDRO Reg 2003b, Regent, Sainte-Foy, Quebec, Canada). The ring width was measured in four directions for each disk and in two directions (north and south) for each core, with a precision of 0.001 mm. To identify false rings, the year of each tree ring was confirmed by visually comparing ring width patterns between samples.

Determination of $\delta^{13}C$

Whole wood tissue contains some mobile compounds, such as resin and phenolics, which may move across ring boundaries (Leavitt and Danzer 1993). The value of $\delta^{13}C$ in lignin differs from that in cellulose, and the lignin-to-cellulose ratio varies not only among annual rings but also between early and late wood in each annual ring (Wilson and Grinsted 1977). Thus, it was necessary to extract holocellulose from the wood samples to determine the annual $\delta^{13}C$ in early and late wood. We modified the chlorite method of Jayme and Wise (Wise et al. 1946; Green 1963; Kuroda 2000) in order to extract holocellulose from a large number of samples at once.

Before the extraction, tree-ring samples were sliced into sections of several hundred microns with a knife and divided into early and late wood of each annual ring. Southward-growing tree rings were used for the determination of $\delta^{13}C$. Around 10 mg of sliced samples were placed into small 300-mesh nylon bags and labeled with plastic nametags. The samples in the bags were dried overnight in a vacuum oven at 40°C to avoid possible changes to the chemical composition within the samples due to high temperatures. After removing resin with ethanol-benzene, the holocellulose was extracted from samples in 50 to 60 bags at once using the standard Wise method (Kuroda 2000).

The holocellulose samples were ground into a fine powder using a mixer mill (MM200, Retsch, Haan, Germany). Not all samples could be analyzed since at least 3 mg of sample was necessary for each measurement; we therefore could not determine the $\delta^{13}C$ in tree rings narrower than 0.3 mm due to the loss of material during grinding. The $\delta^{13}C$ of samples was determined using an isotope mass spectrometer (Delta Plus System, ThermoQuest, San Jose, CA, USA). We repeated measurements for both the standards and the tree-ring samples three times. The $\delta^{13}C$ of standard samples was measured among tree-ring samples. The standard deviation of $\delta^{13}C$ in the standard samples was 0.04-0.18‰. Not all measurements could be used in the analyses, since woody plants in the juvenile stage generally have a low $\delta^{13}C$ in the wood and have wide tree rings (Francey and Farquhar 1982; Marshall and Monserud 1996). Therefore, only the $\delta^{13}C$ for tree rings after 1992 were used for analysis (a total of 129 samples).

To analyze the difference of $\delta^{13}C$ values between untreated wood and holocellulose in a pine tree, we determined the $\delta^{13}C$ of both untreated wood and holocellulose (sample no. P2 in Table 1). In this analysis, the $\delta^{13}C$ values of tree rings before 1992 were used (Figure 4 and 5).

Statistical Analysis

We compared the $\delta^{13}C$ values between untreated wood and holocellulose using the t–test, and compared the values of $\delta^{13}C$ and tree-ring width between early and late wood samples using the Tukey–Kramer HSD test (α = 0.05). For correlation analysis we used the normalized value of $\delta^{13}C_{nor}$ calculated as:

$$\delta^{13}C_{nor} = \delta^{13}C \text{ in each year} - \text{average } \delta^{13}C \quad (4)$$

The normalization of the $\delta^{13}C$ was necessary because the absolute values of $\delta^{13}C$ differed among individual trees.

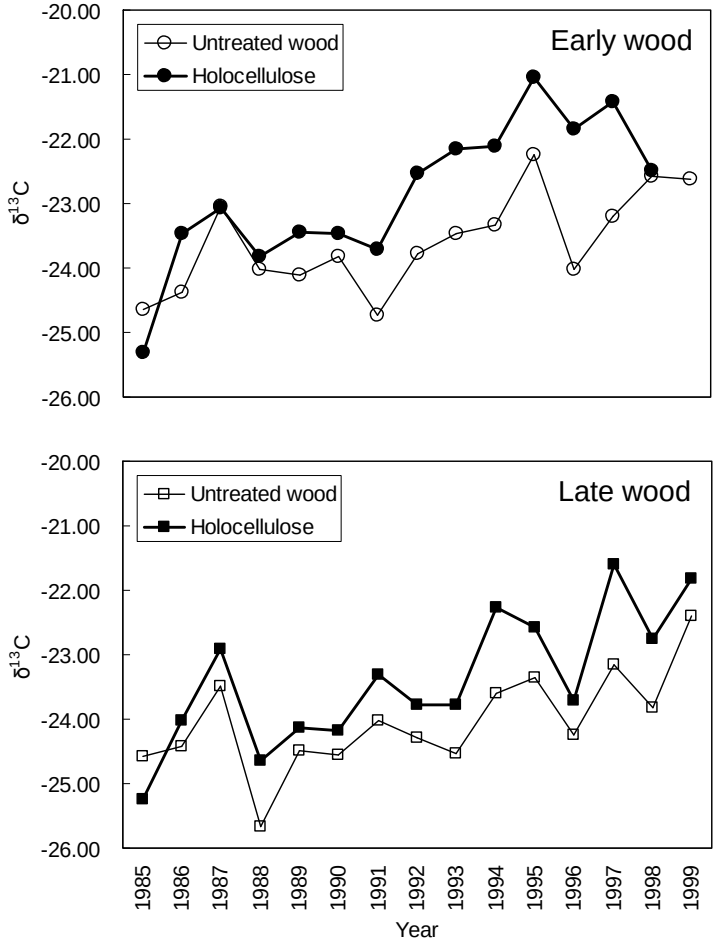

Figure 4. Annual fluctuation of $\delta^{13}C$ in untreated wood and holocellulose in a pine tree (Ssmple no. P2 in Table 1).

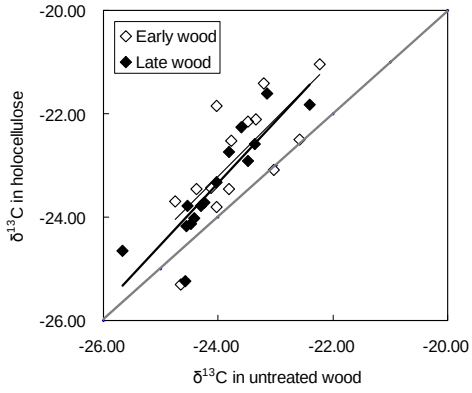

Figure 5. Relation of $\delta^{13}C$ values between untreated wood and holocellulose of pine tree (Ssmple no. P2 in Table 1). The correlation coefficients for early and late wood are 0.7351 and 0.884, respectively

Tree-ring widths toward four or two directions were averaged for each year. The mean tree-ring widths were normalized with a spline function (normalized width: ring index) using the software ARSTAN (Cook et al. 1990). The correlations were examined for each month and for periods of all possible lengths from 2 to 22 months starting from January of the previous year to October of the current year. The rainfall during these periods should be the critical determinant of WUE and tree-ring growth according to the phenology of pine and locust trees (Figure 9). The periods with the highest correlation were adopted as the most effective rainfall seasons for interannual variation in the $\delta^{13}C$ and tree-ring width. All statistical analyses including ANOVA and correlations were performed using JMP software (SAS Institute, Cary, NC, USA).

RESULTS

We compared the difference of $\delta^{13}C$ values between untreated wood and holocellulose in a pine tree (Sample no. P2 in Table 1; Table 2). The $\delta^{13}C$ values of untreated wood were lower than those of holocellulose in both early and late wood. In the early wood, the difference of $\delta^{13}C$ values between untreated wood and holocellulose was large in mature rings (Figure 4). The annual fluctuation of $\delta^{13}C$ values was different between untreated wood and holocellulose especially in the early wood. The correlation of $\delta^{13}C$ values between untreated wood and holocellulose was higher in the late wood than in the early wood (Figure 5).

The $\delta^{13}C$ values of holocellulose in the early and late wood of pine trees were significantly higher (less negative) than those in the late wood of locust trees (Table 3), indicating that the WUE was higher in pine trees. The standard deviation of $\delta^{13}C$ was greater in pine trees than in locust trees, indicating that the interindividual variation in WUE is greater in pine trees. The width of early wood was larger than that of the late wood in pine trees, whereas the reverse was true for locust trees. The ratio of early wood width to entire ring width was 79% in pine trees and 26% in locust trees, respectively. Entire ring width was also compared between pine and locust trees, but there were no significant differences. The coefficient of variation in ring width was the smallest in the early wood of locust trees.

Table 2. Mean ± standard deviation of $\delta^{13}C$ in untreated wood, holocellulose and difference of untreated wood and holocellulose in a pine tree (Sample no. P2 in Table 1). Different lowercase letters indicate significant differences within rows (t–test, $\alpha = 0.05$)

Sample	Untreated wood (‰)	Holocellulose (‰)	Difference (‰)
Early wood	-23.23 ± 0.63 b	-21.94 ± 0.55 a	1.29 ± 0.65
Late wood	-23.85 ± 0.52 b	-22.93 ± 0.86 a	0.93 ± 0.40

Table 3. Mean ± standard deviation and coefficient of variation (CV)* of $\delta^{13}C$ in holocellulose and tree-ring width of pine and locust trees. Different lowercase letters indicate significant differences within columns (Tukey-Kramer test, $\alpha = 0.05$)

Sample		$\delta^{13}C$ (‰)	Width (mm)	CV of width
Pine	Early wood	-23.59 ± 1.40 a	1.056 ± 0.657 a	0.623
	Late wood	-23.77 ± 1.54 a	0.284 ± 0.205 b	0.720
	Entire ring	-	1.340 ± 0.803	0.600
Locust	Early wood	-24.13 ± 0.97 ab	0.449 ± 0.127 b	0.282
	Late wood	-24.63 ± 1.17 b	1.262 ± 0.807 a	0.639
	Entire ring	-	1.711 ± 0.796	0.465

* CV was calculated only for tree-ring width

The annual fluctuation of $\delta^{13}C_{nor}$ in pine and locust trees are shown in Figure 6. The interindividual variation of locust trees was smaller than that of pine trees. The interannual variation of early wood in locust trees was small. Similar patterns were found in the annual fluctuation of ring index in pine and locust trees (Figure 7 and 8, respectively).

Periods of the highest correlation of seasonal precipitation with annual values of $\delta^{13}C_{nor}$ and ring index in early and late wood are shown in Table 4 and Figure 9. These periods indicate the most effective rainfall seasons for the interannual variation in WUE for the production of carbon used for xylem formation, and in tree-ring growth.

In the early wood of pine trees, the $\delta^{13}C_{nor}$ was negatively correlated with precipitation from September of the previous year to May of the current year. The ring indices in early wood and in entire rings were positively correlated with precipitation from September to December of the previous year. Rainfall during the dry season affected both the $\delta^{13}C$ and tree-ring width in early wood. In late wood of pine trees, the $\delta^{13}C_{nor}$ was negatively correlated with precipitation from May to August of the current year (i.e., during the growing season in the current year), whereas the ring index was positively correlated with precipitation from April of the previous year to July of the current year (i.e., 16 months covering two growing seasons).

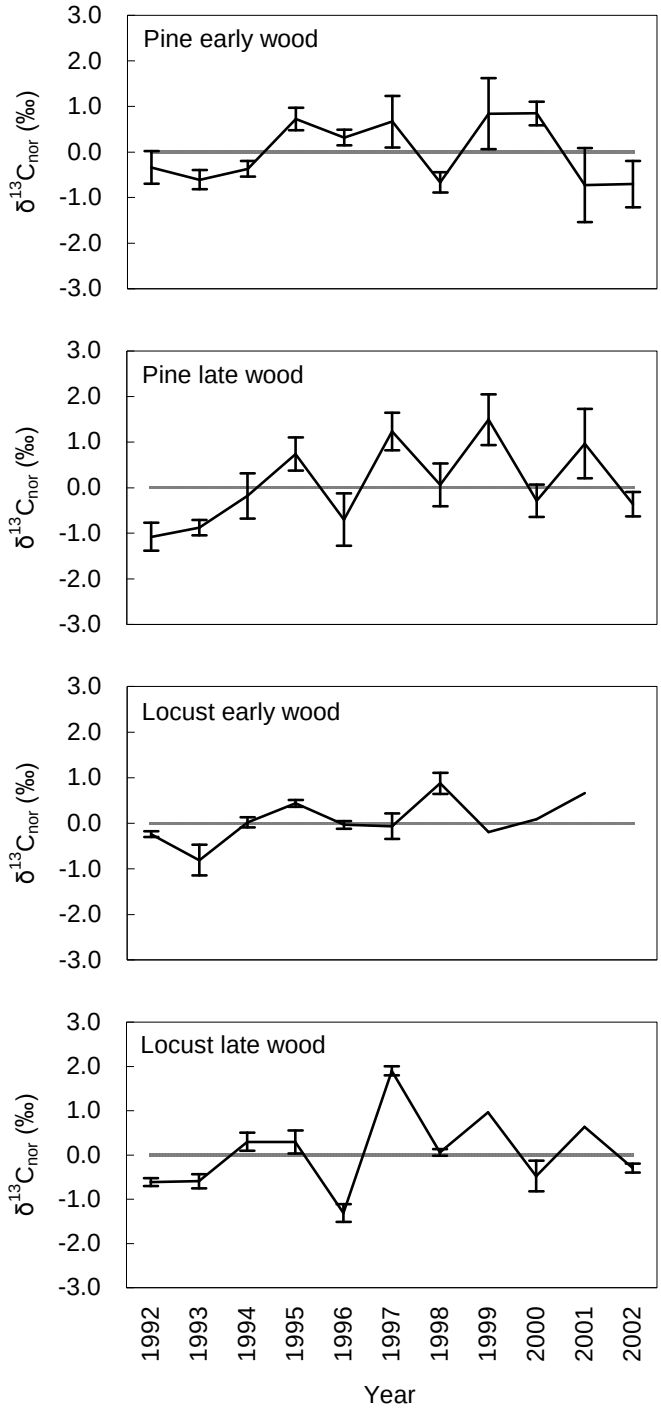

Figure 6. Annual fluctuation of $\delta^{13}C_{nor}$ in early and late wood of pine and locust trees. Error bars indicate ± 1 standard error. The $\delta^{13}C_{nor}$ represents the normalized values of $\delta^{13}C$ by formula (4).

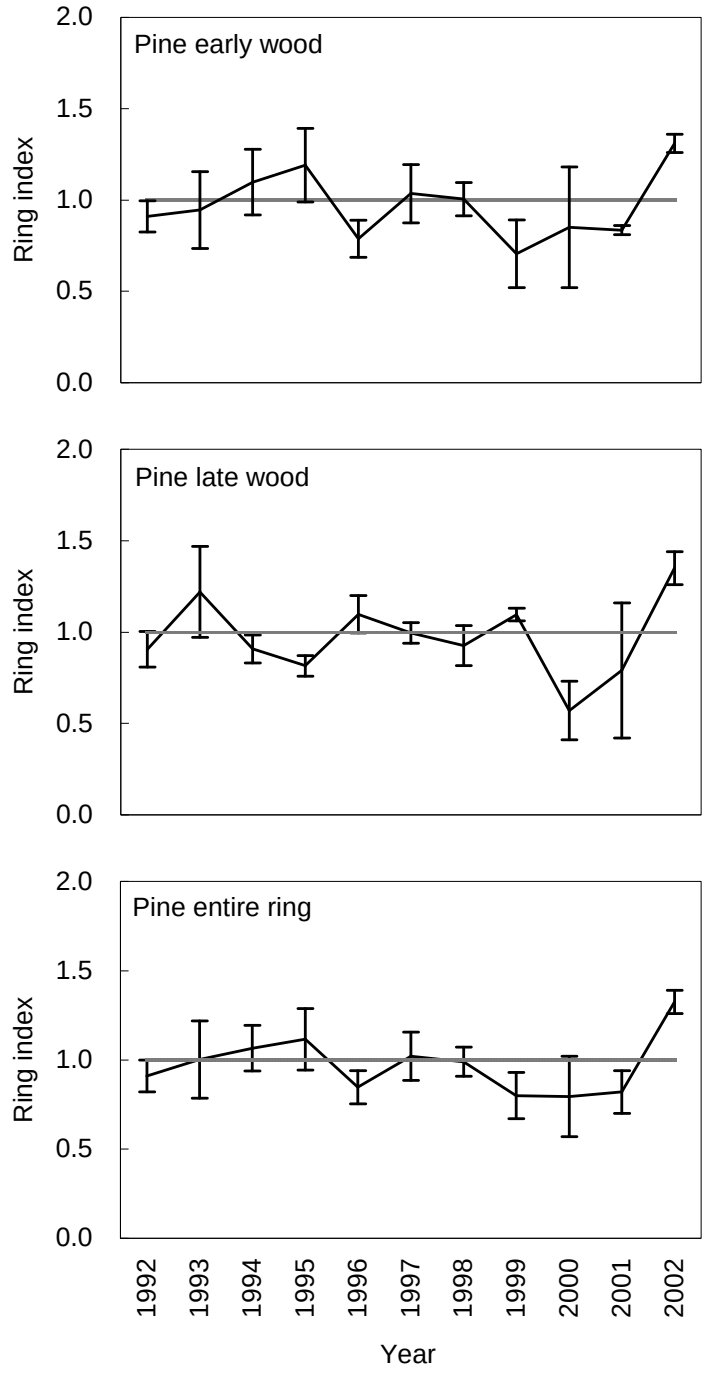

Figure 7. Annual fluctuation of ring index of pine trees. Error bars indicate ± 1 standard error. The ring index represents the normalized values of ring width by spline function.

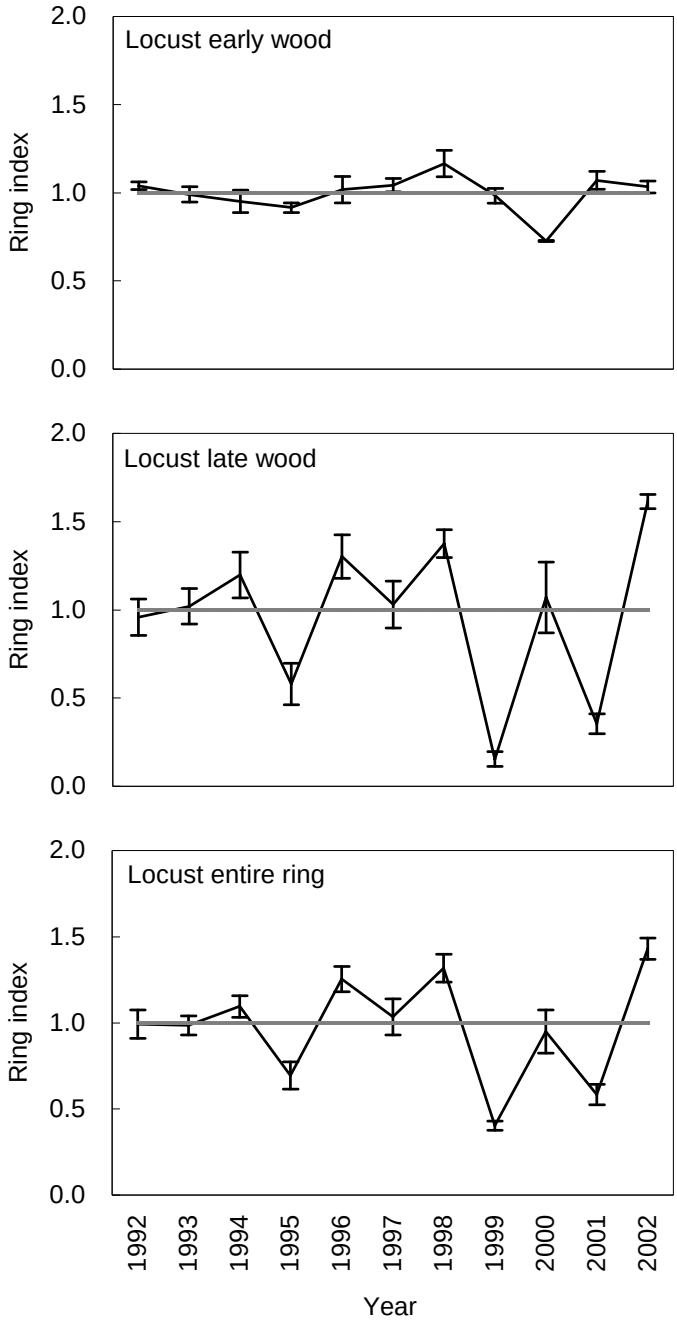

Figure 8. Annual fluctuation of ring index of locust trees. Error bars indicate ± 1 standard error. The ring index represents the normalized values of ring width by spline function.

Table 4. Periods with the highest correlations of precipitation with annual values of $\delta^{13}C_{nor}$ (normalized $\delta^{13}C$) and ring index (normalized ring width) of pine and locust trees

		Early wood		Late wood		Entire ring	
		Period	*r*	Period	*r*	Period	*r*
Pine	$\delta^{13}C_{nor}$	p-Sep. – May	-0.578***	May – Aug.	-0.631***	–	–
	Ring index	p-Sep. – p-Dec.	0.375*	p-Apr. – Jul.	0.572***	p-Sep. – p-Dec.	0.385*
Locust	$\delta^{13}C_{nor}$	p-May – p-Sep.	-0.650***	Jun. – Aug.	-0.825***	–	–
	Ring index	p-Dec. – May	0.574***	Apr. – Jun.	0.674***	Jan. – Jun.	0.710***

r correlation coefficient, p previous year
* $P < 0.05$, *** $P < 0.001$.

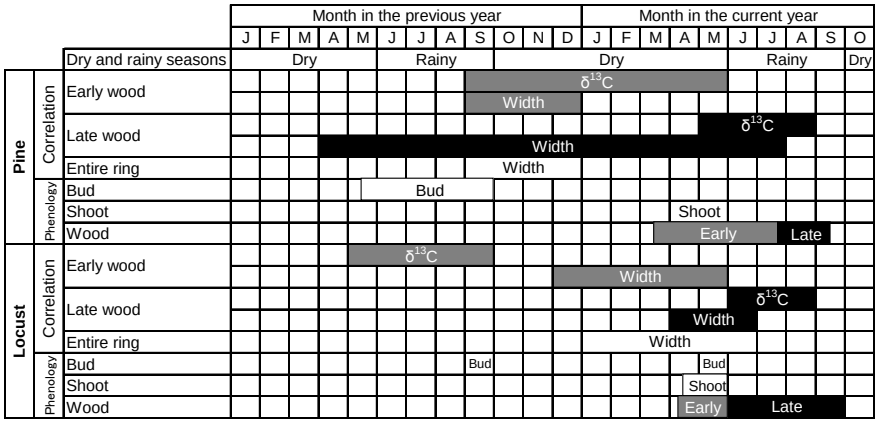

Figure 9. Periods with the highest correlations of precipitation with annual values of $\delta^{13}C_{nor}$ ($\delta^{13}C$) and ring index (Width) in early and late wood, and phenology of pine and locust trees. The period of the highest correlations and phenology are colored in early and late wood with gray and black, respectively.

In locust trees, the $\delta^{13}C_{nor}$ of early wood was negatively correlated with precipitation from May to September of the previous year (i.e., during the growing season of the previous year), while the ring index of early wood was positively correlated with precipitation from December of the previous year to May of the current year (i.e., during the dry season). The $\delta^{13}C_{nor}$ of late wood correlated negatively with precipitation from June to August of the current year (i.e., during the current growing season), and the ring index was positively correlated with precipitation from April to June of the current year (i.e., during the early growing season of the current year). The ring index of entire rings was positively associated with precipitation from January to June of the current year (i.e., the period from the mid dry season to the early growing season of the current year). In both pine and locust trees, the correlation coefficients (*r*) between precipitation and ring indices in early and late wood were lower than those between precipitation and $\delta^{13}C_{nor}$.

We also tested the correlation between the $\delta^{13}C$ values of early and late wood, and found that in pine trees, the correlation was stronger between the values of the same year ($r = 0.6673$, $p < 0.0001$) than between the values of previous and current years. Conversely, in locust trees the early wood $\delta^{13}C$ of the current year was closely associated with the late wood $\delta^{13}C$ of the previous year ($r = 0.7028$, $p = 0.0003$).

DISCUSSION

Rainfall in the previous year and in the early growing season strongly affected the interannual variation in WUE and tree-ring growth of early wood in pine and locust trees. In pine trees, precipitation during the dry season was the most important determinant of the $\delta^{13}C$ (i.e., WUE), and of tree-ring growth in early wood. This suggested that available water stored in the soil before the growing season is used for photosynthesis to form early wood in pine trees. In locust trees, the $\delta^{13}C$ in early wood was negatively associated with precipitation during the growing season of the previous year, and the $\delta^{13}C$ in early wood in the current year was closely associated with that in late wood of the previous year. Ring-porous trees such as locust and oak generally start to form new xylem before leaf bud-break and use the carbon stored in the previous year for early wood formation (Hill et al. 1995, Hauch and Magel 1998; Helle and Schleser 2004). The carbon for xylem formation of early wood in locust trees is thus mainly obtained from starch stored within the plant body in the previous year. Hill et al. (1995) also found that the $\delta^{13}C$ of early wood in the current year was highly correlated to that of late wood in the previous year for *Quercus robur* L., a typical ring-porous tree. In our study, precipitation during the dry season was positively associated with tree-ring growth of early wood in locust trees. This indicates that a decrease in rainfall during the dry season may reduce cambial growth in early wood, since water limitation strongly inhibits cambial activity (Little 1975; Kozlowski 1982). Locust trees have ring-porous wood with large-diameter vessels bearing most of the water conduction in the current-year ring, and these vessels are distributed in early wood (Cochard and Tyree 1990; Hacke and Sperry 2001). In this way, the precipitation during the dry season can determine water transport in the current year, and thus contributes to the overall tree-ring growth in this species.

In late wood of pine trees, tree-ring growth was positively associated with overall precipitation during the previous year. The mechanism of leaf bud formation and the long needle longevity may explain this correlation. In *Pinus* species, the primordia of all leaves for the following season are formed during the growing season of the previous year (Sacher 1954; Sucoff 1971), and the leaf lifespan of the Chinese pine is approximately 1.5 years (Xiao 2003). Previous studies have shown that high precipitation increases leaf area in evergreen tree species (Rico-Gray and Palacios-Rios 1996; Hoff and Rambal 2003). High precipitation in the previous year would promote bud formation in pine trees and consequently increase the total leaf area during the current year. Since the annual increase in stem mass is strongly correlated with the leaf area index in *Pinus* species (Albaugh et al. 2004), higher precipitation in the previous year would affect the tree-ring growth of late wood in the current year.

In the late wood of locust trees, tree-ring growth was positively associated with precipitation during the early growing season of the current year. Most of the canopy leaves of locust form early during the growing season of the current year (Khosla et al. 1995). High precipitation during the early growing season thus increases the leaf area. Because the annual growth of the stem is correlated to the leaf area index in deciduous tree species (Hogg 1999), an increase in leaf area with precipitation during the early growing season of the current year can increase the tree-ring growth of late wood in locusts.

The $\delta^{13}C$ values of holocellulose were higher than those of untreated wood in a pine tree, because the extractives and lignin have low $\delta^{13}C$ values (Wilson and Grinsted 1977). The annual fluctuation of $\delta^{13}C$ values was different between untreated wood and holocellulose.

The extractives move across tree rings, and the lignin-to-cellulose ratio varies among annual rings (Wilson and Grinsted 1977), which probably is the cause of the different annual fluctuation of $\delta^{13}C$ between untreated wood and holocellulose. However, the annual fluctuation of $\delta^{13}C$ values in untreated wood and holocellulose was more similar in the late wood than in the early wood, as indicated by the higher correlation of $\delta^{13}C$ values between untreated wood and holocellulose in the late wood. The richer lignin content in the early wood than in the late wood (Atwell et al. 2003, Siddiqui 1976) may cause the dissimilarity of the fluctuation between untreated wood and holocellulose in the early wood. These results suggest the importance of extraction of holocellulose for $\delta^{13}C$ analysis of tree rings.

The strategy of water use differs between pine and locust trees. The $\delta^{13}C$ in holocellulose was higher in pine than in locust trees, i.e., pine trees have higher WUE and a conservative water use strategy. This is consistent with the results of a previous study showing that water consumption per plant in locust seedlings was 2-3 times more intensive than that in pine seedlings (Han et al. 1994). Liu et al. (2004a) also examined the $\delta^{13}C$ in the cellulose of wood in pine trees on a mountain located approximately 435 km northwest of our study site. The average $\delta^{13}C$ was approximately 2‰ higher than that in our observations. Annual precipitation at their study site was lower than that at our site, suggesting that stomatal responses in pine trees are sensitive to variations in precipitation. The high WUE and high sensitivity of WUE or stomata to rainfall mean that pine trees are highly adaptable to growth in arid areas. In locust trees, the $\delta^{13}C$ was relatively high in early wood compared to late wood. The stored carbohydrate used for early wood formation experiences fractionation due to metabolism in broad-leaved deciduous tree species (Helle and Schleser 2004). The higher $\delta^{13}C$ value of early wood would be caused by the fractionation.

CONCLUSION

The precipitation during the dry season affected the WUE and tree-ring growth of both pine and locust trees, indicating that rainfall during the dry season is important for carbon gain and tree-ring growth during the following growing season. Because locust trees have a low WUE, planting pure locust stands may not be ideal for afforestation in areas where precipitation during the dry season is extremely low. Precipitation during the dry season and the water use of tree species are thus the key factors that determine the suitability of a tree species for afforestation of specific sites on the Loess Plateau.

ACKNOWLEDGMENTS

We thank Dr. Z. Kikvidze for his help in revision of this paper, Prof. Emeritus K. Iiyama for technical advice on extracting holocellulose from tree rings, Dr. K. Katsumata for his help in holocellulose extraction, Dr. H. Sasaki, N. Uehara, and Dr. K. Kojima for their assistance in measuring $\delta^{13}C$ (all from the University of Tokyo). We especially thank K. Matsunaga (Ritsumeikan University) for help with interpretation and the field survey in China.

REFERENCES

Albaugh, T. J.; Allen, H. L.; Dougherty, P. M. and Johnsen, K. H. (2004). Long term growth responses of loblolly pine to optimal nutrient and water resource availability. *For Ecol Manag*, *192*, 3-19.

Atwell, B. J.; Henery, M. L. and Whitehead, D. (2003). Sapwood development in Pinus radiata trees grown for three years at ambient and elevated carbon dioxide partial pressures. *Tree Physiol*, *23*, 13-21.

Cochard, H. and Tyree, M. T. (1990). Xylem dysfunction in *Quercus*: vessel sizes, tyloses, cavitation and seasonal changes in embolism. *Tree Physiol*, *6*, 393-407.

Cook, E. R.; Briffa, K. R.; Shiyatov, S. G. and Mazepa, V. S. (1990). Tree-ring standardization and growth-trend estimation. In: E. R. Cook and L. A. Kairiukstis (Eds.), *Methods of dendrochronology: applications in the environmental sciences* (pp. 104-123). Dordrecht, Kluwer Academic.

Fang, J. Q. and Xie, Z. R. (1994). Deforestation in preindustrial China: the Loess Plateau region as an example. *Chemosphere*, *29*, 983-999.

Farquhar, G. D.; Oleary, M. H. and Berry, J. A. (1982). On the relationship between carbon isotope discrimination and the intercelluar carbon dioxide concentration in leaves. *Aust J Plant Physiol, 9*, 121-137.

Francey, R. J. and Farquhar, G. D. (1982). An explanation of $^{13}C/^{12}C$ variations in tree rings. *Nature*, *297*, 28-31.

Gagen, M.; McCarroll, D. and Edouard, J. L. (2004). Latewood width, maximum density, and stable carbon isotope ratios of pine as climate indicators in a dry subalpine environment, French Alps. *Arct Antarct Alp Res*, *36*, 166-171.

Green, J. W. (1963). Wood cellulose. In: R. L. Whistler (Eds.), *Methods in carbohydrate chemistry* (pp. 9-21). New York, Academic Press.

Guo, H.; Wang, B.; Ma, X. Q.; Zhao, G. D. and Li, S. N. (2008). Evaluation of ecosystem services of Chinese pine forests in China. *Science in China Series C*, *51*, 662-670.

Hacke, U. G. and Sperry, J. S. (2001). Functional and ecological xylem anatomy. *Perspect Plant Ecol Evol Syst*, *4*, 97-115.

Han, R. L. and Hou, Q. C. (1996). Water metabolism characters and photosynthesis capacity of old small Populus trees in growth season. *Journal of Northwest Forestry College*, *11*, 36-40 (in Chinese w.

Han, R. L.; Liang, Z. S.; Hou, Q. C. and Zou, H. Y. (1994). Water consumption properties of adaptable nursery stocks on Loess plateau. *Chin J Appl Ecol*, *5*, 210-213 (in Chinese.

Hauch, S. and Magel, E. (1998). Extractable activities and protein content of sucrose-phosphate synthase, sucrose synthase and neutral invertase in trunk tissues of Robinia pseudoacacia L. are related to cambial wood production and heartwood formation. *Planta*, *207*, 266-274.

He, X. B.; Zhou, J.; Zhang, X. B. and Tang, K. L. (2006). Soil erosion response to climatic change and human activity during the Quaternary on the Loess Plateau, China. *Regional Environmental Change*, *6*, 62-70.

Helle, G. and Schleser, G. H. (2004). Beyond CO_2-fixation by Rubisco - an interpretation of $^{13}C/^{12}C$ variations in tree rings from novel intra-seasonal studies on broad-leaf trees. *Plant Cell Environ*, *27*, 367-380.

Hill, S. A.; Waterhouse, J. S.; Field, E. M.; Switsur, V. R. and Aprees, T. (1995). Rapid recycling of triose phosphates in oak stem tissue. *Plant Cell Environ*, *18*, 931-936.

Hoff, C. and Rambal, S. (2003). An examination of the interaction between climate, soil and leaf area index in a *Quercus ilex* ecosystem. *Ann For Sci*, *60*, 153-161.

Hogg, E. H. (1999). Simulation of inter-annual responses of trembling aspen stands to climatic variation and insect defoliation in western Canada. *Ecol Modell*, *114*, 175-193.

Khosla, P. K.; Toky, O. P.; Bisht, R. P. and Hamidullah, S. (1992). Leaf dynamics and protein content of important fodder trees of the western Himalaya. *Agrofor Syst*, *19*, 109-118.

Khosla, P. K.; Toky, O. P.; Bisht, R. P. and Hamidullah, S. (1995). Growth patterns of early versus late successional multipurpose trees of the western Himalaya. *Trees*, *10*, 108-113.

Kozlowski, T. T. (1982). Water supply and tree growth. *For Abstr*, *43*, 57-99.

Kuroda, K. (2000). Principal component analysis. In: The Japan Wood Research Society (eds) Experimental manual of wood science. *Buneido Publishing, Tokyo, pp 92-97*, , (in Japanese).

Leavitt, S. W. and Danzer, S. R. (1993). Method for batch processing small wood samples to holocellulose for stable-carbon isotope analysis. *Anal Chem*, *65*, 87-89.

Li, Y. K.; Ni, J.; Yang, Q. K. and Li, R. (2006). Human impacts on soil erosion identified using land-use changes: A case study from the Loess Plateau, China. *Physical Geography*, *27*, 109-126.

Li, Z. H.; Leavitt, S. W.; Mora, C. I. and Liu, R. M. (2005). Influence of earlywood-latewood size and isotope differences on long-term tree-ring $\delta^{13}C$ trends. *Chem Geol*, *216*, 191-201.

Little, C. H. A. (1975). Inhibition of cambial activity in *Abies balsamea* by internal water stress: role of abscisic acid. *Can J Bot*, *53*, 3041-3050.

Liu, Y.; Ma, L. M.; Leavitt, S. W.; Cai, Q. F. and Liu, W. G. (2004a). A preliminary seasonal precipitation reconstruction from tree-ring stable carbon isotopes at Mt. Helan, China, since AD 1804. *Glob Planet Chang*, *41*, 229-239.

Liu, Y.; Shi, J. F.; Shishov, V.; Vaganov, E.; Yang, Y. K.; Cai, Q. F.; Sun, J. Y.; Wang, L. and Djanseitov, I. (2004b). Reconstruction of May-July precipitation in the north Helan Mountain, Inner Mongolia since AD 1726 from tree-ring late-wood widths. *Chin Sci Bull*, *49*, 405-409.

Livingston, N. J. and Spittlehouse, D. L. (1996). Carbon isotope fractionation in tree ring early and late wood in relation to intra-growing season water balance. *Plant Cell Environ*, *19*, 768-774.

Marshall, J. D. and Monserud, R. A. (1996). Homeostatic gas-exchange parameters inferred from $^{13}C/^{12}C$ in tree rings of conifers. *Oecologia*, *105*, 13-21.

Porte, A. and Loustau, D. (2001). Seasonal and interannual variations in carbon isotope discrimination in a maritime pine (*Pinus pinaster*) stand assessed from the isotopic composition of cellulose in annual rings. *Tree Physiol*, *21*, 861-868.

Rice, S. K.; Westerman, B. and Federici, R. (2004). Impacts of the exotic, nitrogen-fixing black locust (*Robinia pseudoacacia*) on nitrogen-cycling in a pine-oak ecosystem. *Plant Ecol 174*,, , 97-107.

Rico-Gray, V. and Palacios-Rios, M. (1996). Leaf area variation in *Rhizophora mangle* L (Rhizophoraceae) along a latitudinal gradient in Mexico. *Glob Ecol Biogeogr Lett*, *5*, 30-35.

Sacher, J. A. (1954). Structure and seasonal activity of the shoot apices of *Pinus lambertiana* and *Pinus ponderosa*. *Am J Bot*, *41*, 749-759.

Schleser, G. H.; Helle, G.; Lucke, A. and Vos, H. (1999). Isotope signals as climate proxies: the role of transfer functions in the study of terrestrial archives. *Quat Sci Rev*, *18*, 927-943.

Schmitt, U.; Moller, R. and Eckstein, D. (2000). Seasonal wood formation dynamics of beech (*Fagus sylvatica* L.) and black locust (*Robinia pseudoacacia* L.) as determined by the "pinning" technique. *J Appl Bot*, *74*, 10-16.

Shi, H. and Shao, M. G. (2000). Soil and water loss from the Loess Plateau in China. *Journal of Arid Environments*, *45*, 9-20.

Siddiqui, K. M. (1976). Relationship between cell wall morphology and chemical composition of earlywood and latewood in two coniferous species. *Pak J For*, *26*, 21-34.

Skomarkova, M. V.; Vaganov, E. A.; Mund, M.; Knohl, A.; Linke, P.; Boerner, A. and Schulze, E. D. (2006). Inter-annual and seasonal variability of radial growth, wood density and carbon isotope ratios in tree rings of beech (*Fagus sylvatica*) growing in Germany and Italy. *Trees*, *20*, 571-586.

Sucoff, E. (1971). Timing and rate of bud formation in *Pinus resinosa*. *Can J Bot*, *49*, 1821-1832.

Vaganov, E. A.; Hughes, M. K. and Shashkin, A. V. (2006). *Growth dynamics of conifer tree rings: images of past and future environments*. Berlin, Springer.

Wilson, A. T. and Grinsted, M. J. (1977). $^{12}C/^{13}C$ in cellulose and lignin as paleothermometers. *Nature*, *265*, 133-135.

Wise, L. E.; Murphy, M. and Daddieco, A. A. (1946). Chlorite holocellulose, its fractionation and bearing on summative wood analysis and on studies on the hemicelluloses. *Tech Assoc Pap*, *29*, 210-218.

Xiao, Y. (2003). Variation in needle longevity of Pinus tabulaeformis forests at different geographic scales. *Tree Physiol*, *23*, 463-471.

Xie, J. C.; Sun, B. G. and Yu, M. (2006). Constituents of top fragrance from fresh flowers of *Robinia pseudoacacia* L. occurring in China. *Flavour Fragr J*, *21*, 798-800.

In: Wood: Types, Properties and Uses
Editor: Lorenzo F. Botannini
ISBN 978-1-61668-837-0

Chapter 7

FOSSIL WOOD: A KEY TO THE PAST

B. Ajaykumar[1][1], Shijo Joseph[2], P. C. Abhilash[3,4], Mahesh Mohan[1], K. Anitha[5] and A. P. Thomas[1]

[1]School of Environmental Sciences,
Mahatma Gandhi University, Kerala, India
[2]Forestry and Ecology Division, National Remote
Sensing Agency, Hyderabad, India
[3]Eco-Auditing Group, National Botanical Research Institute,
Lucknow, Uttar Pradesh, India
[4]Department of Botany, University of Lucknow, Lucknow,
Uttar Pradesh, India
[5]Division of Landscape Ecology, Salim Ali Centre for Ornithology and Natural History,
Tamil Nadu, India

ABSTRACT

Palaeo-environmental interpretation using the fossil remains has attained a world wide attention and the palaeontological studies coupled with geochronology and stratigraphy could bring many dimensions to certain obstinate facets of biogeography and promote not only the theory of evolution, but the concept of plate tectonics also. Throughout geological time the omnipresence of fossil wood has provided researchers with a potentially rich archive of data for exploring questions concerning extinct and extant arboreal plant systematics. Fossil woods, both petrified and carbonized wood remains, provide information on bio-geographical trends over space and time. Also, the past distribution and diversity of woody taxa are important for reconstructing the timing of diversification and migration patterns. They have also provided vital information on palaeo-climatic fluxes in reconstructing the palaeo-environmental scenario of a region. The present chapter deals with the importance of fossils woods, types of preservation, their significance in reconstructing the palaeo-climatology and palaeo-environment of a region as well as the limitation in identifying the fossil woods.

[1] Correspondence : Email: jemnair@gmail.com, Telephone : 919447062674, Fax : 91 481 2732620.

INTRODUCTION

In order to understand the distribution of any species in space, one must study its distribution in time. This is because distributions are always changing, sometimes as a response to changing climate and sometimes in response to other changing ecological factors, including the activities of man. The history of a species informs us whether it is on the increase or the decrease, whether its range is expanding or contracting. Such information can often lead us to an understanding of what critical factors underlie the limitation of the range of such species.

Many distribution patterns which appear superficially anomalous can be understood by reference to their histories. An example of this is afforded by species with so-called 'disjunct distributions' (Pigott and Walters, 1954). Many species, now rare in Britain, occur as isolated populations in unstable habitats, e.g. marshes, screes, sand dunes and cliffs. Frequently one finds several scarce plants concentrated together in these habitat fragments. Occasionally, a study of the past history of such species has revealed that they were once of more widespread occurrence and have become restricted because of changes in the environment (Lucchi et al., 2006; Rull et al., 2005). The importance of fossil woods is that they are the most striking and frequently occurring megaplant remains in sedimentary rocks. They store a wealth of information about palaeo-climate, palaeo-ecology, phytogeography as well as evolution and without them, our knowledge about the arborescent plants of the past would have remained largely incomplete (Guleria and Awasthi, 1997).

FOSSILIZATION OF WOODS

Wood may become fossilised in various ways though the main process is always by burial (Guleria and Awasthi, 1997). The burial may be violent as happens in the case of volcanic eruption by lava flows or by extensive floods, but usually it is gradual and gentle as observed in the peat bogs, lakes, rivers and along the sea shores. The wood under preservation often gets flattened forming coaly fossils called compressions. Due to flattening, the original structure of the wood in compression is crushed and is obscured. However, such flattening is generally prevented by the process of fossilisation known as petrifaction and permineralization, in which the wood becomes partly or even completely replaced by minerals, usually by silica, in the form of opal, chalcedony or agate or sometimes by iron pyrites or calcium carbonate (Guleria and Awasthi, 1997). The wood is thus changed into stony fossils and unlike in compressions, the original shape and internal microscopic structures of such woods are well preserved (Figure 1). More over, the petrified woods allow sectioning and examination of the tissue under the microscope. Trivedi and Ambwani (1971) found that many petrified woods such as those of Deccan Intertrappeans are preserved in this way. Since the petrifactions are the most frequently occurring type of fossil wood, their occurrence in the arid and treeless areas of Kutch and Rajasthan, India is of particular significance since they give striking reminder of dense forests which must have flourished these areas millions of years ago. Bark is very rarely found intact in fossil woods. Presence of bark in fossil woods provides an evidence of quick burial. It also indicates that the fossil has

not drifted too far from its place of origin and hence is of considerable significance in determining the provenance of fossil woods (Guleria and Awasthi, 1997).

Petrified wood (wood turned to stone) falls into two categories: casts and permineralizations (Smith and Gannon, 1973). The first step in formation of both of these types of fossils involves quick burial in sediment so that fungal and bacterial decay is retarded due to low oxygen levels. A cast is formed as minerals or other sediments fill and harden within the sedimentary cavity formed as the original wood deteriorates. Casts show the external form of the fossil but do not preserve internal cell structure, and consequently cannot be identified to genus or species levels.

Figure 1. Fossil woods. Petrified wood samples from Myanmar (collected by palaeobotanist Late Prof. Birbal Sahni) displayed at the Botany Department of University of Lucknow. Photo credit: P.C. Abhilash.

Permineralized woods are formed when minerals dissolved in ground waters infiltrate the wood, filling the spaces within and between cells, gradually embedding and preserving the entire tissue. Permineralized woods retain the original cellular structure and therefore can be identified by anatomical study.

RADIO CARBON DATING

Carbon-14 is produced in the upper layers of the troposphere and the stratosphere by thermal neutrons absorbed by nitrogen atoms. When cosmic rays enter the atmosphere, they undergo various transformations, including the production of neutrons. The resulting neutrons (^{1}n) participate in the following reaction:

$$^{1}n + {}^{14}N \rightarrow {}^{14}C + {}^{1}H$$

The highest rate of carbon-14 production takes place at altitudes of 9 to 15 km (30,000 to 50,000 ft) and at high geomagnetic latitudes, but the carbon-14 readily mixes and becomes evenly distributed throughout the atmosphere and reacts with oxygen to form radioactive carbon dioxide. Carbon dioxide also dissolves in water and thus permeates the oceans. Carbon-14 can also be produced in ice by fast neutrons causing spallation reactions in oxygen. Carbon-14 then goes through radioactive beta decay. By emitting an electron and an

anti-neutrino, carbon-14 (half life of 5730 years) decays into the stable (non-radioactive) isotope nitrogen-14. The inventory of carbon-14 in Earth's biosphere is about 300 million Curies, of which most is in the oceans. Radiocarbon dating is a radiometric dating method that uses (^{14}C) to determine the age of carbonaceous materials up to about 60,000 years old. The technique was developed by Willard Libby and his colleagues in 1949 and estimated that the radioactivity of exchangeable carbon-14 would be about 14 disintegrations per minute (dpm) per gram. One of the frequent uses of the technique is to date organic remains from archaeological sites. Plants fix atmospheric carbon during photosynthesis, so the level of ^{14}C in plants and animals when they die approximately equals the level of ^{14}C in the atmosphere at that time. However, it decreases thereafter from radioactive decay, allowing the date of death or fixation to be estimated. The initial ^{14}C level for the calculation can either be estimated, or else directly compared with known year-by-year data from tree-ring data (dendrochronology) to 10,000 years ago, or from cave deposits (speleothems), to about 45,000 years of age. A calculation or (more accurately) a direct comparison with tree ring or cave-deposit carbon-14 levels, gives the wood or animal sample age-from-formation. The technique has limitations within the modern industrial era, due to fossil fuel carbon (which has little carbon-14) being released into the atmosphere in large quantities, in the past few centuries.

SOME CASE STUDIES

Fossil phytolith assemblages from soils and lake sediments have been used to reconstruct palaeo-vegetation patterns, especially forest/grassland ecotones (Alexandre et al., 1997). The modern phytolith assemblages enable the differentiation of subdesertic steppe from wooded riparian forest, and characterise the composition of the C_4-grass associations. Moreover they record local as well as regional vegetation (Barboni et al., 1999).

Deevey (1939) described that changing combination of temperature and moisture conditions could explain the major changes in vegetation and this interpretation is according to the independent information about water – level changes. Time series of palaeontological data provide a record of regional and local vegetation development, which means for biostratigraphic correlation and dating and information about changes in water level (Newby et al., 2000). Caratini et al. (1991) analysed a marine core off Karwar, near the estuary of the Kalindi river, have brought out a distinct major vegetational change in the Western Ghats of the Uttara Kannada District from forest to Savanna during 3,500 YBP which pinpoints the commencement of anthropogenic activity in the region. The work done by Hait et al. (1996) on the late Quaternary sediments and their biotic contents proved that climate fluctuation occurred in a short period during a prolonged climatic phase can also obtain. This is revealed as per the presence of mangrove vegetation noticed by the carbon dating. Chauhan, (1996) revealed that the tree savannahs existed in Bastua and Jagmotha region during 6,720 to 5,000 Years Before Present (YBP) and 6,500 to 4,250 YBP respectively, under cold and dry climate with an ameliorating trend and the formation of Sal dominated tropical deciduous forests commenced simultaneously in Bastua and Amgon regions between 1,050 to 1,200 YBP as a consequence of a moist climate in the regions.

The relation of Middle-Upper Jurassic marine sedimentary cycles of France with climate and sea-level dynamics were studied using fossil woods (Garcia et al., 1998). They showed that the distribution of wood is not controlled by climate but by environmental processes related to relative sea-level changes. Also, the abundance of wood in transgressive deposits related to ravinement of previously emerged areas and/or to the high preservational potential associated with increased accommodation space. Rajagopalan et al. (1997) studied the late Quaternary vegetational and climatic changes in southern India. According to them a progressively negative trend up to 40,000YBP, indicative of a decrease in the proportion of C_4 plants (tropical grasses and sedges), increasing moisture conditions. Quaternary climatic changes in the desert regions of Gujarat and Rajasthan, studied by Allchin et al. (1978) and proposed a dry phase prior to 40,000YBP. Similar results were obtained from tropical Africa where high lake levels have been observed prior to 25,000YBP (Butzer et al., 1972). The study of the fossil remains can give not only the species distribution, but the influence of the past environmental conditions on that particular species also, which ultimately resulted in its bloom or extinction (Vishnu-Mittre and Sharma, 1966). The study of a fragmentary sample coming from a silicified trunk remain of Lunca formation of Eastern Carpathians led to the identification of a wood structure typical to the Cycadaceae family by Iamandei et al. (2003) and a presence of tropical conditions there. Two new fossil fruits belonging to *Sterculia* of Sterculiaceae and *Barringtonia* of Lecythidaceae were described from the Oligocene sediments of Makum Coalfield, Assam, India by Mehrotra (2000). These fruits are reported for the first time not only from the Oligocene of Assam but from the Tertiary of India. Their presence supports the view that evergreen to littoral and swamp forests existed there during the time of deposition.

Fossil woods have been used for paleoecological and paleoenvironmental studies and also helped in reconstructing the floral composition or climatic conditions (Zucol et al., 2005; Philippe et al., 2006; Sweeney et al., 2009; Jeong et al., 2009). Sweeney et al. (2009) studied the unique expressions of wood mineralization and implication for the processes of wood preservation from the middle Cretaceous Moreno Hill Formation. The study suggested that coal inclusions and mineralized wood/coal associations may also be common in other ancient sediments even though weathering may obscure their presence. As such, various stages of wood degradation have been preserved in mineralized samples from the Moreno Hill Formation.

The Late Holocene vegetation change from woodlands to the present desertic pastures of southern Tibet, China has been revealed by radiocarbon dating and fossil wood analysis (Kaiser et al., 2009). Fossil woods obtained from the Miocene El Cien Formation located in Baja California Sur, Mexico has been used for interpreting the floristic similarity between the present floras growing in this region and those existed during the Miocene (Martínez-Cabrera et at., 2006). The fossil wood collected from the sediments indicated the Late Pleistocene floral diversity of the vegetation in El Palmar National Park (Zucol et al., 2005). The fossil woods used for the interpretation of palaeo-climate. The fossil woods of Lower Coal-bearing Formation of Janggi Group at Donghae-myeon, Pohang City, Gyeongsangbuk-do Prefecture, Korea showed that the climate of the Pohang Basin changed from cool-temperate to warm-temperate and subtropical during the early Miocene **(**Jeong et al., 2009).

PETRIFIED FORESTS

A petrified forest is a forest made out of fossil or petrified wood. In other words, a petrified forest is a forest made out of stone trees. A petrified forest becomes such over the course of million of years. Some of the world's largest petrified forests are an estimated 100 million years old. Volcanic ash is sometimes a key step in the process of petrification. In fact, it's not uncommon for a petrified forest to have been covered by mud made out partially by volcanic ash at some time. Volcanic ash produces a chemical reaction in the wood, which in turn accelerates the process of petrification. A petrified forest can take different colours, depending on the type of material once absorbed by the living trees. Cobalt and copper cause a greenish blue tint, while manganese turns the wood pink, and carbon produces gray. Some trees have more than one colour, while others are basically composed of crystal quartz, which are transparent and allow for a view of the grain wood. The world's most impressive petrified forest is in Santa Cruz, Argentina. With trees that are over 10 feet (3 meters) in diameter, the Patagonian petrified forest is one of the best giant examples of wood-stone in the world. As a comparison, the Petrified Forest National Park in northeastern Arizona, considered the best example of petrified wood in North America, boasts trees that barely reach six feet. Canada has the largest petrified forest in the world, covering an area of thousands of kilometres and dating back to the Eocene period. Other significant examples of petrified forest include Petrified Forest of Lesvos (Greece), Thiruvakkarai Village (India), Curio Bay (New Zealand), and Nová Paka (Czech Republic).

WOOD ANATOMY

Many palaeo-botanical studies have dealt with leaf impressions (Lumbert et al., 1984; Ivany et al., 1990), but studies related to fossil woods are few. Fossil woods sometimes retain exquisite details of the original cell structure that can be investigated with the aid of a microscope. Hence the preservation of the tissues has prime importance (Hoffmann and Blanchette, 1997). Such fossils may be identified by comparing their anatomy with that of modern woods or other fossil woods. This method of identification is similar to that used in the identification of timber woods in the forest products industry. Anatomical features such as presence of vessels, vessel size and grouping, distribution of parenchyma, ray size and distribution, are used in wood keys aiding in the determination to family, genus, and in some cases, species. Identification of fossil woods is accomplished through comparison with modern woods and with other known fossil woods. There are good literatures on the anatomy of timbers including keys for quick identification and descriptions and illustrations for thorough comparison (Gregory, 1980; Panshin and de Zeeuw, 1980; Hoadley, 1990; Stewart and Rothwell, 1993). Computerized keys are also available to help in determining modern and fossil woods (Wheeler et al., 1986).

El-Din (2003), by giving detailed wood anatomical descriptions, identified two fossil wood species *Celastrinoxylon celastroides* and *Ficoxylon Cretaceum*, which are reported and described for the first time from the Farafra Oasis in Egypt. Anatomical descriptions were used to identify many fossil woods in India also. *Sterculioxylon pondicherriense* is recorded from the Cuddalore Series of the Lower Miocene of eastern peninsular India (Awasthi, 1981),

while *Sterculioxylon kalagarhense* is recorded from the Miocene of Uttar Pradesh (Trivedi and Ahuja, 1978). *Sterculioxylon varmahii* is recorded from the Mio-Pliocene of Arunachal Pradesh (Lakhanpal et al., 1978). *Sterculioxylon dattai* is recorded from the Tertiary of Assam (Prakash and Tripathi, 1974). Similarly, *Heritieroxylon keralaensis* is described from the Middle Miocene of Kerala (Srivastava and Awasthi, 1993) and *Heritieroxylon arunachalensis* is described from the Mio-Pliocene of Arunachal Pradesh (Lakhanpal et al., 1978). Prakash and Dayal (1964) and Srivastava and Guleria (2000) could identify *Grewioxylon indicum* and *Grewioxylon mahurzariense* in the Inter-trappean Beds of the Eocene (?) and Lakhanpal et al., (1976) could describe the anatomical characters of *Sterrculioxylon deccanensis* from the Inter-trappean Formation (Palaeocene?) of the Deccan of India.

The wood anatomical techniques were used to evaluate the palaeo-environmental conditions of the Meenachil River basin, Kerala, India (Guleria et al., 2008)(Figure 2). The study of these carbonised woods found embedded in palaeo-deposits of sand occurring in terrestrial regions, which are at present located about 15km landward from the present Vembanad Lake, along with its radio-carbon dating suggested that since the *Calophyllum, Spondias* and *Sonneratia* are inhabitant of coastal area, they indicate near shore conditions during the Holocene

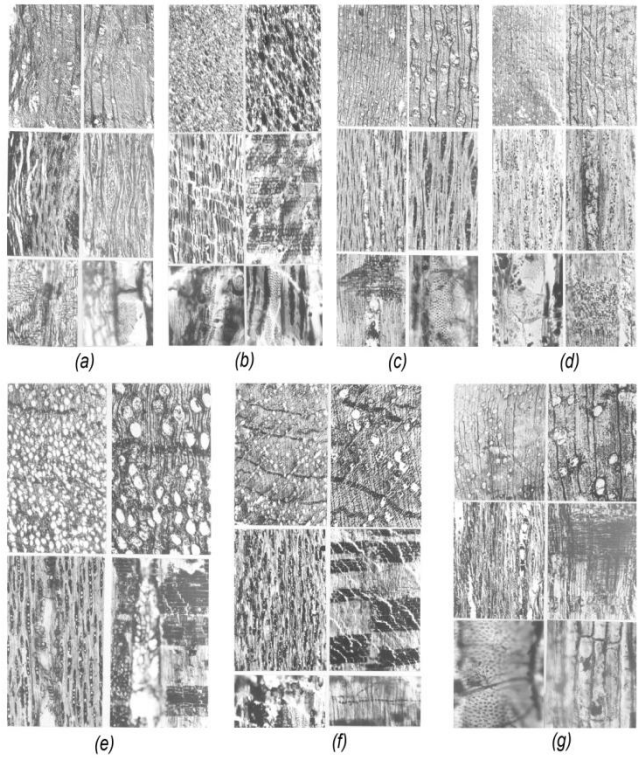

(a) - Artocarpus sp. (Moraceae); (b) - Sonneratia sp. (Sonneratiaceae); (c) - Canarium sp. (Burseraceae); (d) - Spondias sp. (Anacardiaceae); (e) - Calophyllum sp. I (Clusiaceae); (f) - Calophyllum sp. II (Clusiaceae); (g) - Holigarna sp. (Anacardiaceae)

Figure 2. Wood anatomical description of carbonised woods embedded in palaeode- posits of sand from Meenachil River basin, Kerala, India.

Sonneratia is a mangrove tree that occurs in the tidal creeks and littoral forests. *Calophyllum inophyllum*, a comparable species is found all along the coast above high water mark and in the evergreen forests of Western Ghats along the river banks. Likewise, *Artocarpus* (the jack fruit tree), *Holigarna* and *Canarium* are found in the evergreen forests of Western Ghats including Kerala. The assemblage indicates that the area was covered by dense forest and witnessed high rainfall and then prevailed conditions must had been warm and humid, which revealed from the later deposition of *Spondias*. The fungal infection in some of the woods further substantiates the existence of warm and humid conditions. So climatically there is no significant difference since the time of deposition of these woods. However, occurrence of *Sonneratia,* specially indicate the proximity of sea in the area at the time of deposition. Obviously, the sea level was much higher at that time than at present. Evidently, the sea had receded since then. Thus the carbonized woods have provided evidence about the prevailing environmental conditions and sea level fluctuations in the area. It is suggested that Moscow and Ponpally region, which are located about 15 km inland of present Vembanad Lake, had witnessed an episode of marine transgression, regression and contemporaneous geological modifications. It is proven that the wood anatomical techniques can be considered as a reliable tool to analyse the palaeo-environmental conditions.

LIMITATIONS OF THE STUDY BASED ON FOSSILISED WOODS

One problem that Paleobotanists have is that fossil wood is almost never found with leaves or fruit still attached (Wehr 1995). All study of fossil wood was originally based on the comparison to living trees. Now there are more and more published records of fossil wood which have been dated to approximate age, fossil wood can now be compared to other fossil woods. Some Eocene fossil wood's cell structure is so similar to extant genera that it has been named after it. Because some genera's wood structure has changed, Paleobotanists sometimes refer to Eocene fossil wood by the form that the cell structure resembles rather than the name of the extant genus.

Some species of hardwood trees have very distinctive cell structure features while others have structure that closely resembles many other species (Panshin and de Zeeuw, 1980). Some families of hardwoods have genera which are fairly different from one another's cell anatomy (Hall, 1952). Some families of trees have species that have more similarities to other families than members of their own. All of these phenomena make the determination of represented genus of a fossil wood specimen one of the more difficult branches of Palaeo-botany (Prakash and Barghoorn 1961). Because the determination of represented genera of fossil wood samples has little if any commercial value there are very few experts in this field.

CONCLUSION

Fossilized woods are preserved part of plants. They may be petrified woods that are many millions of years old, or bits of charcoal that are only a few hundred years old. Fossilised woods provide substantial information on palaeo-environment and palaeo-ecology. Even though there are some difficulties while reconstructing the preserved ones, it is strikingly true

that without the fossilised wood records, our knowledge about the arborescent plants of the past would have remained largely incomplete.

ACKNOWLEDGMENT

The authors dedicate this work before the treasured memmories of Late Dr. R. Satheesh. They sincerely extend a deep sense of gratitude to Dr. E. V. Ramasamy, Director, School of Environmental Sciences, Mahatma Gandhi University for his help and support. Thanks are also due to Dr. J. S. Guleria, Senior Scientist, Birbal Sahni Institute of Palaeobotany, Lucknow for extending the technical support.

REFERENCES

Alexandre, A., Meunier, J. D., Lezine, A. M., Vincens, A., Schwartz, D. (1997). Phytolith: indicators of grassland dynamics during the late Holocene in intertropical Africa. Palaeogeogr., *Palaeoclimatol., Palaeoecol*. 136: 213-229.

Allchin, B., Goudie, A. S., and Hegde, K. T. M. (1978). The prehistory and Paleogeography of the Great Indian Desert, Academic press, San Francisco, New York, London.

Awasthi, N. (1981). Fossil woods belonging to Sterculiaceae and Lythraceae from the Cuddalore Series near Pondicherry. *The Palaeobotanist*, 27(2): 182 – 189.

Barboni, D., Bonnefille, R., Alexandre, A., and Meunier, J. D. (1999). Phytoliths as palaeoenvironmental indicators, west side Middle Awash valley, Ethiopia. Palaeogeography, Palaeoclimatology, *Palaeoecology.* 152: 87-100.

Butzer, K. W., Isaac, G. L., Richardson, J. and Kamau, W. B. (1972). *Current Science.* 175:1069-1076.

Caratini, C., Fontungne, M., Pascal, J.P., Tissot, C and Bentale, B. I., (1991). A major change at ca. 3,500 years B.P in the vegetation of Western Ghats in North Kanara, Karnataka. *Curr. Sci.* 621 (9-10): 669-672.

Chauhan, M. S. (1996). Origin and history of tropical deciduous sal forests in Madhya Pradesh, India. *Palaeobotanist*. 43: 89-101.

Colalongo, M. L. (1969). Ricerche sugli Ostracodi nei fondali antistantiil delta del Po. *Giorn. Geol.* 36(2): 335-362.

Deevey, E. S. Jr. (1939). Studies on Connecticut lake sediments. I.A. postglacial climatic chronology for southern New England. *American journal of science.* 237: 691-724.

El-Din, M. M. K. (2003). Petrified wood from the Farafra Oasis, Egypt. *IAWA Journal*, 24(2): 163 – 172.

Garcia, J.; Philippe, M. and Gaumet, F. (1998). Fossil wood in Middle-Upper Jurassic marine sedimentary cycles of France: relations with climate, sea-level dynamics, and carbonate-platform environments. Palaeogeography, Palaeoclimatology, *Palaeoecology*, 141(3-4):199-214

Gregory, M. (1980). Wood identification: an annotated bibliography. International Association of Wood Anatomists Bulletin, 1: 3 - 41.

Guleria, J. S. and Awasthi, N. (1997). Fossil woods and their significance. *Current Science*, 72(4): 248 – 254

Guleria, J.S., Srivastava, R., Ajaykumar, B. and Satheesh, R. (2008). Late Holocene vegetation and environment of Meenachil river basin, Kottayam District, Kerala, India. Proceedings of the International Workshop on Climate Change and its impact on flora in the South Asia region, Lucknow.

Hait, A. K., Das, H. K., Ghosh, S., Ray, A. K., and Chanda, S. (1996). Environmental variations in late Quaternary Sequence of Kolaghat, West Bengal, India. *Current Science.* 70(12): 1089-1093.

Hall, J. W. (1952). The comparative anatomy and phylogeny of the Betulaceae. Botanical gazette, 113 (3): 244 - 251

Hoadley, R.B. (1990). Identifying wood; accurate results with simple tools. Taunton Press, Newtown.

Hoffmann, P. and Blanchette, R. A. (1997). The conservation of fossil tree trunk. Studies in Conservation, 42(2): 74 – 82.

Iamandei, E.; Iamandei, S. and Grinea, D. (2003). Cycadoxylon sp. – a Jurassic fossil wood remain from the haghima mountains, Eastern Carpathians. Rev. Roum. Geologie, 47: 43 – 51

Ivany, L.C.; Portell, R.W. and Jones, D.S. (1990). Animal-plant relationships and paleobiogeography of an Eocene seagrass community from Florida. *Palaios,* 5: 244 - 248.

Jeong, E.K.; Kim, K.; Suzuki, M. and Kim, J.W. (2009) Fossil woods from the Lower Coal-bearing Formation of the Janggi Group (Early Miocene) in the Pohang Basin, Korea Review of Palaeobotany and Palynology, 153(1-2):124-138

Kaiser, K.; Opgenoorth, L.; Schoch, W.H. and Miehe, G. (2009).Charcoal and fossil wood from palaeosols, sediments and artificial structures indicating Late Holocene woodland decline in southern Tibet (China). *Quaternary Science Reviews,* 28(15-16): 1539-1554.

Lakhanpal, R. N.; Prakash, U. and Awasthi, N. (1978). Some more dicotyledonous woods from the Tertiary of Deomali, Arunachal Pradesh, India. *The Palaeobotanist,* 27(3): 232 – 252.

Lakhanpal, R. N.; Prakash, U. and Bande, M. B. (1976). Fossil dicotyledonous woods from the Deccan Intertrappean beds of Mandla District in Madhya Pradesh. *The Palaeobotanist,* 25: 190 – 204.

Lucchi, M. R., Fiorini, F., Colalongo, M. L., Curzi, P. V. (2006). Late Quaternary palaeoenvironmental evolution of Lesina lagoon (Southern Italy) from subsurface data. *Sedimentary geology*. 183: 1-13.

Lumbert, S. H.; den Hartog, C.; Phillips, R. C. and Olsen, S. F. (1984). The occurrence of fossil seagrasses in the Avon Park Formation (late middle Eocene), Levy County, Florida (U.S.A.). *Aquatic Botany*, 20: 121 - 129.

Martínez-Cabrera, H.I.; Cevallos-Ferriz, S.R.S. and Poole, I. (2006). Fossil woods from early Miocene sediments of the El Cien Formation, Baja California Sur, Mexico. *Review of Palaeobotany and Palynology,* 138(3-4):141-163.

Mehrotra, R. C. (2000). Two new fossil fruits from Oligocene sediments of Makum Coalfield, Assam, India. Current Science, 79(10): 1482-1483.

Newby, P. E., Killoram, P., Waldorf, M. R., Shuman, N. B., Webb, R. S., and Webb. T. III. (2000). 14,000 Years of sediment, vegetation, and water level changes at the Makepeace Cedar Swamp, South-eastern Massachusetts. *Quaternary Research.* 53: 352-368.

Panshin, A. J. and de Zeeuw, C. (1980). Textbook of wood technology, 4th edition. McGraw-Hill, New York.

Philippe, M.; Barbacka, M.; Gradinaru, E.; Iamandei, E.; Iamandei, S.; Kázmér, M.; Popa, M.; Szakmány, G.; Tchoumatchenco, P. and Zatoń, M. (2006). Fossil wood and Mid-Eastern Europe terrestrial palaeobiogeography during the Jurassic–Early Cretaceous interval. *Review of Palaeobotany and Palynology,* 142(1-2): 15-32

Pigott, C. D. and Walters, S. M. (1954).On the interpretation of the discontinuous distributions shown by certain British species of open habitat. *J. Ecol.*42: 95-116.

Prakash, U. and Barghoorn, E. S. (1962) Miocene fossil woods from the Columbia basalts of Central Washington. *Journal of the Arnold arboretum,* 17 (2): pp 165.

Prakash, U. and Dayal, R. (1964). Fossil woods of Grewia from the Deccan Intertrappean series, India. *The Palaeobotanist,* 12: 121-127

Prakash, U. and Tripathi, P.P. (1974). Fossil woods from the Tertiary of Assam. *The Palaeobotanist*, 21(3): pp 305 – 316.

Rajagopalan, G., Sukumar, R., Ramesh, R., Pant, R. K., and Rajagopalan, G. (1997). Late Quaternary vegetational and climatic changes from tropical peats in southern India- An extended record up to 40,000 years BP. *Current Science.* 73(1): 60-63.

Rull, V., Abbott, M. B., Polissar, P. J., Wolfe, A. P., Bezada, M., and Bradley, R. S. (2005). 15,000-year pollen record of vegetation change in the high altitude tropical Andes at Laguna Verde Alta, Venezuela. *Quaternary Research*. 64: 308-317.

Smith, F.H. and Gannon, B.L. (1973). Sectioning of charcoals and dry ancient woods. *American Antiquity*, 38: 468 - 472.

Srivastava, R. and Awasthi, N. (1993). Carbonised woods of Sterculiaceae and Sapindaceae from middle Miocene sediments of Kerala coast. *The Palaeobotanist,* 42(2): 178 – 182.

Srivastava, R. and Guleria, J. S. (2000). Grewinium, a substitute name for Grewioxylon Shallom non Schuster. *The Palaeobotanist,* 49(3): 531 – 532.

Stewart, W. N. and Rothwell, G.W. (1993). Palaeobotany and the evolution of plants, 2nd edition. Cambridge University Press, New York.

Sweeney, I.J.; Chin, K.; Hower, J.C.; Budd, D.A. and Wolfe, D.G. (2009). Fossil wood from the middle Cretaceous Moreno Hill Formation: Unique expressions of wood mineralization and implications for the processes of wood preservation. *International Journal of Coal Geology,* 79(1-2): 1-17

Trivedi, B. S. and Ahuja, M. (1978). Sterculioxylon kalagarhense sp. nov. from Kalagarh (Bijnor District), U.P., India. *Current Science*, 47(1): 24 – 25.

Trivedi. B. S. and Ambwani, K. (1971). Occurence of Hibiscoxylon Intertrappeum Sp.Nov. from the Deccan Intertrappean series of Mahurzari, near Nagpur (M.P). India. *Current Science*, 40(7): 167-168.

Vishnu-Mittre and Sharma, B. D. (1966). Studies of post-glacial vegetational history from the Kashmir Valley, 1 Haigam Lake. *Palaeobotanist,* 15(1-2): 185-212.

Wehr, W. C. (1995). Early Tertiary flowers, fruits, and seeds of Washington State and adjacent areas. *Washington Geology* 23 (3): pp 7

Wheeler, E.A.; Pearson, R.G.; LaPasha, C.A.; Zack, T. and Hatley, W. (1986). Computer-aided wood identification. North Carolina Agricultural Research Service Bulletin, 474: 1 - 160.

Zucol, A.F.; Brea, M. and Scopel, A. (2005). First record of fossil wood and phytolith assemblages of the Late Pleistocene in El Palmar National Park (Argentina). *Journal of South American Earth Sciences*, 20(1-2): 33-43.

In: Wood: Types, Properties and Uses
Editor: Lorenzo F. Botannini
ISBN 978-1-61668-837-0

Chapter 8

PLASTIC MOLDABLE PINE FIBER BY BENZYLATION

Armando G. McDonald[1] and Lina Ma
Department of Forest Products, University of Idaho, Moscow,
ID 83844-1132, USA

ABSTRACT

The effects of chemical modification of pine wood fiber on the moldability of this material were examined. Pine wood fiber was chemically modified with benzyl chloride under alkaline conditions at various mole ratios of benzyl chloride to wood hydroxyl groups (ratio = 1 to 4) and at different reaction times (2 to 8 h). The extent of benzylation was assessed by weight gain and FTIR and NMR spectroscopies. FTIR spectroscopy revealed the reduction of wood hydroxyl group bands, an increase in aromatic bands, a reduction in cellulose crystallinity, and an increase in acryl and alkyl ether bands, which were consistent with etherification. The thermal and mechanical properties of the benzylated wood fiber were assessed by a combination of differential scanning calorimetry (DSC), dynamic rheometry and dynamic mechanical analysis (DMA). The results from DSC were consistent with data from rheometry. The data have shown that the benzylated wood thermal transition temperature and mechanical properties can be tailored by the extent of benzylation.

INTRODUCTION

In recent years, polymer composite reinforced with wood fibers have attracted considerable interest because of characteristics like low density and high specific modulus [1]. In 2004, the North American wood plastic composites (WPC) outdoor residential decking and railing markets accounted for approximately US$0.9 billion [2]. However, plastic is an expensive and non-degradable material. Therefore, there is an opportunity to develop a wood-based composite material without the use of a resin system. As the most widely used renewable natural material, wood cannot be melted and molded directly. The lack of

[1] corresponding author: E-mail: armandm@uidaho.edu.

thermoplasticity of wood is attributed to three main causes [3]: (i) cellulose in wood has a 50 to 70% crystalline structure, (ii) lignin has a three-dimensional molecular structure, and (iii) the main components of wood are linked by chemical bonds. Cellulose has the highest softening temperature among the wood polymeric components, which is about 240°C [4]. Cellulose properties are due to its strong inter- and intra-chain hydrogen bonds. With substitution of hydroxyl group in cellulose molecule with non-polar groups, thermoplasticity is introduced to cellulose [5].

Wood chemical modification can be obtained by substitution of wood hydroxyl groups with a suitable chemical agent. Generally, there are two primary categories for wood modification [6]: etherification (agent: benzyl chloride, acrylonitrile) and esterification (agent: maleic anhydride, phthalic anhydride, and succinic anhydride). In addition to these categories, modification by alkali is important in the formation of derivatives, because aqueous alkali swells the crystal lattice of cellulose and also creates an intermediate to allow for substitution to occur.

The thermoplasticization of wood by benzyl chloride (BC) created a wood derivative that could be pressed or extruded into films or molded products [7]. Benzylation at the surface of wood blocks and chips for self-bonding of wood surfaces has also been reported [8]. It was also reported that benzylation derivatives of prehydrolyzed rice straw exhibited thermoplastic behaviour with a softening point between 89 and 140^{o}C [9]. Lu and co-workers performed a surface benzylation treatment on sisal fibers which created self-reinforced composite after hot-pressing where the plasticized surface zones serve as matrix and the unplasticized cores of the fibers as reinforcement [10]. The aim of this study is to generate totally wood-based moldable composite materials without the need for synthetic resins. In the present work, pine wood fiber was benzylated to produce thermoplastic like material and the resulting materials characterized.

MATERIALS AND METHODS

Pine wood fiber (100 mesh, American Wood Fibers) was extracted with dichloromethane and dried prior to use. Extractives free pine fiber (5 g) was pre-treated with 10N NaOH (20 mL) for 1h to aid in swelling. The slurry was then transferred into a flask containing BC (6.9 to 27.6 mL) and the reaction was carried at 110 ºC for 2 to 8 h with continuous stirring [7]. Different mole ratios (1 to 4) of BC to wood fiber hydroxyl groups were examined. The modified pine fiber was collected by filtration and exhaustively washed with water and then with ethanol to remove any residuals. The final product (light yellow in color) was vacuum dried at 40^{o}C to constant weight to determine yields. Benzylated pine fiber was molded into bar (2 mm x 10 mm x 35 mm) and disc (2 mm x 25 mm dia) specimens by injection molding at approximately 180˚C using a Dynisco Lab Molding Machine.

Spectroscopy

Fourier transform infrared (FTIR) spectra were obtained on original and benzylated pine fiber in the attenuated total reflectance (ATR) mode (ZnSe) on an Avatar 370 spectrometer

(ThermoNicolet). Benzylation was evidenced by changes of functional group and cellulose crystallinity. Solid state cross polarization-magic angle spinning (CP-MAS) ^{13}C nuclear magnetic resonance (NMR) spectra were obtained on a Bruker Avance DRX-400 solid-state NMR spectrometer operating at a frequency of 100.6 MHz equipped with a Chemimagnetics solids probe (Washington State University NMR center). Samples were ground and packed into a 5 mm zirconia rotor which were spun at 5000 Hz. Spectra were recorded using a 3.75 μs proton preparation pulse followed by a 1 ms cross polarization contact time and a acquisition time of 6.6 μs. Spectral analysis was performed using freeware MestRe-C v2.3a.

Thermal Analysis and Mechanical Properties

Differential scanning calorimetry (DSC) was performed on benzylated pine fiber to determine the glass transition temperature (T_g) according to ASTM D3418 [11]. The benzylated pine fibers were annealed at 100˚C for 4 h prior to DSC analysis (TA Instruments model Q200 DSC, 5mg of sample, 25 to 300˚C at 10˚C/min). Dynamic mechanical analysis (DMA) was performed on molded specimens (in triplicate) in the 3 point bending mode using a TA Instruments model Q800 DMA. Flexural modulus of elasticity (MOE) at 35˚C were obtained from stress-strain curves in the controlled force test using 0.5 N/min ramp force according to ASTM D5934 to maximum strain 0.03% [12]. Data was analyzed by TA Universal Analysis software v4.4A. Dynamic rheometery was performed (in duplicate) using a Bohlin CVO100 rheometer equipped with an extended temperature control module on molded disc specimens in accordance to ASTM D4440 [13]. A negative temperature ramp (250 to 40˚C at -2˚C /min) was performed at 0.3, 1, 3 and 10 Hz with strain of 0.02% [14]. Data was analyzed using Bohlin rheology software v06.32.

Microscopy

Scanning electron microscopy (SEM) was performed on uncoated molded benzylated pine fiber samples on a Hitachi TM-1000 benchtop SEM.

RESULTS AND DISCUSSION

Weight Gain Analysis

The extent of wood fiber benzylation was assessed by weight gain. The degree of substitution (DS) was calculated from the percentage weight gain for pine based on the number of available hydroxyl groups present in pine (0.0148 mol/g) [15]. For fully substituted pine (DS = 1) a theoretical weight gain of 133% would be obtained. An increase in the reaction time from 2 to 8 h was shown to give a 2-fold increase in the DS with a 1:1 ratio of BC to hydroxyl group content (Figure 1). The DS of benzylated wood was shown to increase 4-fold with an increase of the ratio of BC to hydroxyl groups from 1 to 4 (Figure 2) showing that an excess BC was necessary to obtain high DS.

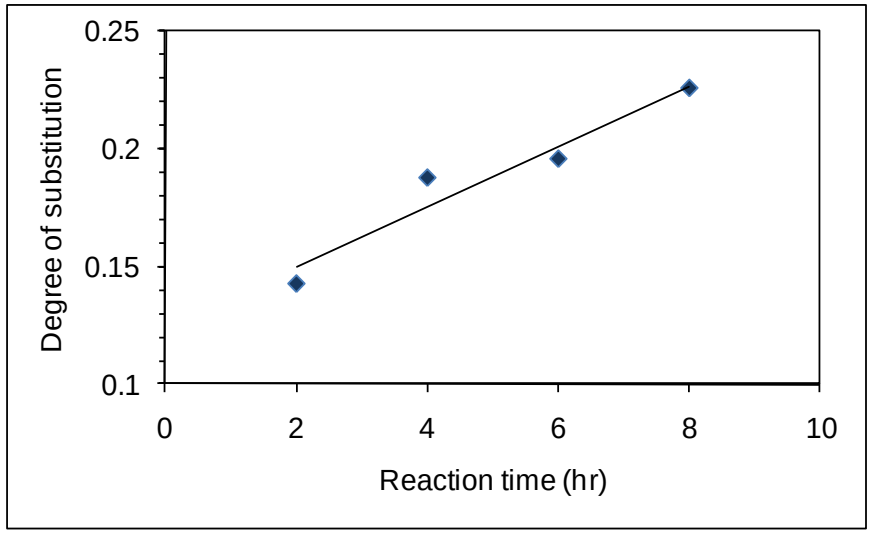

Figure 1. Graph of benzylated pine degree of substitution versus reaction time at a benzylchloride/wood hydroxyl group ratio of 1.

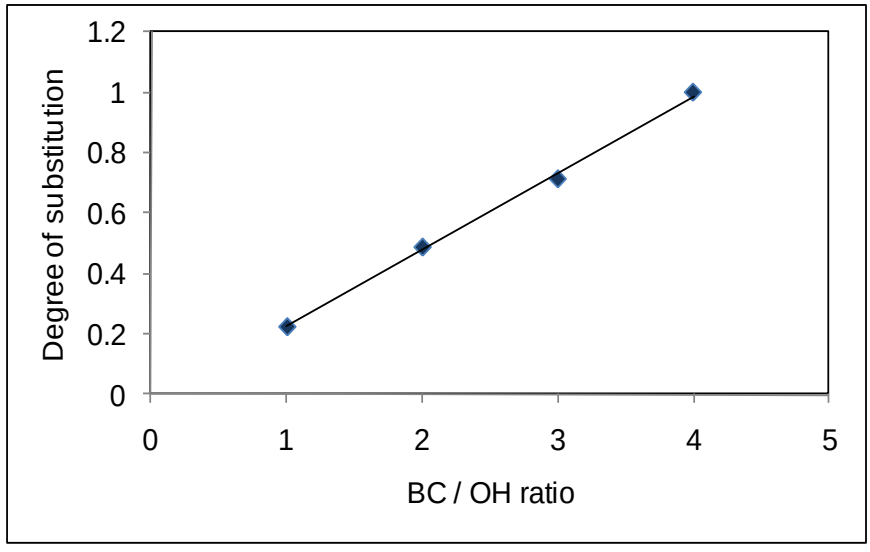

Figure 2. Graph of benzylated pine degree of substitution versus benzylchloride/wood hydroxyl group ratio.

FTIR Spectroscopic Analysis

FTIR spectra of original wood and benzylated pine fiber (DS=1.1) are shown in Figure 3. Benzylation of wood was evidenced [7, 16] by: (i) a reduction in the 3450 cm^{-1} band (OH stretch) and disappearance of 670 cm^{-1} peak (C-OH out-of-plane bending); (ii) appearance of bands at 695 cm^{-1} (aromatic C-C angular deformation), 736 cm^{-1} (aromatic C-H out-of-plane bending, mono-substitution); 1592-1612 cm^{-1} and 1496-1454 cm^{-1} (aromatic C-C axial deformations), 1810 cm^{-1} and 1950 cm^{-1} (out of plane deformation vibrations of adjacent

hydrogens from mono-substituted aromatic rings), and 3030-3088 cm^{-1} (strong multiplet, aromatic C-H stretch) which are attributable to mono substituted benzyl rings; (iii) a decrease in the bands at 1370 cm^{-1} (C-H bending), 895 cm^{-1} (deformation of anomeric CH) and 670 cm^{-1} (C-OH out-of-plane bending) which are assigned to crystalline cellulose; and (iv) an increase of aryl ether band (-C-O-C- stretching) at 1265 cm^{-1} and alkyl ether band at 1150-1060 cm^{-1} (C-O stretch from alkyl-substituted ether). Positive linear relationships between DS and (i) intensity of aryl (1265 cm^{-1}) and alkyl ether (1150 cm^{-1}) peaks and (ii) area of benzyl peak (695 cm^{-1}) were observed (data not shown) for benzylated pine samples. While, a negative relationship was observed between DS and intensity of the hydroxyl group (3450 cm^{-1}). These results are consistent with the literature [7]. Therefore FTIR spectroscopy can be used to determine the DS of benzylated lignocellulosic materials.

NMR Spectroscopic Analysis

The ^{13}C NMR spectrum of pine fiber (Figure 4, top) shows prominent signals between 60 and 110 ppm associated with wood polysaccharides (cellulose and hemicelluloses) [17]. The signals between 60 and 70 ppm are assigned to C6 of cellulose, 70 and 80 ppm to C2, C3, and C5 of cellulose, 80 and 90 ppm to C4 of cellulose, and 98 and 110 ppm to C1 of cellulose. In addition, signals for xylans were observed at 103 ppm (C1), 84 ppm (C4), 72 to 75 ppm (C2, C3), and 65 ppm (C5). However, these signals overlap with the strong cellulose signals [17]. The signal at 92 ppm corresponds to C4 of the crystalline regions in cellulose, whereas the signal at 86 ppm was assigned to the C4 of amorphous regions of cellulose [18]. Furthermore, the signals at 68 ppm and 65 ppm were assigned to C6 of crystalline and amorphous regions in cellulose, respectively. Moreover, resonances at 174 and 21.5 ppm are assigned to an acetyl substituent. The low intensity signals observed at 58 ppm, 115 to 130 ppm, and 152 to 156 ppm, were assigned to methoxyl and aromatic groups of lignin, respectively.

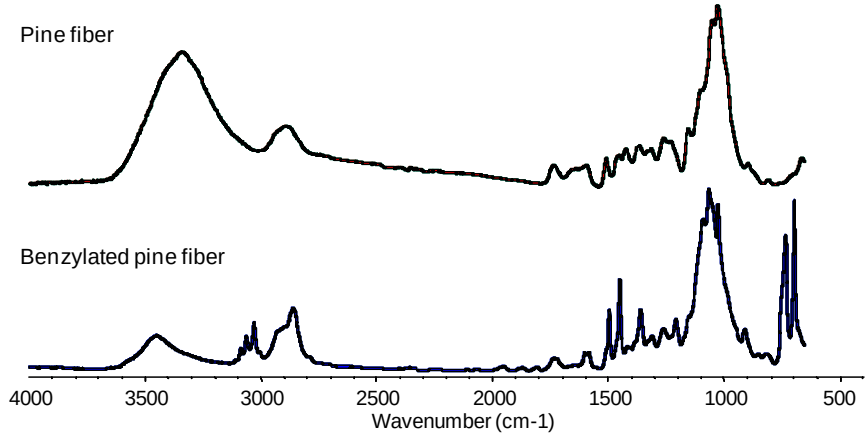

Figure 3. FTIR spectra of pine fiber (top) and benzylated wood fiber with a DS=1.1 (bottom).

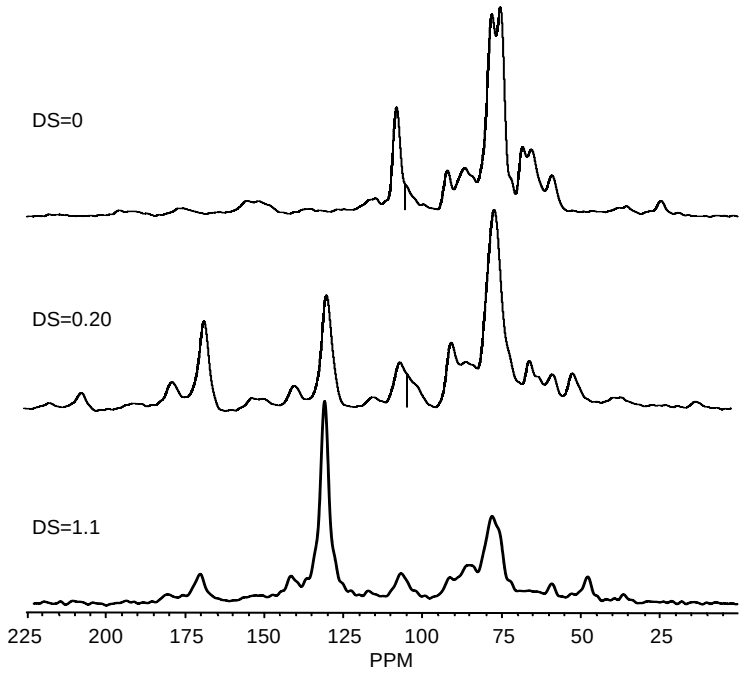

Figure 4. ^{13}C-CP-MAS NMR spectra of pine fiber (top) and benzylated wood fiber with a DS of 0.20 (middle) and 1.1 (bottom).

The other functional groups of lignin, e.g. CHOH, CH_2OH, and C–O–C groups overlapped with the signals from cellulose [17]. These observations are consistent with those reported in the literature [18- 20].

In benzylated pine at a DS of 0.20 (Figure 4, middle) and 1.1 (Figure 4, bottom), an intense signal appeared at 131 ppm and was assigned to aromatic carbons of the benzyl group [21,22]. The intensity was dependent on the DS. The signal at 142 ppm was assigned to C4 on benzylated *p*-hydroxyl phenyl, guaiacyl, and syringl units [21,22]. The sharp signal at 171 ppm was assigned to carbonyl groups. A new signal was observed at 51 ppm and assigned to a methoxyl aryl ether group. The cellulose anomeric carbon signal at 107 ppm and cellulose peaks associated with amorphous (86 ppm (C4)) and crystalline (91.6 ppm (C4) and 67.6 ppm (C6)) were all significantly reduced in intensity upon benzylation [22]. These data show that the relative concentration of wood to benzyl groups decreased upon substitution.

Glass Transition Temperature (T_g)

From the rheological data the temperature at the viscous modulus (G") peak maximum was tentatively assigned to the T_g and was shown to decrease from 161 to 70^{o}C as the extent of wood benzylation increased (DS = 0.20 to 1.25) (Figure 5, Table 1). The T_g was also determined by tan δ (G"/G') peak maximum and were several degrees higher that that determined by G" data (Table 1). These findings are consistent with those reported in the literature [7]. The higher the DS the lower the T_g (start of viscous flow based on G") which indicates an increase in free volume by introducing bulky benzyl substituents and thus increasing molecular mobility [23-24]. To confirm that the transition was a T_g the Arrhenius activation energy (E_a) was determined. Figures 6 show the frequency dependence of G" on

transition temperature. By plotting the results from dynamic rheology of natural log of frequency (*lnf*) against $1/T_g$ the E_a can be determined from the Arrhenius plot (Figure 7) [7]. The E_a of benzylated wood (DS=0.72) was determined at 212 kJ/mol and this transition was attributed to a glass transition. The E_a values for benzylated pine fiber (DS 0.2 to 1.1) are in the range (Table 1) of those published for the α-transition (or T_g) of polymers, such as PS and PVC [25].

Thermal transitions were also analyzed by DSC on the benzylated wood samples and the results are given in Table 1. The T_g was shown to decrease from 172 to 113°C as DS increased from 0.13 to 0.41. This trend is consistent with that obtained by dynamic rheology. However, at higher DS it was difficult to observe a clear transitions by DSC.

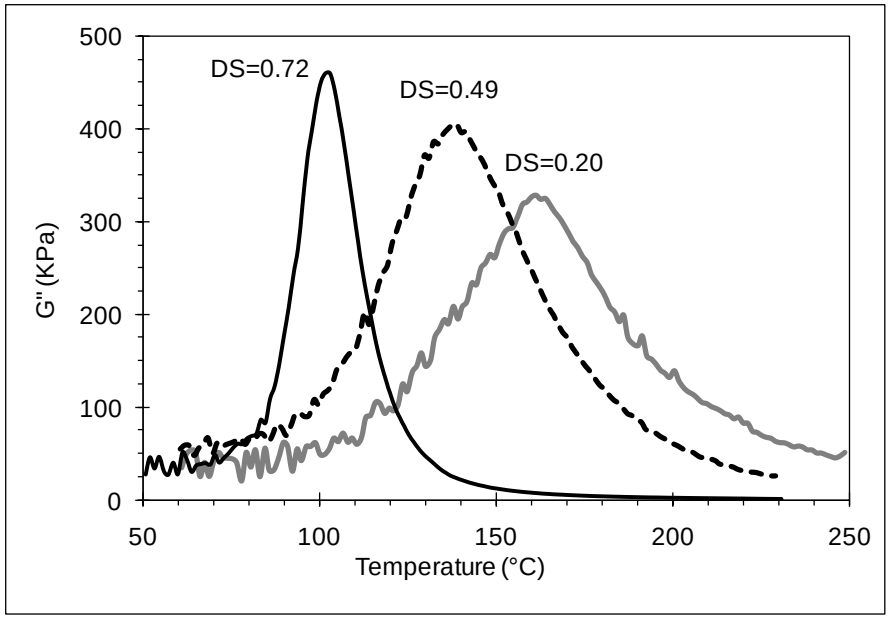

Figure 5. Dynamic rheology thermograms of viscous modulus (G") of benzylated wood.

Table 1. Determined T_g and E_a values for benzylated pine fiber by rheometry and DSC

Benzylated wood (DS)	T_g (°C) by G"	T_g (°C) by tan δ	T_g (°C) by DSC	E_a (kJ/mol)
0.23	161	171	172.6	
0.49	139	155	151.1	251
0.72	102	116	112.7	212
1.10	97	90		140
1.25	70	88		177

Mechanical Properties

Flexural properties were measured by DMA (3 point bending) to determine the modulus of elasticity (MOE) from the stress-strain curves of molded benzylated pine fiber samples

(Figure 8). MOE values of around 2.7 GPa were obtained with low DS benylzated pine while, the MOE significantly decreased as DS increased (Table 2).

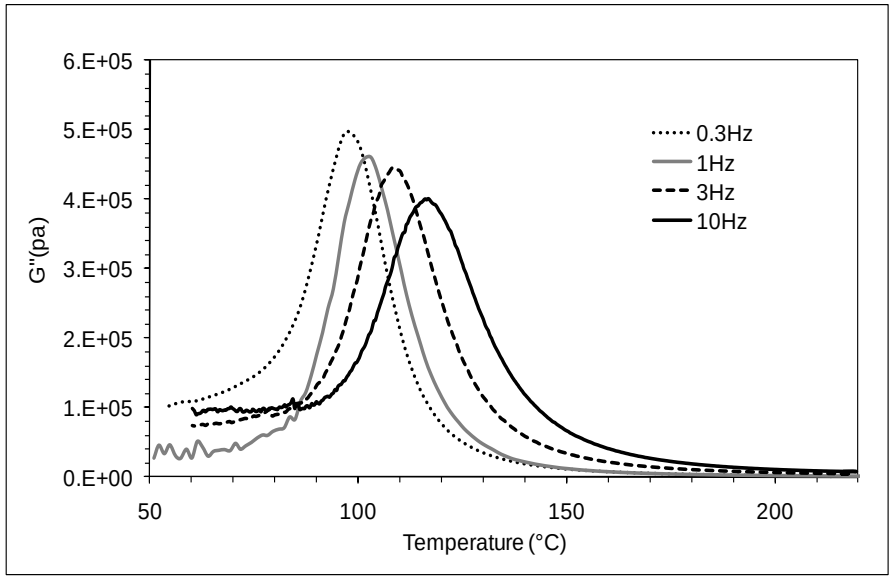

Figure 6. Thermograms of viscous modulus (G") as a function of dynamic frequency for benzylated wood at DS=0.72.

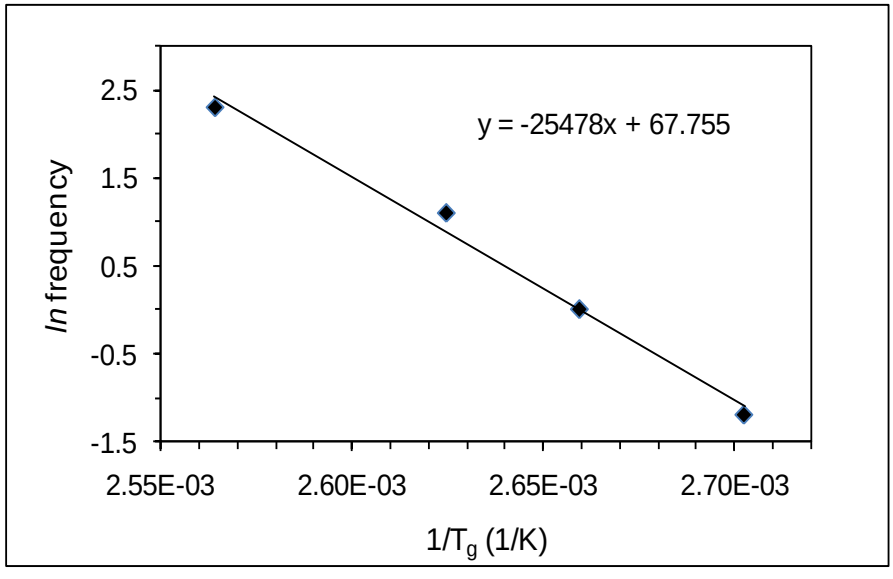

Figure 7. Arrhenius plot (ln *f* versus $1/T_g$) for benzylated pine fiber at DS=0.72.

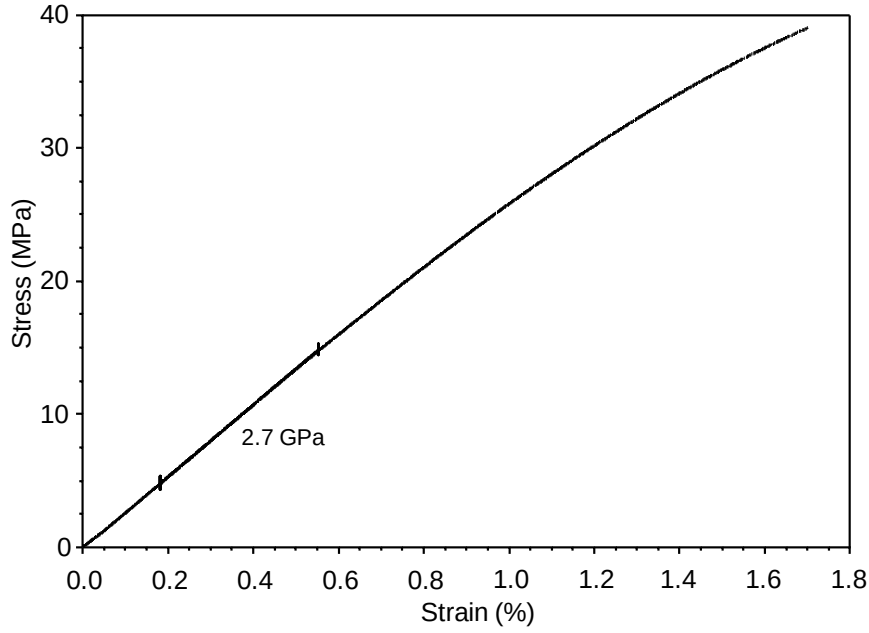

Figure 8. Flexural stress-strain curve for molded benzylated pine fiber at DS=0.20.

Table 2. Flexural properties of benzylated pine fiber

Benzylated wood (DS)	MOE (GPa)
0.23	2.7
0.49	1.4
0.72	0.11

However, at higher DS it was difficult to test the flexural properties of these molded benzylated fibers since they sagged on the test fixtures. The results are in good agreement with values for self-reinforced benzylated composites with MOE values of 3.0 and 1.7 GPa for weights gains of 26 and 60%, respectively [10, 26]. The MOE of benzylated wood fiber, was comparable to values for polypropylene (40%) based WPC at 2.1- 2.8GPa [27].

Morphology

SEM analysis on molded benzylated wood fiber sample (DS = 0.18) showed a smooth surface amorphous matrix phase with some unmelted fibers present (Figure 9) within the matrix. At higher levels of benzylation (DS >0.2) no fibers were observed in the thermoplastic phase. The unmelted fibers can reinforce the matrix and thus enhance the MOE [7].

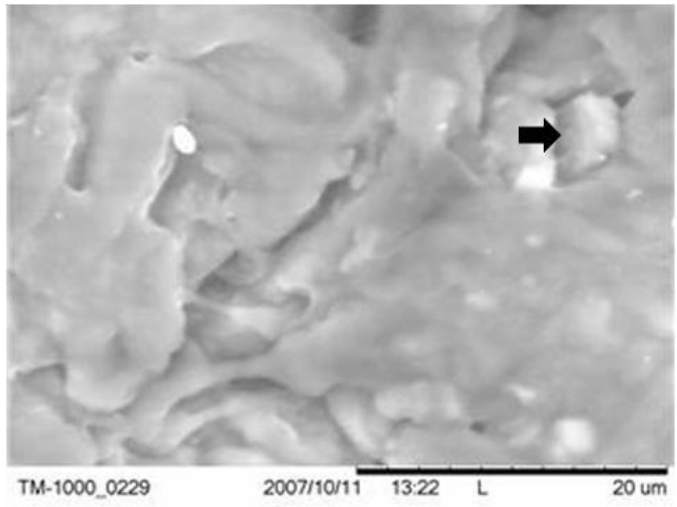

Figure 9. Scanning electron micrograph of molded benzylated pine at DS=0.18 (4000x). Arrow shows unmelted pine fiber.

CONCLUSION

Wood fiber was successfully benzylated in a 2-step process. Cellulose crystallinity was shown to decrease as substitution increased. The extent of benzylation could be governed by either reaction time or ratio of benzylchloride to wood hydroxyl content. The thermal transition properties of benzylated pine fiber were successfully plasticized by benzylation. The modulus of elasticity (MOE) of benzylated pine fiber (2.7 GPa), at low levels of substitution, were shown to be comparable to commodity plastics and wood plastic composites. At low extent of benzylation fragments of wood fibers were embebdded in the benzylated matrix which can reinforce the matrix. However, as the benzyl substitution increased the MOE decreased and the material behaved like a thermoplastic rubber. It is possible to produce such a bio-plastic based on wood benzylation. The outcome of this effort is to develop biobased plastics which will reduce our dependency petroleum based plastics.

ACKNOWLEDGMENTS

The project was supported by USDA-CSREES Wood Utilization Research program; Inland-Northwest Forest Products Research Consortium. The FTIR spectrometer was supported by a USDA-CSREES grant #2005-35103-15243.

REFERENCES

[1] Pickering K.L., Abdallaa, A., Jia, C., McDonald, A.G., and Franich, R.A. (2003) The effect of silane coupling agents on radiata pine fibre for use in thermoplastic matrix composites. *Composites Part A*, *34*, 915-926.

[2] Smith, P.M. and Wolcott, M.P. (2005). Wood-Plastic Composites Emerging Products and Markets. In Proceedings of the 8th International Conference of Woodfiber-Plastic Composites. (pp 335-343). Madison, WI, May 23-25.Shiraishi N. (1991). Wood Plasticization. In D.N.S. Hon and N. Shiraishi (Ed.) Wood and Cellulosic Chemistry. (pp 861-906). Marcel Dekker, Inc., New York.

[4] Dwan, A. (1987) Paper Complexity and the interpretation of conservation research. *Journal of the American Institute for Conservation*, *26(1)*, 1-17.

[5] Sereshti, H., and Mohammadi-Rovshandeh, J. (2003). Chemical Modification of Beech Wood. *Iranian Polymer Journal*, *12(1),* 15-20.

[6] Matsuda, H. (1996). Chemical modification of solid wood. In D. Hon (Ed.) Chemical Modification of Lignocellulosic Materials. (pp 159-183). Marcel Dekker, Inc., New York.

[7] Hon, D.N.S. and Ou, N-H. (1989). Thermoplastization of Wood: Benzylation of Wood. *Journal of Applied Polymer Science Part A, 27,* 2457-2482.

[8] Kiguchi, M. and Yamamoto, K. (1992). Chemical modification of wood surfaces by etherification III. Some properties of self-bonded benzylated particleboard. *Mokuzai Gakkaishi, 38(2)*, 150-158.

[9] Mohammadi-Rovshandeh, J., and Sereshti, H. (2005). The effect of extraction and prehydrolysis on the thermoplasticity and thermal stability of chemically modified rice straw. *Iranian Polymer Journal, 14(10)*, 855-862.

[10] Lu, X., Zhang, M.Q., Rong, M. Z., Shi,G., and Yang, G.C. (2003). Self-reinforced melt processable composites of sisal. *Composites Science and Technology, 63,* 177–186.

[11] American Society for Testing and Materials (ASTM D3418-03) (2008) Standard test method for transition temperatures and enthalpies of fusion and crystallization of polymers by differential scanning calorimetry. ASTM annual book, vol. 08(02). (pp 63-69). Conshohocken, PA.

[12] American Society for Testing and Materials (ASTM D5934-02) (2008) Standard test method for the determination of modulus of elasticity for rigid and semi-rigid plastic specimens by controlled rate of loading using three-point bending. ASTM annual book, vol. 08(03). (pp 311-314). Conshohocken, PA.

[13] American Society for Testing and Materials (ASTM D4440-07) (2008) Standard test method for plastics: Dynamical mechanical properties melt rheology. ASTM annual book, vol. 08(02). (pp 489-492). Conshohocken, PA.

[14] Fox, S.C. and McDonald, A.G. (2005) The esterification of different industrial lignins to form lignin bioplastics. In proceedings of the 37th Society of Advancement of Material and Process Engineering Fall Technical Conference, Seattle, Washington, October 31-November 2.

[15] Hill, C.A.S., and Jones, D. (1996). The dimensional stabilisation of corsican pine sapwood by reaction with carboxylic acid anhydrides. *Holzforschung, 50(5)*, 457–462.

[16] Coates, J. (2000). Interpretation of Infrared Spectra, A Practical Approach. In R.A. Meyers (Ed.) Encyclopedia of Analytical Chemistry (pp. 1-25). John Wiley and Sons Ltd, Chichester.

[17] Sterk, H., Sattler, W., and Esterbauer, H. (1987). Investigations of lignocellulosic materials by the carbon-13 NMR CP MAS method. *Carbohydrate Resource, 164,* 85–95.

[18] Wikberg, H. and Maunu, S.L. (2004). Characterisation of thermally modified hard- and softwoods by 13C CPMAS NMR. *Carbohydrate Polymers, 58,* 461–466.

[19] Newman, R.H. and Hemmington, J.A. (1990). Determination of the degree of cellulose crystallinity in wood by carbon-13 nuclear magnetic resonance spectroscopy. *Holzforschung, 44,* 351–355.

[20] VanderHart, D.L. and Atalla, R.H. (1984). Studies of microstructure in native cellulose using solid-state 13C NMR. *Macromolecules, 17,* 1465–1472.

[21] Mello, N.C., Ferreira, F.C., Curvelo, A.A.S., Mattoso, L.H.C., and Colnago, L.A. (2000). Study on benzylated sisal fibers by 13C solid state NMR. In Proceedings from the 3rd International Symposium on Natural Polymers and Composites (pp 32-36), Sao Pedro, Brazil, May 14-17.

[22] Ramos, L.A., Frollini, E., Koschella, A., and Heinze, Th. (2005). Benzylation of cellulose in the solvent dimethylsulfoxide/tetrabuty lammonium fluoride trihydrate. *Cellulose. 12,* 607–619.

[23] McCrum, N.G., Read, B.E., and Williams, G. (1991). Anelastic and Dielectric Effects in Polymeric Solids. Dover Publications, New York.

[24] Nielsen, L.E., and Landel, R.F. (1994). Mechanical Properties of Polymers and Composites. Marcel Dekker, Inc., New York.

[25] Cervenya,S., Ghilarduccib, A., Salvab, H., and Marzocca, A.J. (2000). Glass-transition and secondary relaxation in SBR-1502 from dynamic mechanical data. *Polymer. 41,* 2227–2230.

[26] Lu, X., Zhang, M.Q., Rong, M.Z., Yue, D.L., and Yang, G.C. (2004). Environmental degradability of self-reinforced composites made from sisal. *Composites Science and Technology, 64,* 1301–1310.

[27] Wechslera, A., and Hiziroglu, S. (2007). Some of the properties of wood–plastic composites. *Building and Environment, 42(7),* 2637-2644.

In: Wood: Types, Properties, and Uses
Editors: Lorenzo F. Botannini
ISBN: 978-1-61668-837-0

Chapter 9

HIGH STRENGTH PHENOL FORMALDEHYDE (PF) RESIN IMPREGNATED WOOD: FUNDAMENTAL ANALYSIS AND FUTURE APPLICATIONS

Md. Iftekhar Shams* *and Hiroyuki Yano*
Kyoto University Uji, Kyoto, Japan

ABSTRACT

This chapter highlights the deforming behavior of PF resin-impregnated wood under transverse compression aiming at obtaining high strength wood at low pressing pressure. The impregnation of PF resin caused significant softening of cell walls resulting in cell wall collapse at low pressing pressure. Pressure holding causing creep deformation of resin impregnated wood was also effective in initiating collapse at lower pressure. Thus, by controlling the processing parameters (resin content, pre-curing temperature, pressing temperature and pressing speed) high strength wood having MOR of 240 MPa and MOE of 22 GPa can be obtained at a pressing pressure of 2 MPa. Removal of matrix substances by $NaClO_2$ treatment prior to resin impregnation is also effective for further enhancing the mechanical properties of resin impregnated wood at lower pressing pressure. This treatment is attractive; nevertheless it is complicated in processing and somewhat difficult to remove the harmful chemical $NaClO_2$ completely from the treated wood, posing a major drawback in the commercial application. Hence, the potentials of steam pretreatment as a substitute of chemical treatment for making highly compressed PF resin-impregnated wood at low pressing pressure was highlighted. Such treated wood elements present a promising surface material in the manufacture of sandwich panels, giving high strength and dimensional stabilization with a moderate specific gravity as a whole product using single shot application.

* Research Institute for Sustainable Humanosphere, Kyoto University Uji, Gokasho, Kyoto 611-0011, Japan, Email: shams@rish.kyoto-u.ac.jp/shams_rish@yahoo.com

1. INTRODUCTION

The establishment of a sustainable society based on renewable and sustainable resources is a real challenge and responsibility of all nations in the 21st century. In this sense, the promotion of wood as a future-oriented material must be emphasized as it is a natural renewable resource that is environmentally friendly. As reserves of coal and oil become exhausting, future advanced materials have to be derived from renewable resources such as wood. For these potentials to be realized and to substitute other resources derived from synthetic plastic, ceramics and metals, the utilization of inherent properties of wood should be taken into account. However, wood as a material has several undesirable properties that need to be overcome so that wood can be used more effectively, and its field of application can be extended. These include dimensional instability due to moisture, low durability due to biodeterioration, and relatively low mechanical properties compared to other engineering materials. In order to enhance the properties of wood, a good number of studies have been carried out through hydrophobisation to prevent water re-softening or plasticization of wood by replacement of hydroxyl groups with hydrophobic groups [1-5], steam or heat stabilization by combination of self adhesion, self cross linking, or releasing the elastic stresses stored in the microfibrils and matrix [6-9], resin impregnation into the wood cell wall and cell lumen to hold the deformation [10-16]

PF resin impregnated compressed wood, named Compreg, is produced by impregnation with PF resin, and compression under pressures of 7 MPa or above. The product has a density of 1.2 to 1.35 g/cm^3, and exhibits high strength, good dimensional stability and high resistance to decay and termites [17-18]. Because of such properties, a lot of research following up Stamm's work has been done, and in recent years the potential strength of PF resin-impregnated compressed wood has been extensively studied [19-23]. When wood selected based on sound velocity was impregnated with low molecular weight PF resin, and hot pressed at a pressing pressure of 50-80 MPa, the bending strength and Young's modulus attained were 500-530 MPa and 50 GPa respectively. Furthermore, when lignin and hemicellulose were removed from the wood and the specimens were impregnated with low molecular weight PF resin and hot pressed at high pressure; the Young's modulus and bending strength attained 62 GPa and 670 MPa, respectively. This value is greater than the value of bending strength of soft steel with a density of 7.8 g/cm3, and is comparable to the strength of duralumin, which has a density of 2.7 g/cm^3. On the other hand, when PF resin impregnated wood elements such as particles and powder were hot pressed under high pressure, a decrease in element size did not result in a decrease in bending strength, due to high interactive forces developed between elements.

The aforementioned research indicates that PF resin-impregnated compressed wood has the potential to be a substitute for other engineering materials. However, considering the production of large size composites, the high pressing pressure required during manufacturing becomes an explicit problem. Although many studies on the compressive deformation of wood as a cellular material have been done [24-27], none have clarified the deforming behavior of low molecular weight PF resin-treated wood where PF resin acts as a plasticizer at first and then loses the effects by polymerizing or curing during hot-pressing. In this chapter, we first presented a method to obtain highly compressed wood at low pressing pressure based on the analysis of the deformation behavior of PF resin-impregnated wood and

then deliberate the potentials of this technique to produce selectively densified wood based materials.

2.1. Compressive Deformation of PF Resin Impregnated Wood

Flat sawn grain of Japanese cedar (*Cryptomeria japonica*), with dimensions of 60 mm (L) X 40 mm (T) X 1.5 mm (R) was used in this study. Oven-dried specimens were soaked in an aqueous solution of 20% low molecular weight PF resin (average molecular weight 300, pH 5.5, and gelation time 10 minutes at 150ºC, Gun-ei Chemical Industry Ltd.). Specimens were kept under vacuuming for 12 hours, after which release pressure and specimens were kept at room temperature for 12 hours. This process was repeated several times in order to obtain complete penetration of the solution into the wood. The weight gain determined using oven-dried weight before and after treatment was 60.8%. Oven-dried specimens were compressed in the radial direction using hot plates fixed to the Instron Universal Testing Machine (Model 5582) [28, 31].

Like the stress-strain curve for all other cellular materials, PF resin-impregnated wood shows a linear region at lower stress, followed by a long collapse region with a roughly constant stress [24-27]. However, PF resin-impregnated wood required lower stress to initiate cell wall collapse compared with untreated wood (Fig. 1a). Furthermore, the stress required to compress wood is greatly influenced by the concentration of PF resin (Fig. 1b). With increasing resin concentration, collapse tends to initiate at a lower stress. For example, in the case of a resin concentration of 3% having a weight gain of 12.5% and volume gain of 5.3%, the collapse is initiated around 1.6 MPa; while at 20% with a weight gain of 62.7% and volume gain of 10.1%, collapse occurs at approximately 1.0 MPa.

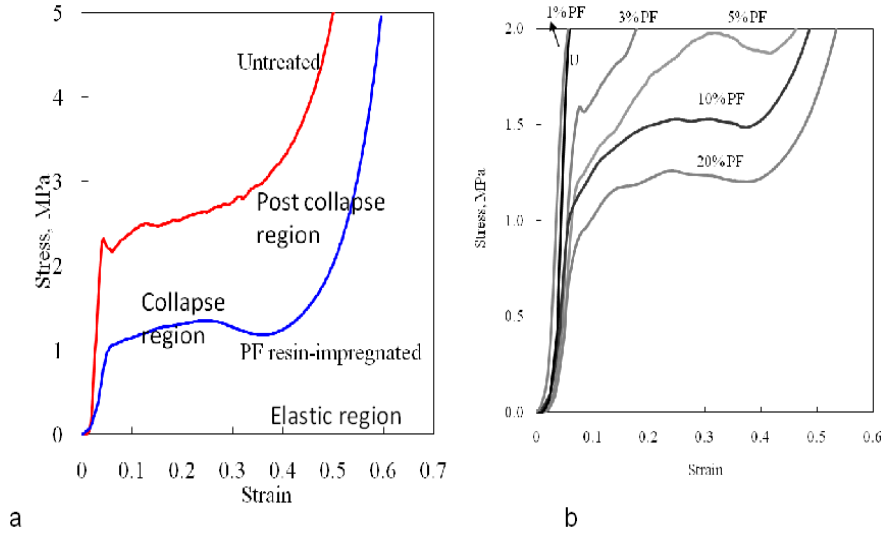

Figure 1. (a) Typical stress-strain curve of oven dried untreated wood and PF resin-impregnated wood compressed in the radial direction at a pressing temperature of 150°C and a pressing speed of 5mm/min (Shams et al. 2004) (Color preferred) (b) Stress-strain curve of wood treated with different concentrations of PF resin during compression (Shams and Yano, 2004)

The relationship between Young's modulus in the radial direction and collapse initiating stress revealed that there is a linear relationship between Young's modulus in the radial direction and collapse initiating stress [29]. The Young's modulus is evaluated by fitting a straight line to the elastic region of the stress-strain curve and determining the inclination. The collapse initiating stress is evaluated as the interception point of the straight line of elastic region and a fitted straight line of the collapse dominant region until the strain of 0.1 mm/mm. This indicates that increasing the amount of PF resin acting as a plasticizer reduces the Young's modulus of cell walls perpendicular to the fiber direction resulting initiation of collapse at lower stress.

Besides, it can be seen in Fig. 1 that a certain strain is required to initiate cell wall collapse, irrespective of PF resin-impregnated or untreated condition. This result implies that the cell wall collapse in the radial direction is strain-dependent rather than stress dependent. Since the occurrence of cell wall collapse was found to be strain dependent, creep deformation of cell walls to initiate collapse at lower pressing pressures was accordingly studied at various pressing pressures ranging from 0.5 to 10 MPa. After reaching desired pressing pressure, the pressing pressure was held for 30 minutes as shown in Fig. 2. When PF resin-impregnated wood was compressed at 0.5 MPa, the effect of pressure holding on density can be negligible. However, when wood was compressed at 1 MPa, a significant increment in density occurred during the pressure holding period. The density increased from 0.52 to 0.84 g/cm^3, which is around 70% higher than the density before pressure holding. At high pressing pressures such as 5 MPa and 10 MPa, the effect of pressure holding on density was not as significant as that at 1 MPa. It illustrated that the resistance of the cell wall against deformation increases with increasing strain at the post collapse region suggesting that a certain balance between cell wall resistance and applied pressure exists during creep deformation in a collapse dominant region. Thus, a proper combination of pressing pressure and holding period is needed to obtain marked deformation of wood at lower pressing pressures.

Furthermore, there was not a significant difference in mechanical properties between pressure holding (with creep deformation) and non holding (without creep deformation) at the same density. As a consequence, at a pressing pressure of 2 MPa utilizing a combination of pressure holding, the density of Japanese cedar impregnated with low molecular weight PF resin increases from 0.45 to 1.1 g/cm^3. Concurrently, the Young's modulus and bending strength increases from 10 GPa and 80 MPa to 22 GPa and 250 MPa, respectively. Thus, effective utilization of collapse is promising process for the production of high strength wood at lower pressing pressures [28].

The above findings indicate that the optimum processing conditions (preheating temperatures, pressing temperature and pressing speed) for obtaining high strength wood at lower press pressure have to be clarified in relation to the viscoelastic properties and behavior of resin impregnated wood. Thus we studied the processing parameters (pre-curing temperature, pressing temperature and pressing speed) that affect the compressive deformation of resin-impregnated wood [29]. By increasing the preheating temperatures, such as 100 ºC for 1 hour, the pressure needed to initiate collapse increases due to the increment of the Young's modulus of the cell wall. An increase in pressing temperature results in the thermal softening of cell wall and causes collapse at a lower pressing pressure level. The wood is compressed effectively, despite the accelerated resin cure. The pressing speed significantly affects the visco-elastic deformation of the cell wall, and the wood is well

deformed with decreasing pressing speed although the differences in density and mechanical properties are relatively small after a pressure holding period of 30 minutes. For all the parameters examined here, the Young's modulus and bending strength increase with increasing density [29].

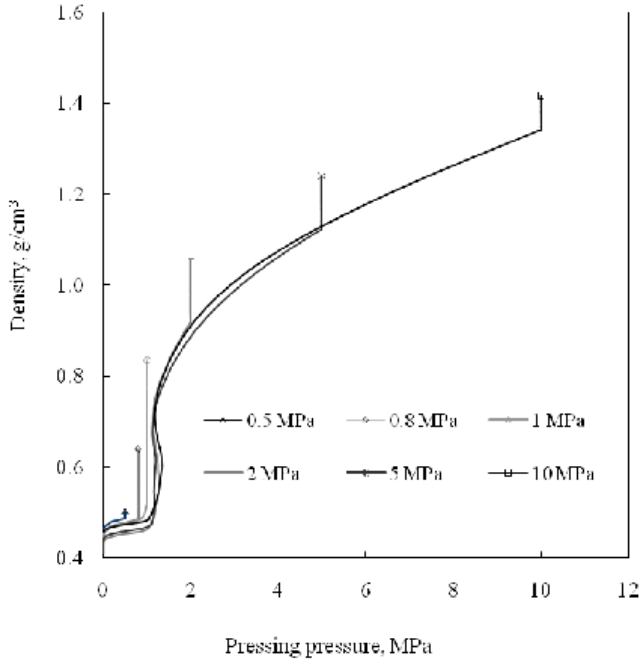

Figure 2. Effects of pressing pressure with pressure holding time on the densification of PF resin-impregnated wood. The bar indicates a holding time of 30 minutes (Shams et al, 2004)

2.2. Pre Treatment Effect on the Compressive Deformation of Resin Impregnated Wood

2.2.1. Removal of Matrix Substances Pre-Treatment Through $Naclo_2$ Treatment and Combination of $Naclo_2$ and Naoh Treatment

To obtain a further deformation of PF resin-impregnated wood under compression, the effect of the removal of the matrix substances from the cell wall prior to resin impregnation was studied [30]. Sawn veneers were used in this study, since it is easier to treat the inside of the veneers with $NaClO_2$ aqueous solution than thicker solid wood. Oven-dried veneers were treated with 2% aqueous solution of $NaClO_2$ at 45ºC for 12 hours. The treatment was repeated up to four times, followed by rinsing with running water for six hours. A weight loss of above 21% was observed due to this treatment. The weight gain due to PF resin was about 60%, regardless of $NaClO_2$ treated or untreated conditions.

$NaClO_2$ treatment did not show any considerable effect on the deformation of resin-impregnated wood at a press pressure of 2 MPa in the oven-dried condition. However, when the moisture content was increased to 10-11%, the deforming behavior was significantly different between the $NaClO_2$ treated and untreated wood. The density of $NaClO_2$ treated wood was almost double compared to untreated wood at the same pressing pressure, with the

greatest benefit seen at 1 MPa (Fig.4). This indicates that adding moisture helps to plasticize the cell wall significantly in $NaClO_2$ treated wood, and results in a considerable reduction of press pressure required to initiate collapse compared to oven-dried wood. Most interestingly that $NaClO_2$ treatment has shown considerable potential for highly compression of PF resin-impregnated wood at lower pressing pressure regardless of molecular weight of resin [31].

In addition, the mechanical properties of $NaClO_2$ treated wood were considerably higher than untreated wood. The Young's modulus and bending strength of four times $NaClO_2$ treated PF resin-impregnated veneer laminated composites compressed at 1 MPa, reached 27 GPa and 280 MPa, whilst those values for the untreated PF resin-impregnated wood reached 16 GPa and 165 MPa, respectively. The mechanical properties of the material were further improved by a combination of $NaClO_2$ and NaOH treatment [32]. The MOE and MOR of the treated compressed materials reached 29 GPa and 310 MPa respectively. This could be attributed to the removal of lignin, in other words, to an increase in the volume ratio of microfibrils, the framework of the cell wall. Thus, the removal of matrix substances is a highly promising approach for increased deformation of PF resin-impregnated wood at lower pressing pressures, especially when moisture is added.

2.2.2. Steam Pretreatment

The above treatment is attractive; nevertheless it is complicated in processing. Furthermore, it is somewhat difficult to remove the harmful chemical, $NaClO_2$, completely from the treated wood, a factor that poses a major drawback in the application of this treatment. For this reason, we have focused on steam treatment as an alternative pretreatment [33]. Specimens were subjected to saturated steam at different temperatures 140°C, 160°C, 180°C, and 200°C for 10 minutes. Steam treated and untreated veneer specimens were immersed in a 20% aqueous solution of PF resin for three days. The weight gain due to resin impregnation was 50-60%.

When solely steam treated wood was compressed at oven-dried condition (St 160°C, OD), we could not detect any collapse deformation up to a pressing pressure of 1 MPa, showing to some extent the similar deformation behavior of untreated oven-dried Japanese cedar (C). As shown in Fig.3, steam treated wood after adding moisture (St 160°C, AD) showed to a great extent deformation compared to oven-dried condition. It started collapsing up to 1 MPa although it is difficult to point out the exact position of the collapse initiating stress. However, as clearly demonstrated the behavior is not as distinct as that of oven-dried PF resin impregnated wood (PF resin impregnated) especially in the collapse dominant region. The collapse-initiating stress was dramatically reduced by the combination of steam treatment and PF resin impregnation (St + PF). Steam treatment at a relatively lower temperature such as 140°C prior to PF resin impregnation reduced the collapse-initiating stress from 0.8 MPa of solely PF resin-impregnated wood to 0.3 MPa. The collapse-initiating stress remained constant over the range of temperatures from 140°C to180°C despite the decomposition of the cell wall polymers demonstrated by increased weight loss, although a long collapse-dominant region with roughly constant stress was distinct at 180°C. The collapse-initiating stress decreased with increasing steaming temperature from 180°C to 200°C, and it was noted that cell wall collapse started at 0.2 MPa when steam treatment was performed at 200°C for 10 minutes.

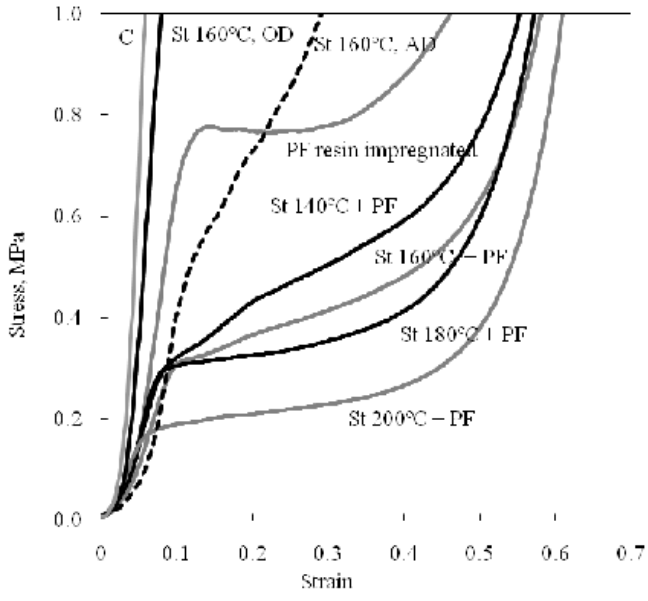

Figure 3. Stress-strain curves of oven-dried PF resin-impregnated wood as a function of steaming temperatures at a pressing temperature of 150°C and pressing speed of 5 mm/min. C, St, PF, OD and AD refer to control (oven-dried untreated Japanese cedar), steam temperature, phenol formaldehyde resin impregnated, oven-dried condition and air-dried condition, respectively. Steaming time was 10 minutes (Shams et al, 2006)

The pressing pressure-density relationship of steam treated resin-impregnated wood is compared in Fig. 4 with those of $NaClO_2$ (a lignin removal treatment) treated resin-impregnated wood [30]**.** The density of $NaClO_2$ treated resin-impregnated wood was 0.7 g/cm^3 for the oven-dried condition ($NaClO_2$ treatment, OD) at a pressing pressure of 1 MPa. After adding moisture of 10-11% to the $NaClO_2$ treated resin-impregnated wood ($NaClO_2$ treatment, AD), the density reached 1.0 g/cm^3. This is similar to the density attained by oven-dried steam treated resin-impregnated wood (200°C). It is worth mentioning that the decomposition of hemicellulose is as effective in increasing the compressibility of PF resin-impregnated wood as is the removal of lignin. Based on the chemical analysis of Higashihara *et al.* [34], it is believed that a large amount of low molecular weight substances derived from decomposition of hemicellulose still remain in the cell wall after steaming. From these facts, it may be speculated that the decomposed hemicellulose maintained in the cell wall acts as a plasticizer in combination with the low molecular weight PF resin, and reduces the Young's modulus of the cell wall.

The Young's modulus and bending strength of PF resin-impregnated wood at a pressing pressure of 1 MPa increased due to steam pretreatment, and attained 20 GPa and 207 MPa, respectively, when the steaming treatment was 200°C and 10 minutes [33]. It is thus recommended that steam treatment can be substituted for chemical treatment in the fabrication of highly compressed PF resin-impregnated wood, since steam treatment is much easier than the $NaClO_2$ treatment and is harmless to humans.

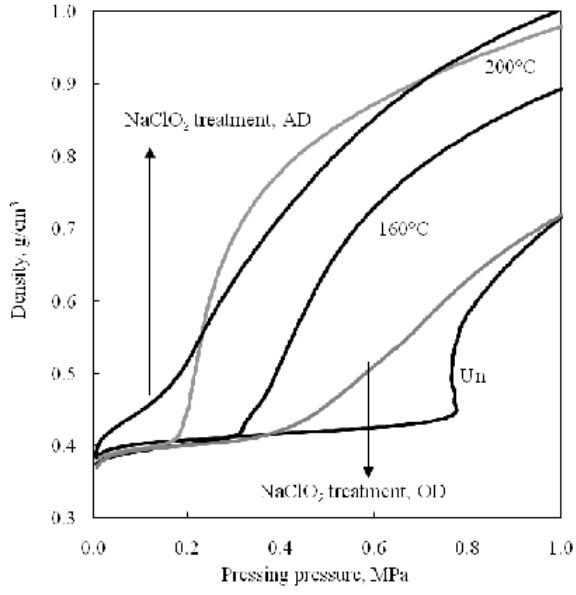

Figure 4. Changes of density of PF resin-impregnated wood as a function of steaming temperatures and comparison with those of $NaClO_2$ treatment (Shams et al, 2005). AD and OD refer to air- dried and oven-dried conditions for $NaClO_2$ treated PF resin-impregnated wood, respectively. Un refers to PF resin impregnated wood. Steaming time was 10 minutes (Shams et al, 2006)

3. FUTURE POTENTIAL APPLICATIONS

Since the Young's modulus and bending strength of untreated oven-dried Japanese cedar used in this study were 5.0 GPa and 40.8 MPa, respectively, the mechanical properties of Japanese cedar improved 4 to 6 folds by the combination of pretreatment ($NaClO_2$ or steam treatment), PF resin impregnation and hot pressing at 1 MPa. Considering that 1 MPa is a typical pressing pressure used for ordinary plywood and LVL production, we expect that when such treated PF resin-impregnated Japanese cedar veneers are laminated on both surfaces of stacked untreated veneers prior to hot pressing, high-strength plywood or LVL having a moderate specific gravity as a whole product can be obtained.

Fig.5 shows an example of one-shot lamination of resin-impregnated veneers to a Japanese cedar block of a density 0.35 g/cm^3. Due to softening pretreatment by $NaClO_2$, three layers of resin impregnated Japanese cedar veneer were compressed until a density of 1.0 g/cm^3 at a pressing pressure of 1 MPa without any deformation to a Japanese cedar block with a density of 0.35 g/cm^3. On the other hand, the resin-impregnated veneers without softening treatment were not compressed so much at a pressing pressure of 1 MPa despite plasticizing effect of phenolic resin. The density of this part is 0.5 g/cm^3.

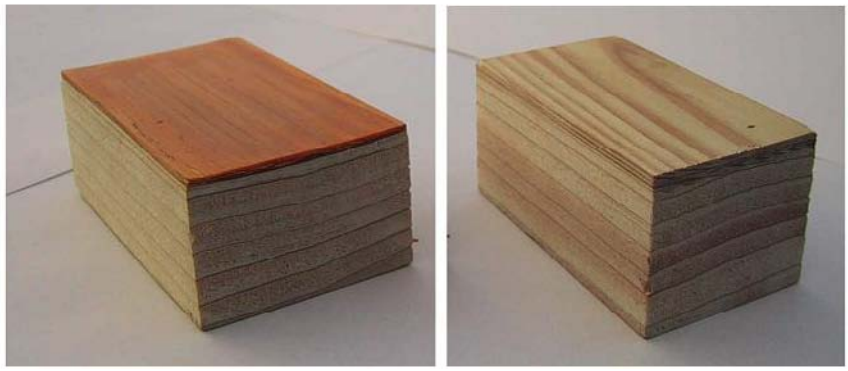

Figure 5. Appearance of veneer lamination wood material. Left: $NaClO_2$ and PF treated veneer, Right: PF treated veneer only. (Color preferred)

Hence, $NaClO_2$ treated resin impregnated veneers were laminated on the both side of commercial MDF [35]. Due to the lamination of treated veneer, MOE and MOR increased significantly although density of the final product increased about 40% (0.68 to 0.93 g/cm^3). The MOE and MOR of the laminated material attained 18 GPa and 177 MPa, respectively. It is interesting to note that the specific MOE and MOR (the ratio of MOE and MOR to specific gravity) of the laminated product were 19.6 GPa and 188 MPa which is almost five folds or four folds higher than commercial MDF [35]. The rate of water absorption of the commercial MDF shielded by the epoxy resin was 160%. On the other hand, surface laminated MDF, when parts other than the surface of the sample were shielded by the epoxy resin, was subjected to 3 hour boiling and further left in cold water for 72 hours; the rate of water absorption was 7.2% [35].

Although the single plate veneer lamination technique is promising, it is somehow difficult to treat large size veneer by $NaClO_2$ treatment. Considering the commercial point of view, $NaClO_2$ treated wafer or $NaClO_2$ treated powder lamination on the particle board (PB) before hot pressing was attempted [35]. The MOR and MOE of wafer overlaid PB were considerably higher than those of PB and the difference was especially remarkable for the MOE. By overlaying $NaClO_2$ treated resin impregnated wafer, the surface became flat and smooth with plastic like appearance, and MOE and MOR reached 7.2 GPa and 40MPa, respectively, about three times and two times higher than those of Japanese cedar PB with a density of 0.80 g/cm^3. Furthermore, it is noteworthy that $NaClO_2$ treated resin impregnated powder laminated board also showed excellent performance compared to particleboard. The MOE and MOR of the board reached 6.17 GPa and 34.0MPa, respectively with a density of 0.76 g/cm^3. The MOE of lauan plywood with a density of 0.78 g/cm3 is reported as 9.7 GPa parallel to the surface fiber direction and 5.1 GPa perpendicular to the surface fiber direction. The MOR in both directions is reported as 73MPa and 58MPa, respectively [36]. Considering the difference in the density between plywood and $NaClO_2$ treated resin impregnated wafer/powder overlaid PB, it could be said that the production of particleboards having similar mechanical properties to plywood is possible by overlaying plasticized wafer/powder. The application of steam treated PF resin impregnated veneer lamination in making high-performance plywood and LVL is presently underway.

CONCLUSION

Low molecular weight PF resin has a significant effect on the deformation behavior of wood during compression. With an increase of PF resin content, the Young's modulus of the cell wall perpendicular to the fiber direction decreases, and collapse-initiating pressure decreases linearly with the Young's modulus. This indicates that the occurrence of cell wall collapse is strain dependent. By controlling the processing parameters, combination of PF resin impregnation and pressure holding, a high strength wood was produced at low pressing pressures, such as 2 MPa. The removal of matrix substances by pretreatment with $NaClO_2$ and NaOH had a further effect to enhance the mechanical properties of resin-impregnated wood. Since $NaClO_2$ treatment is complicated in processing and harmful to environment, we proposed steam treatment as a substitute for chemical treatment in the fabrication of high strength wood at low pressing pressure. This technique allows the producer to impart high strength, improved durability and an attractive surface to wood composite material using conventional hot press equipment.

ACKNOWLEDGMENT

The authors would like to thank Gui-E-Chemical Industry Ltd. For supplying different types of phenol formaldehyde (PF) resins. M. I. Shams is indebted to the financial support of the JSPS Postdoctoral Fellowship for Foreign Researchers from the Japan Society for the Promotion of Science.

REFERENCES

[1] Hill, C. *Wood modification: chemical, thermal and other Processes*. Wiley, (2006) 233pp
[2] Rowell, R.M. *Chemical modification of wood.* In: Handbook of wood chemistry, wood composites, Rowell RM (ed) Chap. 14. CRC Press, Boco Raton, (2005) pp 381–420
[3] Rowell, R.M. *Forest Prod. J*. 2006. 56(9):4-12
[4] Rowell, R.M. *Forest Products Abstracts.* 1983.6(12):363-382
[5] Rowell, R.M. and Norimoto, M. J. Japan *Wood Res. Soc*. 1987. 33(11):907-910
[6] Hsu, W.E, Schwald, W., Schwald, J., Shields, A. *Wood Sci Technol.* 1988. 22:281-289
[7] Inoue, M., Norimoto, M., Tanahahi, M., Rowell, R.M. *Wood Fibre Sci.* 1993. 25:224-235
[8] Sekino, N., Inoue, M., Irle, M., Adcock, T. *Holzforschung*. 1999. 53:435-440
[9] Dwianto, W., Morooka, T., Norimoto, M., Kitajima, T. *Holzforschung*. 1999. 53:541-546
[10] Anwar, U.M.K., Paridah, M.T, Hamdan, H., Sapuan, S.M., Bakar E.S. *Industrial Crops and Products*. 2009. 29: 214-219
[11] Deka, M., Saikia, C.N. *Bioresource Technology*. 2000. 73: 179-181
[12] Gabrielli, C.P., Kamke, F.A. *Wood Sci. Tech*. DOI 10.1007/s00226-009-0253-6
[13] Furono, T., Imamura, Y., Kajita, H. *Wood Sci. Tech*. 2004. 37: 349-361

[14] Gindl, W., Zargar-Yaghubi, F., Wimmer, R. *Bioresource Technology.* 2003 87: 325-330
[15] Inoue, M., Norimoto, M., Otsuka, Y., Yamada, T. *Mokuzai Gakkaishi*.1991. 37 (3): 234-240
[16] Ryu, J.Y., Takahashi, M., Imamura, Y., Sato, T. *Mokuzai Gakkaishi*. 1991. 37 (9): 852-858
[17] Stamm, A.J., Seborg, S.M. *Forest Product Lab. Report* 1381 Rev. 1955.
[18] Stamm, A.J. *Wood and Cellulose Science*. Ronald Press Company, (1964) 349 pp
[19] Yano, H., Hirose, A., Inaba, S. J. *Mater. Sci. Lett*.1997. 16: 1906-1909
[20] Yano, H., Ozaki, M., Hata, T. *Holzforschung*.1997. 51: 287-288
[21] Yano, H., Hirose, A., Collins, P.J., Yazaki, Y. J. *Mater. Sci. Lett*. 2001. 20: 1125-1126
[22] Yano, H. J. *Mater. Sci. Lett.* 2001. 20: 1127-1129
[23] Yano, H., Mori, A.K, Collins, P.J., Yazaki, Y. *Holzforschung*. 2000. 54: 443-447
[24] Bodig, J. *For Prod J.* 1965.15: 197-202
[25] Gibson, L.J., Ashby, M.F. *Cellular Solids: Structure and Properties.* Cambridge University Press, (1997) pp 278-315
[26] Wolcott, M.P., Kamke, F.A., Dillard, D.A. *Wood and Fiber Sci.*1990. 22 (4): 345-361
[27] Wolcott, M.P., Kamke, F.A., Dillard, D.A. *Wood and Fiber Sci.* 1994. 26(4): 496-511
[28] Shams, M.I., Yano, H., Endou, K. *J Wood Sc*i. 2004. 50: 337-342
[29] Shams, M.I., Yano, H. *J Wood Sci*.2004. 50: 343-350
[30] Shams, M.I., Yano, H., Endou, K. *J Wood Sci.* 2005. 51:234-238
[31] Shams, M.I., Yano, H. *Wood Sci. Technol.* 2010 (In press)
[32] Shams, M.I., Yano, H. *J. Tropical Forest Sc*i. 2009. 21(2)175-180
[33] Shams, M.I., Morooka, T., Yano, H. *J Wood Sci.* 2006. 52, 389-394
[34] Higashihara, T., Morooka, T., Hirosawa, S., Norimoto, M. *Mokuzai Gakkaishi.* 2004. 50,159-167
[35] Shams, M.I., Yano, H. *J. Wood and Wood Products*. 2009. 67: 169-172
[36] Ebihara, T. *Wood composites board* (in Japanese). In: Mokuzai Katuyo jiten. Sangyo Chosakai, Uemura T (ed), (1994) 437p

In: Wood: Types, Properties, and Uses
Editors: Lorenzo F. Botannini
ISBN: 978-1-61668-837-0

Chapter 10

CRYSTALLIZATION AND MELTING BEHAVIOUR OF POLYPROPYLENE / WOOD FLOUR COMPOSITES

R. Bouza[1], C. Marco[2], G. Ellis[2], Z. Martín[2], M.A. Gómez[2] and L. Barral[1]

[1] Dept. of Physics, E.U.P. Ferrol, Universidad de A Coruña, Ferrol, Spain.
[2]Institute of Polymer Science & Technology, CSIC, 28006 Madrid, Spain.

ABSTRACT

Wood polymer composites (WPC's) are a new generation of reinforcing materials, using polymeric thermoplastic matrices such as polyolefins, and renewable materials such as woodflour. As a contrast to other mineral fillers, WPC materials have experienced growing interest over recent years due to the combination of a variety of factors, such as high performance, high versatility, processing advances, reasonable costs and biodegradability. However, there are some limitations. The most important disadvantage is their reduced resistance and low efficiency during stress transfer due to the incompatibility between hydrophilic polar fibres and hydrophobic apolar isotactic polypropylene, iPP. This creates repulsion forces that lead to poor adhesion, if at all, during blending. The use of compatibilizers increments the adhesion between components by reducing the interfacial tension and improving the stress transfer between phases. Since iPP is a semicrystalline polymer the understanding of the crystallization and melting behaviour of this matrix in the iPP/WF system, and the study of the influence of the compatibilizer on the crystalline parameters, and both the kinetics and thermodynamics of crystallization of iPP, are essential to the understanding of the solid-state properties in these materials. In this chapter we review the crystallization and melting processes of iPP/wood composites, under both dynamic and isothermal conditions, as a function of the thermal history, the content of the filler and the presence of interfacial agents as compatibilizers. The kinetic parameters and the evolution of the energies associated with crystalline nucleation of polypropylene in this type of composites and their relationship with the possible existence of a compatibilization processes between the polypropylene matrix and the wood reinforcement are discussed.

INTRODUCTION

For various decades plastic materials have played a fundamental role in our daily life. As an integral part of their technological evolution, both mineral and organic fillers have been added to polymeric matrices with the objectives of cost reduction, and increased stiffness and toughness. For this reason polymer composites have been the object of growing scientific and technological interest. However, the increased awareness and concern for environmental issues has generated the need for the reduction and/or rationalization in the use of polymeric materials, firstly because of their non-biodegradability, and secondly due to the short term consumption of non-renewable energy sources such as petroleum. These are the fundamental reasons for the interest in polymer composites that employ natural organic fillers, e.g. WPC's, especially via combinations with recyclable and/or degradable polymer matrices (green composites), as well as the different advantages that they offer when compared to polymer composites with inorganic mineral fillers.

Interest in biodegradable polymer composites, or those which present a very low environmental impact, is enormous and there is profuse activity in the study of composites based on materials of vegetable origin with synthetic polymers which incorporate biodegradable bonds, such as Mater-Bi, polylactic acid, poly(hydroxy-butyrate-co-hydroxyvalerate), polyvinyl alcohol, polybutylene succinate, polyester amide and polycaprolactone (1-20).

The main advantages in the use of natural fillers derived from wood, WF, are their ecological implications and reduced costs, since they are extracted from generally highly abundant plants, and frequently from sources of urban or industrial waste. Furthermore, these fillers are generally less abrasive for processing equipment than inorganic fillers, are of lower density, have good thermal and acoustic insulating properties, and on incineration can present lower health risks if inhaled. In recent years, the use of natural organic fillers in polymers sourced from post-consumer recycling and municipal solid waste has received growing interest due to the advantages derived from cost, aesthetic properties and environmental impact (21-27).

Fillers derived from wood, especially in the form of sawdust or fibres, have made an important impact in the thermoplastic polymer industry, mainly as a result of their penetration in the construction industry as both structural and semi-structural materials. Examples such as decking, fencing, siding, roof tiles, door and window frames, indoor and garden furniture are already abundant, and there is rapid growth in the transport, industrial and consumer sectors. However, WPC's also present some disadvantages. Amongst these it is important to consider their high sensitivity to humidity and their tendency to swell. Given that WPC's are low maintainence solutions for exterior applications, the understanding of water absorption and transport properties is fundamental in order to estimate the effect of humidity on phenomena related to the loss of mechanical properties or biological attack such as mildew (28-39). Further, since these WPC's can experiment undesirable colour changes, warping, swelling, chalking, etc. it is essential to assure their behaviour with respect to environmental factors. Thus the development of a better understanding of the mechanisms responsable for their degradation due to external agents, and methods that improve their environmental resistance are required (40-44).

Whilst there are numerous studies in the area of composite materials based on polymers with fillers of vegetable origin (45-47), by far the major research and technological efforts have been directed towards polyolefin matrices, fundamentally polyethylene, PE (48-57) and isotactic polypropylene (58-67). When compared with mineral fillers, the principal disadvantage of vegetable fillers resides in their low compatibility with hydrophobic matrices, especially polyolefins, which reduces the possibility for efficient dispersion of the polar particles in the apolar matrix, or adhesion with the polymeric chains. This often leads to the formation of aggregates during processing with a subsequent reduction in, or loss of, mechanical properties. In order to remedy this a major effort has been directed towards increasing the adhesion between the vegetable filler and the polymer, and the improvement of the dispersion of the filler in the matrix. Both aspects are of great importance and have been faced by two different approaches. Firstly, the addition of a third component, known as a coupling, interfacial or compatibilizing agent that, due to its inherent characteristics, can improve the interfacial adhesion through the formation of bonds between the filler and the matrix. Secondly, chemical treatment and surface modification of the fillers. There is much information available on the modification or interfacial adhesion in PE or iPP with vegetable fillers (68-85).

Isotactic polypropylene has been employed in the design and development of an endless variety of polymeric blends and composites (86-90). Since iPP is a semicrystalline polymer, the understanding of its crystallization and melting behaviour in composites with vegetable fillers is essential. Further, the analysis of the influence of interfacial or compatibilizing agents or filler surface treatments on the crystalline parameters, as well as the crystallization kinetics and thermodynamics of iPP are intrinsic to the understanding of the solid state properties of these composites.

In this chapter we present a revision of the crystallization and melting processes of iPP in its composites with vegetable fillers, under both dynamic and isothermal conditions, and as a function of the type, concentration and surface modification of the filler, and/or presence of compatibilization agents. The kinetic parameters of crystallization, and the evolution of the energies associated with the crystalline nucleation process of iPP in this type of composites, and phenomena such as polymorphism and transcrystallinity, are also revised.

DYNAMIC CRYSTALLIZATION

From a kinetics viewpoint the phenomenon of crystallization from the melt ocurrs via two fundamental processes: crystalline nucleation and subsequent crystalline growth. The first stage is the formation from the melt of stable crystalline nuclei, that is, ordered structures whose dimensions have reached a critical value that allow them to experience subsequent growth. This nucleation process can be homogeneous or heterogeneous. In homogeneous nucleation the nuclei form sporadically and at random due to statistical fluctuations in the polymer segments in the melt. This occurs at a constant rate. In the case of heterogeneous nucleation, the presence of foreign particles induces nucleation at the surface of the particle. This occurs at a non-constant rate. In practice, the nucleation phenomenon usually occurs through intermediate mechanisms, either due to the presence of impurities or through particles specifically introduced into the melt. This is the case for additives that impart

specific characteristics to the polymer, or those that accelerate the nucleation stage denominated *nucleating agents*, whose specific aim is to increase the crystallization rate of the polymer.

Once the nuclei are formed, either homogeneously or heterogeneously, these can undergo unidimensional, two-dimensional or three-dimensional growth, generating crystalline lamellae whose organization and packing give rise to the supracrystalline strutures which constitute the morphology of the polymer (91-94). As a general rule, in the crystallization of polymers the phase transition occurs at temperatures relatively far from the melting temperature, i.e. at relatively large undercooling, $\Delta T = T_m - T_c$, where T_m and T_c are the melting and crystallization temperatures respectively. The reason lies in the high interfacial free energies associated with the basal plane of the crystalline nuclei, and the difficult access to macromolecular sequences or segments of sufficient length to undergo chain folding from a random, disordered melt.

The nucleation rate, N, depends on the free energy necessary for the formation of a critically sized nucleus, denominated the free energy of nucleation, ΔG^*, and on the free energy necessary for the transport of the polymeric segments through the melt-crystal interphase, E_d, and can be expressed as:

$$N = N_0 \exp [(-E_d - \Delta G^*)/RT_c] \quad [1]$$

At high T_c , i.e. low undercooling, ΔG^* is high and dominates over the transport term. Thus, both the nucleation rate and the overall rate of crystallization are low. As the T_c is diminished, ΔT increases, ΔG^* is reduced, and the transport term gradually becomes more important as the viscosity of the melt increases. The result is that the nucleation rate falls and with it the overall crystallization rate. The balance between these two energies of nucleation and transport generates a maximum in the crystallization rate, which is a general fact in the crystallization of polymers.

From a technological point of view polymeric materials are processed from the melt generally by cooling at a controlled rate, which provokes crystallization under dynamic conditions. The incorporation of additives or nucleation agents during the process is of normal practice in the polymer industry with the following objectives; to increase the number of production cycles, thus reducing costs, and to improve materials properties. These agents increase the crystallization rate by influencing the nucleation stage through the reduction of the energetic barrier of the process.

Isotactic polypropylene is especially sensitive to the activity of both inorganic and organic nucleating agents [95], and these have been used to improve both mechanical properties directly related to the rigidity of the material and optical properties, as a function of the induced crystalline structure. Particles of vegetable origin, both as dust (or flour) or fibres, can exert a nucleating effect on the crystallization of iPP. Under dynamic conditions this activity is manifested by an increase in the temperature corresponding to the minimum of the crystallization exotherm, T_p, when the composite is cooled from the melt at a controlled cooling rate.

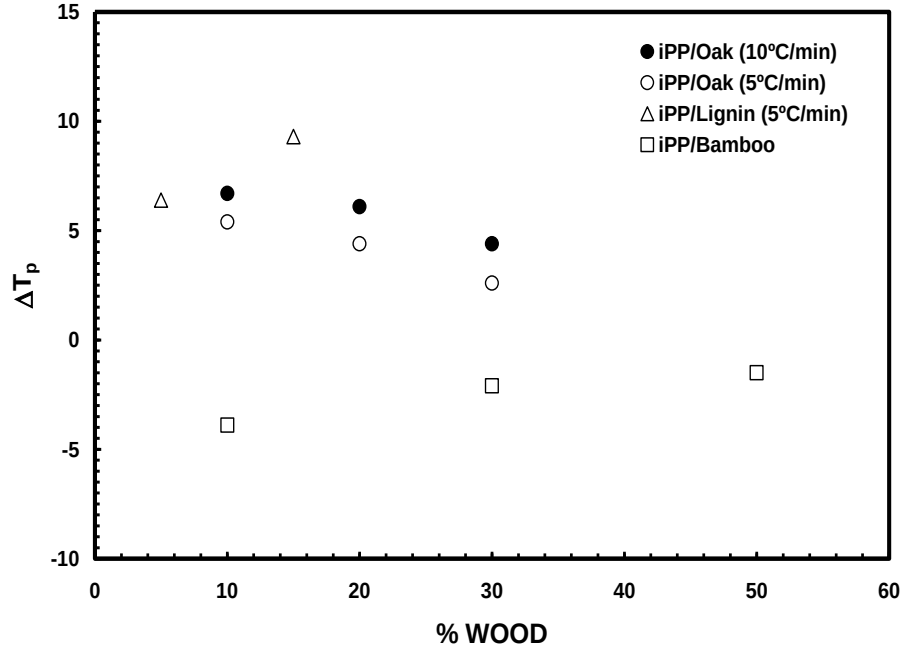

Figure 1. Variation of ΔT_p for iPP in the composites described with respect to the composition of vegetable filler (96-98).

Figure 1 shows the value of ΔT_p , considered as the difference between the values of T_p corresponding to iPP in the iPP/WF composite and the value of T_p for neat iPP obtained at the same cooling rate, for different types of wood. In the case of oak (96) and lignin (97) particles, the ΔT_p values are positive, i.e. T_p for iPP in the composites is higher than that for neat iPP, thus manifesting the nuclating activity of the wood particles. Further, this phenomenon depends on the cooling rate, and is more important at lower rates. However, although nucleating activity exists in both aforementioned cases, it varies as a function of the composition. For oak the value of ΔT_p falls with filler concentration, whereas the contrary occurs in the case of lignin. This can almost certainly be attributed to the better dispersion of the lignin particles in the iPP matrix, whilst in the case of oak the formation of particle aggregates occurs with increasing concentration. However, the most relevant case is that presented by the iPP/Bamboo composites (98), where not only is the nucleating effect absent, but there is also a depression in the value of T_p.

The presence of an interfacial agent generally reduces this nucleating effect, as can be observed in Figure 2, where the dynamic crystallization exotherms corresponding to cooling from the melt are compared for a PP/Oak system compatibilized with an ethylene-methacrylic acid ionomer at different compositions (99). The exotherms shift to lower temperatures in the presence of the interfacial agent, i.e. both the temperatures associated with the start of crystallization and the exotherm maxima are lower than those corresponding to the composites without the compatibilizing agent. As an example, Figure 3 shows the value of the maximum in ΔT_p for iPP/Oak and iPP/Bamboo composites in the presence of organosilane coupling agents (74, 98, 100, 101), or treatment of the wood with NaOH and other procedures (102).

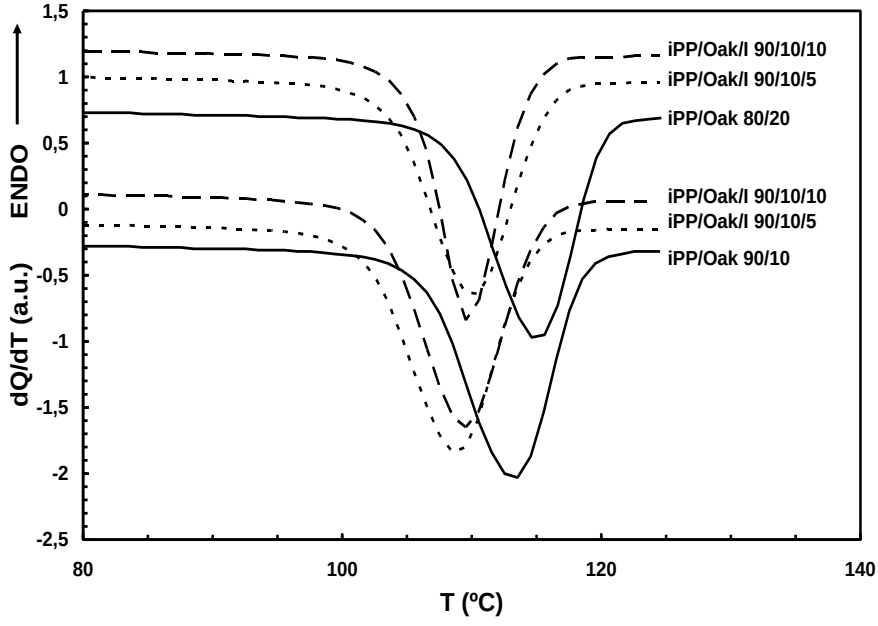

Figure 2. Crystallization exotherms correponding to cooling from the melt at a rate of 10ºC/min of the PP/Oak system, compatibilized with a ethylene-methacrylic acid copolymer, I, at the given compositions (99).

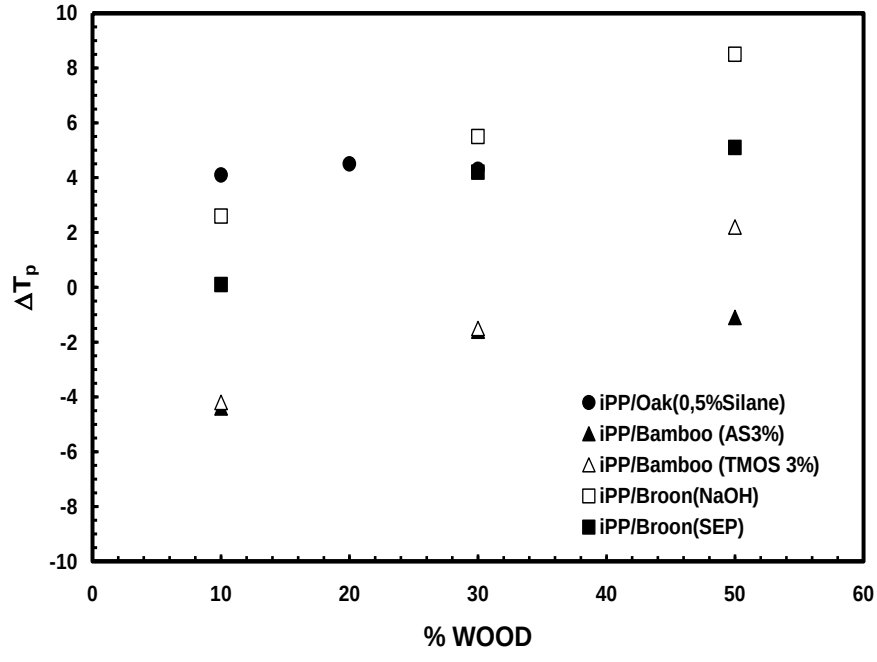

Figure 3. Variation in ΔT_p for iPP in the composites described with respect to the vegetable filler (74, 98, 100-102).

In iPP/Pine and iPP/Beech composites the influence of prior chemical treatment of the fibres with NaOH and subsequent esterification with maleic, propionic, crotonic, succinic and

phthallic anhydrides has been studied (103), and an important increase of between 5 – 9 ºC in the crystallization temperature was found compared to that for neat iPP. It was also found that the values of T_p are dependant on the chemical treatment, with an increase of around 1 – 4 ºC observed in the composites with chemical modification with respect to those without. Superior activity was observed for pine wood modified with maleic or succinic anhydride, and beech wood esterified with succinic anhydride.

Furthermore, the relationship between the supramolecular structure of iPP and the kinetic crystallization parameters have been studied in iPP/Flax and iPP/Hemp composites. The chemical modification of the lignocellulose fibres reduces both the nucleation density and the crystallization rate. On the other hand, the increase in the crystallization rate observed in the presence of un-modified fibres was attributed to the ability to generate another polymorphic phase of iPP (104). The experimental evidence currently available confirms the fact that the local chemical nature of the lignocellulose component plays an important role in the nucleation process of iPP (105).

In some cases the presence of an interfacial agent has been reported to slightly reduce the crystallization temperature of iPP, for example in iPP/WF composites in the presence of different concentrations of a styrene-ethylene-butadiene-styrene copolymer grafted with maleic anhydride, SEBS-g-MA, due to the fact that the interaction between the anhydride group and the WF inhibits the molecular mobility in the interphase, with a consequent restriction in the crystalline nucleation (106). Other interfacial agents based on isocyanates have also been used as compatibilizers to improve interfacial adhesion in iPP composites with cellulose derivatives (107). In all cases a nucleating effect on the crystallization of iPP was described in the presence of the vegetable filler. The addition of the compatibilizer reduces the values of T_p, although they remain superior to those for neat iPP, indicating that the chemical bond between the isocyanate group and the surface OH groups of the WF increments the interfacial adhesion, increasing the melt viscosity of the system, and limiting the molecular packing of the iPP macromolecules.

The observation of the fracture surfaces of iPP/WF composites by scanning electron microscopy, SEM, provides useful information on the levels of interaction between the thermoplastic matrix and the filler (25, 49, 85). Figure 4 shows the fracture surface corresponding to an iPP composite with Oak woodflour, both without compatibilizer and compatibilized with vinyltrimethoxysilane (74, 80).

The cellular structure of the wood particles can be easily distinguished, and shows either empty cavities, or cavities filled with the iPP matrix. Gaps between the polymer and the particles can be clearly observed at the walls of the cellular niches, and the fracture surfaces are seen to be very clean and devoid of flaking or adhered particles, which is a result of the poor adhesion between the components, Figure 4a. This effect can be more clearly observed in the microphotograph of the composite with 50% woodflour, Figure 4b. The coupling of the surface of the filler with an interfacial agent such as vinyltrimethoxysilane contributes to the reduction of the interfacial tension, generating a more isotropic fracture surface and increasing the level of wetting, as observed in Figure 4c where it is very difficult to differentiate between the particles as their dispersion in the matrix is increased and the interphase improved.

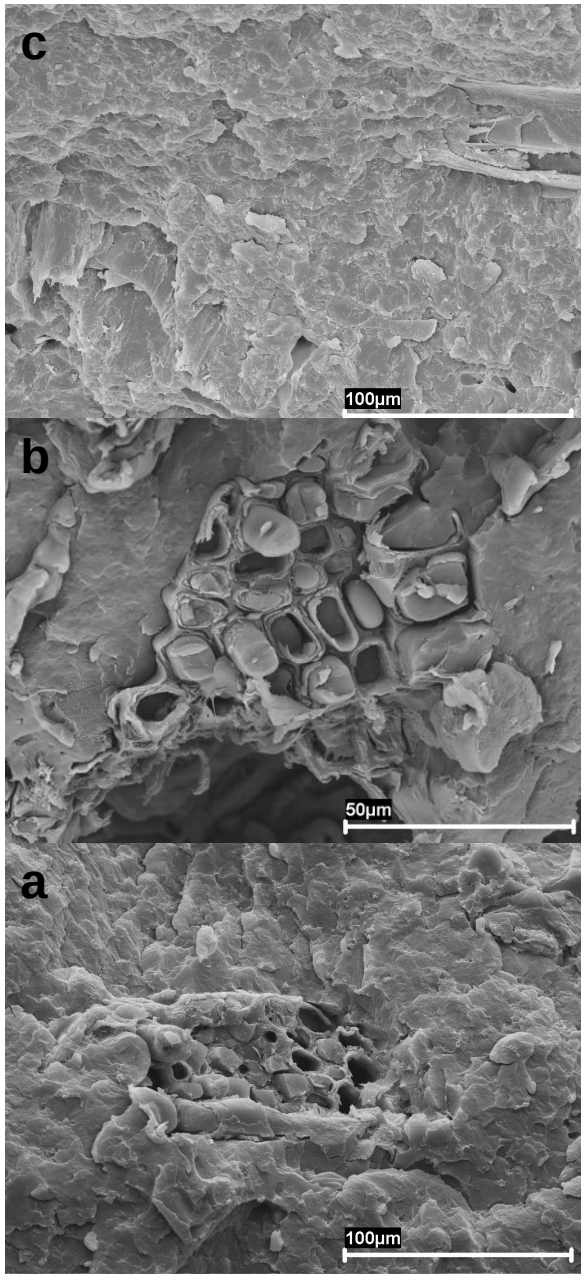

Figure 4. SEM microphotographs of the fracture surfaces of an iPP composite with (a) 10% Oak woodflour without compatibilizer, (b) 50% Oak woodflour without compatibilizer, (c) 10% Oak woodflour compatibilized with vinyltrimethoxysilane (74, 80).

CRISTALLINITY AND POLYMORPHISM

Generally the levels of crystallinity of iPP are affected by the type of filler, its surface treatment, and the presence of compatibilizing agents, as well as the crystallization

conditions. However, in some cases the degree of crystallinity is unaffected independently of the cooling rate employed, for example, iPP composites with sisal fibres (108). The same behaviour can be observed for PP-g-MA with treated or untreated Broom fibre, treated either with NaOH or by the steam explosion extraction process (SEP) (102), and for treated microcrystalline cellulose-filled iPP (109). However, in iPP composites with untreated Bamboo fibre the crystallinity falls dramatically at high fibre content, clearly indicating an inhibition of the crystallization process in iPP due to the presence of the vegetable filler, although silane treatment of the fibre can significantly re-establish the crystalline order (98). Conversely, in iPP/WF composites an increase in crystallinity has been observed with increasing WF content, justified by epitaxial crystallization of iPP on the surfaces of the WF particles, which is unaltered by the presence of a PP-g-MA compatibilizer (75). However, a reduction in the degree of crystallinity was reported in the presence of m-isopropenyl-α,α-dimethylbenzyl isocyanate grafted polypropylene (71).

With respect to the melting behaviour of iPP in vegetable filled composites after dynamic crystallization from the melt, either in the presence of interfacial agents or chemically treated fillers, the existing results appear to indicate that in the absence of an interfacial agent no significant variations in the melting temperature of iPP are observed, for example, in the case of iPP/Broom (treated) (102), iPP/Bamboo (98), iPP/Oak (99), or PP/Sisal (110) composites. However, in some cases an important depression in the melting temperatures of iPP can be found; around 6 ºC for composites of iPP / blend of Spruce, Maple, Pine and Oak in the presence of PE-g-MA (111), between 2 – 4 ºC for iPP / silane treated Bamboo composites (98), or slightly lower temperatures as is the case for iPP/Oak composites in the presence of an ethylene-methacrylic acid copolymer (99).

A relevant fact in the melting behaviour of iPP in some vegetable filled composites is the presence of a characteristic double melting endotherm corresponding to the existence of crystalline polymorphism in iPP. Isotactic polypropylene can present four crystal forms, known as monoclinic or α, trigonal or β, orthorrhombic or γ and smectic (112-114). It is known that the processing conditions are an influencing factor on the crystalline structure of iPP in vegetable filled composites. When they are molded by compression or extrusion, only the monoclinic form is encountered, whereas when they are processed by injection, both monoclinic and trigonal polymorphs are present. The fraction of each polymorph appears to depend on the type and concentration of filler, and process variables such as temperature and mold cooling rate, i.e. the crystallization conditions.

In iPP/Lignin composites two melting endotherms are observed, corresponding to the α and β polymorphs, whose fractions are influenced both by the concentration of lignin and the cooling rate (97). In an 80%/20% iPP/Oak system in the presence of an ethylene-methacrylic acid copolymer interfacial agent (99), a double endotherm was also detected, and the formation of the trigonal polymorph was also confirmed by x-ray diffraction as a function of temperature. As an example, Figure 5 shows the evolution of wide angle x-ray scattering (WAXS) diffractograms obtained using synchrotron radiation, corresponding to a heating cycle from room temperature (96). At 30 ºC a reflection can be clearly observed at $2\theta = 16.2º$ associated to the (300) plane of the trigonal polymorph, along with the reflections at 14.2 , 17.0, 18.8 , 21.2 and 22.0º, respectively associated to the (110), (040), (130), (111) and (041) planes corresponding to the monoclinic structure. At a temperature of 155 ºC the reflection at 16.2º dissapears, corresponding with the melting of the trigonal crystallites, and between 165 – 170 ºC the reflections associated with the monoclinic structure also disappear.

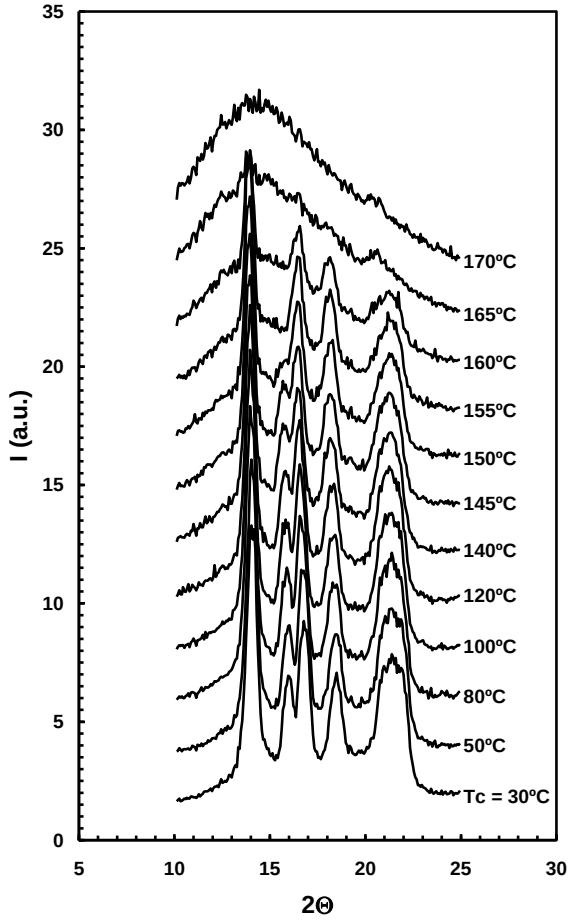

Figure 5. WAXS diffractograms corresponding to a heating cycle from room temperature of an iPP/Oak 80/20 composite compatibilized with an ethylene-methacrylic acid copolymer (96).

In the heating thermograms after the crystallization of iPP with Pine and Beech treated with NaOH and posterior esterification with maleic, propionic, crotonic, succinic and phthallic anhydrides, the presence of a small endotherm at around 150 ºC has also been detected, and corresponds to the melting of β crystals associated to the presence of between 4 – 6 % of the trigonal phase. The differences found in the polymorphs formed, depending on the chemical modification of the wood, suggest that the formation of the trigonal phase is associated with, on the one hand, the different nucleating capacities of the surface of the wood, and on the other, the crystalline growth rate (103).

The comparative analysis of flax fibres, unmodified and modified with acetic anhydride, shows that the modification provokes a reduction in the crystalline growth rate and consequently in the fraction of the trigonal polymorph. A similar effect has been found in composites of iPP with silane or octylisocyanate modified flax fibres (104). The formation of the trigonal polymorph in composites of iPP with treated and untreated flax and hemp, is dependant on the temperature of the melt in which the fibre is dispersed, such that at lower temperature the trigonal fraction increases. Chemical modification of the fibre significantly reduces the concentration of this polymorph (115). Also in the case of iPP/PP-g-

MA/Teawood flour composites, a small fraction of trigonal crystals are formed, which disappears when the fibre is treated with maleic anhydride (116). In iPP/Sisal composites, trigonal polymorph fractions of around 0.3 have been observed, which diminish in the presence of a compatibilizing agent such as SEBS-MA (117). This polymorph has also been detected in iPP/Cellulose composites (118) and in iPP/acetyl Jute or grafted with poly(methyl methacrylate), PMMA (119).

ISOTHERMAL CRYSTALLIZATION

In polymeric materials the isothermal crystallization process generally takes place at high crystallization temperature intervals, i.e. low undercooling, where the free energy of nucleation is high and consequently the crystalline nucleation rate is low, leading to crystalline growth rates and global crystallization rates that are also low. It is under these conditions that the differences that exist in the process of crystalline nucleation are best observed.

In Figure 6 the evolution of the crystallization exotherms obtained by differential scanning calorimetry for neat iPP are compared over a range of crystallization temperatures between 126 and 136 ºC, after cooling from the melt at 210 ºC (120).

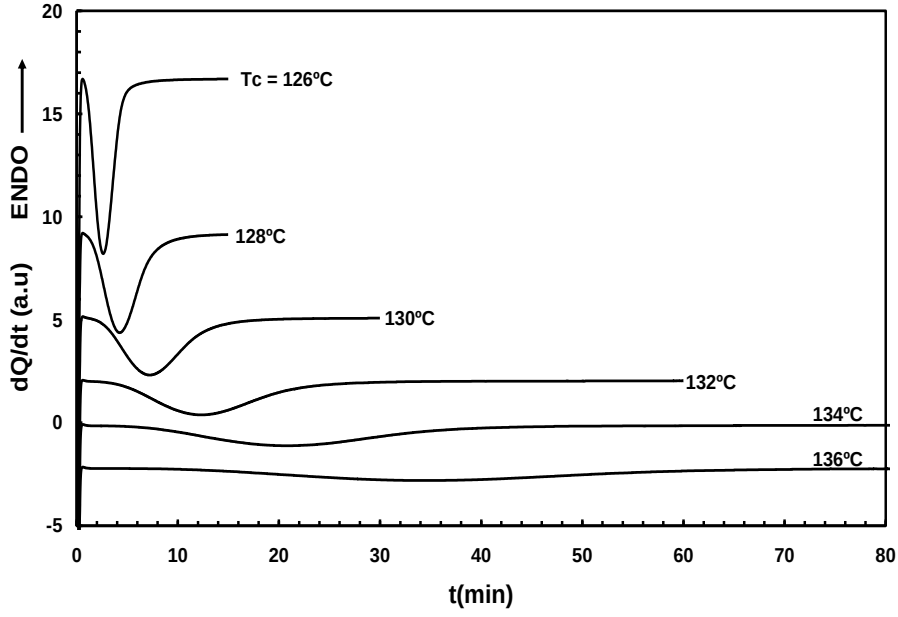

Figure 6. Crystallization exotherms for iPP at the crystallization temperatures indicated (120).

It is observed that the induction period, the width of the exotherm and the time necessary to complete crystallization all increase with T_c, reflecting a diminishing overall crystallization rate with the reduction of the undercooling of the system. This dependency of the rate with the temperature implies that the crystallization process is controlled by the nucleation stage for the system.

In binary iPP/WF composites, the presence of the vegetable filler provokes a reduction in the induction time and a shift in the exotherm minima to shorter times with respect to neat iPP for the same crystallization temperatures. This effect can be observed in iPP/Oak flour composites for a T_c of 130 ºC in Figure 7, and represents the existence of a nucleating effect of the WF particles on the crystallization of the iPP (120).

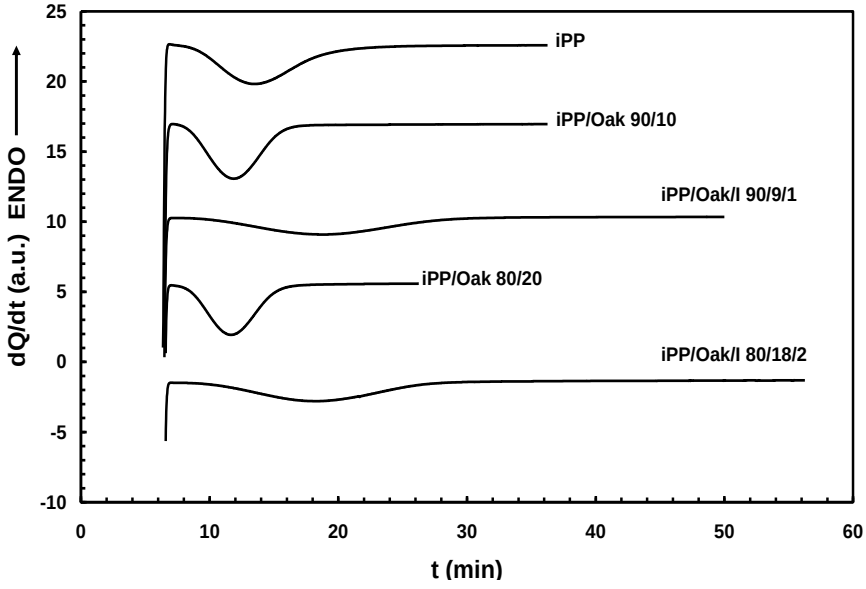

Figure 7.- Crystallization exotherms at T_c = 130 ºC, for iPP in composites of iPP/Oak and iPP/Oak/Ethylene-Methacrylic acid copolymer, I, at the compositions indicated (120).

The crystallization rate can be analysed using the values of τ_i , which corresponds to the time necessary to reach a degree of crystalline transformation of *i*, where *i* is between 0 (no transformation) and 1 (complete transformation). This parameter represents the overall or global crystallization rate, *G*, considering that $G \sim (\tau_i)^{-1}$. In Figure 8, the evolution of $\tau_{0.5}$ as a function of T_c is shown for a wide range of systems based on iPP and vegetable fillers. A pronounced change in the crystallization rate can be seen as T_c is increased, manifesting a clear nucleating effect as a function of the presence of the vegetable filler.

The crystallization kinetics can be followed using the models of Avrami and Göler and Sachs (91). The Avrami model, or restricted growth model, takes into account the perturbation of adjacent nuclei, whilst the Göler-Sachs model assumes free growth. Both models coincide when the crystallization process is analysed at low conversion and/or low degrees of crystallinity, and provide the rate constant for the process, *k*, and the parameter *n*, generally denominated as the Avrami exponent, that defines the type of nucleation and the growth geometry of the polymer crystals. In the case of iPP/WF composites diverse values of *n* have ben obtained, oscillating between 2 and 4 for the case of iPP composites filled with flax fibres, sisal fibres, oak flour or lignin (97, 108, 120-123), amongst others. In the majority, the value of *n* depends on the type of vegetable filler employed and the crystallization conditions, where the contribution of different types of nucleation and growth is common in the crystallization of these systems.

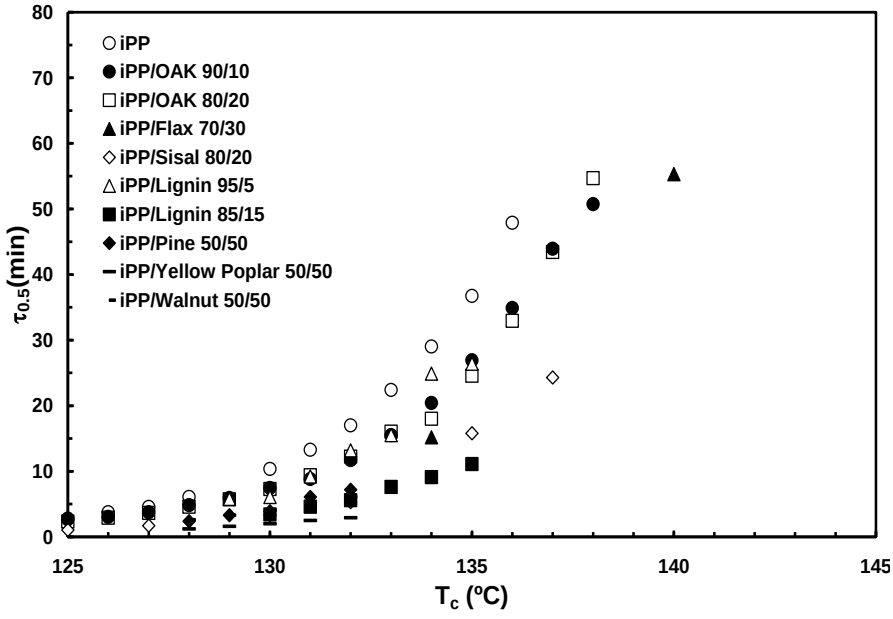

Figure 8. Variation in $\tau_{0.5}$ as a function of T_c for the iPP/WF composites described (97, 108, 120-123).

The determination of the mode of crystalline nucleation and growth permits the analysis of the overall crystallization rate, either from the value of the rate constant k at each crystallization temperature, determined from the Avrami and/or Göler-Sachs models, or by calculation from the expression (124):

$$k = ln\ 2/ (\tau^n_{0.5}) \qquad [2]$$

where $\tau_{0.5}$ is the time necessary to reach 50% crystalline transformation. In this manner the rate constants associated to different vegetable fillers can be compared. Table I presents the values of k at a T_c of 130 ºC, where the differences observed can be due to the surface morphology of the different vegetable fillers.

Table I. Crystallization rate constants for iPP/WF composites at T_c = 130 ºC

WF	Mass WF (%)	$k.10^3$ (min^{-n})	Ref.
Sisal	20	35	108
Lignin	5	3	97
Lignin	15	17	97
Pine	50	31	122
Red Cedar	50	1400	122
Cherry	50	880	122
Maple	50	57	122
Hickory	50	190	122
Osage Orange	50	43	122
Yellow Poplar	50	138	122
Walnut	50	25	122

Assuming spherulitic growth, the number of primary nuclei per unit volume, **N**, i.e., the density of crystalline nuclei, can be calculated from the relation (91):

$$\mathbf{N} = (k/\Gamma^3)[3\rho_\alpha(1-\lambda)_\infty/4\pi\rho_c) \quad [3]$$

where Γ is the radial growth rate, $(1-\lambda)_\infty$ is the degree of crystallinity at infinite time and ρ_α and ρ_c are the densities of the amorphous and crystalline phases respectively. It can also be calculated using the Kowalewsky and Galeski approximation (125):

$$\mathbf{N} = 3k^{3/n}/4\pi\Gamma^3 \quad [4]$$

The effects of the vegetable filler and the crystallization temperature on the nucleation density has been analysed in some systems (97, 108) and, as an example, Figure 9 shows the variation in the rate of spherulitic growth and nucleation density with T_c for iPP composites with lignin compared with that for neat iPP (97). A reduction in the crystalline growth rate and the nucleation density with T_c can be observed. However, whilst the variation observed in the growth rate due to the presence of lignin is practically negligible, the increase experienced in the nucleation density is very important in the presence of this filler. The values of **N** calculated for the composites are superior by 2 or 3 orders of magnitude than those for neat iPP, which is directly related to the effect of the lignin particles on the nucleation stage in iPP.

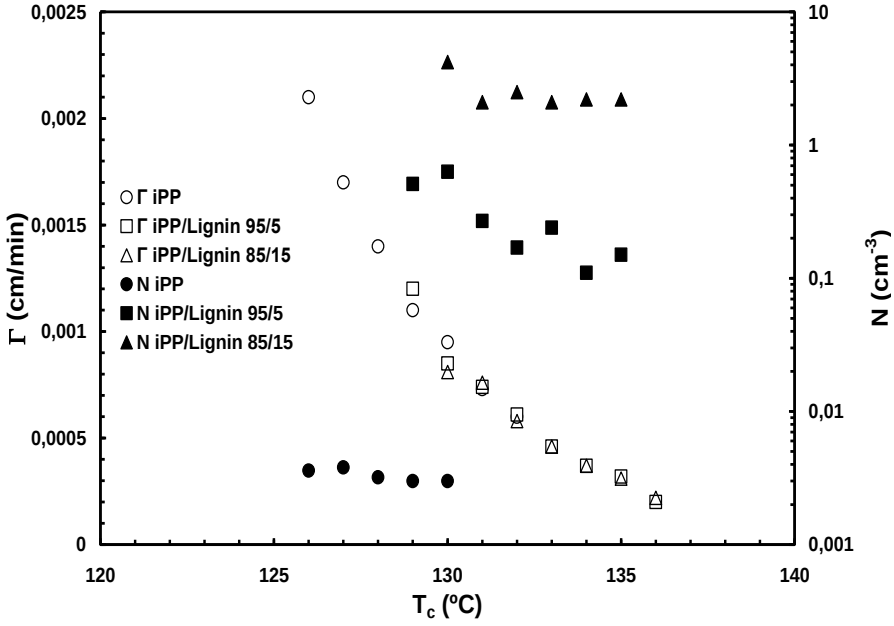

Figure 9. Variation in the nucleation density and the crystalline growth rate with crystallization temperature for iPP/lignin composites (97).

In composites of iPP with Oak flour containing an ionomeric interfacial agent, ethylene-methacrylic acid copolymer, I, a reduction in the rate of crystallization is observed with

respect to that of neat iPP, since the crystallization exotherms shift to longer crystallization times for the same T_c, Figure 7. This reduction in the global crystallization rate is not only manifested by this shift, but also by a reduction in the isothermal crystallization rate constant with respect to both neat iPP and iPP in the binary composites (120), Figure 10. This suggests that, on the one hand the interfacial agent cancels the nucleating effect, and on the other a compatibilization phenomenon is generated between the iPP matrix and the surface of the vegetable filler. Nevertheless, in the treatment of flax fibre with PP-g-MA in composites with iPP the same nucleating effect has not been observed (121).

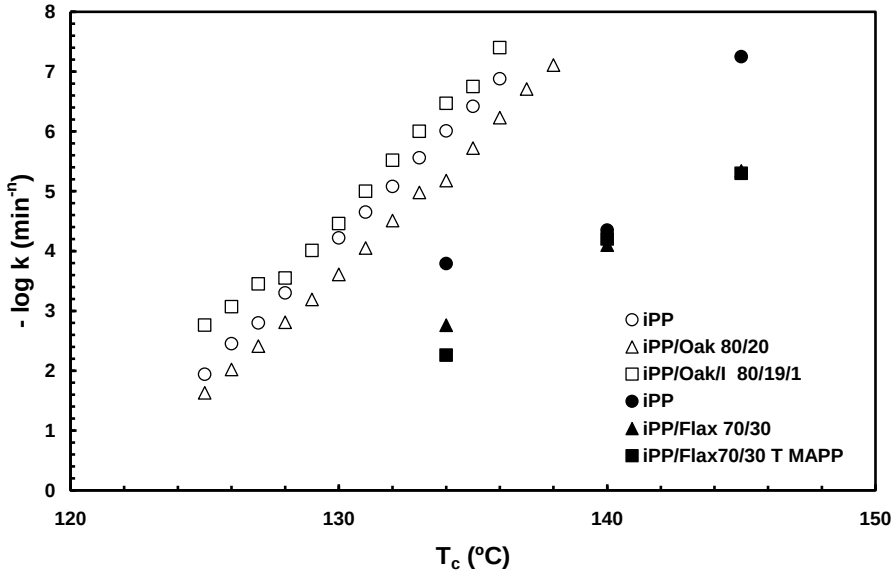

Figure 10. Variation of the crystallization rate constant with T_c for iPP/Oak and iPP/Flax composites in the presence of compatibilizing agent (120, 121)

The melting of iPP in its composites with vegetable fillers is not generally very different to that of neat iPP. Depending on the molecular weight and the conditions of isothermal crystallization, the melting endotherms of neat iPP present a maximum with an associated shoulder at lower temperature, Figure 11a. (120). Both shift to higher temperature as the T_c is increased. This is related to families of iPP crystallites whose size also increases as the level of undercooling decreases. The more imperfect crystals melt giving rise to the lower temperature shoulder in the endotherm, and the melting of the larger crystals constitute the main part of the endotherm, without excluding the existence of simultaneous processes of melting-recrystallization-melting. The presence of a vegetable filler such as oak flour, with or without the presence of an interfacial agent, does not substantially alter this behaviour, Figures 11b-c. Neither does the presence of other vegetable fillers such as flax or sisal (97, 108, 121, 126). The levels of crystallinity also remain practically invariable with respect to neat iPP, although the degree of crystallinity has been reported to increase very slightly for systems with untreated flax fibres, and to fall below the values for neat iPP in the case of treated flax fibres (121).

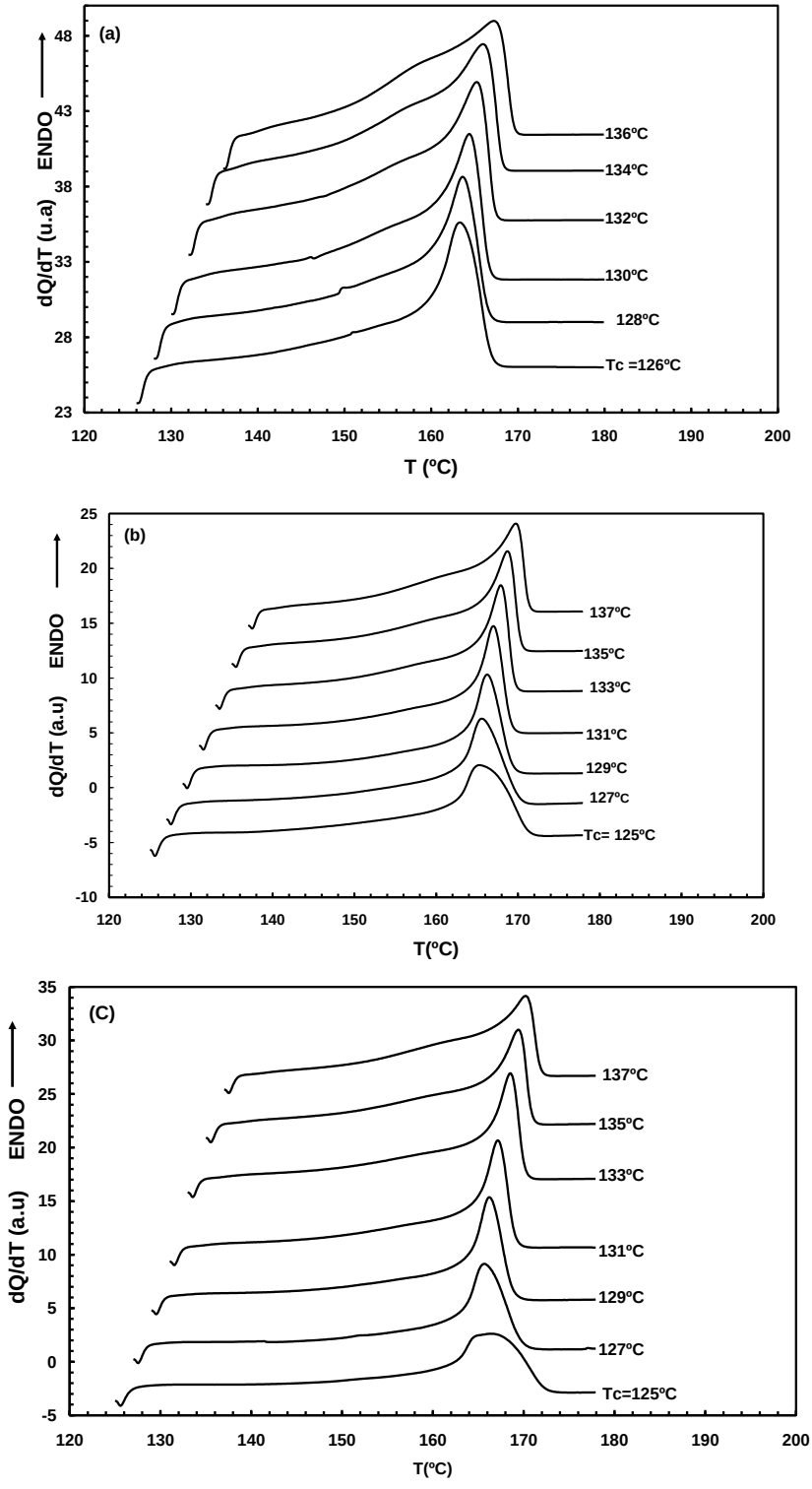

Figure 11. Heating thermograms after isothermal crystallization of (a) neat iPP, (b) iPP/Oak 80/20, (c) iPP/Oak/I 80/18/2, at the T_c values indicated (120)

TRANSCRISTALLINITY

Transcrystallinity appears when the density of crystalline nuclei on the surface of a fibre in contact with the molten polymer is markedly higher than that in the polymer itself. The lateral growth of these crystalline nuclei at the surface of the fibre is almost completely impeded parallel to the surface, due to the presence of neighbouring nuclei. Thus, only growth perpendicular to the surface, i.e. to the fibre axis, is possible and as a consequence a crystalline orientation develops resulting in the appearence of a region denominated *transcrystalline*, TCL, which emerges parallel to the surface. Transcrystallization is possible if the energetic conditions for nucleation are more favourable at the surface than in the unperturbed polymer melt, i.e. the surface should present heterogeneous nucleation activity (112, 127).

Both nucleation and crystalline growth are highly influenced by the temperature gradient of the interphase, the chemical composition and topography of the surface and its crystalline morphology, the surface energy, the presence of nucleating agents and the existence of epitaxial phenomena. Some debate exists on the nucleation mechanisms and their influence on the mechanical properties of the composites (128-131). The capacity of different cellulose fibres to induce transcrystallinity in iPP has been well described in the literature (102, 118, 122, 126, 132).

Figure 12. Microphotograph obtained by polarized light microscopy of an iPP/Sisal fibre system crystallized by cooling from the melt at 210 ºC. Cooling rate = 5 ºC/min.

One of the most interesting cases is that of composites of iPP with Sisal fibres. The incorporation of Sisal fibres results in an apparant increase in the crystallization temperature and the degree of crystallinity of iPP (126). Whilst some authors only observed the existence

of transcrystallinity in this type of PP/Sisal fibre system at high undercooling (108), others have demonstrated the formation of transcrystallinity bands under both dynamic and isothermal conditions (126). In Figure 12, a transcrystalline band in iPP, generated by heterogeneous nucleation on a sisal fibre by cooling from the melt at 210 ºC with a cooling rate of 5 ºC/min, can be observed in a spherulitic matrix.

Under isothermal conditions the dimensions of these bands are a function of the both T_c and time. Figure 13 compares the development of the TCL band on a sisal fibre under isothermal conditions, at T_c = 137 ºC, as a function of time.

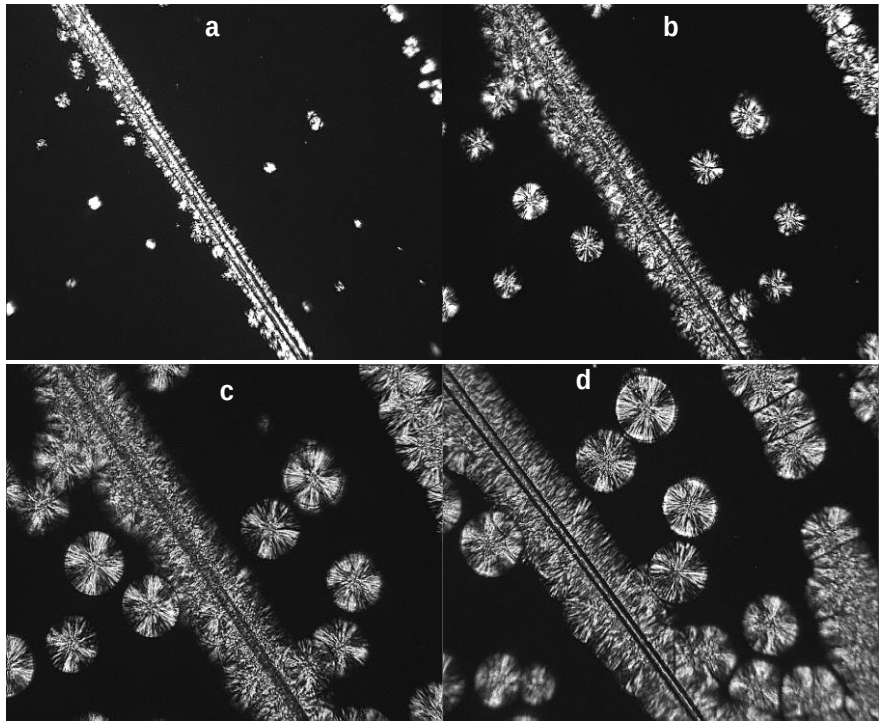

Figure 13. Evolution of the TCL band in a PP/Sisal composite at a crystallization temperature of 137 ºC, at the following times (a) 5, (b) 15, (c) 25 and (d) 40 minutes.

It should be pointed out that the spherulitic radius and the dimension in the growth direction of the TCL band with crystallization time at the same T_c are practically identical (121). Figure 14 shows the evolution of the sperulitic radius and the thickness of the TCL bands grown in a PP/Sisal composite crystallized isothermally at 137 ºC.

In the process of transcrystallization, the nucleation density at the surface of the fibre and in the bulk iPP melt falls with increasing T_c, reducing the crystallization rate and increasing the final dimensions of the transcrystalline layer (133, 134). It has been found that the cooling rate before reaching the crystallization temperature had no effect on the isothermal crystallization process in PP/Flax fibres (132).

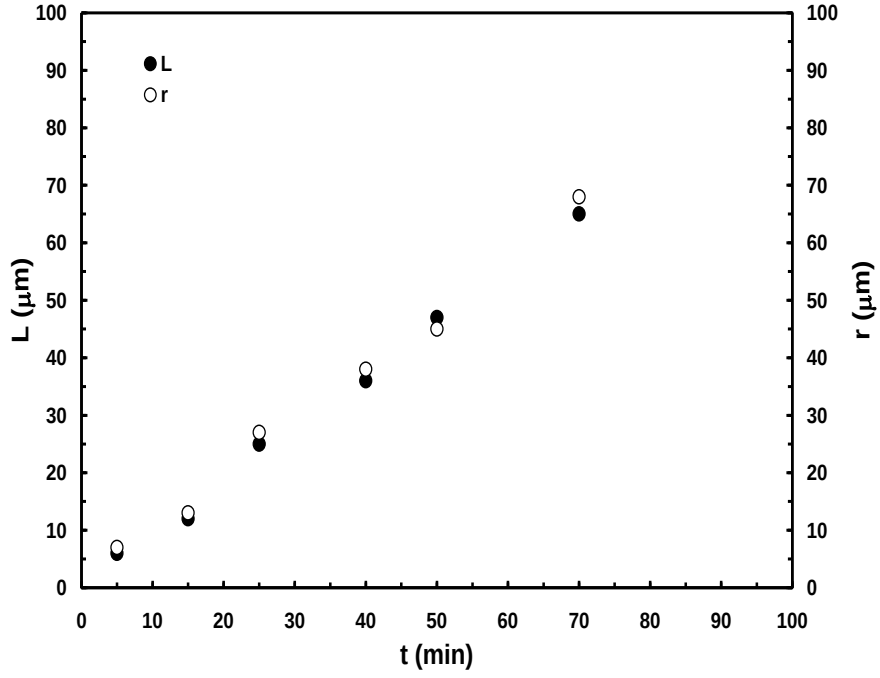

Figure 14. Variation in the thickness of the TCL band and the spherulitc radius in a PP/Sisal composite. T_c = 137 ºC.

Some of the most interesting aspects of the transcrystallization process in this type of composite are related with the influence of the existence of stress during crystallization. Shearing or "pulling" the fibres through the melt at or near T_c is one example of stress induced crystallisation, which reduces the formation time for the TCL band, compared to the time for that originated by normal, or quiescent crystallization (126). Further, it has been found that whilst a TCL band is observed in the isothermal crystallization of PP/untreated Flax fibre, when the surface of the fibre is treated transcrystallization is not observed (121). Thus, the crystalline morphology in fibre-reinforced thermoplastic composites is strongly influenced by the surface treatment of the fibre, as well as the crystallization temperature. In the case of iPP composites with cellulose it has been demonstrated that pre-treatment of the surface of the vegetable fibre with different chemical agents inactivates the surface phenomena responsible for transcrystallinity (135), and it has been pointed out that the coupling agent that improves the interfacial interaction between the cellulose and the matrix must be localised at the interface (118), thus causing an inhibition of the process of transcrystallization, or at least a significant reduction in the nucleation density on the fibre surface. Other authors have found that in the PP/untreated Cellulose fibre system transcrystallinity was observed (109). However, when the fibres were treated no TCL bands were observed, and they propose a possible mechanism for the appearance of the transcrystallinity band which involves the crystalline structures in the matrix and the treated and untreated filler.

Finally, when a nucleating agent is incorporated in order to generate a specific polymorph in the iPP matrix, whether it be monoclinic or trigonal (136, 137), the nucleating activity of the vegetable fibre is lower than that of the nucleating agent and as such the density of

nucleation in the melt is higher than at the fibre surface. Thus the process of transcrystallization is practically eliminated, both under dynamic and isothermal crystallization conditions. Figure 15 shows the typically spherulitic morphology obtained in the case of neat iPP, Fig.15a, along with those obtained in the presence of a nucleating agent inducing the monoclinic polymorph, Fig.15b, sisal fibre, Fig.15c and a sisal fibre with the same nucleating agent, Fig.15d, at a T_c of 137 ºC. In the presence of the nucleating agent, Fig. 15b, the birrefringent structures correspond to crystalline entities of less than 1 μm in diameter, resulting from the high nucleation density induced by the nucleating agent, whose presence inhibits the nucleating effect of the fibre surface, Fig. 15d.

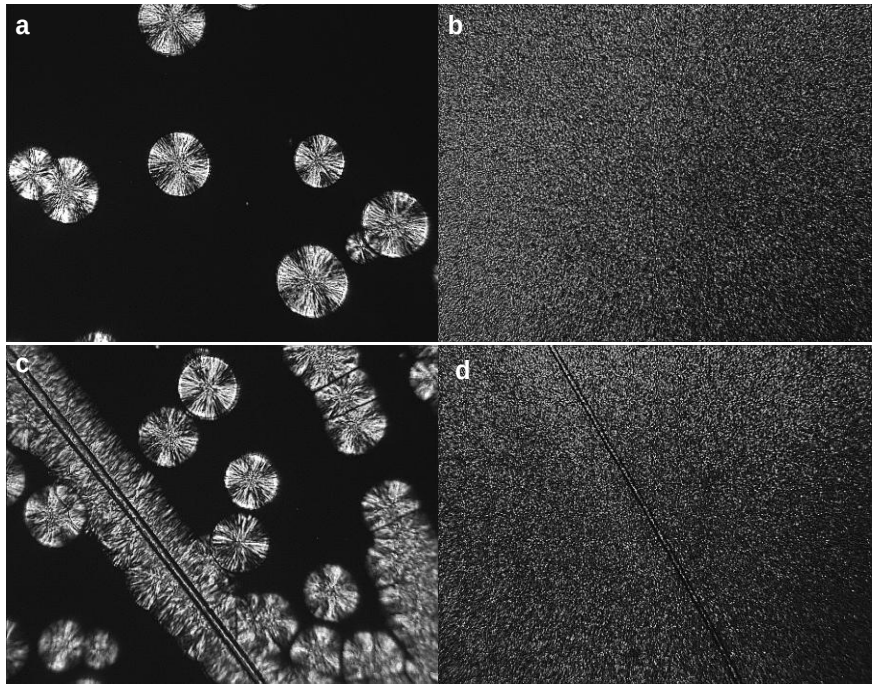

Figure 15. Polarized light microphotographs corresponding to the isothermal crystallization at T_c = 137 ºC of (a) neat iPP, (b) iPP/monoclinic nucleating agent, (c) iPP/Sisal, (d) iPP/Sisal/monoclinic nucleating agent.

TEMPERATURE COEFFICIENT

We have already seen that when crystallizing polymeric materials at low undercooling, i.e. high crystallization temperatures, the rate of crystallization is higher the larger the undercooling, and the crystallization process is controlled by the nucleation stage, i.e. by the free energy of nucleation, ΔG^*, which can be given by the expression:

$$\Delta G^* = \frac{4 b_0 \sigma_u \sigma_e T_m^0}{\Delta H_{100} \Delta T} \qquad [5]$$

The terms σ_e and σ_u are the basal and lateral interfacial free energies of the crystallite, respectively, b_0 = 6.26 Å and represents the thickness of each crystalline monolayer added during growth, T_m^0 represents the equilibrium melting temperature of iPP, and ΔH_{100} corresponds to the melting enthalpy of 100% crystalline iPP.

The presence in the iPP melt of a foreign substrate frequently provokes a reduction in the critical size of the crystalline nucleus necessary for subsequent growth, because the generation of an interphase between the polymeric crystal and the substrate may be more favourable than the creation of a crystalline nucleus from the melt. Heterogeneous nucleation actually occurs through the reduction of the free energy of nucleation, producing a higher nucleation rate and consequently a higher crystallization rate. In iPP three crystallization regimes exist (138-147) and can be associated with discontinuities in the temperature coefficients as a consequence of different modes of crystal growth. The transition from regime III to regime II takes place at T_c values between 135 – 137 ºC, and that from regime II to regime I between 148 – 155 ºC (141, 142, 148). According to the kinetic theory of crystallization (92, 145, 149), the crystallization rate, G can be given by:

$$\log G + \left[\frac{U}{2.3R(T_c - T_\infty)}\right] = \log G_0 - \left(\frac{K_{g(III)}}{2.3T_c\Delta T}\right) \qquad [6]$$

where $U/2.3R(T_c\text{-}T_\infty)$ represents the transport term through the melt – crystal interface at T_c (150), and $K_{g(III)} = 4\ \sigma_u\sigma_e b_0 T_m^0 / k\ \Delta H_{100}$ for regime III, with k in this case corresponding to the Boltzmann constant. The viscosity of the system is infinite at the temperature T_∞ and is equivalent to T_g – 30, which corresponds to 231.1 K for iPP. The influence of the increase in ΔH_{100} can be eliminated by applying the Hoffman, Davis and Lauritzen approximation (92), where the interfacial free energy is given by:

$$\sigma_u = \alpha\Delta H_{100}(a_0 b_0)^{1/2} \qquad [7]$$

where $\alpha \approx 0.1$ and $a_0 b_0$ = 34.37 Å^2 representing the chain cross section in the iPP crystal, and the values of the basal interfacial free energy, given in Table II, can be obtained from the following expression:

$$\sigma_e = \frac{kK_{g(III)}}{4b_0 T_m^0 \alpha (a_0 b_0)^{1/2}} \qquad [8]$$

where T_m^0 was taken as 210 ºC (120).

Information in the literature on the basal interfacial free energy associated with the isothermal crystallization of iPP in composites with vegetable fillers is scarce. Previous studies on the isothermal crystallization of iPP with 5% by weight WF do not show any variations in the value of the basal interfacial free energy (151).

Table II. Nucleation parameters for the isothermal crystallization of iPP/Oak (120)

iPP (mass%)	Oak (mass %)	Ionomer (mass %)	σ_e x 10^{10} (kJcm$^{-2)}$	G (min^{-1})	ΔG^* x10^{-16} (kJ)
100	0	0	1.71	0.047	163.7
90	10	0	1.50	0.063	143.6
90	9.5	0.5	1.57	0.037	150.3
90	9.0	1.0	1.55	0.032	148.4
80	20	0	1.56	0.063	150.3
80	19	1.0	1.68	0.034	160.8
80	18	2.0	1.70	0.028	162.7

It seems clear that the reduction in the values of σ_e in binary iPP/WF composites, with values of 1.50 and 1.56 x 10^{-8} kJ cm^{-2} for the 90/10 and 80/20 composites, respectively, compared to that of 1.71 x 10^{-8} kJ cm^{-2} in the case of neat iPP, Table II, is associated with the nucleating effect of the vegetable filler (120). This behaviour is in agreement with Beck (152), and is similar to that which occurs when nucleating agents (153-156) or nanofillers (157) are present, or there are different types of fibres where transcrystallization is observed (158). However, the presence of the interfacial agent in the ternary composites, especially in the case of the 80/20 composites, compensates for or practically eliminates the nucleating effect of the vegetable filler.

The free energy of nucleation increases with decreasing undercooling, and is lower for the iPP/Oak composites than for neat iPP at the same T_c, confirming that the energy barrier for nucleation is lower when the WF component is present, leading to an increase in the overall rate of crystallization, Table II. The interfacial agent present in the ternary composites clearly cancels out the nucleating effect of the WF through a reduction in the crystallization rate, as mentioned earlier. This effect is accompanied by an important change in the values of the respective basal interfacial free energies. In many binary semicrystalline – amorphous polymeric systems it is well known that a reduction in the crystallization rate of the semicrystalline component indicates the existence of miscibility between the systems (159). Moreover, in binary semicrystalline – semicrystalline polymer systems where one component has a nucleating effect on the other, the corresponding increase in the rate of crystallization disappears when a compatibilizing agent is present (160). Factors such as the existence of interactions between the matrix and the interfacial agent will undoubtedly generate some compatibilization in the system.

CONCLUSIONS

The presence of wood particles exerts a nucleating effect on the crystallization of iPP, which is manifested in the increase in the crystallization rate and the nucleation density. This effect depends on the characteristics and concentration of the vegetable filler and its surface treatment, the presence of interfacial agents, and the crystallization conditions of the composite. Generally the surface modification or the presence of compatibilizing agents cancels the crystalline nucleation effect. The melting behaviour of iPP is on the whole

unaffected by the aforementioned factors. However, significant fractions of trigonal crystalline polymorphism can be induced in composites generally prepared via injection.

Different cellulose fibres present the capacity to induce a transcrystallization process through the energetically favourable heterogeneous nucleation at the fibre surface. The phenomenon of the formation of transcrystalline bands is affected by the surface morphology of the fibre, its chemical composition, its crystalline structure and, of course, the crystallization conditions. The dimensions of the transcrystalline bands are conditioned by the crystallization temperature and time, and the surface treatment of the fibre or the presence of interfacial coupling or compatibilizing agents, whose presence inhibits in the same manner the nucleation process. In the presence of other nucleating agents, transcrystallinity is eliminated both under dynamic and isothermal crystallization processes.

The fundamental cause of the reduction in the values of the basal interfacial free energy of iPP in the presence of vegetable particles compared to that for neat iPP is the nucleating effect of the filler, which is similar to that observed for other conventional nucleating agents or nanofillers. For the same undercooling, the free energy of nucleation for iPP is lower in the presence of a vegetable filler, which results in a higher crystallization rate. The presence of an interfacial agent increases the interfacial energies, and consequently inhibits the nucleating effect.

REFERENCES

[1] Scaffaro, R.; Morreale, M.; Re, G. L.; La Mantia, F. P. *J. Appl. Polym. Sci*. 2009, *114*, 2855-2863

[2] Mathew, A. P.; Oksman, K.; Sain, M. *J. Appl. Polym. Sci*. 2005, *97*, 2014-2025

[3] Jiang, L.; Huang, J.; Qian, J.; Chen, F.; Zhang, J.; Wolcott, M. P. Y. Zhu *J. Polym. Environ*, 2008, *16*, 83-93

[4] Pilla, S.; Gong, S.; O´Neill, E.; Yang, L.; Rowell, R. M. *J. Appl. Polym. Sci*. 2009, *111*, 37-47

[5] Arbelaiz, A.; Fernández, B.; Valea, A.; Mondragón, I. *Carbohydr. Polym.* 2006, *64*, 224-232

[6] Tserki, V.; Matzinos, P.; Zafeiropoulos, N. E.; Panayiotou, C. *J. Appl. Polym. Sci*. 2006, *100*, 4703-4710

[7] Shah, B. L.; Selke, S. E.; Walters, M. B.; Heiden, P. A. *Polym. Compos.* 2008, *29*, 655-663

[8] Lee, S. Y.; Kang, I. A.; Doh, G. H.;Yoon, H.G.; Park, B. D.; Wu, Q. L. *J. Therm. Compos. Mat.* 2008, *21*, 209-223

[9] Reinsch, V.; Kelley, S. *J. Appl. Polym. Sci*. 1997, *64*, 1785-1796

[10] Fernandes, E. G.; Pietrini, M.; Chiellini, E. Biomacromolecules 2004, *5*, 1200-1205

[11] Van De Velde, K.; Kiekens, P. *Polym. Test*. 2002, *21*, 433-442

[12] Luo, S.; Netravalli, N. A. *J. Mater. Sci*. 1999, *34*, 3709-3719

[13] Alvarez, V. A.; Ruseckaite, R. A.; Vazquez A. *Polym. Degrad. Stab*. 2006, *91*, 3156-3162

[14] Jonson, R. M.; Tucker, N.; Barnes, S. *Polym. Test*. 2003, *22*, 209-215

[15] Huda, M.; Drzal, L. T.; Mohanty, A. K.; Misra, M., *Comp. Sci. Tech*. 2008, *68*, 424-432

[16] Bax, B.; Mussig, J. *J. Compos. Sci. Tech*. 2008, *68*, 1601-1607
[17] García, M.; Garmendia, I.; García, J. *J. Appl. Polym. Sci*. 2008, *107*, 2994-3004
[18] Keller, A. *Comp. Sci. Tech*. 2003, *63*, 1307-1316
[19] Iman, S. H.; Cimelli, P.; Gordon, S. H.; Chiellini, E. *J. Polym. Environ*. 2005, *13*, 47-55
[20] Kim, H. S.; Yang, H. S.; Kim, H. J. *J. Appl. Polym. Sci*. 2005, *97*, 1513-1521
[21] Spinace, M. A. S.; Fermoselli, K. K. G.; De Paoli, M. A. *J. Appl. Polym. Sci*. 2009, *112*, 3686-3694
[22] Kaci, K.; Hamma, A.; Pillin, I.; Grohens, Y. *Macromol. Mat. Eng*. 2009, *295*, 532-540
[23] Adhikary, K. B.; Pang, S. S.; Staiger, M. P. *Compos. Part B* 2008, *39*, 807-815
[24] Lei, Y.; Wu, Q. L.; Yao, F.; Su, Y. J. *Compos. Part A* 2007, *38*, 1664-1674
[25] La Mantia, F. P.; Morreale, M. *Polym. Eng. Sci*. 2006, *46*, 1131-1139
[26] Cui, Y. H.; Tao, J. *J. Appl. Polym. Sci*. 2009, *112*, 1250-1257
[27] Ismail, H.; Osman, H.; Mariatti, J. *J. Vinyl Add. Technol.* 2008, 143-151
[28] Mansour, S. H.; Asaad, J. N.; Iskander, B. A.; Tawfik, S. Y. *J. Appl. Polym. Sci*. 2008, *109*, 2243-2249
[29] Arbelaiz, A.; Fernández, B.; Ramos, J. A.; Retejí, A.; Llano-Ponte, R.; Mondragón, I. *Compos. Sci. Tech.* 2005, *65*, 1582-1592
[30] Mishra, S.; Verma, J. *J. Appl. Polym. Sci*. 2006, *101*, 2530-2537
[31] Kaci, M.; Cimmino, S.;, C.; Duraccio, D.; Benhamida, A.; Zaidi, L. *Macromol. Mater. Eng*. 2006, *291*, 869-876
[32] Steckel, V.; Clemons, C. M.; Thoemen, H. *J. Appl. Polym. Sci*. 2007, *103*, 752-763
[33] Nachtigall, S. B. M.; Cerveira, G. S.; Rosa, S. M. L. *Polym. Test*. 2007, *26*, 619-628
[34] Beg, M. D. H.; Pickering, K. L. *Compos. Part A* 2008, *39*, 1748-1755
[35] Yeh, S. K.; Gupta, R. K. *Compos. Part A* 2008, *39*, 1694-1699
[36] Najafi, S. K.; Kiaefar, A.; Tajvidi, M. *J. Appl. Polym. Sci*. 2008, *110*, 3116-3120
[37] Hassan, M. M.; Mueller, M.; Wagners, M. H. *J. Appl. Polym. Sci.* 2008, *109*, 1242-1247
[38] Nekkaa, S:; Guessoum, M.; Haddaoui, N. *Int. J. Polym. Mat.* 2009, *58*, 468-784
[39] Zhang, Y. C.; Toghiani, H.; Zhang, J. L.; Xue, Y. B.; Pittman, C. *J. Mater. Sci.* 2009, *44*, 2143-2151
[40] La Mantia, F.P. *Polym. Deg. Stab*. 2008, *93*, 1252-1258
[41] Ndiaye, D.; Fanton, E.; Moriat-Therias, S.; Vidal, L.; Tidjani, A.; Gardette, J. L. *Compos. Sci. Technol.* 2008, *68*, 2779-2784
[42] Fabiyi, J. S.; McDonald, A. G.; Wolcott, M. P.; Griffiths, P. R. *Polym. Deg. Stab*. 2008, *93*, 1405-1414
[43] Beg, M. D. H.; Pickering, K. L. *Polym. Deg. Stab*. 2008, *93*, 1939-1946
[44] Kiguchi, M.; Kataoka, Y.; Matsunaga, H.; Yamamoto, K.; Evans, P. D. *J. Wood Sci.* 2007, *53*, 234-238
[45] Dikobe, D. G.; Luyt, A. S. *J. Appl. Polym. Sci*. 2007, *104*, 3206-3213
[46] Rimdusit, S.; Kampangsaree, N.; Tanthapanichakoon, W.; Takeichi, T.; Suppakarn, N. *Polym. Eng. Sci*. 2007, *47*, 140-149
[47] Jahani, Y. *Polym. Eng. Sci*. 2007, *47*, 2041-2048
[48] Zhang, J. J.; Park, C. B.; Rizvi, G. M.; Huang, H. X.; Guo, Q. P. *J. Appl. Polym. Sci.* 2009, *113*, 2081-2089
[49] Xiong, C.; Qi, R. R.; Wang, Y. L. *J. Appl. Polym. Sci*. 2009, *114*, 1160-1168
[50] Bengtsson, M.; Oksman, K.; Stark, N. M. *Polym. Compos.* 2006, *27*, 184-194

[51] Tajvidi, M.; Takemura, A. *Polym. Compos.* 2009, *30*, 1226-1233
[52] Yang, H. S.; Wolcott, M. P.; Kim, H. S.; Kim, S.; Kim, H. J. *Compos. Struct.* 2007, *79*, 369-375
[53] Zhong, Y.; Poloso, T.; Hetzer, M.; De Kee, D. *Polym. Eng. Sci*. 2007, *47*, 797-803
[54] Shi, H.; Li, B.; Chen, C.; Jia, Y. L. *J. Appl. Polym. Sci*. 2007, *104*, 3161-3170
[55] Li, B.; Jiang, H. L.; Guo, L. H.; Shi, H. C. *J. Appl. Polym. Sci*. 2008, *107*, 2520-2530
[56] Huang, H. X.; Zhang, J. J. *J. Appl. Polym. Sci*. 2009, *111*, 2806-2812
[57] Godard, F.; Vincent, M.; Agassant, J. F.; Vergnes, B. *J. Appl. Polym. Sci*. 2009, *112*, 2559-2566
[58] Zhang, S. W.; Rodrigue, D.; Riedl, B. *Polym. Compos.* 2005, *26*, 731-738
[59] Hristov, V.; Krumova, M.; Michler, G. *Macromol. Mater. Eng.* 2006, *291*, 677-683
[60] Chauhan, S. S.; Karmarkar, A.; Aggarwal, P. *J. Appl. Polym. Sci*. 2006, *102*, 1706-1711
[61] Bledzki, A. K.; Faruk, O. *Compos. Part A* 2006, *37*, 1358-1367
[62] Mirbagheri, J.; Tajvidi, M.; Hermanson, J. C.; Ghasemi, I. *J. Appl. Polym. Sci.* 2007, *105*, 3054-3059
[63] Kuboki, T.; Lee, Y. H.; Park, C. B.; Sain, M. *Polym. Eng. Sci*. 2007, *47*, 1148-1155
[64] Bengtsson, M., Le Baillif, M.; Oksman, K. *Compos. Part A* 2007, *38*, 1922-1931
[65] Bettini, S. H. P.; Uliana, A. T.; Holzschuh, D. *J. Appl. Polym. Sci*. 2008, *108*, 2233-2241
[66] Renner, K.; Moczo, J.; Pukanszky, B. *Compos. Sci. Technol.* 2009, *69*, 1653-1659
[67] Pan, M. Z.; Zhou, D. G.; Bousmina, M.; Zhang, S. Y. *J. Appl. Polym. Sci*. 2009, *113*, 1000-1007
[68] Coutinho, F. M. B.; Costa, T. H. S.; Carvalho, D. L. J. *J. Appl. Polym. Sci*. 1997, *65*, 1227-1235
[69] Raj, R.; Kokta, B. V. *Polym. Eng. Sci*. 1991, *31*, 1358-1362
[70] Oksman, K.; Lindberg, H.; Holmgren, A. *J. Appl. Polym. Sci*. 1998, *69*, 201-209
[71] Guo, C. G.; Wang, Q. W. *J. Appl. Polym. Sci.* 2008, 109, 3080-3086
[72] Qiu, W. L.; Zhang, F. R.; Endo, T.; Hirotsu, T. *J. Mater Sci*. 2005, *40*, 3607-
[73] Nair, K. C. M.; Thomas, S. *Polym. Compos* 2003, *24*, 332-343
[74] Bouza, R.; Lasagabaster, A.; Abad, M. J.; Barral, L. *J. Appl. Polym. Sci*. 2008, *109*, 1197-1204
[75] Salemane, M. G.; Luyt, A. S. *J. Appl. Polym. Sci*. 2006, *100*, 4173-4180
[76] Selke, S. E.; Childress, J. in *Wood Fiber-Polymer Composites: Fundamental Conceps, Process and Material Options*; Wolcott M. P.; Ed.; Forest Product Society, Madison, Wisconsin, 1993, 109
[77] Bledzki, A. K.; Gassan, J. *Prog. Polym. Sci*. 1999, *24*, 221-274
[78] Wang, Y.; Yeh, F. C.; Lai, S. M.; Chan, H. C.; Shen, H. F. *Polym. Eng. Sci*. 2003, *43*, 933-955
[79] Lu, J. Z.; Wu, Q.; Negulesco, I. I. *J. Appl. Polym. Sci*. 2005, *96*, 93-102
[80] Bouza, R.; Abad, M. J.; Barral, L.; Ladra, M. *Polym. Eng. Sci*., 2009, 324-332
[81] Azizi, H.; Ghasemi, I. *Polym. Compos*. 2009, 429-435
[82] Dányádi, L.; Janecska, T.; Szabó, Z.; Nagy, G.; Móczo, J.; Pukánszky, B. *Compos. Sci. Technol*. 2007, *67*, 2838-2846
[83] Li, T.; Yan, N. *Compos. Part A* 2007, *38*, 1-12
[84] Lai, S. M.; Yeh, F. C.; Wang, Y.; Chang, H. C.; Shen, H. F. *J. Appl. Polym. Sci*. 2003, *87*, 487-496

[85] Acha, B. A.; Reboredo, M. M.; Marcovich, N. E. *Compos. Part A* 2007, *38*, 1507-1516
[86] *Handbook of Polypropylene and Polypropylene Composites*, Karian H. G.; Ed.; Marcel Dekker Inc., N.Y. 1999
[87] *Structure, Blends and Composites*, Karger-Kocsis J.; Ed., Chapman&Hall, London 1995, Vol.3
[88] *Polyolefin Blends and Composites*, Nwaburma, D; Kyu T.; Eds.; John Wiley, 2008, Vol.2
[89] *Polypropylene. An A-Z Reference*, Karger-Kocsis, J.; Ed; Springer-Verlag, 1999
[90] *Wood-polymer Composites*, Oksman, K.; Sain. M.; Eds.; Taylor&Franscis Inc., 2008
[91] Mandelkern, L. in *Crystallization of Polymers*, Cambridge University Press, McGraw-Hill, N.Y. 2002, 2nd Ed., Vol.1
[92] Hoffman, J. D.; Davies, G. T.; Lauritzen, J. I. in *Treatise on Solid State Chemistry*, Hannay N. B.; Ed.; Plenum Press, N.Y. 1976, Vol. 3
[93] Wunderlich, B. *Macromolecular Physics*, Academic Press, N.Y. 1973, Vol.1
[94] Schultz, J. M. *Polymer Crystallization. The development of Crystalline Order in Thermoplastic Polymers*, American Chemical Society, Washington D.C., Oxford University Press, Oxford, 2001
[95] Marco, C.; Ellis, G.; Gómez, M.; Arribas, J. M. in *Recent Research Developments in Applied Polymer Science*, Pandalai S. G. Ed., Research Signpost, Trivandum, India, 2002, Vol.1, 587-610
[96] Bouza, R.; Martín, Z.; Gómez, M. A.; Marco, C.; Barral, L. *J. Ann. Rep. Desy-Hasylab. Soft Condensed Mater.*, 2004, 753-754
[97] Canetti, M.; De Cirico, A.; Audisio, G. *J. Appl. Polym. Sci*. 2004, *91*, 1435-1442
[98] Lee, S. Y.; Chun, S. J.; Doh, G. H.; Kang, I. A. *J. Compos. Mat*. 2009, *43*, 1639-1657
[99] Bouza, R.; Marco, C.; Martín, Z.; Gómez, M. A.; Ellis, G.; Barral, L. *J. Appl. Polym. Sci*. 2006, *102*, 6028-6036
[100] Matsuda, H.; Ueda, M.; Mori, H. *Wood Sci. Technol*. 1988, *22*, 21-32
[101] Toynbee, J. *Polymer* 1994, *35*, 438-440
[102] Avella, M.; Casale, L.; Dell´Erba, R.; Focher, B.; Martuscelli, E.; Marzetti, A. *J. Appl. Polym. Sci.* 1998, *68*, 1077-1089
[103] Borysiak, S. *J. Therm. Anal. Cal*. 2007, *88*, 455-462
[104] Garbarczyk, J.; Paukszta, D.; Borysiak, S. *J. Macromol. Sci. Part B Physics* 2002, *41*, 1267-1278
[105] Borysiak, S.; Doczekalska, B. *Eur. J. Wood Prod.* 2006, 64, 451-454
[106] Guo, C. G.; Wang, Q. W. *J. Reinfor. Plast. Compos.* 2007, *26*, 1743-1752
[107] Gironés, J.; Pimenta, M. T. B.; Vilaseca, F.; De Carvalho, A. J. F. *Carbohydr Polym*. 2007, *68*, 537-543
[108] López Manchado, M. A.; Biagiotti, J.; Torre, L.; Kenny, J. M. *Polym. Eng. Sci*. 2000, *40*, 2194-2204
[109] Quillin, D.T.; Mengping, Y.; Koutsky, J. A.; Caulfield, D. F. *J. Appl. Polym. Sci*. 1994, *52*, 605-615
[110] Albano, C.; Reyes, J.; Ichazo, M.; González, J.; Brito, M.; Moronta, D. *Polym. Degrad. Stab*. 2002, *76*, 191-203
[111] Tasdemir, M.; Biltekin, H.; Caneba, G. T. *J. Appl. Polym. Sci*. 2009, *112*, 3095-3102
[112] Varga, J. in *Polypropylene, Structure, Blends and Composites*. *Structure and Morphology*, Karger-Kocsis J.; Ed.; Chapman & Hall, Cambridge 1995, Vol 1, 56-115

[113] Meille, S. V.; Ferro, D. R.; Brückner, S.; Lovinger, A. J.; Padden, F. J.. *Macromolecules* 1994, *27*, 2615-2622
[114] Lotz, B.; Wittman, J. C.; Lovinger, A. J. *Polymer* 1996, *37*, 4979-4992
[115] Garbarczyk, J.; Borysiak, S. *Int. J. Polym. Mater*. 2004, *53*, 725
[116] Mishra, S.; Verma, J. *Polym. Plast. Technol. Eng.* 2006, *45*, 1199-1205
[117] Xie, X. L.; Fung, K. L.; Li, R. K. Y.; Tjong, S. C.; Mai, Y. W. *J. Polym. Sci. Polym. Phys.* 2002, *40*, 1214-1222
[118] Son, S. J. *J. Mat. Sci*. 2000, *35*, 5767-5778
[119] Bhattacharya, S. K.; Shembekar, V. R. *Macromol. Rep.* 1995, *A32*, 485
[120] Bouza, R.; Marco, C.; Ellis, G.; Martín, Z.; Gómez, M. A.; Barral, L. *J. Therm. Anal. Cal*. 2008, *94*, 119-127
[121] Arbelaiz, A.; Fernández, B.; Ramos, J. A.; Mondragón, I. *Termochim. Acta 2006, 440*, 111-121
[122] Kim, J. W.; Harper, D. P.; Taylor, A. M. *J. Appl. Polym. Sci*. 2009, *112*, 1378-1385
[123] López Manchado, M. A.; Torre, L.; Kenny, J. M. *J. Appl. Polym. Sci*. 2001, *81*, 1063-1074
[124] Kim, S. H.; Park, S. W.; Gil, W. S. *J. Appl. Polym. Sci*. 1998, *67*, 1383-1392
[125] Kowalewsky, T.; Galeski, A. *J. Appl. Polym. Sci*. 1986, *32*, 2919-2934
[126] Joseph, P. V.; Joseph, K.; Thomas, S.; Pillai, C. K. S.; Prasad,V. S.; Groeninckx, G.; Sarkissova, M. *Compos. Part A* 2003, *34*, 253-266
[127] Nelly, A.; Zweben, C. "Comprehensive composite materials, Polymer Matriz Composites", Vol. 2, Chapter 2.25, Elsevier, Oxford, 2000
[128] Felix, J. M.; Gatenholm, P. *J. Mater. Sci*. 1994, *29*, 3043-3049
[129] Wang, C.; Hwang, L. M. *J. Polym. Sci. Polym. Phys*. 1996, *34*, 47-56
[130] Gray, D. G. *J. Polym.Sci. Polym. Lett*. 1974, *12*, 509-515
[131] Folkes, M. J. in *Polypropylene. Structure, blends and composites. Structure and Morphology*; Karger-Kocsis, J.; Ed; Chapman&Hall, London, 1995, Vol.3, 340-370
[132] Zafeiropoulos, N. E.; Baillie, C. A.; Matthews, F. L. *Compos. Part A* 2001, *32*, 525-543
[133] Loos, J.; Schimanski, T.; Hofman, J.; Peijs, T.; Lemstra, P. J. *Polymer* 2001, *42*, 3827-3834
[134] Wagner, H. D.; Lustiger, A.; Marzinsky, C. N.; Mueller, R. R. *Comp. Sci. Technol*. 1993, *48*, 181-184
[135] Amash, A.; Zugenmaier, P. *Polymer* 2000, *41*,1589-1596
[136] Marco, C.; Gómez, M. A.; Ellis, G.; Arribas, J. M. *J. Appl. Polym. Sci*. 2002, *84*, 2440-2450
[137] Marco, C.; Gómez, M. A.; Ellis, G.; Arribas, J. M. *J. Appl. Polym. Sci*. 2002, *86*, 531-539
[138] Lovinger, A. J.; Chua, J. O.; Gryte, C. C. *J. Polym. Sci. Polym. Phys.* 1977, *15*, 641-656
[139] Cheng, S. Z. D.; Janimag, J. J.; Zhang A.; Hsieh, E. T. *Polymer* 1991, *32*, 648-655
[140] Wlochowicz, A.; Eder, M. *Polymer* 1981, *22*, 1285-1287
[141] Ibhadon, A. O. *J. Appl. Polym. Sci*. 1999, *71*, 579-584
[142] Monasse, B.; Haudin, J. M. *Coll. Polym. Sci*. 1988, *266*, 679-687
[143] Bartczak, Z.; Galeski, A. *Polymer* 1990, *31*, 2027-2038
[144] Martuscelli, E.; Silvestre, C.; Abate, G. *Polymer* 1982, *23*, 229-237
[145] Clark, E. J.; Hoffman, J. D. *Macromolecules* 1984, *17*, 878-885
[146] Allen, R. C.; Mandelkern, L. *Polym. Bull*. 1987, *17*, 473-480

[147] Ding, Z.; Spruiell, J. E. *J. Polym. Sci. Polym. Phys.* 1997, *35*, 1077-1093
[148] Bond, E. B.; Spruiell, J.E.; Lin, J. S. *J. Polym. Sci. Polym. Phys.* 1999, *37*, 3050-3064
[149] Hoffman, J. D. *Polymer* 1983, *24*, 3-26
[150] Hoffman, J. D.; Frolen, L. J.; Ross, G. S.; Lauritzen, J. I. *J. Res. Natl. Bur. Stand*. 1975, *79A*, 671
[151] Mucha, M.; Królikowski, Z. *J. Therm. Anal. Cal*. 2003, *74*, 549-557
[152] Beck, H. B. *J. Appl. Polym. Sci*. 1975, *19*, 371-373
[153] Menczel, J.; Varga, J. *J. Therm. Anal. Cal*. 1983, *28*, 161-174
[154] Fena, Y.; Jin, X.; Hay, J. N. *J. Appl. Polym. Sci*. 1998, *69*, 2089-2095
[155] Yin, J.; Wang, S.; Zhang, Y.; Zhang, Y. *J. Polym. Sci. Polymer Phys*. 2005, *43*, 1914-1923
[156] Li, C.; Zhang, D.; Li, Z. *J. Appl. Polym. Sci*. 2002, *85*, 2644-2651
[157] Ma, J.; Zhang, S.; Qi, Z. Z.; Li, G.; Hu, Y. *J. Appl. Polym. Sci*. 2002, *83*, 1978-1985
[158] Wang, C.; Liu, C. R. *Polymer* 1999, *40*, 289-298
[159] Runt, J. P. Crystalline Polymer Blends, *Polymer Blends*, Vol. 1, D.R. Paul D. R.; Bucknall C. B. Eds., John Wiley & Sons, New York 2000
[160] Marco, C.; Ellis, G.; Gómez, M. A.; Fatou, J. G.; Arribas, J. M.; Campoy, I; Fontecha, A. *J. Appl. Polym. Sci*. 1997, *65*, 2665-2677

INDEX

C

D

E

F

G

H

I

J

K

L

M

N

O

P

Q

R

S

T

U

V